



Durham E-Theses

Petrology and geochemistry of gabbroic and ultrabasic rocks from eastern Rhum

Faithfull, John William

How to cite:

Faithfull, John William (1986) *Petrology and geochemistry of gabbroic and ultrabasic rocks from eastern Rhum*, Durham theses, Durham University. Available at Durham E-Theses Online:
<http://etheses.dur.ac.uk/6867/>

Use policy

The full-text may be used and/or reproduced, and given to third parties in any format or medium, without prior permission or charge, for personal research or study, educational, or not-for-profit purposes provided that:

- a full bibliographic reference is made to the original source
- a [link](#) is made to the metadata record in Durham E-Theses
- the full-text is not changed in any way

The full-text must not be sold in any format or medium without the formal permission of the copyright holders.

Please consult the [full Durham E-Theses policy](#) for further details.

PETROLOGY AND GEOCHEMISTRY OF GABBROIC AND
ULTRABASIC ROCKS FROM EASTERN RHUM

John William Faithfull
B.Sc (Dunelm)

Geology Department

Durham University

The copyright of this thesis rests with the author.
No quotation from it should be published without
his prior written consent and information derived
from it should be acknowledged.

Thesis submitted for the degree of
Doctor of Philosophy
University of Durham

1986



13 FEB 1987

THE UNIVERSITY OF CHICAGO
DIVISION OF THE PHYSICAL SCIENCES

DEPARTMENT OF CHEMISTRY

PHYSICAL CHEMISTRY

PH.D. THESIS

Thesis
1986/FAI

Author: [Faint text]
Title: [Faint text]
Date: [Faint text]

Abstract

This work is concerned with the lower part of the Eastern Layered Series (LELS) of Rhum, and with the marginal relationships of the ultrabasic complex in eastern Rhum.

The Lower Eastern Layered Series comprises approximately Units 1-5 of previous workers. Remapping has revealed considerable along-strike lithological variation in the units of the L.E.L.S. It is suggested, on the basis of field and geochemical evidence, that two layers formerly regarded as 'conformable intrusive sheets of fine grained olivine gabbro', may be evolved allivalite layers rather than later intrusions. Xenolith suites in these layers and elsewhere, indicate a component derived from the roof or walls of the magma chamber. Cryptic variation is more extensive in the L.E.L.S. than in other parts of Rhum: olivine forsterite content varies from 85.6 to 70, and clinopyroxene $MgX100/(Mg+Fe)$ varies from 88 to 74. Post-cumulus effects and sub-solidus re-equilibration have altered the initial compositions of the mineral phases. The migration of interstitial liquids has had a major effect on mineral chemistry. Replacement of plagioclase-rich rocks by peridotite is a significant process in parts of the sequence. This is ascribed to disequilibrium between migrating pore liquids and plagioclase. The data are consistent with a model of repeated replenishment by picritic magma, although the replenishing liquids may have been slightly less magnesian than those subsequently available during the formation of the upper ELS.

Re-examination of the eastern margin of the ultrabasic complex suggests that the ultrabasic rocks formed more or less in situ, and that fragments of the roof to the intrusion occur in places. Locally under these roof fragments variolitic olivine-rich gabbros are developed, which may represent the chilled margin to the ultrabasic complex.

DECLARATION

The work described in this thesis is my own, except where otherwise stated, and has not been submitted for degree in this or any other university.

The copyright of this thesis rests with the author. No quotation from it should be published without his prior written consent, and information derived from it should be acknowledged.

TABLE OF CONTENTS

Chapter 1	Introductory remarks	
1.A	Introduction	1
1.B	Rhum geology - general	1
1.B.1	Lewisian rocks	3
1.B.2	Torrisonian rocks	3
1.B.3	Mesozoic rocks	3
1.B.4	Early Tertiary rocks	4
1.C	Previous work on the LELS	6
1.D	The present work	7
Chapter 2	Marginal Relationships	
2.A	Torrisonian rocks	8
2.B	Morphology of the margin	10
2.C	Field relations	10
2.D	Petrography	16
2.D.1	Basic rocks	16
2.D.2	Intermediate rocks	22
2.D.3	Acid rocks	22
2.E	Conclusions	22
Chapter 3	The Layered Rocks	
3.A	Sub-division of the LELS	24
3.B	Field relations	27
3.B.1	Unit 1	27
3.B.2	Unit 2	28
3.B.3	Unit 3	32
3.B.4	Unit 4	35
3.B.5	Unit 5	37
3.B.6	Gabbro plugs and sheets	41
3.C	Petrography	41
3.C.1	Peridotites	41
3.C.2	Peridotite/allivalite contacts	54
3.C.3	Allivalites	61
3.C.4	Gabbro plugs and sheets	72
3.D	Conclusions	74
Chapter 4	Bulk-rock chemistry	
4.A	The Marginal Suite	76
4.B	Gabbro plugs and sheets	84
4.C	The layered rocks	86
4.C.1	Cluster analysis	86

4.C.2	CIPW norms	92
4.D	Conclusions	92
Chapter 5	Mineral Chemistry	
5.A	The layered rocks	93
5.A.1	Olivines	93
5.A.2	Clinopyroxenes	99
5.A.3	Olivine/clinopyroxene relationships	105
5.A.4	Plagioclases	107
5.A.5	Orthopyroxenes	107
5.A.6	Sulphides	109
5.A.7	Kaersutites	111
5.A.8	Hydrous minerals in allivalites	113
5.B	Some aspects of xenolith mineral chemistry	113
5.B.1	Pigeonite	113
5.B.2	Fassaite-bearing xenoliths	115
5.C	Conclusions	118
Chapter 6	Cryptic Variation	
6.A	General	120
6.B	Discussion	122
6.C	Variation in clinopyroxene minor elements	132
6.C.1	Aluminium	132
6.C.2	Titanium	132
6.C.3	Chromium	132
6.D	Conclusions	134
Chapter 7	Discussion and conclusions	
7.A	The formation of the LELS	135
7.A.1	Types of small-scale layering	136
7.A.2	The origins of small-scale layering	137
7.B	Parental magmas, contamination and evolution.	140
7.C	Fingers and replacement	145
7.C.1	Discussion	146
7.D	Evolution of the ultrabasic complex.	148

7.E	Emplacement of the complex	149
BIBLIOGRAPHY		150
ACKNOWLEDGEMENTS		158
APPENDICES		
1.	XRF analyses of international standards.	159
2.	XRF analyses of Rhum samples	164
3.	Sample locations	175
4.	Published articles arising from this work.	178

FIGURES

Fig. 1.1	Sketch map of Rhum, showing the general geology of the island.	2
Fig 2.1	Geology of the LELS and adjacent rocks.	9
Fig 2.2	Partially melted Rubha na Roine Grit.	11
Fig 2.3	Basic dyke breaking up in partially melted Bagh na h-Uamha shale.	11
Fig 2.4	Schematic diagram showing marginal relationships in the Cnapan Breaca/ Allt Mhor na h-Uamha area.	14
Fig 2.5	Skeletal olivine crystals in variolitic -textured picrite.	17
Fig 2.6	Skeletal olivine crystals in variolitic gabbro.	17
Fig 2.7	Olivine gabbro (cumulate?).	19
Fig 2.8	Gabbro from Marginal Suite.	19
Fig 2.9	Analcime-rich mesostasis.	20
Fig 2.10	Clinopyroxene altering to secondary green fibrous amphibole and biotite.	20
Fig 2.11	Inverted tridymite crystals in melted Rubha na Roine Grit.	21
Fig 2.12	Microgranite with clear quartz, turbid alkali feldspar, biotite and magnetite.	21
Fig 3.1	Revised map of the LELS, and stratigraphic section.	25
Fig 3.2	Finger structures cutting low-angle slump folds in unit 2 allivalite.	29
Fig 3.3	Upper part of unit 2 allivalite heavily disrupted by finger structures.	29
Fig 3.4	"Inverted mushroom" style load structures in unit 2 allivalite.	31
Fig 3.5.	Slumped and mixed peridotite/allivalite in the lower part of unit 3 allivalite.	31
Fig 3.6	Fine-grained plagioclase rich layer in the lower part of unit 3 allivalite.	33
Fig 3.7	Deformed "xenolith" of troctolitic allivalite in clinopyroxene-rich	

	allivalite of unit 4.	33
Fig 3.8	Gradational contact between unit 5 peridotite and allivalite.	38
Fig 3.9	Layering in unit 5 allivalite.	38
Fig 3.10	Allivalite layer occurring in the lower part of unit 6 peridotite.	39
Fig 3.11	Disappearance of unit 6 allivalite through fingering.	39
Fig 3.12	View looking down on fingers in unit 6.	42
Fig 3.13.	Feldspathic peridotite with low density of olivine crystals.	42
Fig 3.14	Peridotite from unit 5.	44
Fig 3.15	Peridotite from unit 5.	44
Fig 3.16	Peridotite from unit 5.	46
Fig 3.17	Peridotite from unit 2.	46
Fig 3.18	Intersecting laminations in peridotite	47
Fig 3.19	Preferential concentration of chrome-spinel crystals on the upper surfaces of olivines.	47
Fig 3.20	Hydrous minerals in peridotite from unit 2.	50
Fig 3.21	Interstitial orthopyroxene crystal being made over to hornblende etc.	50
Fig 3.22	Pyroxene-syenite vein from unit 1 peridotite.	52
Fig 3.23	Teschenitic vein from unit 2/3 peridotite.	52
Fig 3.24	Composite sulphide bleb from unit 1.	53
Fig 3.25	Magnetite/sulphide intergrowth.	53
Fig 3.26	Chrome-spinel layer from the lower part of unit 3.	55
Fig 3.27	Mixed peridotite/allivalite layer.	55
Fig 3.28	Deformed peridotite/allivalite contact	56
Fig 3.29	Finger sectioned at 90 ^o to its axis.	56
Fig 3.30	Finger from unit 8 allivalite.	57
Fig 3.31	Gradational peridotite/allivalite contact.	59
Fig 3.32	Gradational allivalite/peridotite contact.	60

Fig 3.33	Allivalite from unit 5.	62
Fig 3.34	Contact between coarse and fine grained layers in unit 3 allivalite.	62
Fig 3.35	Clinozoisite-rich "clot" in allivalite	64
Fig 3.36	Small dispersed sulphide blebs.	64
Fig 3.37	Exsolution lamellae of pentlandite in large pyrrhotite grain.	66
Fig 3.38	Composite sulphide bleb from unit 1.	66
Fig 3.39	Beerbachite xenolith from unit 5.	68
Fig 3.40	Beerbachite xenolith from unit 4 with "clots" of calc-silicate minerals.	68
Fig 3.41	Outer margin of fassaite zone from a calc-silicate clot.	71
Fig 3.42	Large (cumulus?) hypersthene crystal.	71
Fig 3.43	Inverted pigeonite oikocryst.	73
Fig 3.44	Gabbro xenolith from unit 5 allivalite	73
Fig 4.1a	Ba vs Cr plot for the Marginal Suite.	77
Fig 4.1b	Ba vs K_2O plot for the Marginal Suite.	77
Fig 4.2a	MgO vs P_2O_5 plot for the Marginal Suite.	79
Fig 4.2b	MgO vs TiO_2 plot for the Marginal Suite.	79
Fig 4.3	Trace-element compositions of various Torridonian sediments and felsite.	81
Fig 4.4a,b	Trace element compositions of the Marginal Suite.	83
Fig 4.5	MgO vs Zn plot for the Marginal Suite	85
Fig 4.6	Trace element compositions of gabbro plugs and sheets.	85
Fig 4.7	MgO vs CaO plot for the LELS rocks.	87
Fig 4.8	MgO vs P_2O_5 plot for the LELS rocks.	87
Fig 4.9	Dendrogram for the LELS allivalites, "sheetrocks", and gabbro plugs and sheets.	88
Fig 4.10	Normative compositions of LELS rocks.	91
Fig 5.1	Olivine Fo-NiO relationships for U1.	94
Fig 5.2a	Fo content vs MnO for U1 olivines.	97
Fig 5.2b	Fo content vs CaO for U1 olivines.	97
Fig 5.3	Clinopyroxene compositions for LELS rocks.	98

Fig 5.4a	MGN, vs Al per 6 oxygens for LELS clinopyroxenes.	101
Fig 5.4b	Al in tetrahedral sites vs MGN for LELS clinopyroxenes.	101
Fig 5.5	MGN vs Ti per 6 oxygens for LELS clinopyroxenes.	102
Fig 5.6	MGN vs Cr per 6 oxygens for LELS clinopyroxenes.	102
Fig 5.7	MGN vs Na per 6 oxygens for LELS clinopyroxenes.	104
Fig 5.8	Relationship between olivine Fo content and Mgn of clinopyroxenes.	104
Fig 5.9	Relationship between olivine Fo content and Mgn of orthopyroxenes.	108
Fig 5.10	Compositions of epidotes from sample U3A2.	108
Fig 5.11	Host-lamellae relationship in inverted pigeonite.	114
Fig 5.12	Pyroxene compositions in the zone surrounding a garnet/diopside clot.	117
Fig 6.1.	Variation of olivine Fo content and clinopyroxene Mgn with height.	121
Fig 6.2	Variation in LFo-LMgn with height.	124
Fig 6.3	Density variation with MgO content of basic liquids.	128
Fig 6.4	Variation of clinopyroxene total Al and Al(iv) contents with height.	131
Fig 6.5	Variation of clinopyroxene Ti and Cr contents with height.	133

ADDENDUM

An 1:10000 geological map of eastern Rhum, based on the fieldwork of the present author, A.R. Butcher, J.A. Volker, and J. McClurg is enclosed at the back of this volume. It is based on an original prepared by A.R. Butcher.

Electron microprobe analyses obtained during the course of this work are deposited with the Department of Geological Sciences, University of Durham.

TABLES

Table 4.1 Analyses of possible acid end-members for the hybrids of eastern Rhum.	80
Table 5.1 Ranges in olivine composition from different parts of the Rhum complex.	93
Table 5.2 Liquid Fe/Mg ratios calculated from olivines and clinopyroxenes in selected LELS rocks.	106
Table 5.3 Analyses of various sulphide phases from Unit 1.	110
Table 5.4 Selected analyses of minor phases from the LELS.	112
Table 5.5 Analyses of various phases associated with calc-silicate "clots" in beerbachites.	116
Table 7.1 Various proposed parental magmas.	141

CHAPTER ONE

1.A. INTRODUCTION

The island of Rhum is remarkable among the Tertiary volcanic centres of western Scotland for the extensive development of layered ultrabasic rocks. These rocks outcrop principally in central and eastern Rhum; to the west is an older Tertiary granophyre, while the northern and extreme eastern parts of the island are made of Precambrian clastic sediments.

The ultrabasic rocks have recently been divided into three lithostratigraphic units: the Western and Eastern Layered Series, and the Central Series (fig 1.1)

The Western Layered Series (WLS), first defined by Wadsworth (1961) and modified by McClurg (1982), is almost wholly comprised of crescumulate rocks. At its base, on the western side of Harris Bay, these are olivine-plagioclase crescumulates, while further up the sequence olivine-rich rocks are dominant.

The Central Series (CS), defined by McClurg (1982) and Volker (1983) has a transgressive contact with the WLS and post-dates it. It forms a lobate mass, elongated north-south, comprising a wide variety of ultrabasic cumulates and intrusion breccias. Layering is only locally well developed and is often highly deformed. The CS also shows a transgressive relationship to the Eastern Layered Series.

The Eastern layered Series (ELS) was first defined by Brown (1956) although McClurg (1982) and Volker (1983) were the first to map its western boundaries. The ELS is characterised by regular, large-scale rhythmic layering, with alternating layers of olivine- and olivine-plagioclase cumulates, the latter known locally as allivalites (Harker, 1908).

This work is concerned with the lower parts of the ELS, hereafter known as the LELS, and with the eastern marginal relationships of the ultrabasic mass.

1.B. RHUM GEOLOGY- GENERAL

In order that the LELS rocks can be sensibly



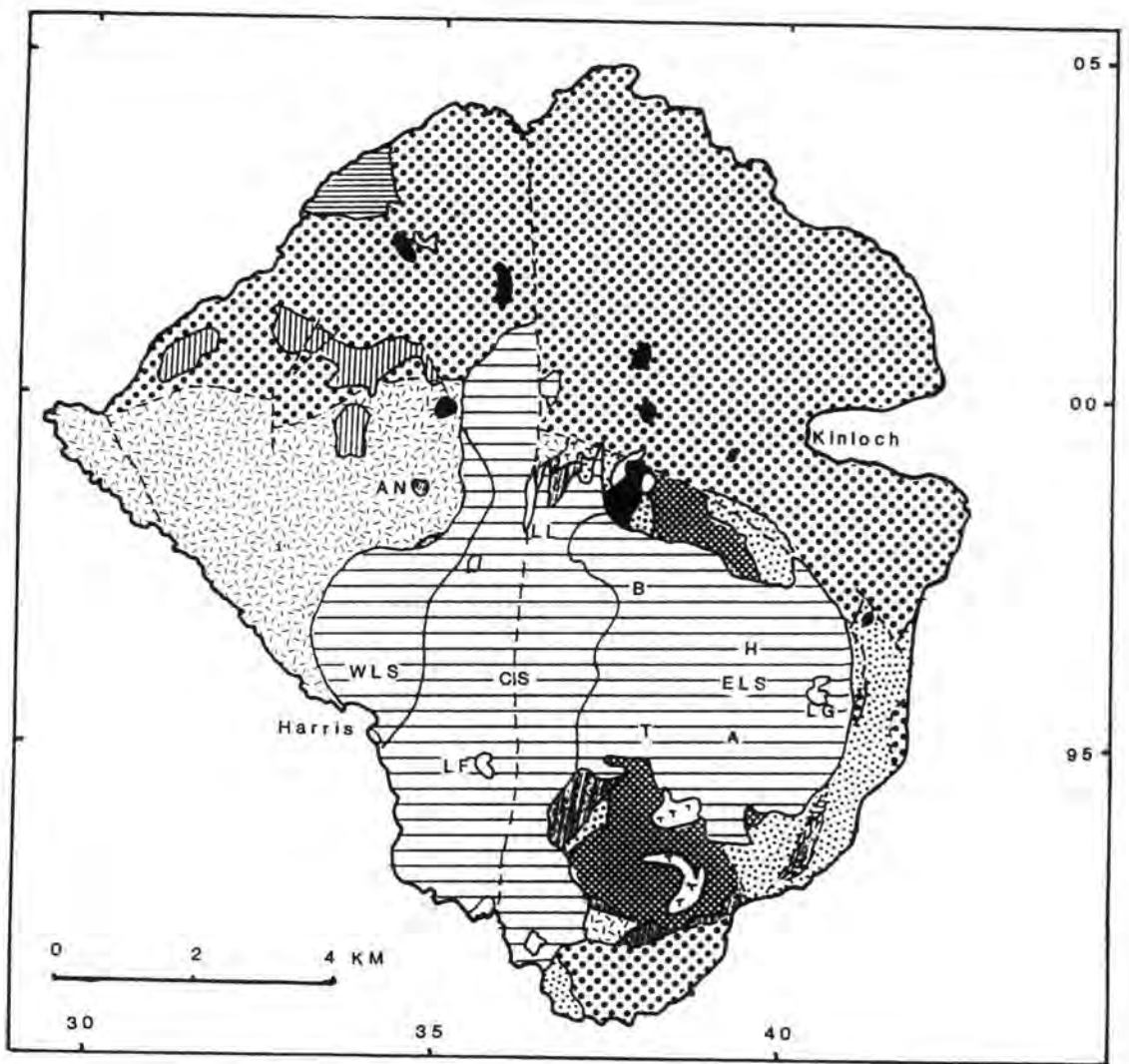


Fig. 1.1 Sketch map of Rhum, showing the general geology of the island (modified from Emeleus et al., 1985).

discussed, it is necessary to put them in their geological context; this requires an outline of the general geology of the island. The following account refers to fig. 1.1.

1.B.1 Lewisian Rocks

Lewisian gneisses occur at a number of places around the island. However, all occurrences are within the ring fractures which surround the central complex. This clearly indicates an episode of central uplift (Bailey, 1945). In a few localities the gneisses can be seen in unconformable contact with basal Torridonian sediments (Dunham and Emeleus, 1967). Gneisses form the roof rocks to the Western Granophyre, on the summit and eastern slopes of Ard Nev.

1.B.2 Torridonian Rocks

The sandstones of northern and eastern Rhum were early recognised as Torridonian in age (eg Geikie, 1897). Black and Welsh (1961) subdivided the sequence, and correlated it with the Diabeg group of the Scottish mainland. The basal group of coarse sandstones only occurs within the ring fracture system. Away from the central complex the Torridonian sediments have a gentle regional dip to the west or north-west.

1.B.3 Mesozoic Rocks

Outcrops of Triassic sediments with conodonts occur in north-west Rhum (Bailey, 1945), probably representing the eastern margin of the Minch basin.

Slivers of limestone have long been known in eastern Rhum, near the margin of the ultrabasic complex (Geikie, 1897; Hughes, 1960). Although considered Lewisian by Hughes (1960), later work produced a few fossils of Mesozoic age (Dunham and Emeleus, 1967). Recent work by Smith (1985) has shown these limestones to be associated with sandstones and shales, and that they are probably equivalent to the Jurassic Broadford Beds of Skye and Raasay. The sequence occurs as a fault slice in the ring fracture zone, just inside another

5

fault slice containing Lewisian gneiss. While the distribution of gneiss provides evidence for central uplift, the presence of these rocks, stratigraphically higher than anything else seen in the pre-Tertiary of Rhum, is clear evidence for central downfaulting (Emeleus et al, 1985).

1.B.4 Early Tertiary Rocks

Basaltic dykes occur right through the period of Tertiary activity on Rhum; these are not discussed here. A thorough account of recent ideas on early Tertiary activity can be found in Emeleus et al, (1985), on which the following account is largely based.

(a) Explosion Breccias

The first major signs of Tertiary activity on Rhum are seen in explosion breccias (but see section (d)). These occur only within the ring fractures around the central complex, although they are probably related to a subsidence event along one of these faults, and it is rather difficult to disentangle the effects of tectonic and explosive brecciation. They are mostly made of shattered basal Torridonian rocks, although gneiss and gabbro are also found. This explosive volcanism is clearly a near-surface phenomenon.

(b) Felsites and Tuffisites

Intimately associated with the explosion breccias, and cutting them, are felsite masses and tuffisite dykes. At least some of the felsites are probably ignimbrites formed subaerially (Williams, 1985).

(c) Granophyres

A large mass of granophyre occurs in western Rhum. Its contacts with the Torridonian sediments to the north are faulted. This is presumably a continuation of one of the ring fractures seen in the eastern part of the complex, but correlation is difficult due to poor exposure of the faults, later movement on the north-south Long Loch fault, and the intrusion of the ultrabasic complex across the line of the ring fractures. Other small granophyres occur near the north end of Long Loch, and at Papadil.

(d) Basalts

Basalts occur in two distinct settings in Rhum. A few flows of basalt, hawaiite and icelandite occur in western Rhum, infilling Tertiary river valleys cut into the granophyre and the Torridonian sediments. Conglomerates under these flows include clasts of peridotite, allivalite and other rocks from the central complex. These lavas are thus a late feature, following erosion and unroofing of the central complex (Black, 1952; Emeleus, 1985).

Basalts also occur with the Mesozoic sediments of eastern Rhum (Emeleus and Forster, 1979; Smith, 1985). They are highly sheared and altered, with zeolites and epidote in amygdales. Smith (1985) states that they are in unfaulted, unconformable contact with the Jurassic rocks. They are therefore much older than the basalts of western Rhum, and if the explosion breccias and felsites really are surface products, they must pre-date them as well, having been eroded off by the time the explosive volcanism occurred. They may be the only remnants of pre-Central Complex Tertiary plateau basalt activity left on Rhum. Such activity might be expected, as most of the other Tertiary centres of western Scotland have plateau basalts formed before the onset of central activity.

(5) The Ultrabasic Complex

The ultrabasic rocks were first examined in detail by Harker (1908). He regarded them as having been produced by successive, more or less conformable injections of peridotite and allivalite magmas. Wager and Brown (1951) recognised similarities with the rocks of Skaergaard, and proposed a cumulate origin for the layered rocks. Subsequent work by Brown (1956) and Wadsworth (1961) supported this idea. Both stressed the role of periodic replenishment in the Rhum magma chamber. Rhum was used as one of the type examples in the development of cumulate terminology (Wager, Brown and Wadsworth, 1960).

Harker (1908) regarded the ultrabasic rocks as a laccolith, more or less sitting on top of a Palaeozoic

thrust. Bailey (1945) reinterpreted the thrust as a ring fault. Brown (1956) agreed with Bailey that there had been uplift along a ring fault, but that a second, later inner ring fault had brought up the layered rocks, in a semi-solid state, this later ring fault now being filled by a gabbroic ring dyke. Dunham (1962, 1964) examined the marginal relationships around Meall Breac and Cnapan Breaca and found intrusion breccias and hybrid rocks developed between the marginal gabbro ring dyke and the country rocks.

This "uplift-with-ring-dyke" model has recently been questioned (Faithfull, 1985; Emeleus et al, 1985). Many contacts between the ultrabasic rocks and the country rocks are not steeply inclined; low-angle contacts are found with the Western Granophyre on Ard Nev and Ard Mheall, and with Torridonian and early Tertiary rocks on Cnapan Breaca and Beinn nan Stac. It has been suggested that some or all of these contacts may be unfaulted igneous contacts (this work; Emeleus et al 1985; R. Greenwood, pers comm 1985), implying that what had previously been regarded as a later gabbro intrusion may be, at least in part, the marginal facies of the ultrabasic magma chamber.

Brown (1956) and Wadsworth (1961) could find little or no cryptic variation in the Rhum cumulates; however more recent work (Dunham and Wadsworth, 1978) has confirmed its presence on a rather limited scale, in both the ELS and the WLS.

1.C. PREVIOUS WORK ON THE LELS

Harker (1908) noted that the layered rocks low down on the eastern slopes of Hallival and Askival differed from those higher up. The lower rocks had less well developed layering and lamination, and they were mineralogically more complex, rarely showing the mono- or bi-minerallic modes of the upper rocks. Accordingly, he mapped the lower part of the layered sequence as a separate "eucrite" intrusion.

Brown (1956) noted the same differences, but instead interpreted them in terms of interstitial liquid

retention in the lower rocks, in contrast to the upper ELS where adcumulus growth had displaced the melt.

Since then, no systematic work has been carried out on the LELS, although various studies on isolated topics have been made. Such works will be referred to in the text as and when appropriate.

1.D. THE PRESENT WORK

The present work is based on fieldwork carried out during 1980, 1981 and 1982. Remapping of the LELS and its margins was undertaken as existing maps (Brown, 1956) proved to be lacking in the necessary detail. Mapping was carried out on aerial photographs and transferred to the 1:10000 topographic map produced by Glasgow University. During the course of this work it became apparent that much of what had been mapped as intrusive gabbro cutting the layered rocks, was itself layered and shared many features of the LELS allivalites. In addition the LELS proved to exhibit marked lithological changes along strike. Studies of bulk-rock and mineral geochemistry were undertaken to examine the extent of cryptic variation in the cumulates, and to examine the relationships between the various gabbros and the layered rocks. In conjunction with other contemporary workers on Rhum, considerable evidence has been built up supporting an important role for post-cumulus processes in shaping the chemistry and modal mineralogy of the layered rocks now seen.

The margins of the complex were also re-examined. The "Marginal Gabbro" ring-dyke of Brown (1956) is reinterpreted as a complex zone of hybrids and gabbros, which may represent the original margins to the ultrabasic magma chamber. In a number of localities fragments of the roof are preserved.

CHAPTER TWO

MARGINAL RELATIONSHIPS

The layered rocks of eastern Rhum are bounded to the east by a zone of gabbros and hybrid rocks, hereafter referred to as the Marginal Suite, largely occupying the line of a previously existing ring fracture. The country rocks outside this zone are mainly Torridonian sediments. These also occur locally within the ring fracture, where they are extensively cut by early Tertiary acid intrusive rocks and basaltic dykes.

This chapter deals with the igneous rocks of the Marginal Suite, and the country rocks immediately adjacent (fig 2.1).

2.A. TORRIDONIAN ROCKS

As mentioned above, the complex is bounded to the east by a series of Torridonian sediments with a regional dip of about 10° to 20° to the north-west. Thus as the contact is followed to the east and south, the complex abuts against successively lower members of the sequence.

The Torridonian sediments of Rhum have been divided (Black and Welsh; 1961) into 5 units, of which only the lowest three occur in the area mapped. The Basal Grit occurs only within the ring fractures, where it forms the area around Cnapan Breaca, overlying the layered rocks. At this locality the rocks are tightly folded and very steeply dipping or vertical (Dunham, 1968). They comprise coarse gritty sandstones with rare shaly or silty intercalations. Further outcrops of this sandy facies occur in the Allt nam Ba valley. Here they are neither so tightly folded nor steeply dipping. Above the basal grits which are about 100m thick, lies a thick (400m+) sequence of dominantly silty or shaly clastic sediments known as the Bagh na h-Uamha shale. This is found both within the ring fractures, where it is seen to overlie the basal grit, and outside, where it is the lowest exposed member of the Torridonian. Outside, and

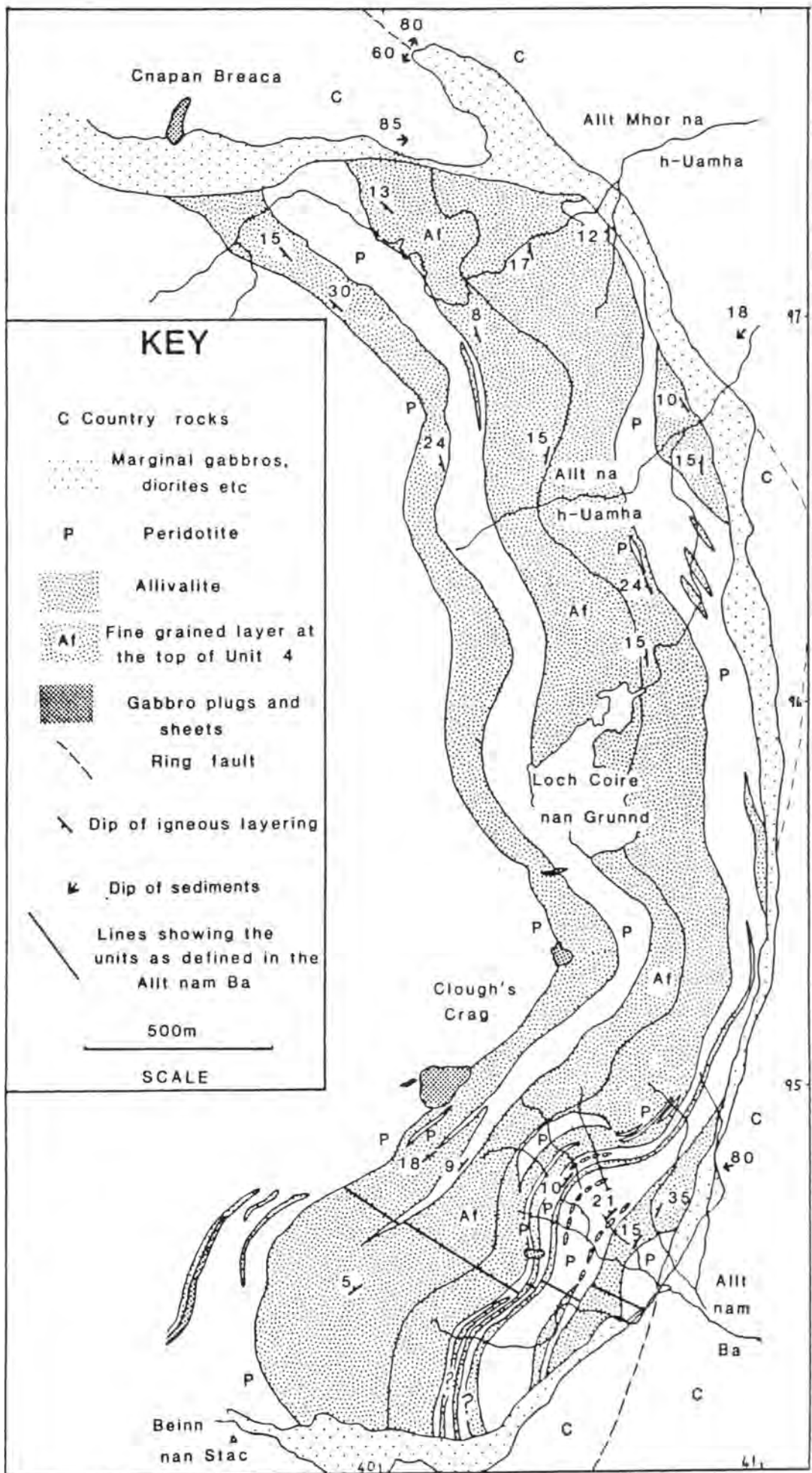


Fig 2.1 Geology of the LELS and adjacent rocks.

away from the ring faults the Torridonian rocks have a gentle regional dip to the north-west, and hence along most of the eastern contact of the complex these shaly rocks comprise the country rocks to the intrusion.

Above the shale lies the Rubha na Roine grit. This comprises some 1200m of pebbly grits and arkosic sandstones of rather different mineralogy to the basal grits (Black and Welsh, 1961). The distribution of the Rubha na Roine grit and the Bagh na h-Uamha shale along the eastern contact of the intrusion is complicated by numerous small faults, some of which (e.g. at NM410964) are probably associated with the ring faulting, while others may be much earlier, perhaps associated with the thrusting at Welshman's Rock (Emeleus, 1980).

2.B. MORPHOLOGY OF THE MARGIN

Where the Marginal Suite is roughly coincident with the trace of the ring fracture, between the Allt nam Ba and Cnapan Breaca, it forms a zone between 0-140m wide although it is usually 10-100m across. Over this area the zone occupied by the Marginal Suite is approximately vertical. Although often deeply weathered, the rocks show no signs of shearing or faulting which might be related to movement on the ring fracture, and in places the Marginal Suite appears to cut the ring fault (NM40989675). It thus post-dates movement on the ring fractures.

Where Torridonian and early Tertiary rocks occur within the ring fractures, they overlie rocks of the Marginal Suite. Thus, at Cnapan Breaca, the contact between the Marginal Suite and the older rocks dips about 10° to the NE at the eastern end, and about 40° to the N at the W end. At Beinn nan Stac the contact dips at about 15° to the SE. These low-angle contacts appear to pass laterally, and downwards into the vertical contacts mentioned previously.

2.C. FIELD RELATIONS

Torridonian sediments show signs of thermal

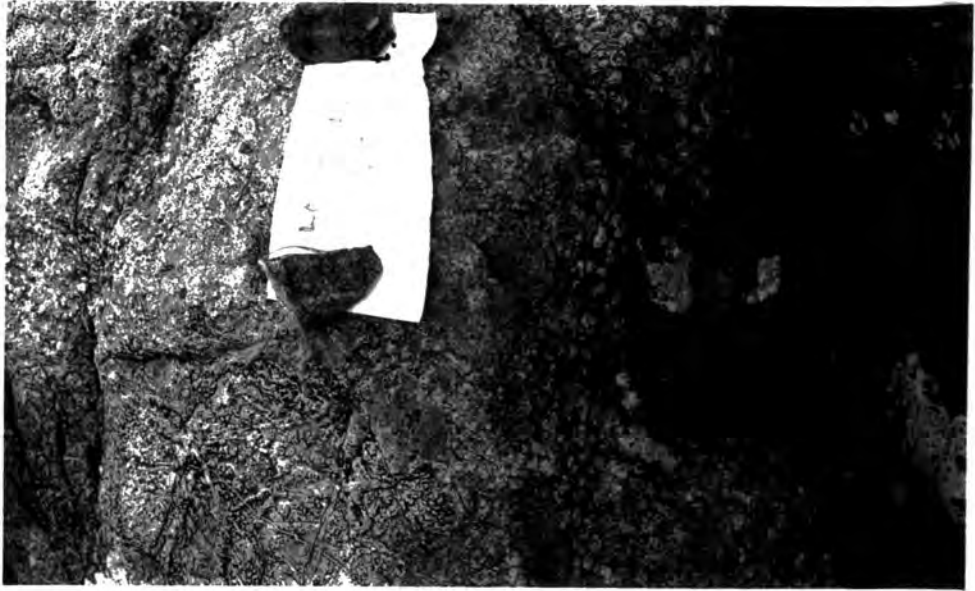


Fig 2.2 Partially melted Rubha na Roine Grit, showing spherulitic devitrification texture. Loc 78. NM40649731.



Fig 2.3 Basic dyke breaking up in partially melted Bagh na h-Uamha shale. Note flow banding of melted sediment. Locality 169. NM40989638.

metamorphism for some distance from the margin of the central complex. Bleaching of the normally pink Rubha na Roine Grits is developed in a zone several hundred metres wide. Closer to the complex the sediments show signs of partial melting with the development of small veins and segregations of quartzo-feldspathic material. This generally occurs within 100m or so of the Marginal Suite. These veins are noticeably more common in the Rubha na Roine Grits than in the Bagh na h-Uamha shales, as might be expected from the lower solidus temperatures of arkosic assemblages. Within 10-20m of the Marginal Suite melting is often very extensive: in the sandy facies a spherulitic texture (Fig 2.2) indicates the presence of devitrified glass, and in the shaly rocks a swirling flow banding is often developed suggesting that the rocks were very mobile. Further evidence for this can be seen at NM40989638, where remobilised Bagh na h-Uamha shales contain dykes which break up into trails of blocks (Fig 2.3) towards the Marginal Suite. At this same locality the melted sediments include a block of coarse-grained (cumulate? -see section D) olivine gabbro perhaps derived from the layered rocks. Similiar occurrences of peridotite blocks are seen on the NNE flank of Ainsival (C.H. Emeleus, pers comm).

The Torridonian rocks are variably deformed in the zone around the central complex. Much of this deformation may be associated with early movements on the ring fractures rather than the emplacement of the ultrabasic rocks (Emeleus et al, 1985). At the northern end of the area, around Cnapan Breaca, the sediments dip steeply away from the ring fracture; around the Allt Mhor na h-Uamha the dips are variable and hard to determine where the rocks are melted. South of the Allt na h-Uamha a steep anticline running N-S is preserved within a fault (ring fracture? - Emeleus et al, 1985). To the south of this dips tend to increase in towards the central complex, up to 80° in places.

In this inner melted zone, and particularly in sandy or arkosic rocks, veins of intrusion breccia with fragments of fine-grained basic material in an acid

groundmass are locally common. In some cases small dykes with chilled margins have caused extensive melting around their contacts, and have been back-veined and hybridised, implying that the sediments were very hot at the time of intrusion.

Intrusion breccias generally form the edge of the Marginal Suite against the sediments, although again they tend to be better developed against sandy rocks than shaly ones. At Meall Breac the breccia includes a block of peridotite (C.H. Emeleus, pers comm), although normally they consist of fine-grained basalt and gabbro fragments set in a matrix of melted Torridonian sediments. Hybrid rocks are common in small quantities associated with these breccias in the outer parts of the Marginal Suite. In places however, more extensive bodies of hybrids occur egs NM40879472, NM40629438. These seem often to have behaved as discrete intrusive bodies, injecting back into the gabbros of the inner marginal zone, or out into the country rocks. Locally chilled contacts can be seen between different bodies of hybrids, a good example being at NM40339746 where two distinct diorites can be seen in contact.

Large masses of hybrid rocks are formed under the low-angle contacts at Cnapan Breaca and Beinn nan Stac. At the latter locality, Bagh na h-Uamha shales and Tertiary felsite are underlain by a zone of melted material with the development of acid and intermediate hybrids. In places (NM39599418) underlying these a fine-grained basic rock can be seen chilled against the hybrids. This rock coarsens rapidly away from the contact, with a strong variolitic texture developed at right angles to the contact. Given the position of this dolerite, overlying layered rocks, it is possible that it may represent the chilled margin of the ultrabasic intrusion, but unfortunately the relationship between the chilled rock and the layered rocks cannot be determined due to lack of exposure. It is worth noting that a similiar situation occurs at NM38259460, in upper Glen Dibidil where felsite is underlain by a zone of hybrids, which in turn are underlain by a chilled

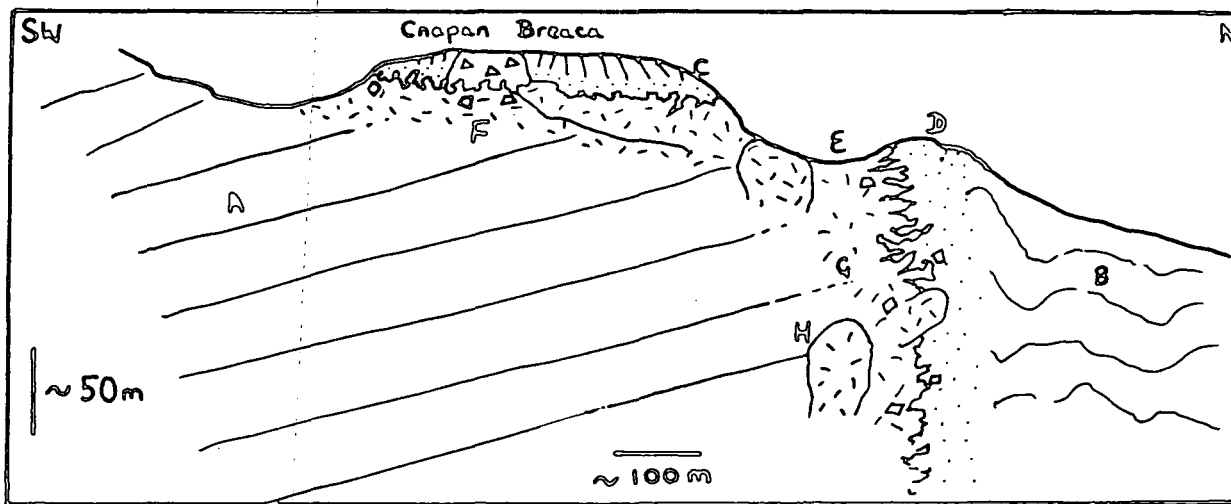


Fig 2.4 Schematic diagram showing marginal relationships in the Cnapan Breaca/ Allt Mhor na h-Uamha area. Key as follows:

- A Rocks of the Eastern Layered Series.
- B Rubha na Roine Grits (Torridonian).
- C Basal Grits (Torridonian) cut by explosion breccias and felsites (early Tertiary).
- D Partially or largely melted Rubha na Roine Grits. May include xenoliths of basalt, gabbro, or cumulates.
- E Gabbros and diorites, locally chilled against one another, cut by acid rheomorphic veins. Intrusion breccia at vertical outer margin.
- F Nearly flat-lying zone of gabbro and hybrid bodies with intrusion breccia at upper margin.
- G Gradational contacts of layered rocks with Marginal Suite.
- H Layered rocks sharply cut by Marginal Suite gabbro.

variolitic-textured gabbro rich in olivine. Not far below layered gabbros (allivalites?) can be seen. A schematic representation of the situation under Cnapan Breaca and the area to the south is shown in Fig 2.4.

Generally, over most of its extent in eastern Rhum, the marginal suite is very badly exposed, weathering to a lush green trench, although the more dioritic and acid rocks are often rather more resistant to weathering. Good exposures are found in the Allt na h-Uamha, where the river has cut through deeply weathered gabbro. Some of the freshest gabbro specimens have come from the cores of weathered gabbro spheroids at this locality.

It is often difficult to distinguish the gabbroic rocks of the marginal suite from altered allivalites occurring in places just within the contact. This has led to an overestimate of the extent of the marginal gabbro on the maps of Brown (1956) and Emeleus (1980). The criteria used here to distinguish the two types of rock are : 1. lack of layering structures in the marginal gabbro. 2. lack of good cumulus textures in the marginal rocks, although large olivine phenocrysts are occasionally seen and sub-ophitic texture is often found. 3. clinopyroxene generally has a distinctive granular habit, and often has abundant fine exsolution lamellae of Fe-Ti oxides in the marginal rocks. 4. abundance of green fibrous amphibole in the marginal rocks. 5. Fe-Ti oxides usually occur as large well-formed crystals in the marginal suite. 6. abundance of quartz-rich mesostasis in even quite fresh marginal rocks.

The contacts of the marginal gabbro are not well exposed. While the intrusion breccias and acid hybrids along the outer margin are frequently exposed the main body of mafic and dioritic rocks cannot generally be seen in contact with them. The contact with the layered rocks is even more poorly exposed. In the Allt na h-Uamha a nearly continuous exposure through highly weathered gabbro to allivalite can be seen but sharp contacts are lacking. In the Allt Mhor na h-Uamha

the contact between the layered rocks and the marginal suite is marked by a waterfall, and appears to be fairly sharp. On the north side of Beinn nan Stac peridotite can be seen cut by a coarse gabbro (NM39719412), but whether this gabbro is part of the marginal suite is not certain. Normally the layered rocks are undeformed towards the Marginal Suite, however just north of the Allt nam Ba, the allivalites of Unit 1 develop steep dips to the west (up to 40°) near the margin.

Apart from rheomorphic veins, acid rocks are rare within the main marginal complex. One interesting occurrence is a small vertically zoned body found within gabbro at NM40679722. This consists of coarse grained mafic diorites at the base, grading through fine grained diorites up to mafic microgranite with clots of diorite caught up in it, all over a distance of 2.5m.

Another acid rock, which may or may not be genetically linked to the marginal suite is seen at NM40449661. Here a small composite sheet, 10cm to 30cm thick is seen cutting allivalite, with a dip of 13° to the west. This has felsic margins and a basic core of basalt which is chilled against them. This is only the second recorded example of an acid intrusion cutting the layered series (Volker, 1983), away from the marginal zone.

2.D. PETROGRAPHY OF THE MARGINAL SUITE

There is a wide range of rock types represented in this suite, from granitic and microgranitic facies to olivine bearing gabbros with a wide range of intermediate types. Grain size is also highly variable, although the olivine bearing rocks are often fairly coarse grained (up to 5mm) and the acid varieties rather fine grained.

For the purposes of petrographic description the suite will be divided into three groups: basic types, intermediate types and acid types.

(1) The Basic Rocks.

These are gabbros or dolerites with or without



Fig 2.5 Skeletal olivine crystals in variolitic
-textured picrite. SR209A. NM39709407.



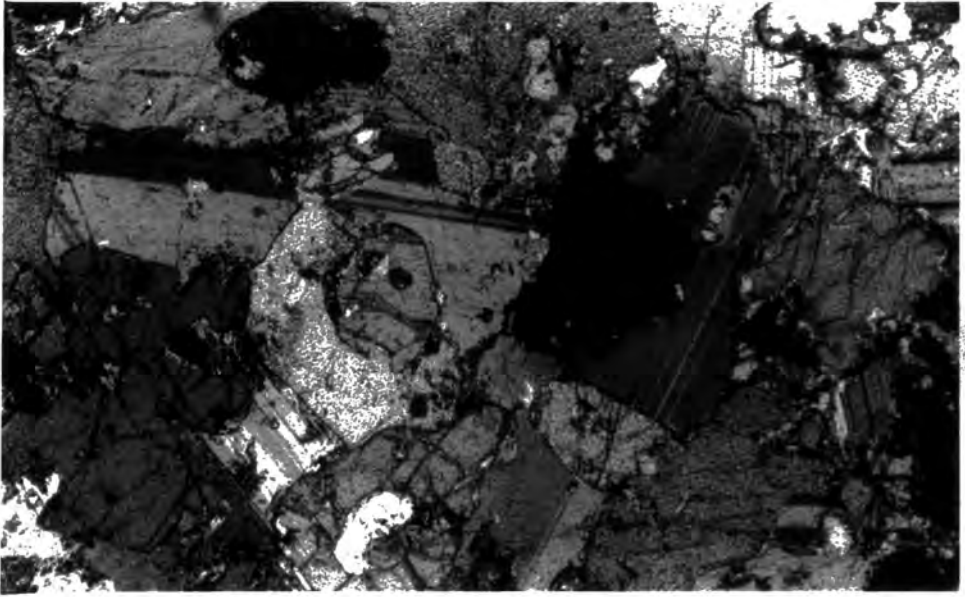
Fig 2.6 Skeletal olivines in variolitic-textured
gabbro. Loc 53A. NM38609549.

olivine. The most basic varieties are olivine-rich gabbros and dolerites, although these are very rare. One such is the fine-grained chilled picrite seen on Beinn nan Stac. The olivines in this rock are skeletal and show good optical zoning (Fig 2.5), presumably due to rapid quenching, with little time for equilibration. This may imply a late age for this picrite, as elsewhere zoning seems to have been removed by slow annealing. A similiar rock (53a), rather coarser in grain size occurs in upper Dibidil (Fig 2.6), although olivine zoning is less marked. Another rock with skeletal olivines occurs as a xenolith within partially melted Bagh n h-Uamha shale (see section B.). In this case the olivines are enclosed in plates of plagioclase and clinopyroxene (Fig 2.7); somewhat similiar rocks occur in places within the LELS.

By far the bulk of the marginal suite is composed of gabbros, often with a little olivine. Commonest are gabbros with subhedral olivines and plagioclases and subophitic augite and a little orthopyroxene (especially rimming olivine). Euhedral or blebby Fe-Ti oxides are common. Amphibole and biotite may be minor phases, rimming oxides or pyroxenes. A little quartz-alkali feldspar-rich mesostasis may occur. Olivine is generally unzoned, at least not visibly in thin section. Clinopyroxene generally shows zoning, often picked out by a clear rim on a core showing exsolution of opaques and plagioclase is usually normally zoned, especially around the mesostasis areas. Where enclosed in clinopyroxene plagioclases may be only weakly zoned.

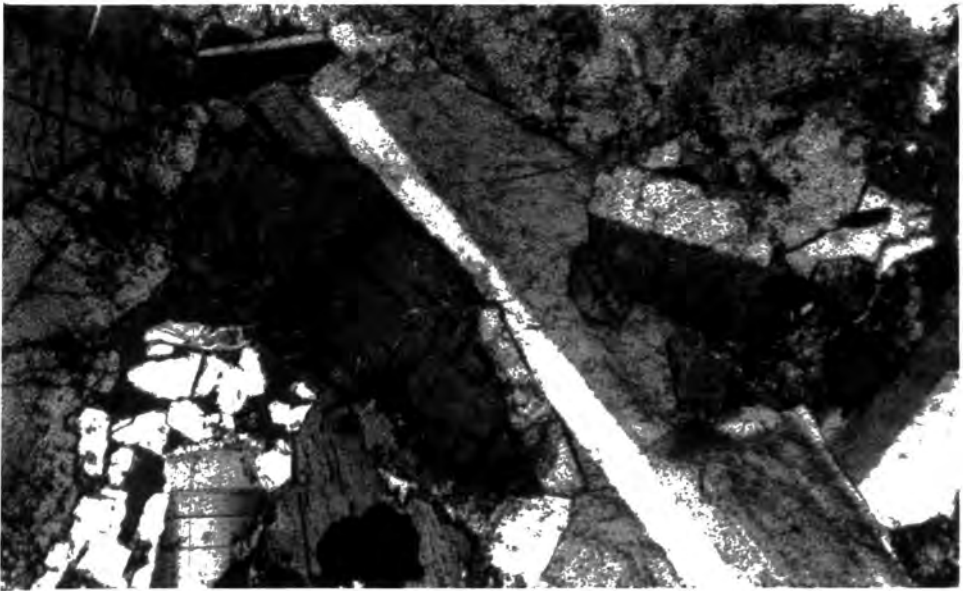
In the olivine-free varieties, the clinopyroxenes normally have a distinctive granular texture (Fig 2.8) and are often clustered with oxide grains. Twinning is common in these granular pyroxenes.

Just NW of the summit of Beinn nan Stac, adjacent to a large hybrid diorite exposure, abundant loose blocks of a spectacular 'black and white' ophitic gabbro occur. This rock contains no olivine, but unusually for the Marginal Suite, shows alkaline



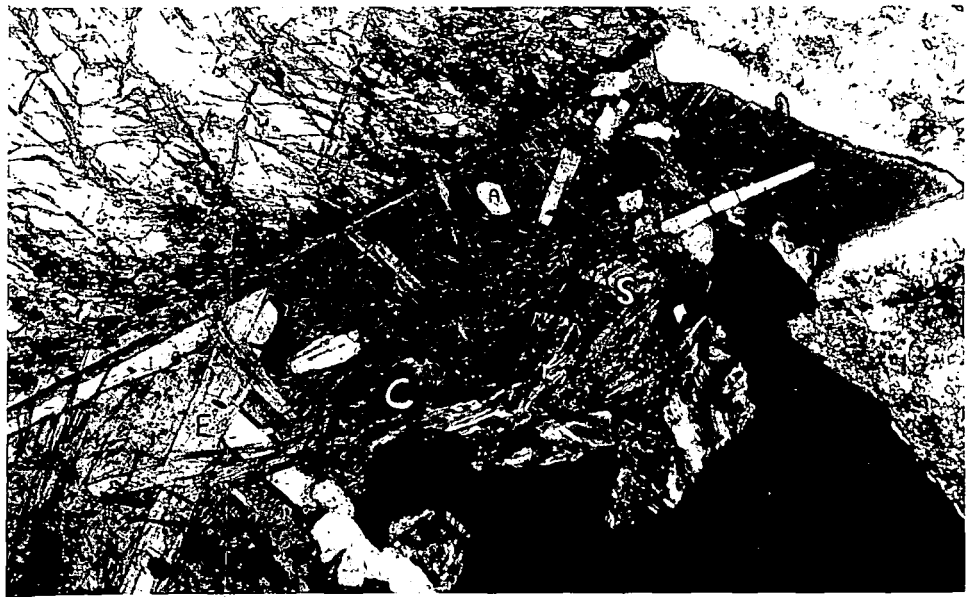
1 mm

Fig 2.7 Olivine gabbro (cumulate?). Note poikilitic plagioclase and pyroxene. Loc 169A. NM40989638.



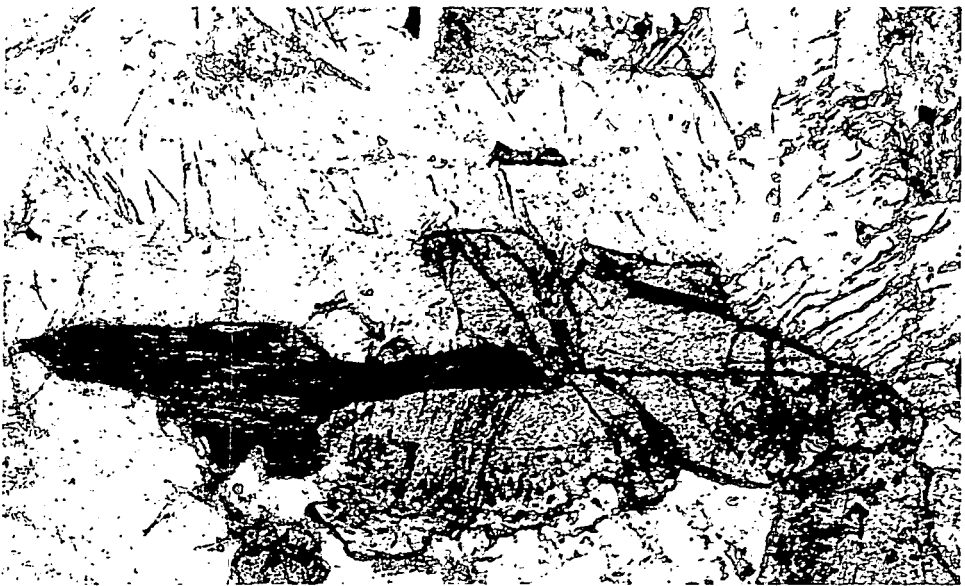
1 mm

Fig 2.8 Gabbro from Marginal Suite. Note habit of clinopyroxene and presence of presence of quartz-rich mesostasis (lower left). Loc 46A. NM39389417.



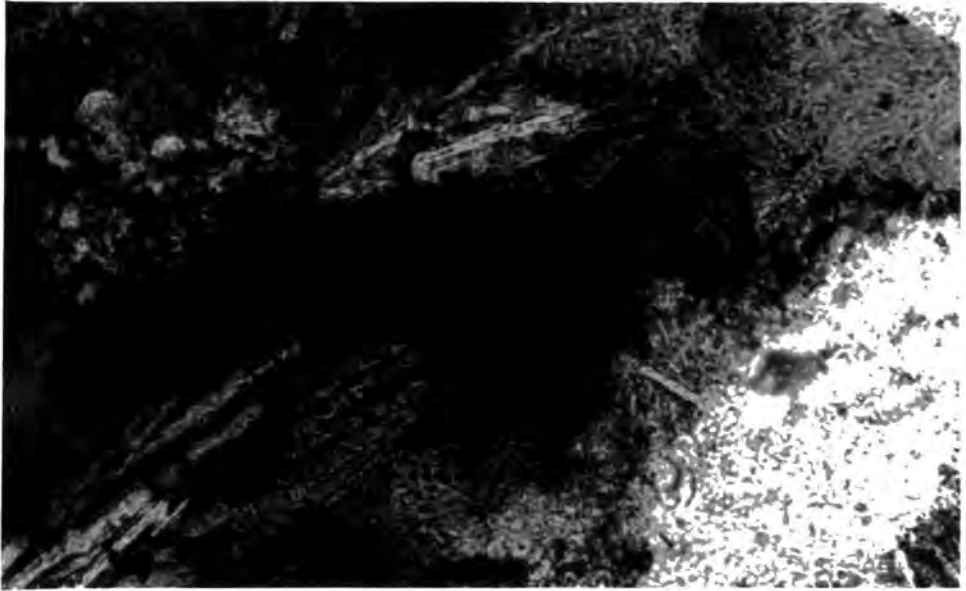
1 mm

Fig 2.9 Analcime-rich mesostasis with apatite (A), sphene (S), epidote (E), and spherulitic chlorite (C). The small dark fibres in the analcime are probably a dark brown amphibole. Loc 47. NM39309419.



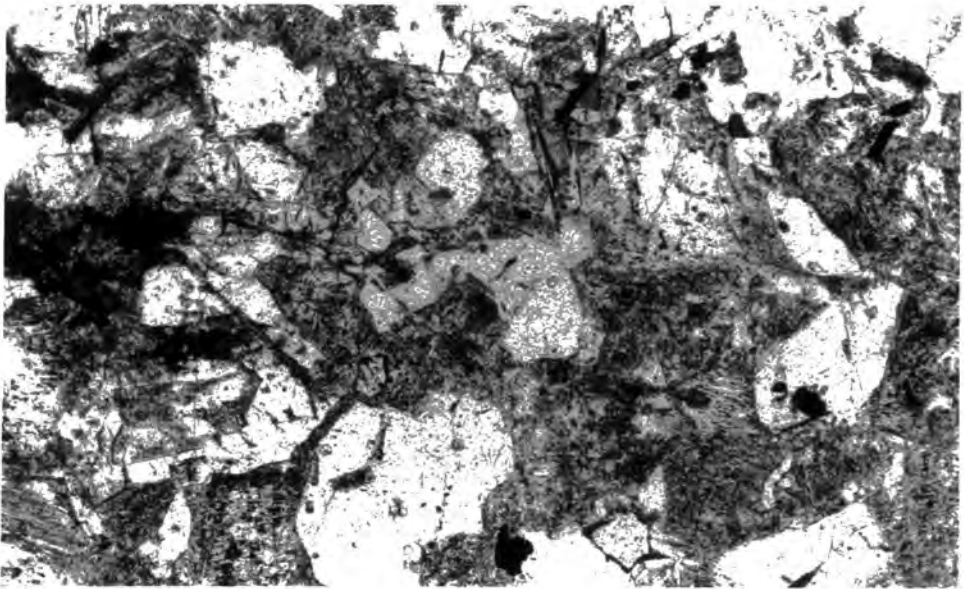
~1mm

Fig 2.10 Clinopyroxene altering to secondary green fibrous amphibole (A) and biotite (B). Note also clear rim of pyroxene on cloudy core. Loc. 175B. NM40909672.



0.1 mm

Fig 2.11 Inverted tridymite crystals in melted Rubha na Roine Grit. Note corroded clastic quartz grain (lower right). Loc 78. NM40649731.



1 mm

Fig 2.12 Microgranite with clear quartz, turbid alkali feldspar, biotite and magnetite. Loc 179B. NM40449661.

affinities. The mesostasis in this rock consists of clear analcime which includes euhedral crystals of sphene, apatite, amphibole, epidote and spherulitic chlorite (Fig 2.9) Almost identical assemblages have been described from teschenite veins near Long Loch (Kitchen, 1985), who argued for a late-magmatic origin for the analcime.

(2) Intermediate Rocks.

The intermediate types are marked by the abundance of amphibole and the lack of olivine. Frequently an acicular habit is marked, particularly in mafic phases - this is rare in the basic varieties. Fresh clinopyroxene is not common although much of the amphibole is clearly secondary after clinopyroxene (Fig 2.10). Orthopyroxene is locally abundant as acicular crystals with strong red-green pleochroism. Subhedral grains of magnetite or ilmenite are very abundant in some rocks but others contain very little.

(3) Acid Rocks.

These appear generally to be slightly contaminated varieties of melted Torridonian or acid Tertiary country rocks.

A frequent occurrence in the partially melted Torridonian rocks is of fine grained gritty rocks with a spherulitic texture, especially well picked out on weathered surfaces (Fig 2.2). In thin section these show relict corroded clastic grains set in a fine grained quartzo-felspathic matrix, often containing acicular inverted tridymites (Fig 2.11).

The acid rock from the composite sheet is shown in Fig 2.12. It is a drusy granophyric microgranite consisting of quartz, rather altered perthite, magnetite and biotite. A little apatite, pyrite and zircon are also present. Whether this is related to the marginal suite is uncertain.

E. CONCLUSIONS

(1) The Marginal Suite is not a simple ring-dyke. The inner and outer contacts are generally sub-parallel and are either vertical, or dipping out

from the centre of the central complex at low to moderate angles. It is a complex zone containing many distinct bodies of intermediate and basic rocks.

(2) The outer contact is marked by melting of the Torridonian sediments, and the development of intrusion breccias and hybrid rocks. Fragments of rocks from the layered series are occasionally caught up in these intrusion breccias.

(3) Under some of the low-angle contacts chilled picrites and olivine-rich gabbros are found between hybrid rocks and the layered series.

(4) In places the Marginal Suite may show an intrusive relationship to the layered rocks; in others there is an almost insensible gradation between the two, and the Marginal Suite may represent a marginal facies to the magma chamber in which the layered rocks were formed.

(5) There is no direct evidence that the Marginal Suite occupies a ring fracture. Although it follows generally the traces of older ring fractures, in places it transgresses them.

CHAPTER THREE

THE LAYERED ROCKS

The LELS comprises some 250m of olivine and olivine-plagioclase-(clinopyroxene) cumulates. Whereas the upper ELS rocks are mainly adcumulate and heteradcumulate peridotites and troctolites, in the LELS orthocumulates and mesocumulates are common (Brown; 1956), and troctolitic allivalite is relatively rare. Peridotite forms the bulk of the upper ELS sequence; in the LELS, about 60% of the thickness is allivalite. Chrome-spinel seams and harrisite layers are often associated with the upper ELS peridotites, but chrome-spinel seams are rare, and harrisites unknown in the LELS. Many of the "allivalites" of the LELS are locally rather deficient in olivine; these gabbroic rocks are included in the term "allivalite" to emphasise their relationship to the layered rocks, rather than the later gabbro plugs and sheets.

3.A. Sub-division of the LELS

Brown (1956) divided the Eastern Layered Series into 15 units, each of which he considered represented the products of crystallisation of at least one pulse of basaltic magma. Each unit he defined as "olivine rich rock passing gradually up into one rich in plagioclase." Some units present no problems in definition: for example units 1,7,9,10 consist of a peridotite layer overlain by an allivalite. Other units are more complex: for example units 2,3,8,11,12 contain subsidiary "units" - with thin allivalites within the peridotite, and/or peridotites within the allivalite. It is thus rather arbitrary whether these are designated as single units or as many distinct units. Brown recognised this problem and argued that units should be defined on the basis of laterally persistent dominant lithologies, ignoring thin or impersistent layers.

Remapping (Fig 3.1) has revealed however that the lateral lithological change is a common feature of

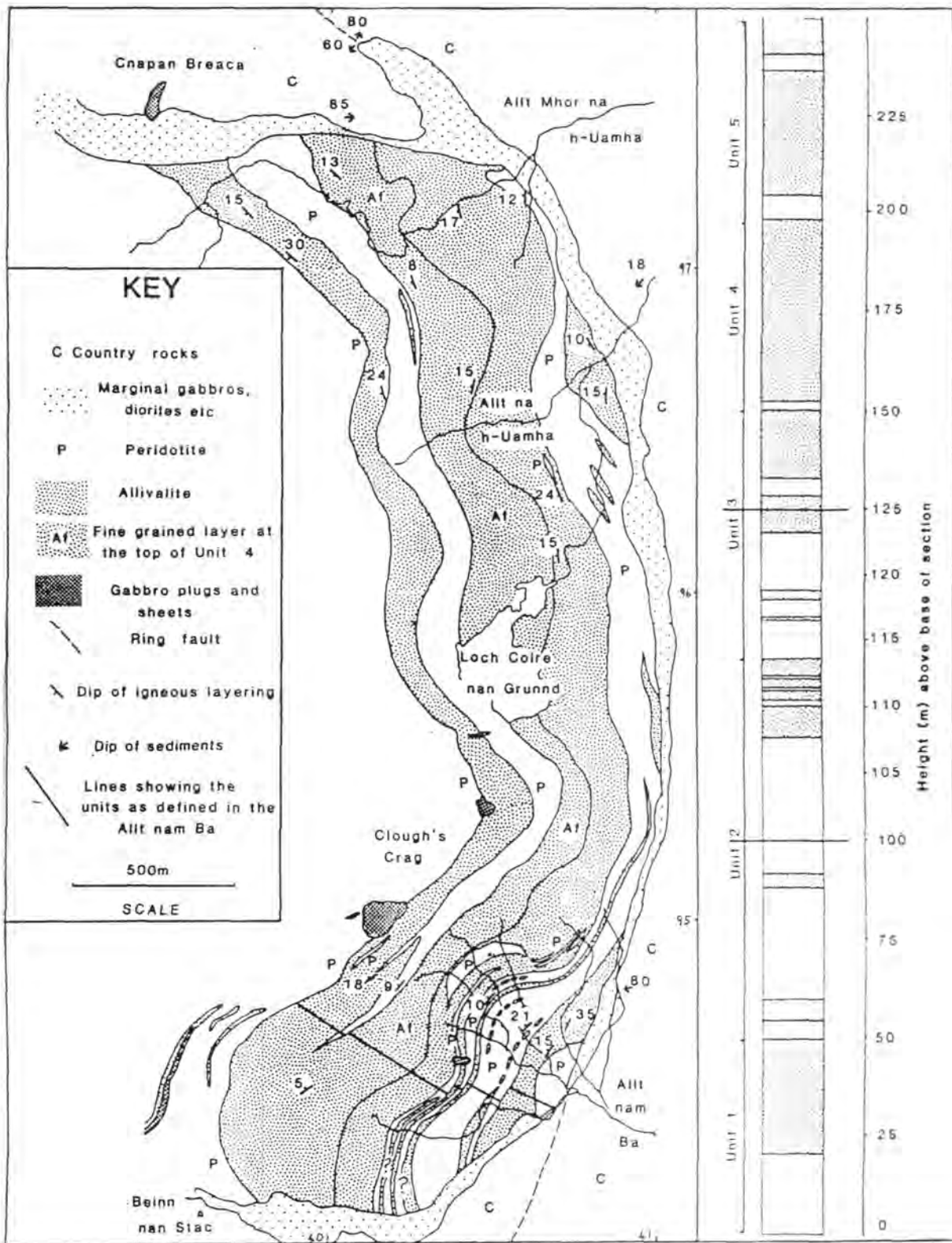


Fig 3.1 Revised map of the LELS, and stratigraphic section. The numbers around the edge of the map are National Grid lines at 1km intervals. The section above, and the cryptic variation sample traverse were taken from NM 40719452 - NM40479486, and from NM 40369470 - NM40109495. Note the partially expanded vertical scale on the section.

the LELS, and this means that it is not possible to subdivide the LELS into 5 units, each comprising a persistent peridotite overlain by a persistent allivalite. Poor exposure away from the Allt nam Ba area makes it impossible to correlate exposures along strike accurately. This causes certain problems in the nomenclature of units away from the type section. For example, the peridotite defining the base of Unit 4 in the Allt nam Ba thins and disappears to the north, and the allivalite of Unit 3 passes up into that of Unit 4. Due to poor exposure it is not possible to determine accurately where Unit 3 ends and Unit 4 begins: this thick allivalite is thus referred to as Unit 3/4 allivalite. The main allivalite of Unit 2 in the Allt nam Ba also disappears to the north, and the peridotites of Units 2 and 3 pass directly into one another. The resultant peridotite is referred to as Unit 2/3 peridotite.

Since the work of Brown (1956) each unit has been interpreted as the product of the crystallisation of a pulse of basaltic magma. However, as discussed later (Section 6.8) this needs to be extended to each minor peridotite/allivalite alternation. Thus no genetic significance can be attached to the term "Unit" - some units do represent the crystallization products of one magma pulse, others represent a complex sequence of crystallization and replenishment. The term "unit" is merely one of convenience.

A further complication is introduced by the role of post-cumulus processes in shaping the present day distribution of peridotite and allivalite layers. There is good evidence, in Units 2,3, and 6, and elsewhere in Rhum (Butcher, 1984; Young, 1984) that allivalite layers have suffered post-cumulus replacement by peridotite. This is discussed in detail elsewhere (section 7.C), but it seems clear that many allivalites have been reduced in thickness and/or lateral extent by these processes. It is even possible that whole allivalite layers have been completely replaced by peridotite. This makes it even more difficult to relate

the peridotite/allivalite cycles now seen to the original cumulates formed from distinct batches of magma.

Bearing all this in mind, the LELS has been divided into 5 units on the basis of a measured section in the Allt nam Ba where exposure is best. These units are used purely for stratigraphic convenience. In view of the considerable differences between Brown's (1956) map and that of the current work, it is likely that not all of the units defined here correspond exactly to those defined by Brown.

3.B. Field Relations

3.B.1 Unit One

This unit can only be identified with certainty in the Allt nam Ba, where it comprises some 20m of peridotite (base not exposed), overlain by 30m of allivalite.

The peridotite, which is rather poorly exposed, is highly weathered. It is mostly unlayered, although one outcrop does show a diffuse 5 - 10 cm scale layering, caused by variations in the proportions of intercumulus clinopyroxene and plagioclase. At NM4067 9451, it is cut by several irregularly orientated coarse gabbroic veins. These are regarded as late "squirts" of interstitial liquid emplaced into fractures in the cooling cumulate pile. (Brown; 1956, Butcher; 1985). Blebs of sulphide minerals up to about 1cm across are fairly common in the peridotite.

The contact with the allivalite is exposed in the stream bed of the Allt nam Ba, and in two small tributary streams to the north. It seems to be sharp and planar, although close examination is difficult due to the steady flow of water. The basal parts of the allivalite are poorly layered and troctolitic. Large blebs of sulphide minerals are common in the lowest 2 - 3m, up to about 1cm across. With increasing height, clinopyroxene becomes more abundant and the rocks develop good layering. The layering is on a 1 - 30cm scale and is rather diffuse, reflecting slight

variations in clinopyroxene content. It is best picked out on weathered surfaces.

The middle and upper parts of the allivalite are very poor in olivine - none is seen in thin section, although rare rusty-weathering crystals on the outcrops suggest it may not be totally absent. This part of the sequence is characterised by wispy layering, with coarse grained, well laminated clinopyroxene-rich rock enclosing fine grained lensoid layers of plagioclase-rich rock.

In the topmost parts of the allivalite olivine is again abundant, and clinopyroxene content is reduced.

Xenoliths are not uncommon in the allivalite. Most of these are slab-like masses of beerbachite lying sub-parallel to the layering. They are especially common on the ridge formed by the allivalite, just to the north of the Allt nam Ba (about NM407957). Xenoliths are absent from the peridotite.

To the north of the Allt nam Ba, a number of allivalite outcrops may be tentatively described as laterally equivalent to the Allt nam Ba sequence. The scattered and poorly exposed outcrops at NM410955 may belong to Unit 1; they appear to wedge out to the north. The allivalite outcrops in the Allt na h-Uamha may also be equivalent, although they are rather more feldspar-rich and clinopyroxene-poor compared to the Allt nam Ba sequence. Just inside the marginal gabbro in the Allt Mhor na h-Uamha, a small outcrop of allivalite underlies peridotite; it resembles the allivalite of the upper part of Unit 1, although it is only faintly layered.

3.8.2 Unit Two

Of all the units in the LELS, Unit 2 bears the greatest resemblance to those of the upper ELS. Peridotite is predominant over allivalite (50m of peridotite; about 15m of allivalite) and the allivalite is a clinopyroxene-poor troctolite.

The Unit has a slightly undulating or nearly planar contact with the underlying allivalite of Unit 1.

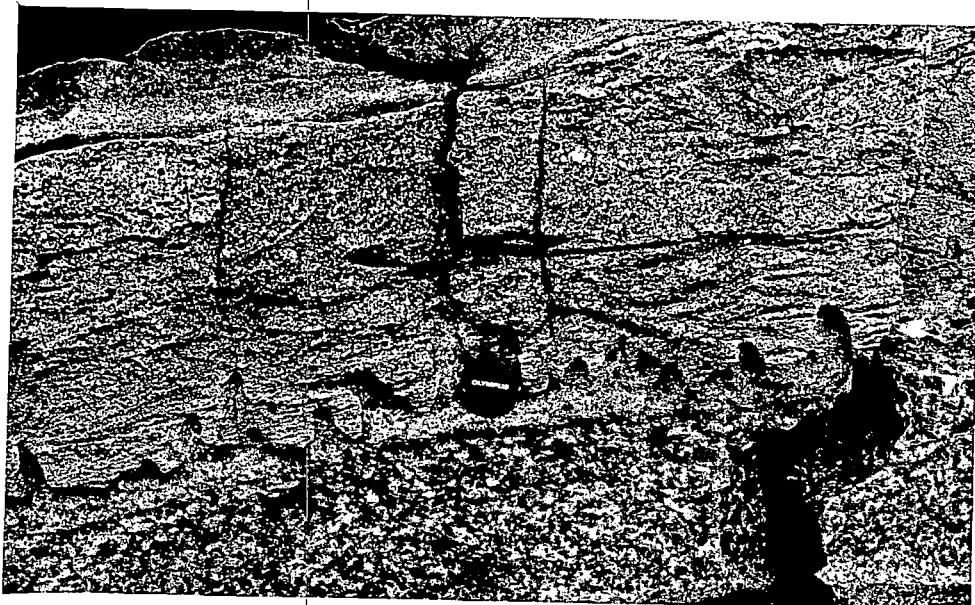


Fig 3.2. Finger structures cutting low-angle slump folds in unit 2 allivalite. Loc 220. NM40509477.



Fig 3.3. Upper part of unit 2 allivalite heavily disrupted by finger structures. The honeycomb-textured peridotite above the overhang is unit 3 sensu stricto. The underlying, more feldspathic rock includes unrotated relict blocks of allivalite. Loc 198. NM40549478.

well exposed in several of the streams comprising the Allt nam Ba. There is no basal chrome spinel seam. A few metres above the base an allivalite layer is developed. This layer is quite thick and coherent in the southernmost exposures but to the north it becomes increasingly disturbed, being mixed with the enclosing peridotite by slumping and loading. Although exposures are not particularly good, the slump folds appear to have no constant closure directions, and hence slumping caused by down-slope movement is less likely than deformation under conditions of fluidisation perhaps induced by shock. There is also a suggestion of along-strike lithological change in this layer. The material which has been mixed in with peridotite is well laminated and poor in clinopyroxene, while the coherent outcrops to the south show little lamination and are richer in clinopyroxene.

Above this deformed layer is a considerable (25m +) thickness of poorly exposed peridotite, which is unlayered or shows a 5 - 15cm scale diffuse layering on weathered surfaces. It is overlain by a thin (3m) disturbed layer of troctolitic allivalite, rather discontinuous along strike. The upper surfaces of many of the peridotite loads within this layer show the development of finger structures. This allivalite is only seen between NM40489460 and NM40629472.

The upper part of Unit 2 peridotite above this layer consists of 14m of well layered honeycomb peridotite, rather more feldspathic than the peridotite lower down in the unit.

The main allivalite of Unit 2 in the Allt nam Ba shows evidence of a complex history. The bottom contact is not well exposed but seems to be planar and sharp. In the exposures at NM40509474, the allivalite contains three thin peridotite layers which are not seen to the south. Each of these has a sharp planar base (no chrome spinel seams) and an upper surface marked by upward protrusions of peridotite into allivalite - hereafter referred to as finger structures. The allivalite above the lowest peridotite has well



Fig 3.4. "Inverted mushroom" style load structures in unit 2 allivalite. The upper surfaces of the loads show small finger structures. Loc 198. NM40549478.



Fig 3.5. Slumped and mixed peridotite/allivalite in the lower part of unit 3 allivalite. Allt nam Ba.

developed recumbent slump folds - these are sharply cut across by the finger structures (Fig 3.2). A little to the north these peridotites thicken somewhat, and deformation becomes marked, with the peridotite layers becoming locally discontinuous due to loading, with flame structures of allivalite injecting the peridotites. Finger structures are more prominent than they are further south. A few tens of metres further north, the allivalite presents a different spectacle (Fig 3.3). The upper part has been extensively disrupted by finger development, with merging of the subsidiary peridotites leaving only a few relict fragments of allivalite. All these relict fragments have their lamination and layering parallel to the general dip of the layering. The peridotites often show "inverted mushroom" style load structures, the upper surfaces of which show the development of small fingers (Fig 3.4). These structures, and other similar ones are abundant in Rhum, and they are taken as evidence of replacement (Robins, 1982; Butcher et al, 1985). They are discussed in more detail in section 7.C.

The main allivalite of Unit 2 cannot be traced north beyond NM40949540, and the peridotites of Units 2 and 3 cannot be accurately distinguished. However, in the stream around NM408964, a number of small isolated allivalite outcrops are seen, which may perhaps be ascribed to Unit 2.

3.B.3 Unit Three

Unit 3 is the most extensive in the LELS, exhibiting considerable lateral changes in lithology. The boundary with Unit 4 is only clear-cut in the southern part of the area; to the north the allivalite of Unit 3 merges with that of Unit 4 due to the northward thinning of Unit 4 peridotite. In the measured section in the Allt nam Ba the unit is about 36m thick, of which 23m is allivalite.

The contact with Unit 2 is well exposed in the Allt nam Ba, and is sharp and planar, except where finger structures (see previous section) have cut

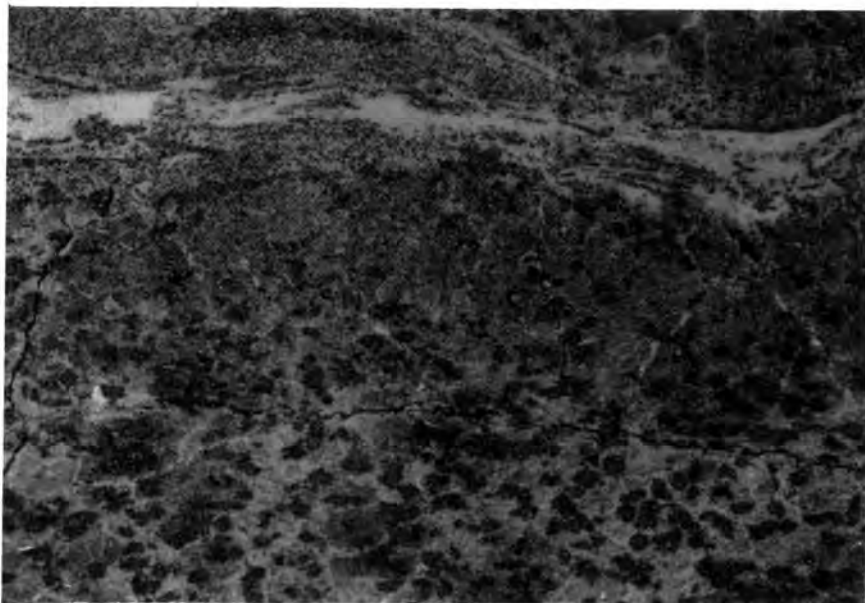


Fig 3.6. Fine-grained plagioclase rich layer in lower part of unit 3 allivalite. Note deformed margins. Cut slab. Approximately life size. Loc 183. NM40799620.



Fig 3.7. Deformed "xenolith" of troctolitic allivalite in clinopyroxene-rich allivalite of unit 4. Xenolith approx. 0.4m long. Loc 184. NM40739613.

... ..

... ..

through the underlying allivalite. There is no chrome spinel seam. About 2m above the base is a thin, discontinuous and highly disturbed allivalite layer. A metre above this is a small anorthositic allivalite layer with small (ca. 1cm) finger structures along its base. This layer shows no sign of deformation. The top surface is sharp and planar and is overlain by 5m of honeycomb-weathered peridotite. Above this is 27m of allivalite. The lowest parts are highly deformed, with schlieren and lenses of peridotite, which slightly further up form a slightly more coherent layer (Fig 3.5). Above this the allivalite becomes increasingly rich in clinopyroxene and less well laminated. The pyroxene-rich upper parts have a vague layering on a 5cm - 1m scale, picked out by variations in pyroxene content and the presence or absence of large (1cm) poikilitic olivines. This same part of the sequence is prone to crumbly weathering and has a rather altered appearance. This may be related to a nearby gabbro intrusion (see next section).

The peridotite of Unit 3 is not well exposed to the north of the Allt nam Ba, and north of NM409954 it merges with that of Unit 2. Exposures at NM40859621 show peridotite overlying a thin troctolite layer. The upper part of this layer is anorthositic and has a chrome-spinel seam developed along the top of it. Two thinner, and rather deformed chrome-spinel seams occur within the peridotite one or two cm above. These are the only chrome-spinel seams seen in the LELS, and this is the only place where peridotite overlies anorthositic allivalite. The association of chrome-spinel seams with anorthosite-peridotite contacts is a marked feature of the ELS, the contacts between Units 7 and 8, and Units 11 and 12 being good examples.

To the north of the Allt nam Ba the troctolitic lower part of Unit 3 allivalite is less well developed, and clinopyroxene is a major phase throughout. Minor peridotite layers do occur in the lower parts, but it is not possible to correlate these with those seen in the Allt nam Ba. Good exposures of

the main allivalite can be seen in the lower parts of the cliff 300m NNE of Loch Coire nan Grund. At NM40799620 abundant lensoid layers of fine grained anorthositic material can be seen. These layers are generally 1-5cm thick, and can be traced along strike for up to a meter or so. They have sharp, although often deformed contacts with the material above and below (Fig 3.6). A little further up the cliff, at NM40759625, an unusual (for Rhum) channel-like structure can be seen. This contains a number of dish-like layers, separated by erosive(?) surfaces. The axis of the channel dips at 24° to the WSW, about the same as the adjacent rocks. These dish-like layers are stacked approximately vertically, and extend several meters up the cliff face. Although the upper parts are somewhat inaccessible, they appear to be richer in olivine than those lower down. The width of the "channel" is difficult to gauge due to the steepness of the terrain, but is at least 10m.

In the Allt Mhor na h-Uamha, at NM40369716, a fine-grained clinopyroxene rich layer contains abundant tiny blebs of sulphide minerals.

Xenoliths of beerbachite are not uncommon in the middle and upper parts of Unit 3 allivalite.

3.B.4 Unit Four

The peridotite which defines the base of Unit 4 in the Allt nam Ba is very thin (<3m). Where it is best exposed, around NM40489483, it has a very weathered and altered appearance. Veins of gabbro are common in this area, and it may be that a sub-surface gabbro intrusion has affected the cumulates. To the south the peridotite becomes rather fresher in appearance, while to the north it thins and cannot be traced north of NM40519485.

The peridotite has a sharp and planar contact with the overlying allivalite, which is a well layered troctolitic type, at least in the Allt nam Ba. This passes into poorly layered clinopyroxene and Fe-Ti oxide rich material with abundant xenoliths of beerbachite, gabbro and ultrabasic rocks. To the north of the Allt

nam Ba the troctolitic facies is not well developed, and the orthocumulates of the upper part of Unit 3 pass up into those of Unit 4 with no clear boundary.

This part of Unit 4 allivalite to the east of Loch Coire nan Grund contains "xenoliths" of troctolitic allivalite set in a clinopyroxene rich cumulate. These xenoliths were obviously in a soft plastic stage as they are deformed and folded in with the enclosing material (Fig 3.7). Above these deformed cumulates in this area are undeformed, well layered orthocumulates with layers rich in magnetite. Epidote is common as an interstitial mineral in certain layers. This facies is not developed elsewhere: generally the xenoliths become more abundant with height until suddenly there is a sharp decrease in grain size over about 2m. The upper part of Unit 4 allivalite over its entire exposed length is comprised of this fine grained facies. Just below this fine-grained layer in the Allt nam Ba at NM404948 a thin (1 - 2m) peridotite layer occurs, cut by abundant gabbro veins like those seen at the base of Unit 4 nearby.

This fine-grained layer is very rich in xenoliths and was mapped by Brown (1956) as an intrusive sheet of olivine gabbro, although he seems to have used the presence of xenoliths to delineate its contacts, thus obscuring the fact that xenoliths appear much lower down in the sequence than the fine-grained rock types. Brown states that "[the gabbro] ...is free from any form of banding or igneous lamination...". Re-examination during the course of the present work however, has revealed that abundant vague wispy layering, and lamination of plagioclase is also common. The conformable, gradational nature of the bottom contact and the presence of xenoliths in both the underlying allivalite and in the fine-grained layer may cast doubt on an intrusive origin for this body of rock.

A preliminary examination of the Askival Plateau Gabbro (APG), a body of rock superficially resembling the fine grained facies in Unit 4, show it to be clearly intrusive with abundant net-veined contacts.

The APG clearly cross-cuts the layering of Units 9 and 10, and has caused considerable deformation of the layering in these units. Butcher (1984) in a more detailed study also found a ghost stratigraphy preserved in the APG based on the distribution of xenoliths.

None of these features are seen in the fine grained layer of Unit 4, suggesting a different origin, although the lithologies are very similar even down to the presence of layering within the APG ..

3.8.5 Unit Five

Unit 5 peridotite forms a thick, continuous layer from Cnapan Breaca south to the corrie just north of Beinn nan Stac, where it thins and disappears. It is not well exposed, but where seen shows a faint honeycomb layering.

In the measured section it is about 6m thick, and neither the upper nor lower contacts are exposed. Above this is about 3m of troctolitic allivalite, which passes up into the main allivalite which is very rich in clinopyroxene. Elsewhere this troctolitic layer is absent; the peridotite passes gradationally upwards into the allivalite. This is unusual in Rhum; most peridotite/allivalite contacts are very sharp. The contact is gradational over about 2m, and is well layered on a 2-5cm scale, with alternating olivine-rich and plagioclase-rich layers, the former becoming thinner and less clearly marked upwards (Fig 3.8).

The allivalite of Unit 5 corresponds to the upper "intrusive sheet of fine-grained olivine gabbro" of Brown (1956). As with the lower sheet, it is difficult to disprove an intrusive origin, although the gradational lower contacts, lack of net-veining and deformation in the surrounding rocks, and the presence of good layering suggest similarities with the LELS allivalites rather than the intrusive gabbros.

The Unit 5 allivalite is not so rich in xenoliths as the fine-grained facies of Unit 4, although beerbachite and gabbro xenoliths are locally common. The latter are particularly common in the upper part of the



Fig 3.8. Gradational contact between unit 5 peridotite and allivalite. Height of outcrop approx. 1m. Loc 178. NM40179674.



Fig 3.9. Layering in unit 5 allivalite. An ilmenite-rich layer occurs along the line marked X-X. This truncates the underlying layering in places (A). Loc 203. NM40149483.

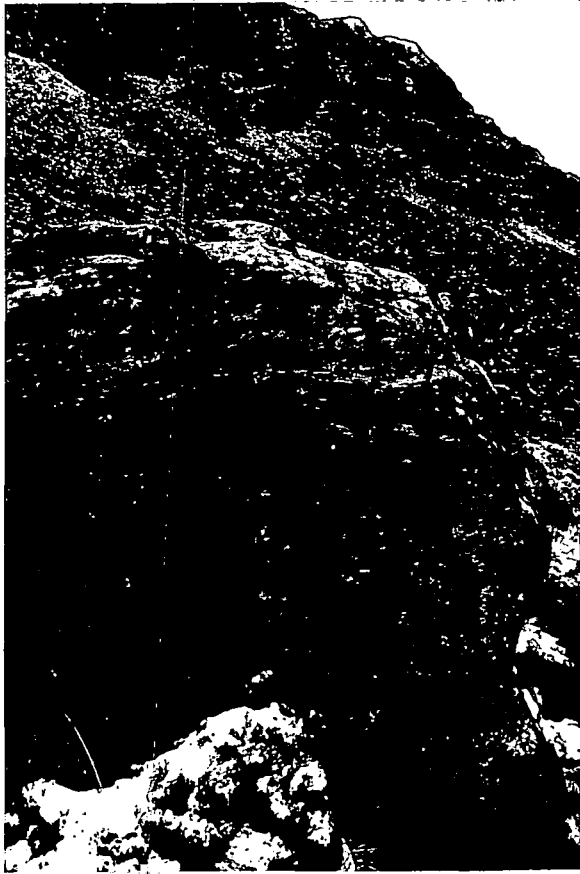


Fig 3.10. Allivalite layer occurring in the lower part of unit 6 peridotite. Almost the entire thickness of the layer is shown. Loc 234. NM39629455.

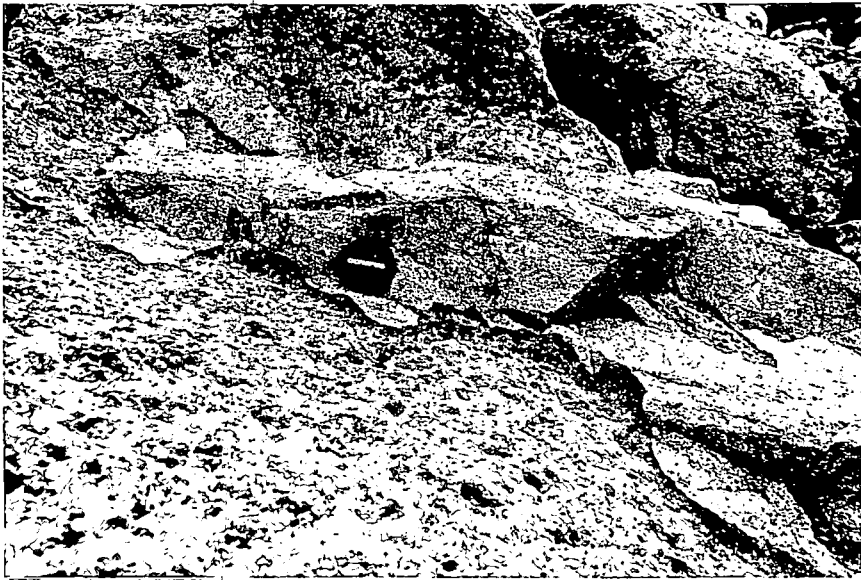


Fig 3.11. Disappearance of unit 6 allivalite through fingering. A few metres to the right of this photograph the allivalite is over 2m thick. Loc 235. NM39629466.

allivalite in Bare Corrie (NM398971); they are frequently magnetic.

Layering is well developed in places within Unit 5 allivalite, mostly rather diffuse and without dramatic changes in modal mineralogy between layers. Locally however, striking concentrations of ilmenite occur as thin layers (Fig 3.9). At this locality the oxide-rich layer appears to divide around a beerbachite xenolith, and there is a suggestion of an unconformable contact, the oxide-rich layer cutting off the underlying layering which has a slightly steeper dip.

In the measured section, Unit 5 allivalite contains a thin lensoid peridotite layer about 10m below the top. This peridotite has a gradational lower contact, and a fairly sharp upper contact. It displays excellent lamination of elongate olivines in its basal portions.

The upper part of Unit 5 allivalite develops in places (eg NM39699718) a rather pale, well layered facies. Brown (1956) interpreted these as relics of the allivalite which had been intruded by the sheet, but explicit evidence for this is lacking. A very similar facies is developed in Unit 8 allivalite at NM94859683.

Brown's (1956) map shows the "upper sheet" cutting across the allivalites of Units 5, 6 and 7 below Clough's Crag, and used this as evidence for the intrusive nature of the sheet. However the sheet is nowhere seen in contact with the allivalites, and lateral wedging out of the layers (seen at eg NM) is a more likely explanation.

Between the top of Unit 5 allivalite and Unit 6 allivalite at NM, a previously unmapped allivalite layer occurs. It is of distinctive appearance, the lower part being troctolitic with scattered large green clinopyroxene oikocrysts, and the upper part being much finer grained and richer in pyroxene (Fig 3.10). One might be tempted to term this Unit 5.5, but for the sake of terminological simplicity, and to avoid setting dubious precedents, it is perhaps better included as a sub-unit of Unit 6.

The main allivalite of unit 6 is highly discontinuous along strike, due to the "fingering" process mentioned earlier (3.B.2). This is shown in Figs 3.11 and 3.12.

3.B.6 Gabbro plugs and sheets

Previous maps of the LELS have shown differing numbers of small gabbro intrusions in a variety of places. Much of this confusion has stemmed from the rather "gabbroic" appearance of the LELS rocks, together with the extent of lateral lithological variation, which was not previously recognised. Most of these have been reinterpreted as clinopyroxene-rich allivalite in the present work. However, several small plugs and inclined sheets of gabbro have been mapped on the basis of transgressive or chilled margins and lack of layering. Two of these are intruded across the upper contact of unit 5 allivalite, cutting both it, and the overlying peridotite.

3.C. PETROGRAPHY

Good accounts of the petrology of the LELS are given by Brown (1956) and Harker (1908). For the sake of brevity, and to avoid excessive duplication, only a general account, together with some new observations, will be given here.

3.C.1 Peridotites

The peridotites are composed of four main minerals: olivine, plagioclase, clinopyroxene, and chrome-spinel. Olivine and chrome-spinel are the only cumulus phases. Other minerals occur in small quantities: phlogopite, kaersutite, orthopyroxene, hornblende, various sulphide minerals, and a variety of secondary alteration products such as chlorite, talc(?), and serpentine.

3.C.1.a Textures

Olivine forms between 40% and 80% by volume of the LELS peridotites. The dunitic facies locally developed in

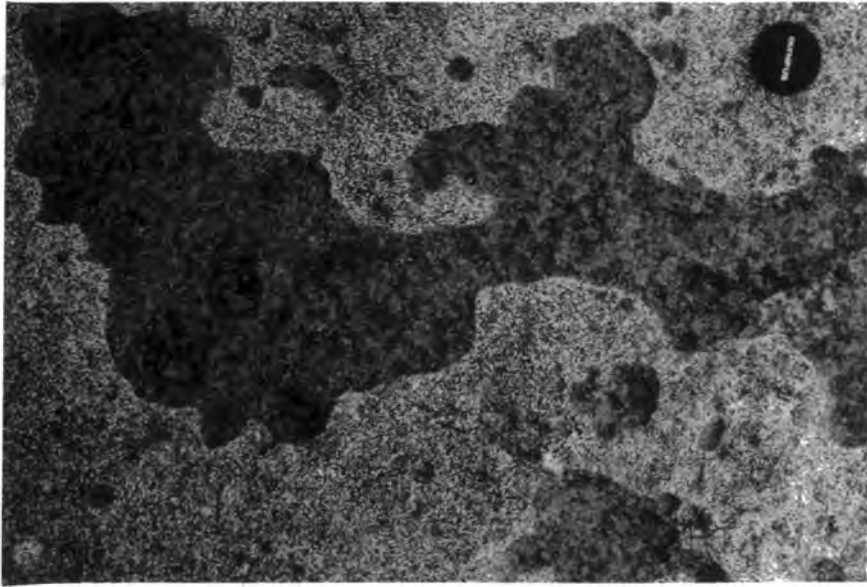
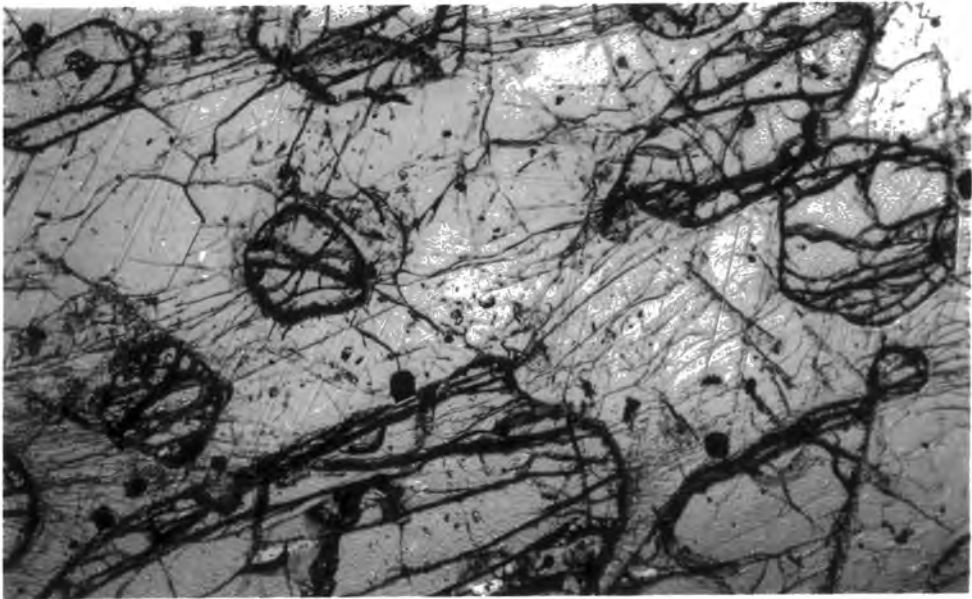


Fig 3.12. View looking down on fingers in unit 6. Same locality as previous photograph.

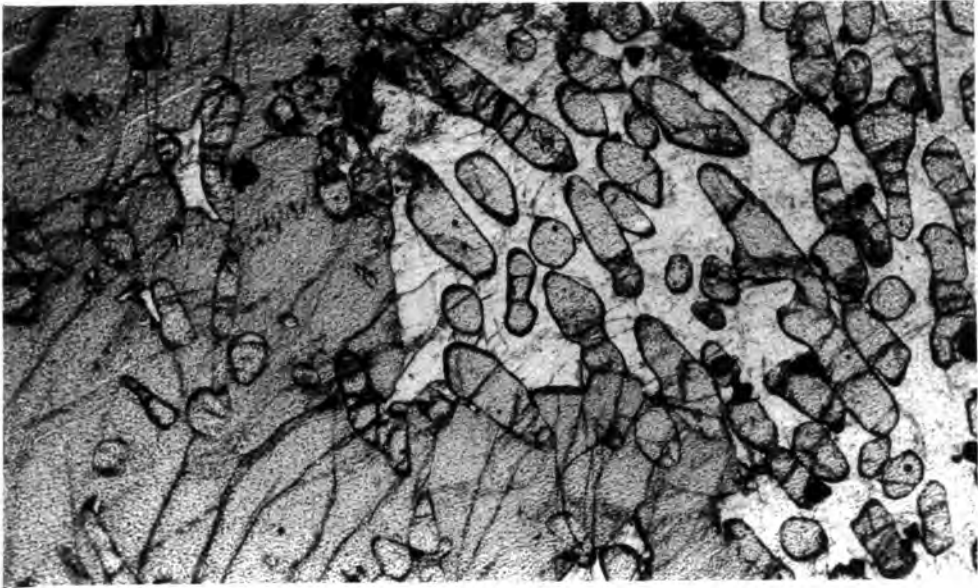


1mm

Fig 3.13. Feldspathic peridotite with low density of olivine crystals. Note high proportion of intercumulus material and non-touching grains. PPL. Sample U2P11.

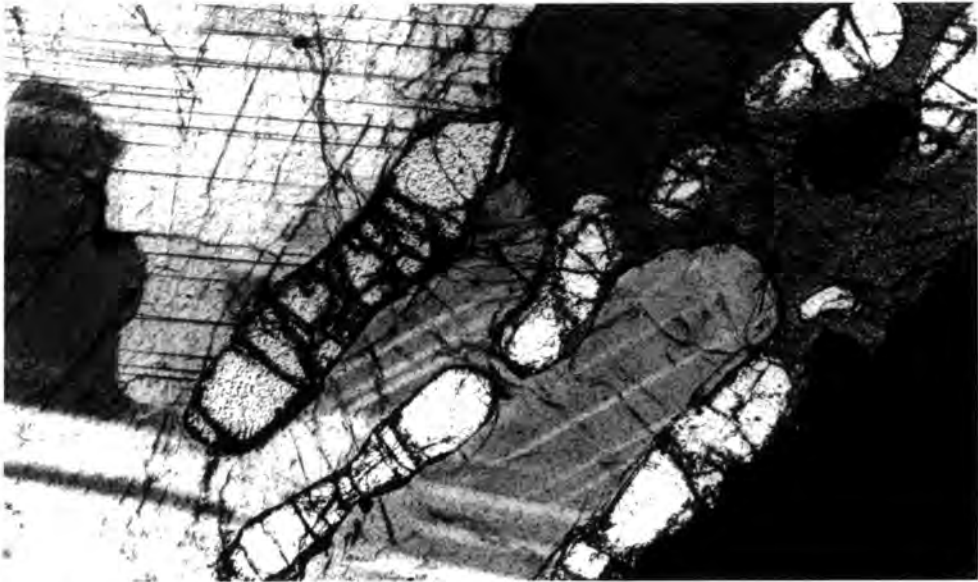
other parts of the ultrabasic complex are not seen in the LELS. Some of the rocks seen in the peridotite layers of the LELS are not strictly peridotites, being rather deficient in olivine, however they are included here on the basis of association, and in the absence of cumulus plagioclase. Indeed, according to some definitions, certain of the peridotites would not be regarded as cumulates at all, as the cumulus grains (olivine) do not form a touching crystal framework (Fig 3.13). However, in view of their close association with rocks of impeccable cumulate credentials, and the fact that they are clearly not representative of liquid compositions, this is not considered crucial. According to McKenzie (1985), compacting layers of olivine + basic melt may well develop upward-moving melt-rich "waves" with non-touching grains. This is a plausible process in layered intrusions (Sparks et al, 1985), and this may account for the local absence of grain supported textures. A similar process has been invoked by Donaldson (1982) to explain the formation of certain harrisite layers.

Olivine crystals tend to be smaller and more widely spaced when enclosed in clinopyroxene oikocrysts than when enclosed in plagioclase (Fig 3.14). This is at first sight somewhat paradoxical, as clinopyroxene normally crystallises after plagioclase in Rhum. Thus early crystallising plagioclase might be expected to preserve the high-porosity, uncompacted cumulus textures, and prevent further growth of the enclosed olivines, while the later-formed pyroxene would crystallise in the interstices of better compacted, larger grains. A number of factors may be significant here. Delayed nucleation of plagioclase, so that it nucleates simultaneously with pyroxene, has been suggested by McClurg (1982) as an explanation for enhanced Al_2O_3 contents of CS clinopyroxenes. There is some evidence that Al_2O_3 contents of LELS clinopyroxenes tend to be higher than those of the upper ELS (section), however this textural phenomenon has been observed by Volker (1983) in many upper ELS peridotites, so this is



1 mm

Fig 3.14. Peridotite from unit 5, showing small size and wide spacing of olivines within clinopyroxene. PPL. Sample U5A17i.



0.5 mm

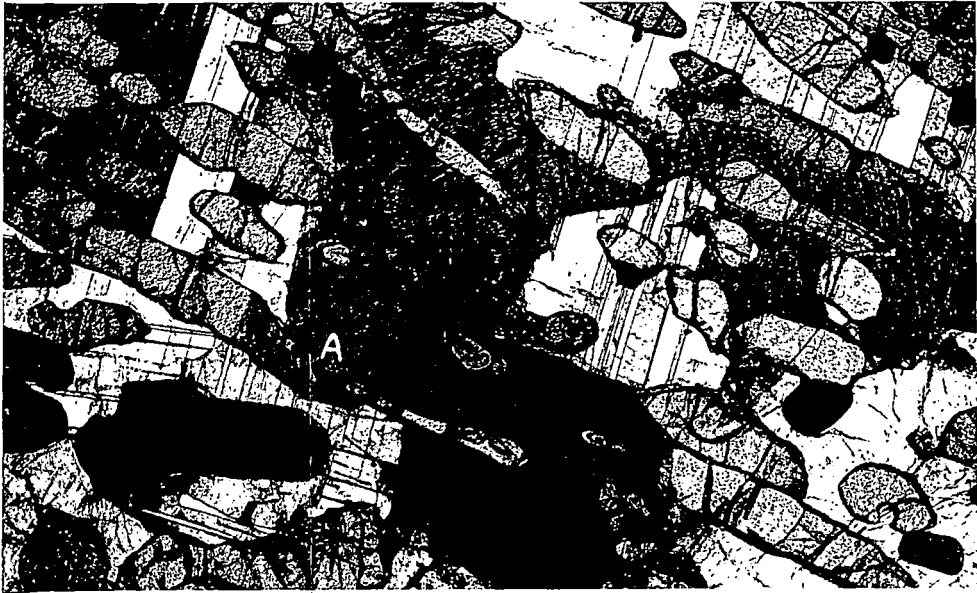
Fig 3.15. Peridotite from unit 5. Note break-up of elongate olivines into trails of small blebs as they cross from plagioclase oikocryst to clinopyroxene oikocryst. XP. Sample U5A17ii.

unlikely to be sufficient explanation.

Recent work at Cambridge University by D. McKenzie and R. Hunter (R. Hunter, pers comm) suggests that the small-scale structures of many cumulate rocks may be controlled by the post-cumulus minimalisation of grain-boundary energies, ie textural equilibration. If all grains are of the same phase, and mechanically isotropic, this will eventually result in 120° triple junctions. However equilibrium inter-grain angles for mixed grain assemblages may be very different. Thus clinopyroxene will tend to creep along olivine-olivine, plag-plag, or plag-olivine boundaries. This is frequently seen (Fig 3.15). Likewise, interstitial basic melts may form open channels along grain boundaries, and be expelled from the crystal pile as the matrix of cumulus grains deforms. This process may be important in producing adcumulates.

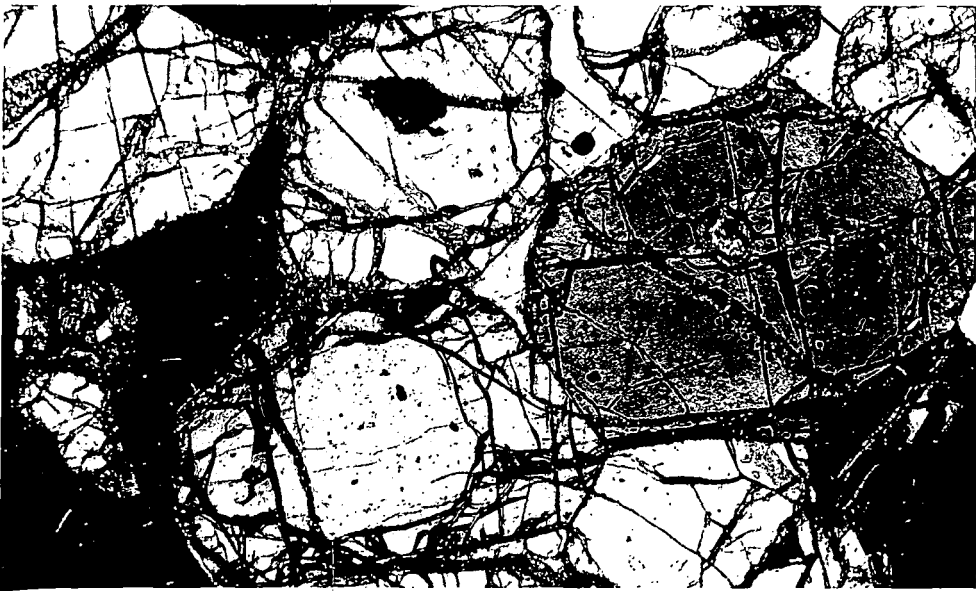
Similar processes may explain the smaller and scarcer olivines within clinopyroxene oikocrysts. There is good evidence in some specimens for considerable post-cumulus textural modification of olivines enclosed within pyroxenes. Elongate olivine crystals in sample U5A17 break up into trails of rounded blebs when an individual crystal crosses from a plagioclase oikocryst to a clinopyroxene (Fig 3.15), the blebs remaining in optical continuity. In this same rock "necking" of olivine crystals in pyroxenes can be seen (Fig 3.16), similar to that often seen in elongate or planar fluid inclusions in fluorite or quartz. Incipient "necking" of olivine crystals in plagioclase is also seen, but is less well developed.

Given this, is it possible to say anything about the original textures of LELS rocks? Approach to textural equilibrium is indicated by constant inter-grain angles at any given type of grain boundary. Thus all plag-plag-plag or olivine-olivine-olivine contacts would be 120° and all plag-plag-olivine contacts would have a constant angle, as would plag-plag-cpx, and so on. This is rarely seen in the LELS except in very fine-grained layers, and in the



1 mm

Fig 3.16. Peridotite from unit 5. Note "necking" and break-up of elongate olivine at point A. XP. Sample U5A17ii.



1 mm

Fig 3.17 Peridotite from unit 2 showing very local development of 120° triple junctions between olivine grains. XP. Sample U2P9.

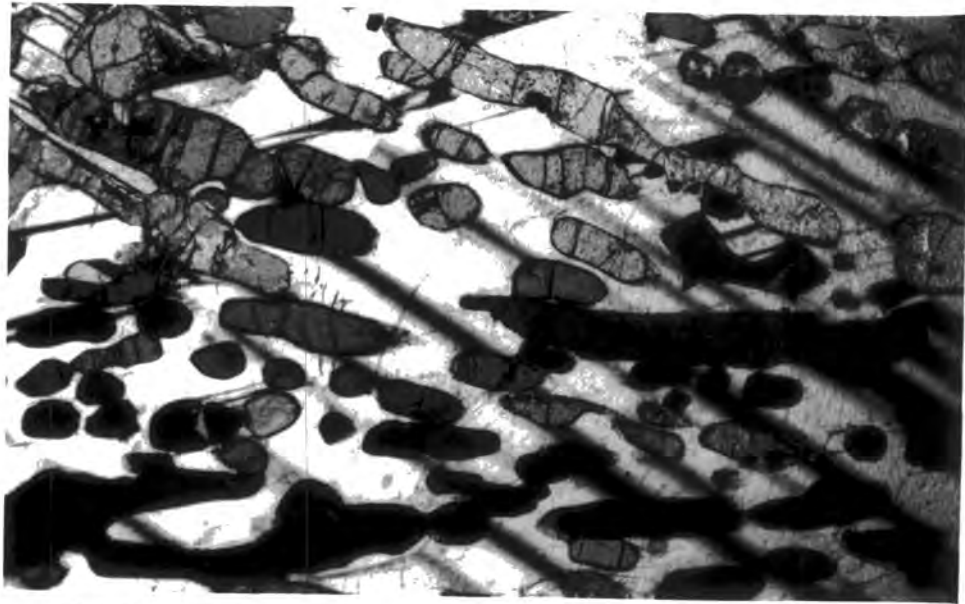


Fig 3.18. Intersecting laminations in peridotite from unit 5. Olivines parallel to the bottom of the photograph are in extinction. XP. Sample U5A17iii.

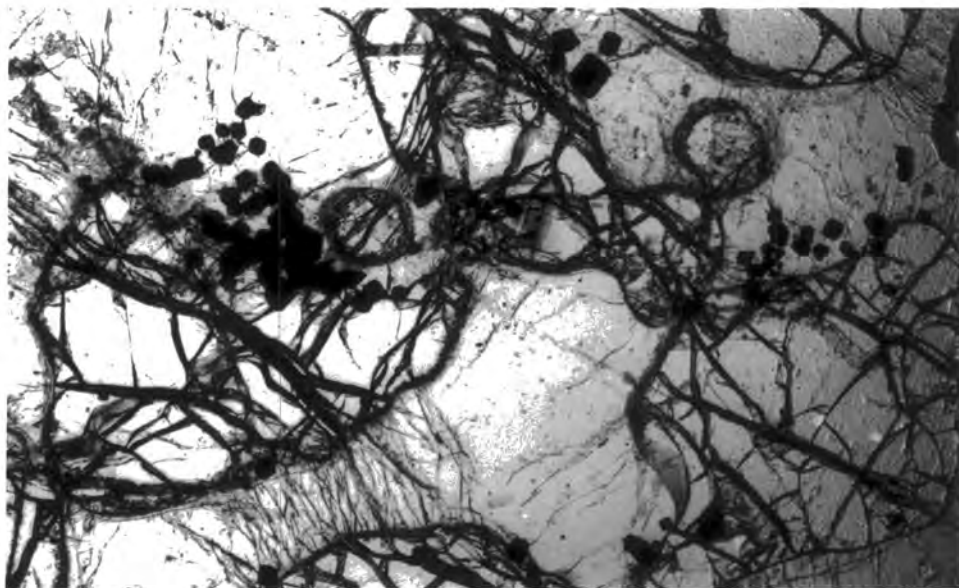


Fig 3.19. Preferential concentration of chrome-spinel crystals on the upper surfaces of olivine crystals in peridotite from unit 2. PPL. Sample U2P5.

xenoliths from Units 4 and 5. Very local textural equilibrium is sometimes developed, but adjacent grains may not be in equilibrium (Fig 3.17). Thus most of the LELS rocks are some way from equilibrium, and thus retain, to a greater or lesser degree, their original textures.

The normal habit of olivine is rounded-granular, but locally, particularly in the peridotites of units 4 and 5, elongate habits are common. In these cases the olivines display lamination, roughly parallel to the general dip of the layering. The lamination of olivine crystals is independent of the enclosing oikocrysts (Fig 3.32c), unlike that seen in plagioclases in the allivalites (section 3.C.3.a). In a specimen from the minor peridotite within unit 5 allivalite, there appear to be two intersecting laminations (Fig 3.18). Similar structures in Unit 9 allivalite have been ascribed to nucleation and growth of "pseudo-cumulus" olivine crystals within the crystal mush (Young and Donaldson, 1985). In this case a more likely explanation is that the lamination sets each represent sections across two large, and only sub-parallel, platy olivine crystals. Sections cut at right-angles to that in Fig 3.18 show a few large crystals of complex habit, showing little lamination or elongation, rather than large numbers of small sub-parallel crystals.

Elongate and/or skeletal habits are more common in the basal parts of peridotites; the middle and upper parts are usually dominated by the rounded-granular habit. This is particularly well marked in the peridotites associated with unit 5.

A feature shown by several peridotite samples is the preferential concentration of chrome-spinel crystals on the upper surfaces of olivine grains (Fig 3.19). Volker (1983) observed this in peridotites of the upper ELS on Trallval, and considered it evidence for the sinking of chrome-spinels within the interstitial liquid. This seems likely, particularly as several of the LELS chrome-spinel concentrations show fining-upward

size grading (Fig 3.19). This has implications for the rheology of the interstitial liquid. Such small chrome-spinels would be most unlikely to sink if the interstitial magma had a significant shear strength, as suggested by McBirney and Noyes (1978). The sinking of these small crystals suggests that earlier sinking of the olivines, which would have much larger Stokes settling velocities, is quite plausible, although they do not show evidence for size-grading.

3.C.1.b Peridotite mesostasis minerals

As mentioned above, a number of hydrous phases are found in the LELS peridotites. These typically occur as interstitial clots up to 5mm or so in diameter, and they may enclose cumulus olivines. The commonest assemblage is kaersutite/phlogopite with lesser amounts of green hornblende, apatite, and chloritic alteration products. The kaersutite may form discrete crystals, or, more commonly, overgrowths at the margins of intercumulus pyroxene crystals. Frequently the kaersutite has an overgrowth of green hornblende (Fig 3.20). The core of these clots is usually a chlorite/ fibrous amphibole assemblage, which may include apatite crystals, or discrete amphibole crystals with brown kaersutite cores, and green hornblende rims. Phlogopite is usually found associated with kaersutite in the outer part of the clot, although phlogopite also occurs as isolated flakes without other accompanying hydrous phases. Large plates may poikilitically enclose olivine crystals, which show no signs of alteration.

Orthopyroxene occurs in several peridotite samples, and has been found in peridotites from all the LELS units. It normally forms poikilitic plates similar in habit to clinopyroxene, although enclosed olivines tend to be rather ragged in outline, suggesting a reaction relationship. Wherever orthopyroxene occurs, it seems to be unstable, often altering to, or being rimmed by, kaersutite or hornblende (Fig 3.21). Most orthopyroxene crystals are largely altered, even where adjacent olivine or clinopyroxene is fairly fresh.



Fig 3.20. Hydrous minerals in peridotite from unit 2. Clinopyroxene (c) has overgrowth of kaersutite (k), which in turn has a rim of green hornblende (h). A large flake of phlogopite (p) is also visible. PPL. Sample U2P11.



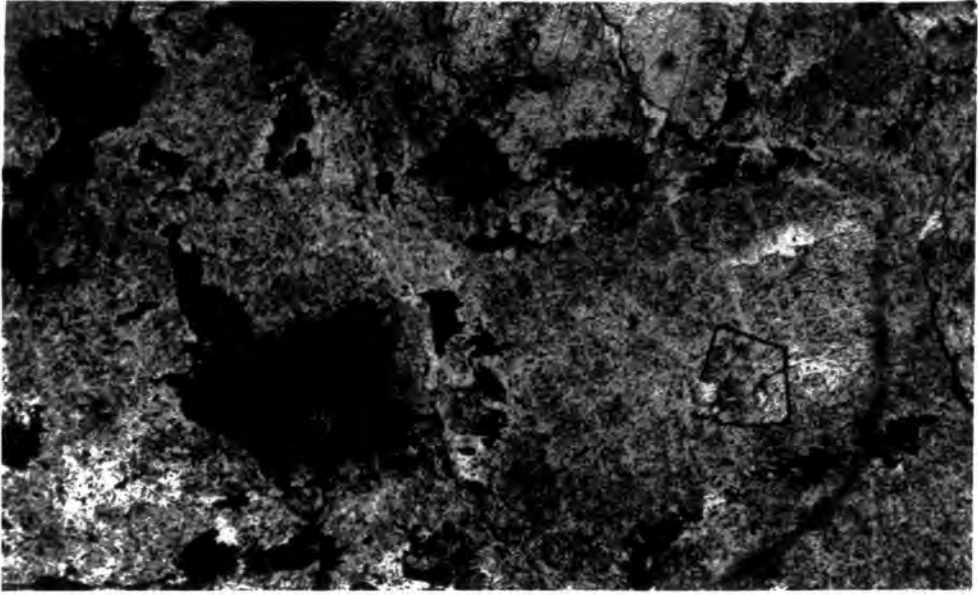
Fig 3.21. Interstitial orthopyroxene crystal being made over to hornblende, kaersutite, and chlorite. XP. Sample U1P4.

Further indications of late-stage liquids available in the peridotites are provided by veins cutting the peridotites of units 1 and 2/3. These are coarse-grained and unchilled, and are very similar in appearance to the "contemporaneous ultrabasic veins" described by Brown (1956) and Butcher (1985). However the veins examined in the LELS are all highly fractionated, and are teschenitic or syenitic rather than ultrabasic. They all have clinopyroxene, as large neutral-coloured irregular crystals, which may be rimmed by dark-blue amphibole or chlorite (Fig 3.22), alkali feldspar, and abundant Fe-Ti oxides. Some veins have abundant plagioclase, showing intense normal zoning over a more homogeneous calcic core; in others perthitic alkali feldspar is dominant. Zircon and sphene occur widely in small quantities; apatite is very abundant (Fig 3.23); a pale greenish yellow mineral with high birefringence and straight extinction forming tiny elongate crystals, and more rarely, thin overgrowths on clinopyroxene may be aegirine. Kaersutite is not uncommon, usually as small inclusions within the large clinopyroxene crystals. Fibrous zeolites and possibly analcime also occur in small quantities. Kitchen (1985) has described similar veins in CS peridotites from near Long Loch. The presence of both silica oversaturated (orthopyroxene) and undersaturated alkaline (kaersutite, analcime, aegirine) assemblages associated with LELS peridotites is curious. The alkaline assemblage seems to be later, in that orthopyroxene is out of equilibrium wherever seen, being made over to the amphibole-rich assemblage. The liquids available at very late stages to form veins when the peridotites were cool enough to undergo brittle fracturing are thoroughly alkaline.

3.C.1.c Sulphide minerals

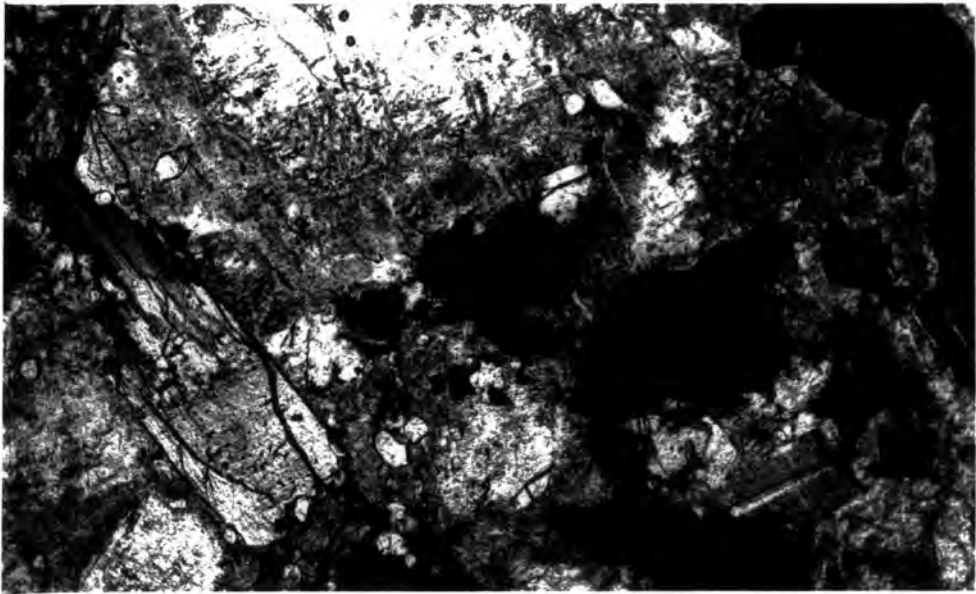
Sulphide minerals are not uncommon in trace quantities in Rhum peridotites (Volker, 1983), however unit 1 of the LELS is strikingly rich in sulphide blebs of large size, which may form 5% of the rocks.

The sulphide minerals in unit 1 peridotite



1 mm

Fig 3.22. Pyroxene-syenite vein from unit 1 peridotite. Augitic pyroxenes are set in perthitic alkali feldspar. Many of the pyroxenes are rimmed by deep blue amphibole and/or chlorite. Small zircons and sphenes occur in the perthite. PPL. Loc 153. NM40679451.



1 mm

Fig 3.23 Teschenitic vein from unit 2/3 peridotite. Consists of intensely zoned plagioclases with altered rims, augite with blue amphibole overgrowths, and abundant apatite and magnetite. Loc 163. NM 40719696.

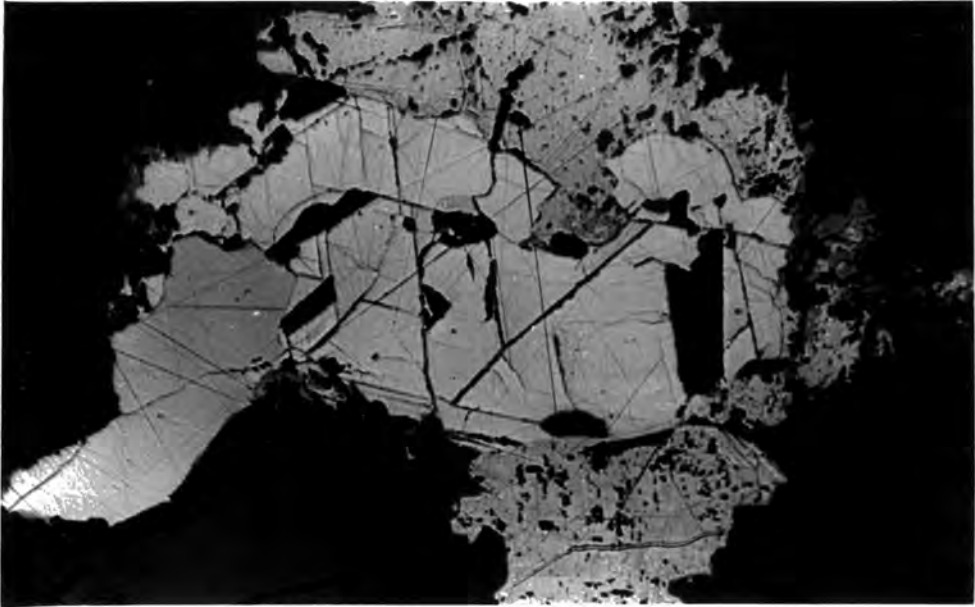


Fig 3.24 Composite sulphide bleb from unit 1 peridotite. Consists of chalcopyrite (c), pentlandite (pn) and pyrrhotite (po). Partially uncrossed polars. Sample U1P2.

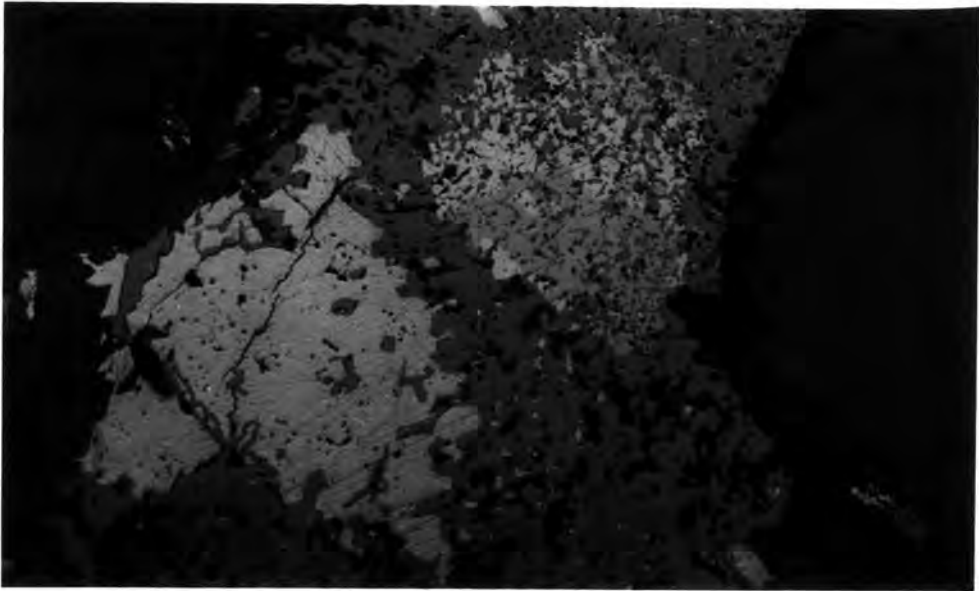


Fig 3.25 Magnetite/sulphide intergrowth between olivine crystals in unit 1 peridotite. Partially uncrossed polars. Sample U1P3.

form intercumulus blebs and masses which are locally large enough to enclose several olivine crystals. Sulphides are not seen as inclusions within olivine crystals (cf Volker, 1983) nor are they associated with chrome-spinel (cf Young, 1984, and Dunham and Wilkinson, 1985). The mineralogy is fairly simple: pentlandite, magnetite, pyrrhotite and a little chalcopyrite. This is a common assemblage found in many layered basic and ultrabasic complexes. Pentlandite and pyrrhotite usually form coarse-textured composite grains (Fig 3.24), or smaller dispersed blebs intergrown with fine-grained magnetite, which may coalesce to form larger masses poikilitically enclosing magnetite crystals (Fig 3.25). The largest magnetite/sulphide blebs, which may enclose many olivine crystals, tend to be sulphide-poor at the margins, with large sulphide aggregates in the central parts. Exsolution of pentlandite within pyrrhotite grains is rare (cf sulphides in unit 1 allivalite).

3.C.2 Peridotite/allivalite contacts

Several types of peridotite/allivalite contact can be distinguished in the LELS.

(i) Contacts which are planar and the boundary between the layers is sharp, on a grain-size scale. Any lamination present is parallel or sub-parallel to the contact. This is the most common type of contact.

(ii) Contacts with chrome-spinel seams. Only one such contact is seen in the LELS (see 3.B.3). In thin section this shows the chrome-spinel layer, and the peridotite sharply truncating the lamination of the allivalite (Fig 3.26). A similar relationship was found by Young (1984) at the Unit 11/12 boundary. He ascribed this to the thermal erosion of the allivalite by overlying picritic liquid, producing a reaction-crust of chromite.

(iii) Contacts which have been deformed by slumping or loading. In thin section these show mixing of the two populations of cumulus grains: rounded olivines and chrome-spinels from the peridotite, and plagioclase and irregular olivines from the allivalite.

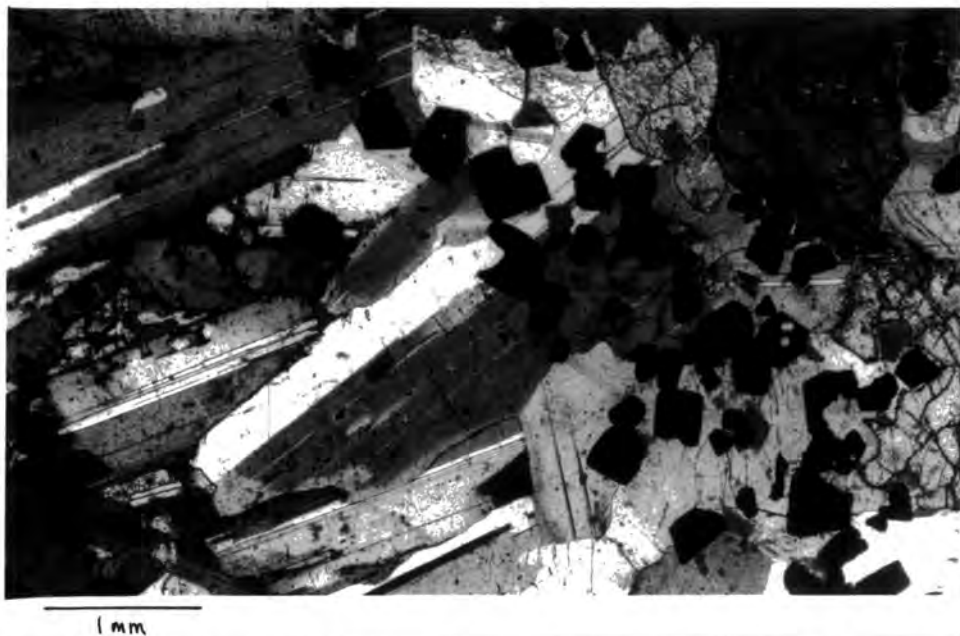


Fig 3.26 Chrome-spinel layer from the lower part of unit 3. The chrome-spinel layer cuts off the lamination of the underlying allivalite. XP. Loc 182. NM40859621.

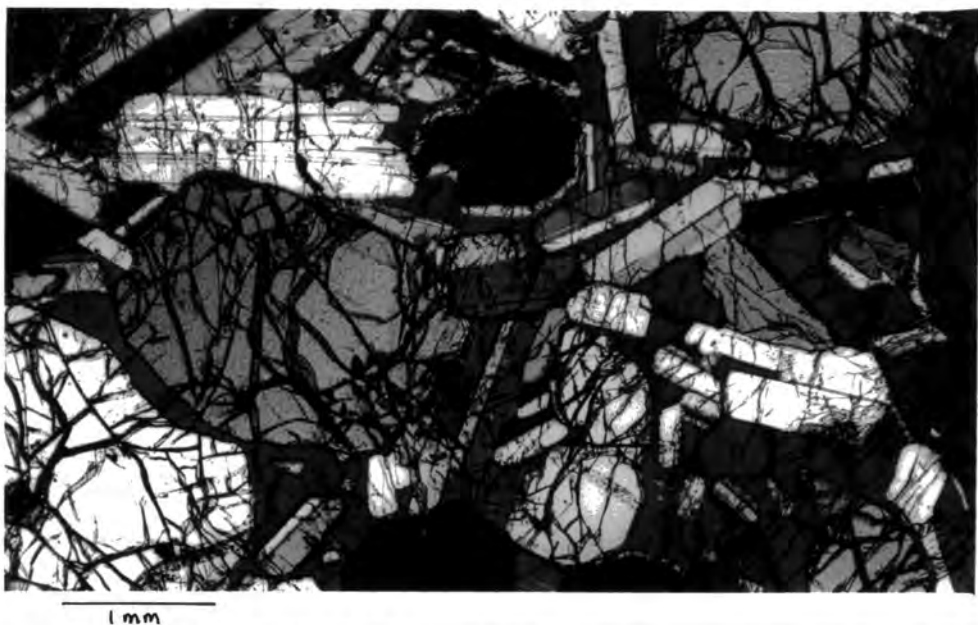


Fig 3.27 Mixed peridotite/allivalite from deformed layer in unit 2. The large olivines are from the peridotite; the smaller ones, and the plagioclases from the allivalite. All are enclosed within a clinopyroxene oikocryst. XP. Sample U2P3.

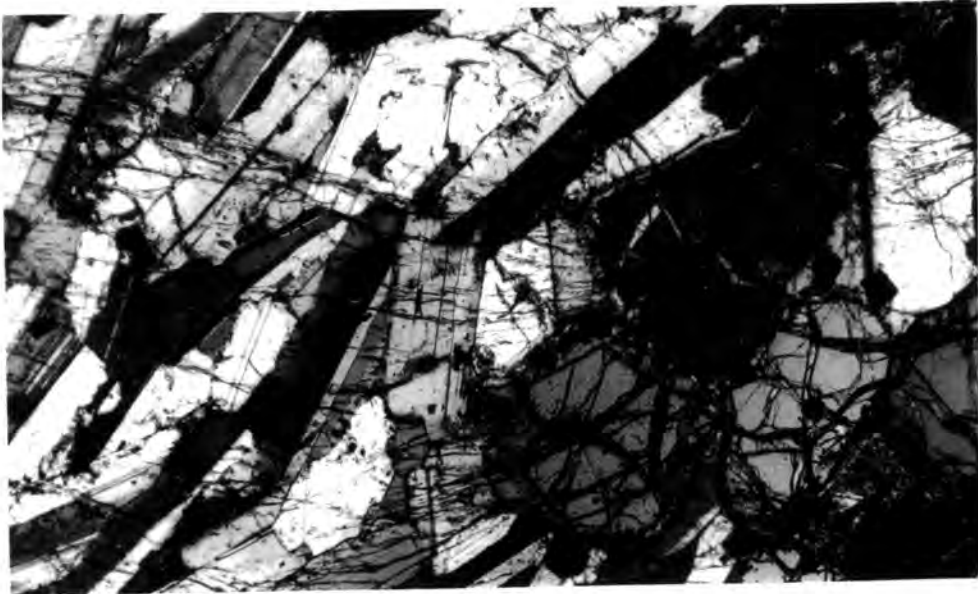


Fig 3.28 Deformed peridotite/allivalite contact from unit 2. In this case there has been little mixing of the cumulus grains. XP. Sample U2P4.

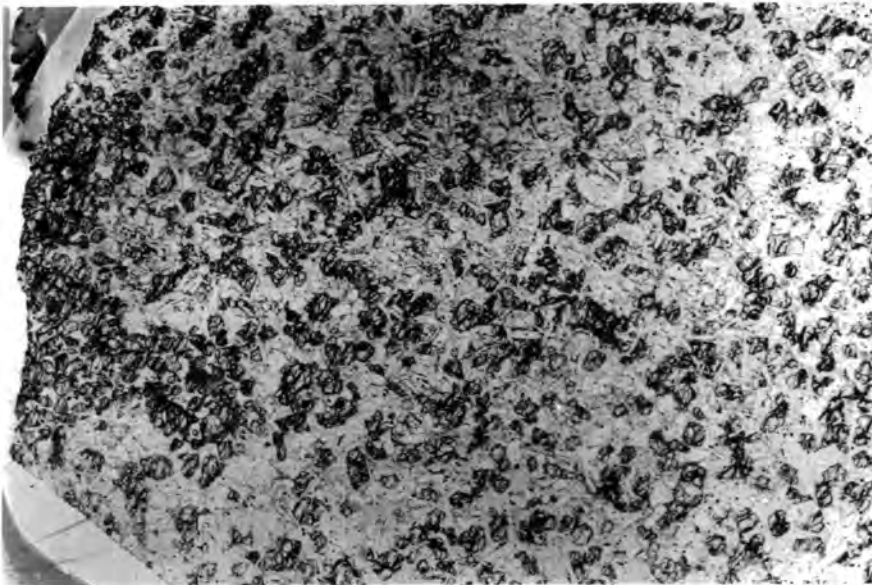
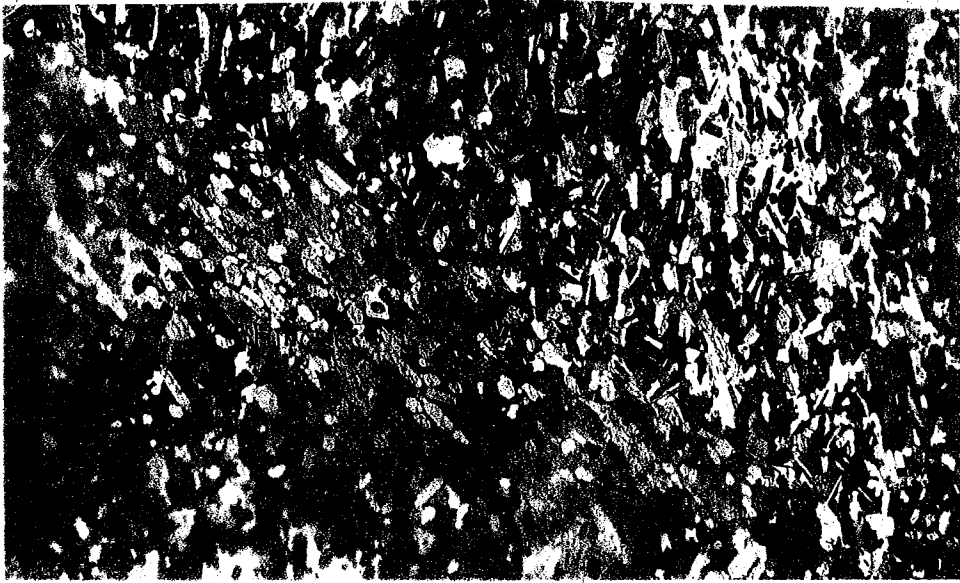


Fig 3.29 Finger sectioned at 90° to its axis, from unit 2 allivalite. There is no evidence of a reaction rim around the finger, although there is a suggestion of depletion of mafic phases in the allivalite around the finger. Loc 217. NM40509474.



WAY UP



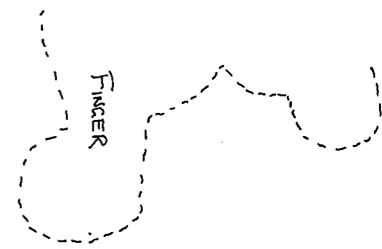
Fig 3.30 Finger from unit 8 allivalite, with elongate olivines in the finger orientated parallel to the finger margins. A few of the cumulus plagioclases show slight upward deflection against the finger. Alan Butcher sample no. GMBFC. Approx 2X.

In some cases the two populations are well mixed (Fig 3.27), in others mixing is less complete (Fig 3.28). The degree of mixing often varies considerably, even within a given layer. This is probably a function of both the severity of the disturbance causing the mixing, and of the degree of consolidation of the cumulates.

(iv) Contacts with finger structures. Despite the evidence from larger-scale field evidence that these are replacement structures, on a microscopic scale they are very similar to type 1 contacts (Fig 3.29), except that the peridotite cuts across allivalite lamination. In a few cases however, a small degree of upward deflection of plagioclase crystals can be seen adjacent to the finger. If elongate olivines are present in the peridotite, these are aligned parallel to the finger margins (Fig 3.30; see also Butcher et al, 1985). This implies that the olivines in the peridotite were much more mobile than the plagioclases in the allivalite, as the olivines have been capable of being rotated, or growing from a melt, while the plagioclases have preserved earlier structures with little deformation.

(v) Contacts gradational on a scale of 10cm - 2m. In the LELS these are mainly found in unit 5. The main peridotite grades up into the overlying allivalite over a distance of about 2m. This zone is clinopyroxene rich peridotite at the base, and olivine-rich allivalite at the top. The intervening rocks are well layered, the layering distinguished by variations in the quantities of olivine + poikilitic clinopyroxene, and cumulus plagioclase + olivine. The cumulus plagioclases show a marked normal zoning, with minor oscillations (Fig 3.31).

The minor peridotite within unit 5 allivalite has a sharp top, but a gradational base. A section across the lower contact is shown in Fig 3.32. Abundant elongate olivines appear in the upper part of the allivalite, and the amount of cumulus plagioclase diminishes with height until it disappears, over a distance of about 0.5m. The olivines in the basal part of the peridotite are skeletal and elongate, but further



2x

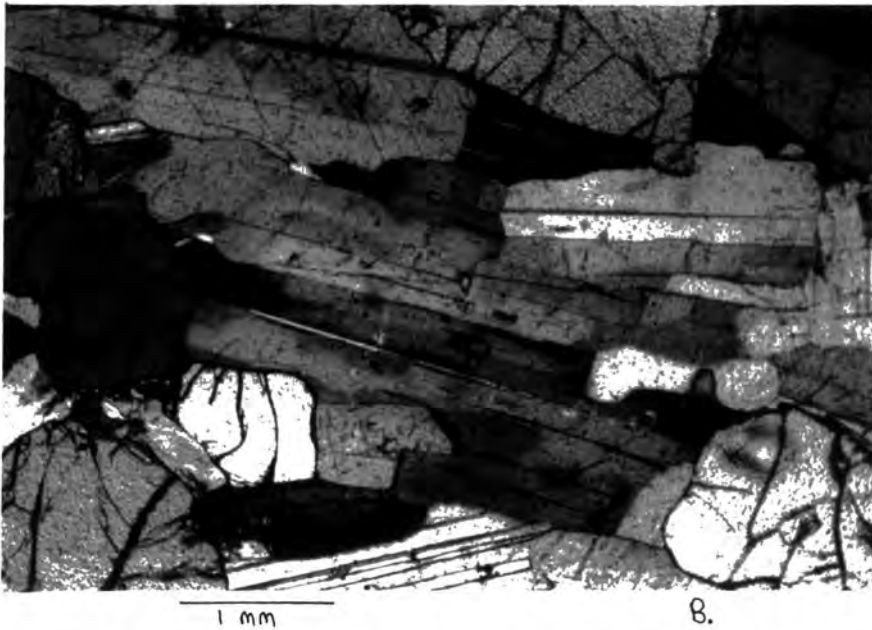
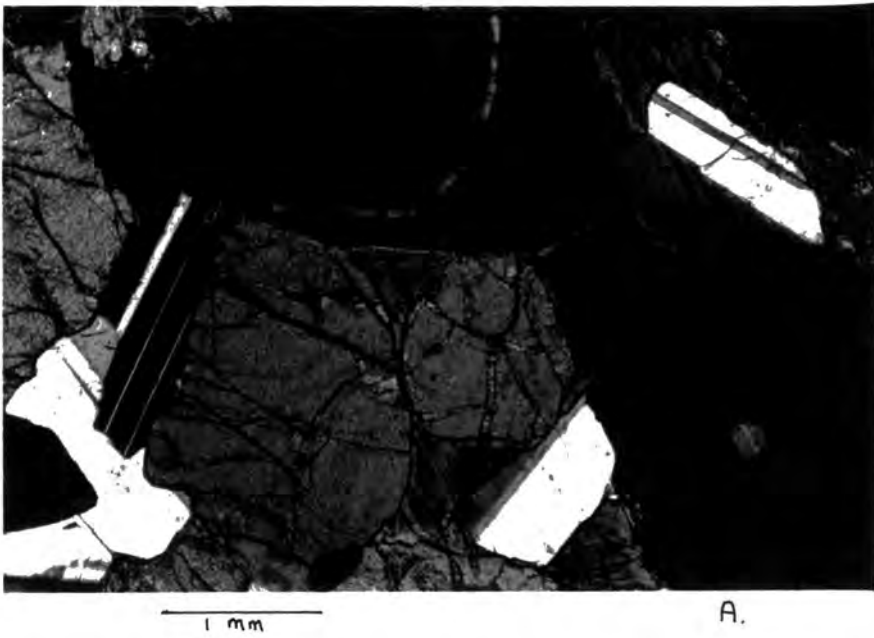


Fig 3.31 a. Olivine-rich layer from the gradational contact at the base of unit 5 allivalite. Note presence of cumulus plagioclase which distinguishes this from normal peridotites.

b. Plagioclase-rich layer just above 3.31a.

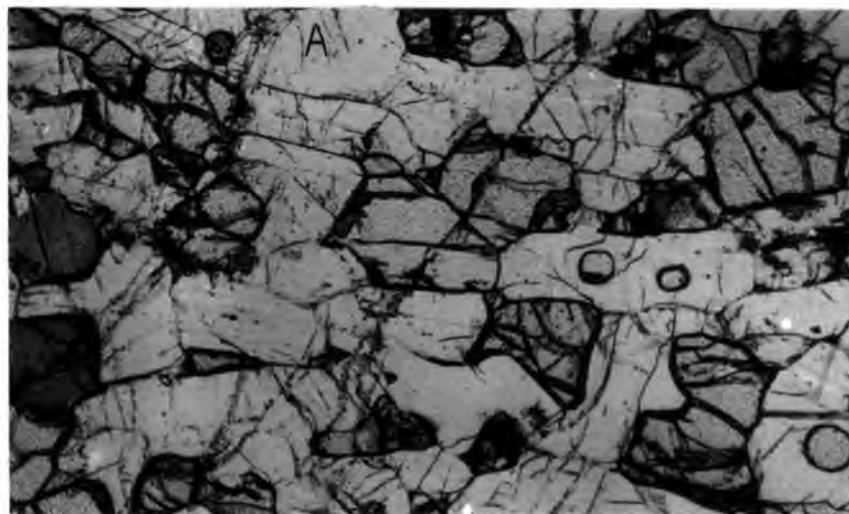
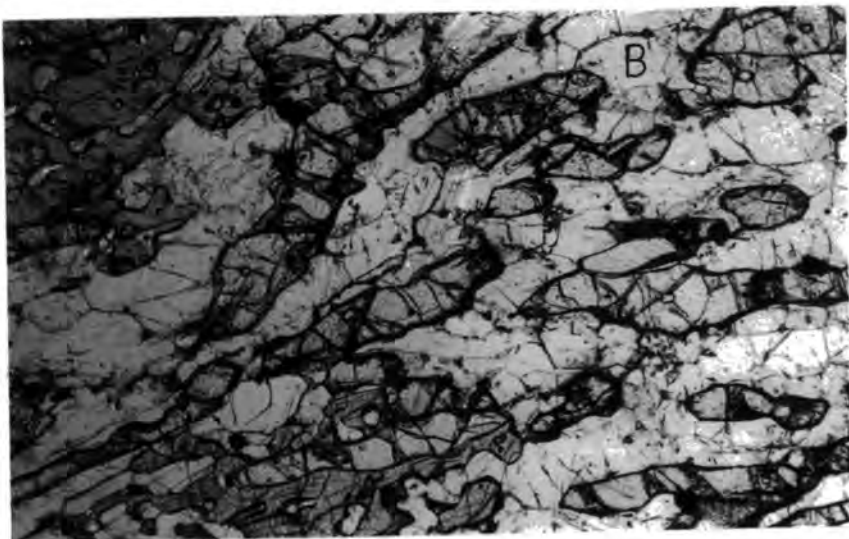
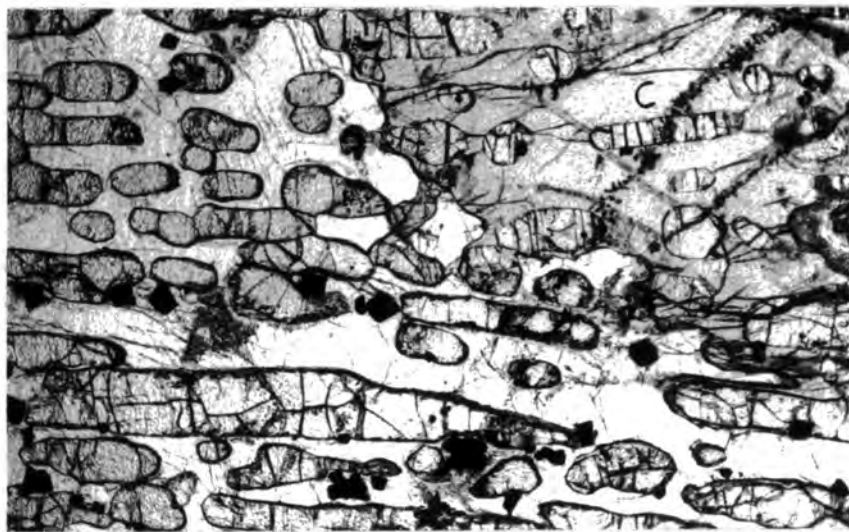


Fig 3.32 a Olivine rich allivalite 1.6m below the minor peridotite within unit 5 allivalite. PPL. Sample U5A15.

b Allivalite with elongate olivines from lower part of gradational contact zone. 1.4m above 3.32a. PPL. Sample U5A16.

c Peridotite from top of gradational contact zone. 0.2m above 3.32b. PPL. Sample U5A17i.

up the rounded-granular habit becomes dominant.

3.C.3. Allivalites

The allivalites are characterised by the presence of cumulus plagioclase. The main minerals are plagioclase, olivine, clinopyroxene, orthopyroxene, and ilmenite, with lesser amounts of phlogopite, zeolites, clinozoisite, hornblende, chlorite, sulphides, apatite, sphene, and locally quartz.

3.C.3.a Textures

Plagioclase forms >50% of all allivalites except locally, in thin laminae which may consist largely of clinopyroxene or olivine.

Plagioclase crystals are often laminated, particularly in rocks with little clinopyroxene. Indeed there is a rough inverse correlation between the amount of clinopyroxene and the development of lamination. In individual specimens lamination is often poorly developed, or absent, where the crystals are enclosed in clinopyroxene oikocrysts, while outside the oikocrysts lamination is pronounced (Fig 3.33). This contrasts with the situation in peridotites where lamination is unaffected by enclosure (Fig 3.32c). There is also a tendency for the density of plagioclase crystals within oikocrysts to be much lower than outside. The same situation occurs where olivine forms oikocrysts enclosing plagioclase, although this is much rarer.

In the case of peridotites this low crystal density was ascribed to post-cumulus textural modification (section 3.C.1) but in allivalites this phenomenon occurs in rocks which are clearly not in textural equilibrium, and it occurs regardless of whether the oikocryst is clinopyroxene or olivine, suggesting that this is not a major factor here. In addition, textural equilibration in peridotites does not affect lamination of the crystals; thus it is proposed that both the low plagioclase crystal density and the lack of lamination are early features of allivalites, which are preserved only where oikocrysts protect them



1 mm

Fig 3.33 Allivalite from unit 5. The plagioclases enclosed in the clinopyroxene oikocryst are unlaminate, while those outside display good lamination. XP. Loc 14b. NM39589721.



1 mm

Fig 3.34 Contact between coarse and fine grained layers in unit 3 allivalite. The fine grained layer shows a high degree of textural equilibration. XP. Loc 183. NM40799620.

from the effects of later compaction. The cumulus plagioclase crystals within oikocrysts often do not form touching crystal frameworks; assuming that the oikocrysts do not conceal cumulus clinopyroxene cores, this implies that settling of plagioclase was not a major factor in producing allivalites.

Some allivalites may have primary lamination. Where chrome-spinel seams truncate the lamination of underlying allivalite, the lamination must have developed at a very early stage, before formation of the oxide layer.

Sudden changes in plagioclase grain size define certain types of layering, particularly common in units 1 and 3 (Fig 3.34). These layers are usually somewhat lensoid in form. Fine-grained layers have been described by Thy and Esbensen (1980) from Lille-Kufjord, and ascribed to fluctuations in the nucleation rate. However these have since been shown to be flattened xenoliths (R.S.J. Sparks, pers comm). The LELS layers show an overlap of grain sizes at the layer boundaries (Fig 3.34), which might suggest a primary "cumulate" origin. However texturally they are very similar to anorthosite xenoliths seen in units 4 and 5 (section 3.C.3.d), including the presence of rare large clustered plagioclase crystals. It is proposed that these layers are xenoliths of plagioclase-rich material which was poorly consolidated when brought to the floor of the magma chamber, and was flattened during deposition and compaction. Pyroxene oikocrysts were able to grow across the xenolith/ cumulate boundary prior to compaction.

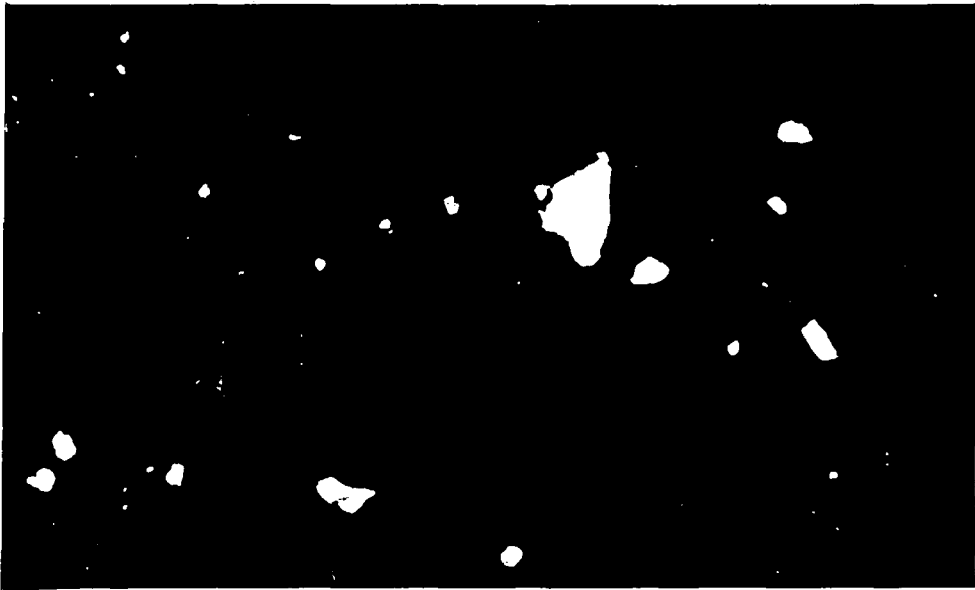
3.C.3.b Minor phases in allivalites

Most allivalites contain small quantities of minerals other than those mentioned above. Phases recorded include clinozoisite, phlogopite, hornblende, fibrous zeolites, apatite and sphene. Using autoradiography of polished slabs, Williams (1978) was able to detect tiny crystals of zirconolite and baddelyite in the mesostasis of LELS rocks, but these have not been definitely identified in this study.



1mm

Fig 3.35 Clinozoisite-rich "clot" in allivalite from unit 3. Other minerals include sphene (s), hornblende (h), prehnite (p) and chlorite (c). The large grain at the top left is an orthopyroxene, much altered to amphibole; at the top right is a plagioclase crystal. PPL. Sample U3A2.



1mm

Fig 3.36 Small dispersed sulphide blebs in unit 1 allivalite. Partially uncrossed polars. Sample U1A3.

Clinozoisite is not uncommon as small patches occupying the interstices between plagioclase crystals. However, locally it forms larger "clots" up to 7mm in diameter, intergrown with hornblende, prehnite, sphene, phlogopite and apatite. An as-yet-unidentified brown mineral is common as tiny radiating masses with high birefringence in the interstices between clinozoisite crystals (Fig 3.35). These assemblages occur in rocks containing fresh olivine, although adjacent to the larger clots olivine is often altered to fine grained talc(?), chlorite or phlogopite. Against these larger clots plagioclase may be slightly sericitised, and may be partially replaced by clinozoisite, although the smaller patches do not appear to be associated with any alteration.

There is some evidence from the Marginal Suite (Fig 2.9) and from alkaline veins in the peridotites near the Long Loch, that clinozoisite may be on the liquidus of certain magmas in the Rhum complex. It is suggested that these clot assemblages are related to local late-stage enrichment in water, and that they crystallised, at least in part, from a melt, rather than forming from previously existing minerals. It is difficult to see how they could be produced by pervasive or channelled hydrous alteration of the cumulates, given the lack of localisation along fractures, and the close association with fresh olivine and plagioclase. These clots are particularly common in the middle parts of unit 4 allivalite, and in unit 3 allivalite.

Allivalites within a few metres of the marginal suite sometimes have small quantities of a granophyric mesostasis.

3.C.3.c Sulphide minerals

The allivalite of unit 1, like the peridotite, is remarkably rich in sulphide blebs. In the basal parts of the allivalite they may form up to 5% of the rock, and the blebs may reach 1cm in diameter. The mineralogy is similar to peridotite assemblage, except that chalcopyrite forms a larger proportion of the blebs in

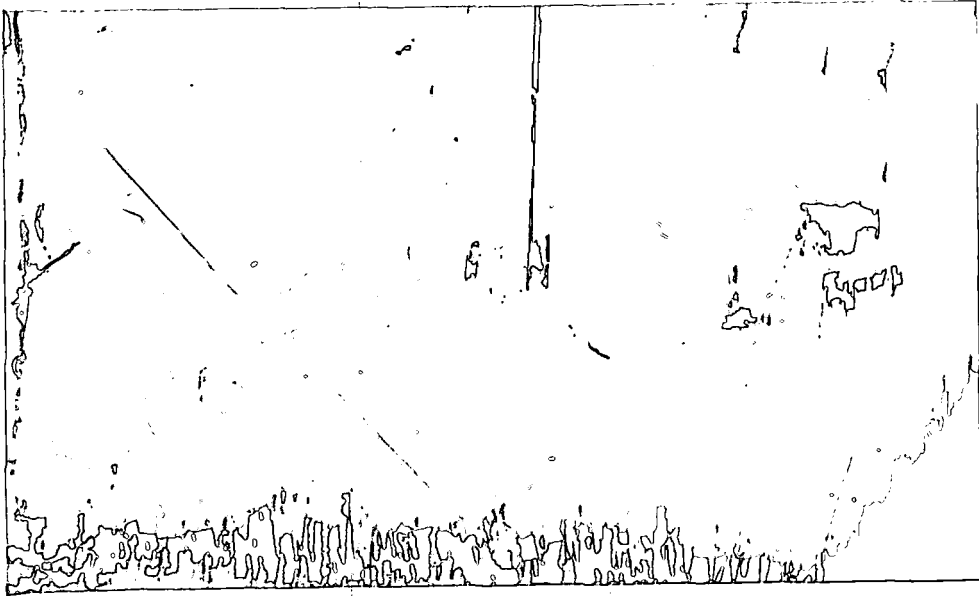


Fig 3.37 Evolution lamellae of pentlandite in large pyrrhotite grain from unit 1 allivalite. Note large, early formed "flame" lamellae, and later, finer and more regular lamellae. Partially uncrossed polars. Loc 152a. NM40649452.

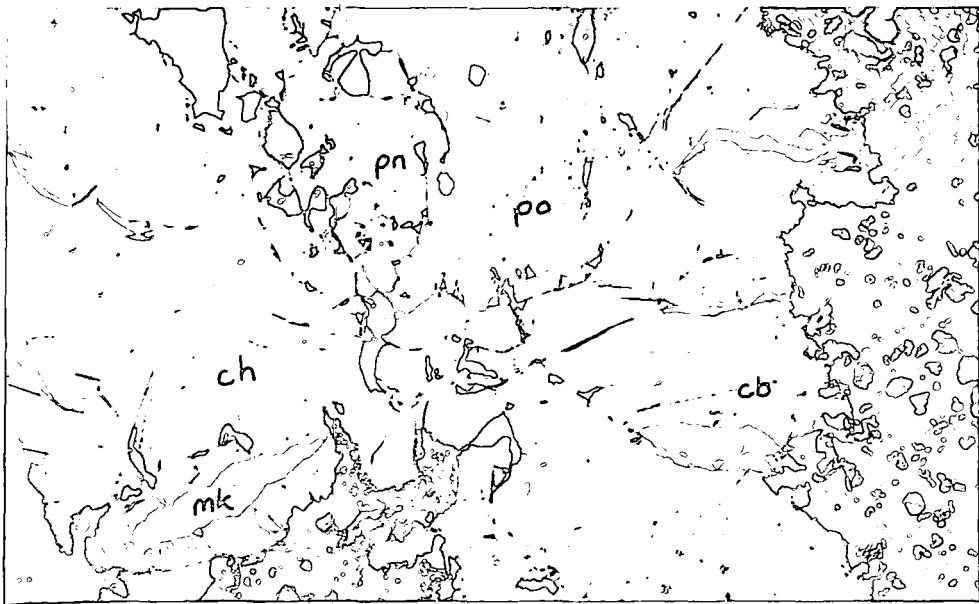


Fig 3.38 Composite sulphide bleb from unit 1 allivalite, consisting of pyrrhotite (po) with pentlandite exsolution, chalcopyrite (ch), pentlandite (pn), mackinawite (mk) and cubanite (cb). The bleb is rimmed by a fine-grained magnetite/sulphide intergrowth. PPL in oil. Loc 152a. NM40649452.

the allivalite, and magnetite is less abundant. The smaller blebs (Fig 3.36) are usually composite grains of pyrrhotite, chalcopyrite and pentlandite. The pyrrhotites show well developed flame and lamellar exsolution of pentlandite, particularly in the larger grains (Fig 3.37). The largest blebs show complex exsolution with lamellae of cubanite and mackinawite in the chalcopyrite (Fig 3.38). In addition to the fine-grained magnetite found around some of the blebs, large cumulus ilmenites are also fairly common in the basal parts of unit 1 allivalite. Further up the allivalite, the sulphide blebs diminish in size and abundance; the proportion of pentlandite also diminishes.

The sulphide-rich layer in unit 3 contains only small composite grains of pyrrhotite and chalcopyrite.

3.C.3.d Xenoliths

The xenoliths found throughout the allivalites of the LELS fall into three main groups: (1) fine-grained basic rocks, sometimes associated with calc-silicates, here termed beerbachites, (2) fine-grained plagioclase-rich rocks often well layered, termed anorthosites and (3) coarser grained gabbroic rocks, termed gabbros.

Xenoliths are almost exclusively restricted to the allivalite layers, although Smith (1985) records a single calc-silicate xenolith in the peridotite of unit 2. Wherever allivalite blocks are enclosed in peridotite in the LELS, they are associated with finger structures and replacement, and thus are not true xenoliths.

(i) Beerbachites

Brown (1956) recorded peridotite xenoliths as being abundant in parts of the LELS. However, all the brown-weathering xenoliths examined here have proved to be fine-grained granular rocks, very similar in texture and mineralogy to the beerbachites reported by from Ardnamurchan. Peridotite xenoliths do occur in Rhum, eg in allivalites of the CS to the north and west of Long Loch, but these retain their cumulate texture (I.Young,

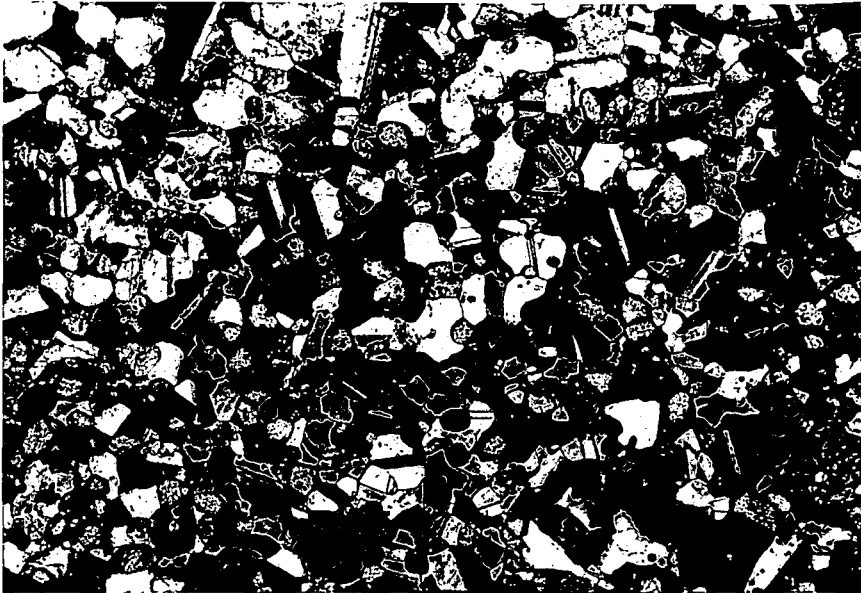


Fig 3.39 Beerbachite xenolith from unit 5, consisting of plagioclase, olivine and clinopyroxene. XP. NM 40199499.



Fig 3.40 Beerbachite xenolith from unit 4 with "clots" of calc-silicate minerals (c), rimmed by fassaite (f). Natural light. Loc 176a.

pers comm). A typical beerbachite is shown in Fig 3.39. They consist mainly of equal-sized polygonal grains of plagioclase, olivine, clinopyroxene, magnetite, and often orthopyroxene. Most inter-grain angles are about 120° , regardless of the phases involved, but clinopyroxene occasionally forms sub-poikilitic grains, or rims around other phases. A faint lamination is often evident. This has probably developed during recrystallisation, as parallel planar structures are absent in these rocks. A few beerbachites contain larger porphyroblasts of plagioclase or olivine. Irregular veins of clinopyroxene or fine-grained plagioclase are common. The latter particularly, are often associated with clots rich in calc-silicates. These are invariably zoned with an outer zone of fassaite, and a core of intergrown garnet, diopside, sometimes plagioclase, and small quantities of vermiculite (Fig 3.40). Where the fassaite adjoins the beerbachite, there is often a zone of intergrown magnetite blebs (Fig 3.41). Across this zone the optical properties of the pyroxene changes, a yellow tint becoming increasingly intense towards the core of the clot, and associated with this, an increase in the dispersion. The innermost fassaites show intense anomalous blue interference colours. A few of these clots contain a little clinozoisite, or low-Fe epidote.

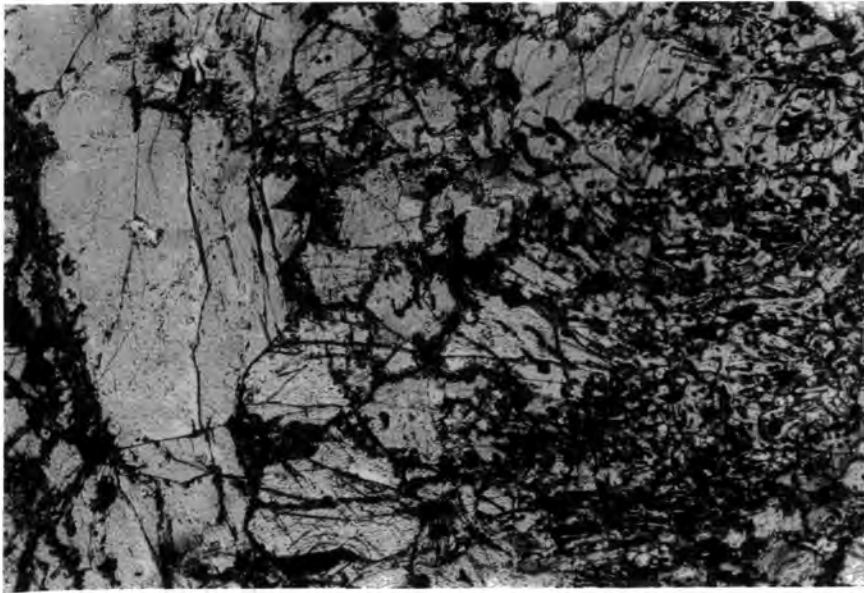
This association of calc-silicates with fine-grained basic hornfels strongly suggests that these rocks were originally amygdaloidal basalts, and thus represent material derived from the country rocks of the intrusion. Amygdale assemblages of calcite, calcium zeolites and celadonite or chlorite would have roughly the correct chemistry to produce the observed metamorphic minerals. The Rhum ultrabasic complex is nowhere seen in contact with amygdaloidal basalts; presumably they formed roof or wall rocks to the upper part of the magma chamber, since eroded away. This implies a high-level origin for the ultrabasic complex, with the magma chamber in contact with hydrothermally altered basalts. Amygdaloidal basalts which pre-date the ultrabasic rocks are seen in the complex fault zone on

the south-east flank of Beinn nan Stac (Smith, 1985).

(ii) Anorthosites

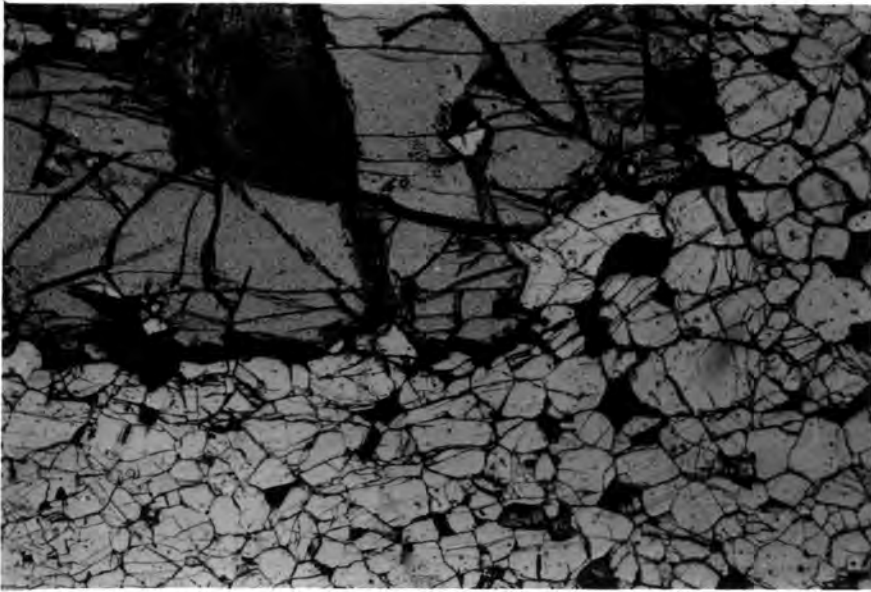
The anorthosite xenoliths are usually angular and well layered and laminated. Mafic minerals are almost invariably poikilitic in habit, although large well-formed orthopyroxenes occur in one specimen (Fig 3.42). The main mafic silicates are clinopyroxene and olivine, although the sample with the large orthopyroxenes contains a thin layer rich in inverted pigeonite (Fig 3.43). Magnetite blebs are locally common. The layering in these rocks is defined mainly by changes in the abundance, or types of mafic minerals present, and to lesser extent, by changes in grain size. The layering is usually on a 1mm-1cm scale. Some layers consist of 100% plagioclase. Optical zoning is faint, or absent in the plagioclases, which are generally bytownites. A few specimens contain larger, sometimes glomeroporphyritic plagioclase crystals. These xenoliths are thus very similar in texture to the lensoid, fine-grained, plagioclase-rich layers seen in units 1 and 3. It may be that these layers formed from "soft", xenoliths of the same material, which was able to deform during deposition and compaction, whereas the angular xenoliths of units 4 and 5 represent better consolidated material.

The strongly layered and laminated aspect of the anorthosites, together with their mineralogy suggests that they may be of cumulate origin. However the grain sizes of both the xenoliths and the fine-grained layers are very similar to those of the beerbachites, and locally, where particularly rich in mafic minerals, they resemble some of the beerbachites. Given the high degree of textural equilibration in these fine-grained rocks, it is difficult to say much about their original textures, however it is unlikely that the anorthosites represent metamorphosed volcanic rocks in view of their high plagioclase content. Unlike the beerbachites the anorthosites are never associated with calc-silicate minerals, further suggesting a different origin. A sedimentary origin is also possible; this



1 mm

Fig 3.41 Outer margin of fassaite zone from a calc-silicate clot. Note the decrease in pyroxene grain size, and the exolution of magnetite towards the beerbachite. Loc 20b. NM 39799715.



1 mm

Fig 3.42 Large (cumulus?) hypersthene crystal in fine grained anorthosite xenolith from unit 4. PPL. Loc 194c. NM40299697.

might explain the layering, but again it is hard to envisage sediments of the correct bulk composition. A cumulate origin is thus preferred.

It is tentatively proposed that while the beerbachites represent the basaltic country rocks, the anorthosites represent fine-grained evolved cumulates formed at the roof of the intrusion. The abundance of orthopyroxene may be explained by the ponding of light magma, contaminated by silicic country rocks at the walls, under the roof. The development of such an upward convecting boundary layer would be very likely, if as has been suggested (chapter 2) the Rhum complex is largely in situ, and walled by low melting-point arkoses and granophyres.

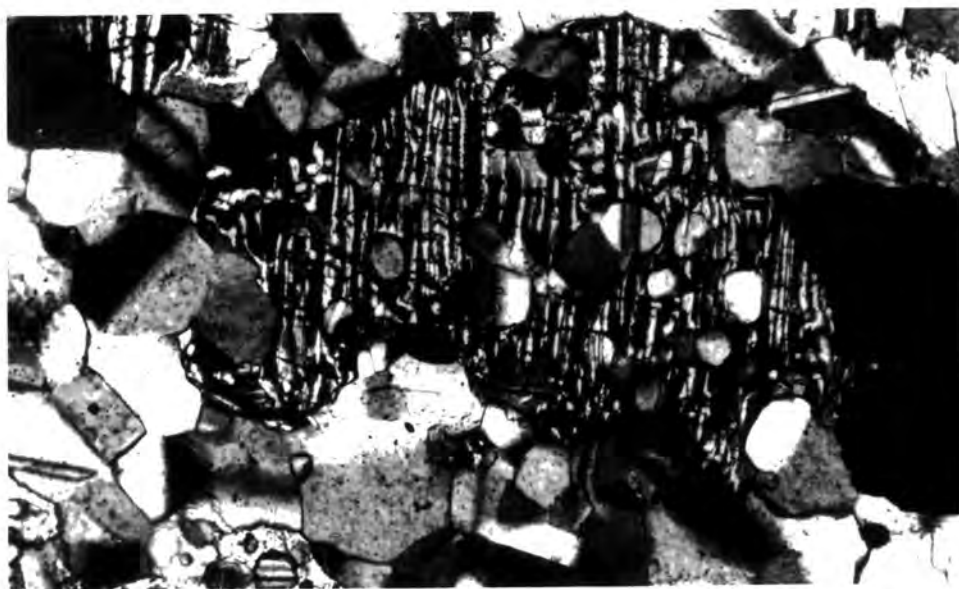
The roof rocks, both cumulates and basalts, were able to sink or be carried down to the floor of the magma chamber throughout the formation of the LELS allivalites. Well-consolidated cumulate material is most abundant in units 4 and 5, where the greatest abundance of beerbachite is found, suggesting that considerable quantities of roof rocks were dislodged during the formation of these units.

(iii) Gabbros

The gabbro xenoliths are coarser than the others, and their textures are very similar to those of the rocks in which they are enclosed (Fig 3.44). They are extremely abundant in parts of unit 5 allivalite, of which they may form >50%. They are characterised in thin section by intense clouding of mafic phases by exsolved magnetite. Many specimens are rich in poikilitic orthopyroxene. As well as cumulate textured gabbros, rocks with sub-variolitic textures are also found.

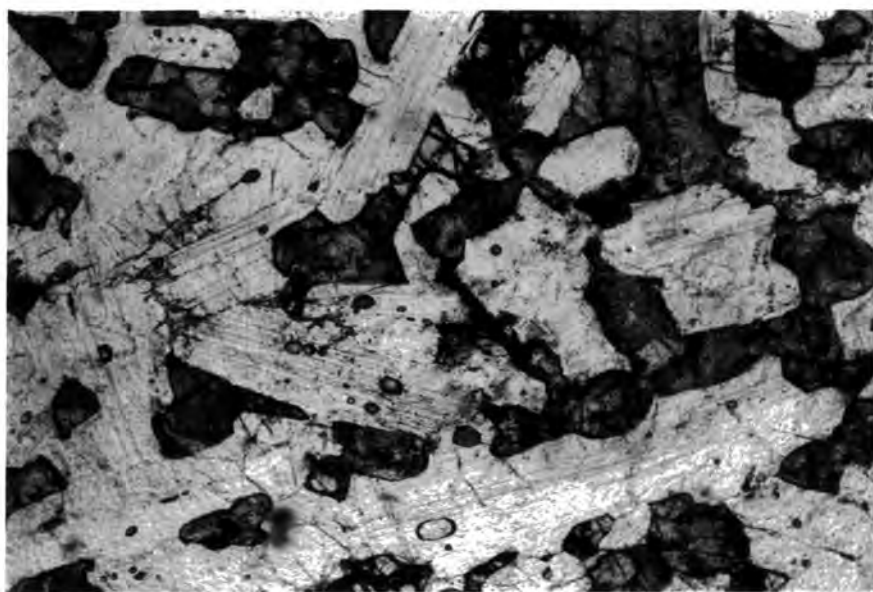
3.C.4 Gabbro plugs and sheets

The main minerals are clinopyroxene and plagioclase. The former is usually pale brown with marked normal zoning. Sector zoning is occasionally well developed. Habit varies from euhedral prisms to ophitic intergrowths with plagioclase. The latter forms narrow laths, generally showing strong continuous normal



0.1mm

Fig 3.43 Inverted pigeonite oikocryst in anorthosite xenolith from unit 4. XP. Loc 194c. NM40299697.



1mm

Fig 3.44 Gabbro xenolith from unit 5 allivalite showing intense clouding of clinopyroxene, and to a lesser extent, of plagioclase. Loc 20c. NM 39799715.

zoning. Other minerals present are Fe-Ti oxides, as large irregular grains; olivine, usually as large altered grains, and green amphibole. A fine-grained mesostasis is often present, usually altered to chlorite; this is one of the best features for distinguishing the gabbros from the clinopyroxene-rich allivalites.

3.D Conclusions

(1) The morphology and distribution of the allivalite and peridotite layers of the LELS have been affected by a number of post-cumulus processes including deformation of poorly consolidated crystal mushes, and later, by replacement of allivalite by peridotite.

(2) The allivalite horizons contain varying quantities of xenolithic material derived from the walls or roof of the magma chamber, including amygdaloidal basalts, which are not now seen as country rocks. This implies a high-level for the magma chamber, not far from its present position.

(3) The layers richest in roof- or wall-derived xenoliths are also richest in orthopyroxene, as are the cumulates seen in these xenolith assemblages. This may suggest ponding of silica rich magmas at the top of the chamber.

(4) There is evidence that some peridotite layers may have been more mobile and permeable than overlying allivalites.

(5) Crystal settling may have been a significant process in the formation of peridotites, but other than the presence of xenoliths, there is no unambiguous evidence in the LELS allivalites for settling being important.

(6) The textures of the cumulates are affected to varying degrees by post-cumulus processes, some of which may be sub-solidus. Most LELS rocks are not in textural equilibrium. Lamination may be a primary feature of olivines in peridotites, but lamination of plagioclase in allivalites mostly originates during compaction. This is not always the case though. Where

lamination is truncated by chrome-spinel seams (unit 3,
unit 11/12) lamination must be a very early feature,
probably primary.

CHAPTER FOUR

BULK-ROCK CHEMISTRY

A selection of rocks from the Marginal Suite, the gabbro plugs and sheets, and the LELS have been analysed by XRF techniques at Durham University. Both major and trace elements were determined on pressed powder pellets. Major element count data, corrected for instrument drift and mass absorption effects, was processed using the program MANAPF4, based on one provided by J. Esson of Manchester University. Trace element data were processed using the program TRATIO, written by R.C.O. Gill at Durham University. Analyses of selected international standards are given in appendix 1.

Particular aims of this work were (i) to examine the chemical variation in the Marginal Suite, and to evaluate possible mixing processes; (ii) to investigate the status of the allivalites of units 4 and 5, which Brown (1956) regarded as intrusive gabbros; (iii) to investigate the relationships between the LELS, the Marginal Suite, and the gabbro plugs and sheets.

4.A THE MARGINAL SUITE

The marginal suite comprises a wide range of compositions from picrites and olivine-rich gabbros, to dioritic and granitic rocks. The field relations (Chapter 2), strongly suggest mixing of mafic magmas and melted country rocks as being an important process in producing the observed variation.

This can be evaluated in a number of ways. Where a suite of rocks covers a wide compositional range (as here), plotting highly compatible elements against highly incompatible ones permits discrimination of mixing and fractionation (Fig 4.1). Using Cr vs Ba, or K_2O , the Marginal Suite falls on a strongly curved trend. Mixing between the most basic and most acid end-members should give a straight line. However this diagram does not show that mixing has not occurred. It

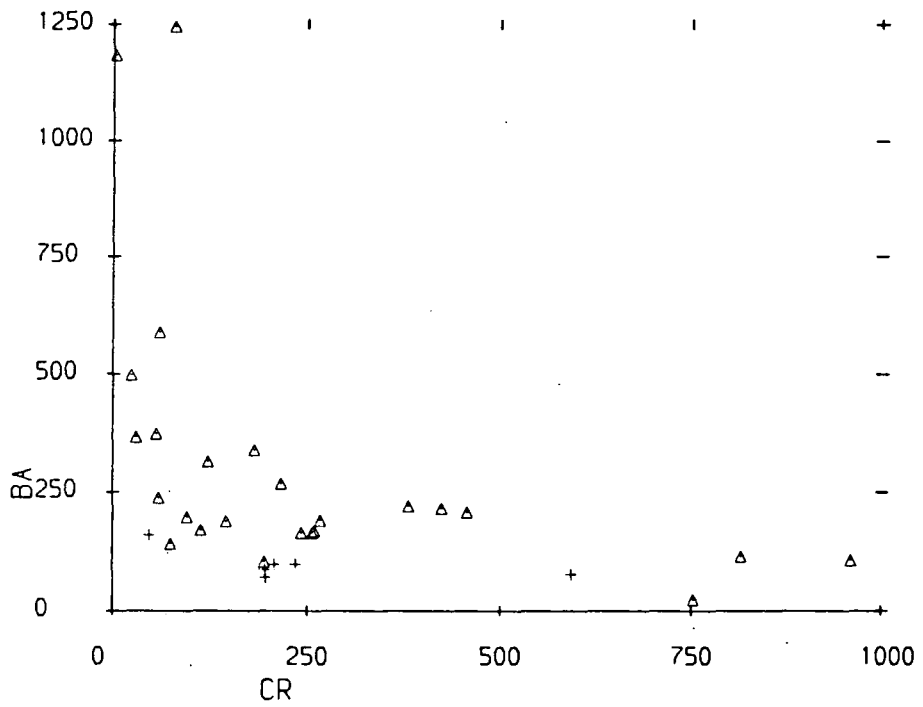


Fig 4.1a Ba vs Cr plot for the Marginal Suite (triangles), and the gabbro plugs and sheets (crosses).

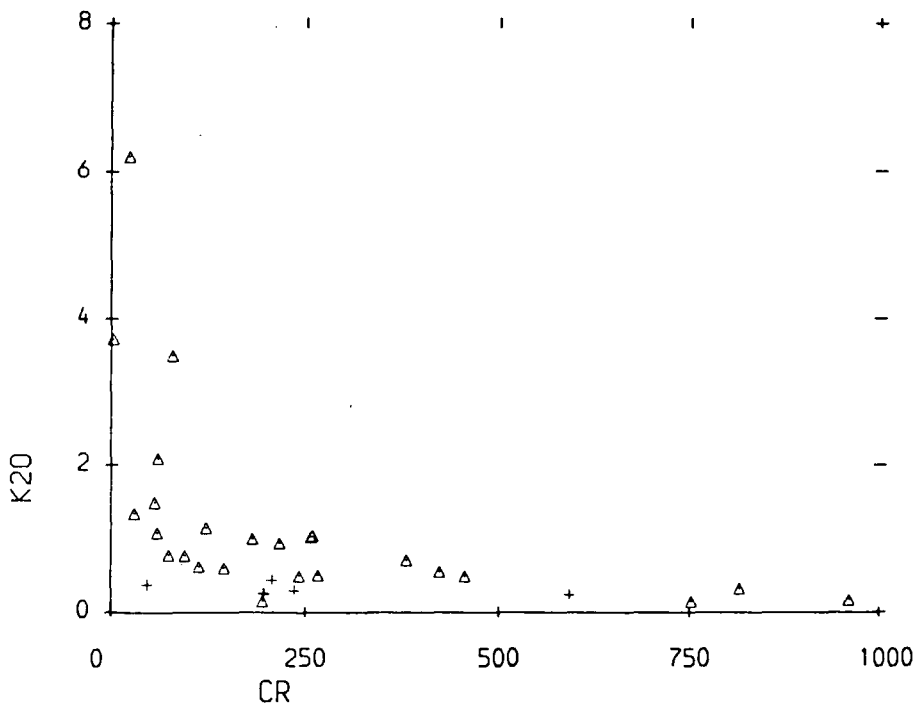


Fig 4.1b Cr vs K₂O plot for the Marginal Suite and the gabbro plugs and sheets. Symbols as above.

does illustrate that most of the intermediate rocks have not been produced by mixing picritic rocks and felsite or sediments, but cannot rule out mixing between low-Cr basic rocks and acid melts. It is noteworthy that several of the basic samples do show slightly enhanced Ba and K_2O , suggesting that small amounts of contamination may have occurred.

Another method for distinguishing fractionation and mixing in tholeiitic sequences has been used by Marshall and Sparks (1984). Ti and P are strongly enriched in intermediate tholeiitic fractionates, while mixing low-Ti,P acid rocks and low-Ti,P basic rocks can only produce low-Ti,P intermediate hybrids. The Marginal Suite shows both trends (Fig 4.2), indicating that some of the diorites are hybrids, while a few are fractionates. The maximum TiO_2 and P_2O_5 contents occur at about 7% MgO; this is higher than the value in other tholeiitic suites where it is usually about 4-5% (see for example Marshall and Sparks, 1984) However the number of samples on the fractionation trend is relatively small and cannot be regarded as a complete sample.

To quantify mixing processes, it is essential to identify the correct end-members. Although picrites occur in the Marginal Suite, they do not seem to have mixed with acid material on a large scale (see above). The only evidence of contamination in these rocks is enhanced incompatible trace elements. Fig 4.2 suggests that more fractionated gabbros (about 10% MgO) may be the usual basic end member, as this is the value at which the mixing and fractionation trends diverge. Picritic liquids may not mix readily with acid melts for several reasons. There is likely to be a considerable viscosity difference, even if the acid melts are locally superheated, and this inhibits mixing (Campbell and Turner, 1986). High density contrasts would also decrease the tendency to mix, and the great difference in liquidus temperatures between picrite and granite may result in quenching of the picrite before mixing could occur. Thus it appears that hot picritic liquids were not prone to mixing with acid melts; only cooler, less

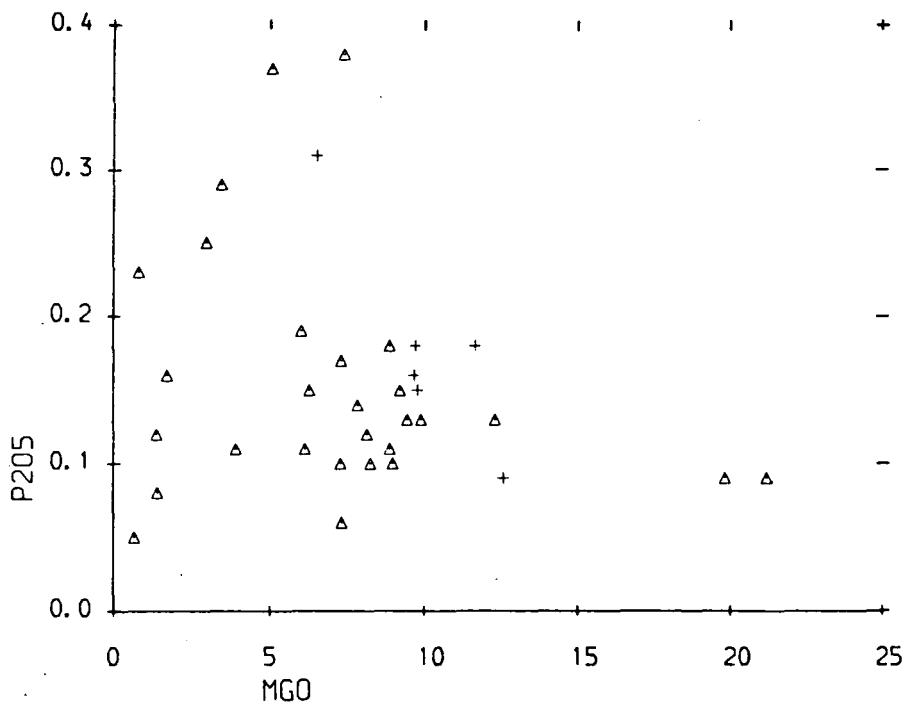


Fig 4.2a MgO vs P₂O₅ plot for the Marginal Suite (triangles) and the gabbro plugs and sheets (crosses).

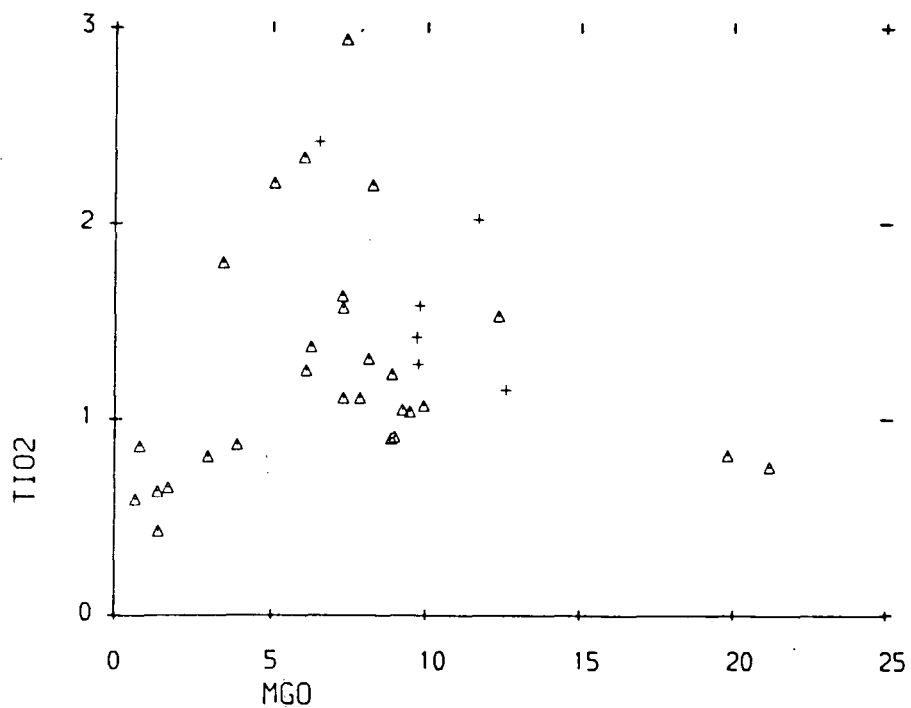


Fig 4.2 b MgO vs TiO₂ plot for the Marginal Suite and gabbro plugs and sheets. Symbols as above.

Name	AV.SLT	LNDSHL	BNSSST	6.48
SiO2	73.64	71.40	79.67	69.80
TiO2	0.63	0.65	0.59	0.86
Al2O3	12.86	13.64	10.56	12.40
Fe2O3	0.46	0.49	0.36	0.59
FeO	3.07	3.29	2.38	3.90
MnO	0.01	0.06	0.05	0.09
MgO	1.36	1.71	0.65	0.80
CaO	1.02	1.18	0.68	2.44
Na2O	2.62	2.73	2.34	3.76
K2O	3.13	3.23	2.86	3.72
P2O5	0.12	0.16	0.05	0.23
LOI	ND	ND	ND	ND
Total	98.92	98.55	100.19	98.59

Trace elements in ppm.

BA	912	1007	769	1184
NB	12	11	12	14
ZR	299	291	356	240
Y	24	23	19	39
SR	183	210	141	223
RB	101	100	91	96
ZN	35	39	21	82
CU	--	--	--	27
NI	10	12	5	27
CR	--	--	--	2

Table 4.1 Analyses of possible acid end-members for the hybrids of eastern Rhum. 6.48 is a felsite from Beinn nan Stac. LNDSHL: average Loch na Dal Shale (=Skye equivalent of Bagh na h-Uamha Grit). AVSLT: average Skye Sleat Group (=Rhum Torridonian). BNSSST: average Beinn na Seamhrig Sandstone (=Skye equivalent of Rubha na Roine Grit). Torridonian data from Donnellan (1981).

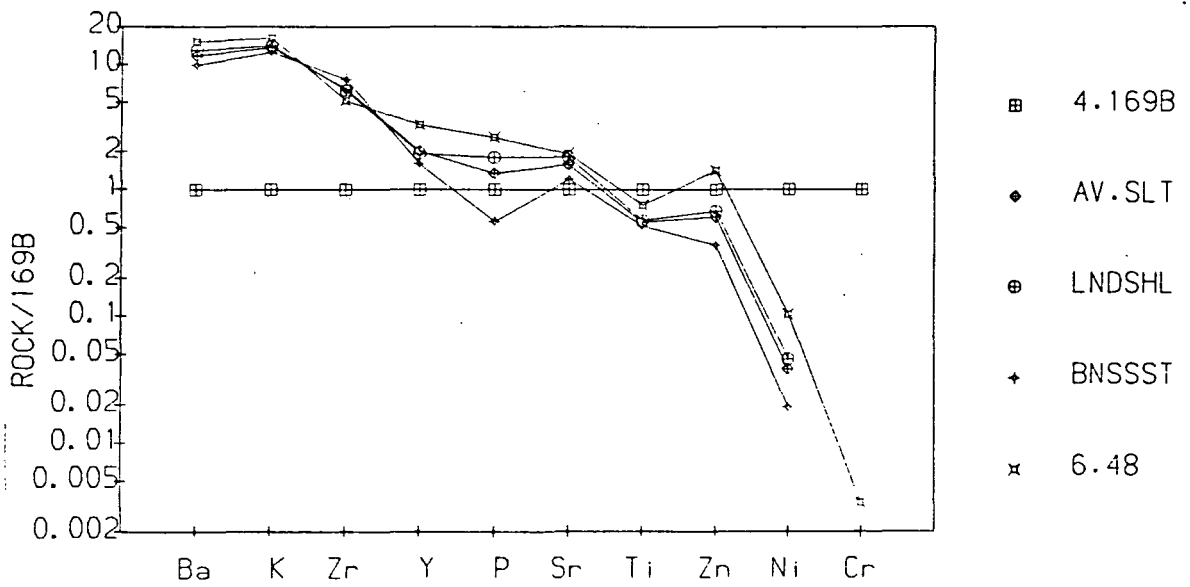


Fig 4.3 Trace-element compositions of various Torridonian sediments and felsite normalised to marginal dyke 169b. Data for Torridonian rocks from Donellan (1981). LNDSHL= Loch na Dal Shale, BNSST= Beinn na Searraig Sandstone, AVSLT= average Sleet Group. These are the Skye equivalents of the Bagh na h-Uamha Shale, the Rubha na Roine Grits, and the Rhum Torridonian respectively.

dense and more viscous basic liquids would mix.

Identification of the acid components is more difficult. Possibilities include Rubh na Roine Grit, Bagh na h-Uamha Shale, and felsite. Detailed chemical data on the Torridonian rocks of Rhum is lacking. However extensive data for the laterally equivalent rocks in Skye is available (Donellan, 1981), and his average values for these units are used in this study. Comparison of these analyses with limited unpublished data for the Rhum Torridonian (R. Greenwood, pers comm) shows good agreement. In the western part of the complex, granophyre is likely to be a major contaminant. Unfortunately the major-element chemistry of these groups is remarkably similar (Table 4.1). In an attempt to resolve this, modified "spidergrams" for the various possible contaminants, normalised to one of the Marginal Suite gabbros, are shown in Fig 4.3. The patterns for the hybrids are shown in Fig 4.4. Assuming that the normalising rock is close to the basic end-member, the hybrids should show patterns parallel to the acid end-member with which they mixed. The patterns for the contaminants are very similar, except for Zn and P, which are > 1 in the felsite, and are < 1 in the Torridonian rocks.

The patterns for the hybrids in most cases are consistent with mixing with these components, although the marked depletion in Ni and Cr, together with -ve Sr anomalies, suggests fractionation combined with mixing for many rocks. The role of felsite and Torridonian rocks is difficult to distinguish. High P hybrids could be explained by felsite contamination; but P also tends to increase with fractionation, so this is not a useful discriminant. Zn does not show much change with fractionation in the gabbro plugs and sheets (Fig 4.5), and thus it may be a better guide to contaminants. Hybrids with Zn markedly greater than 1 on Fig 4.4 must have been contaminated by a high Zn material, ie felsite. Low Zn hybrids may be Torridonian-contaminated.

Palacz (1984), and Palacz and Tait (1985), using Pb and Sr isotopes, argued that the Rhum ultrabasic magma

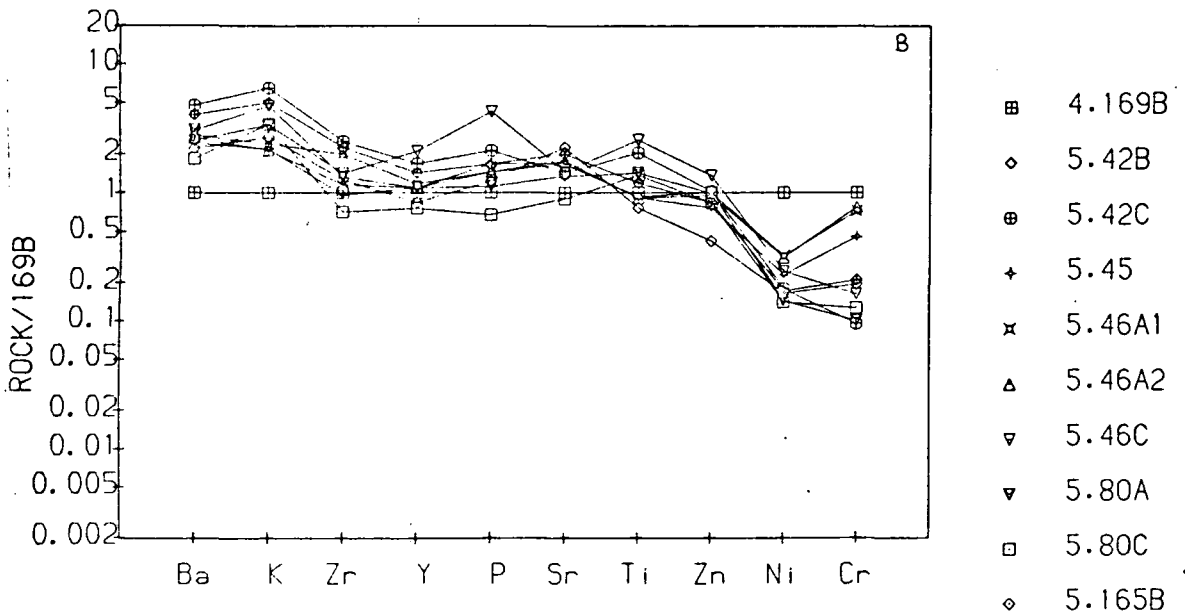
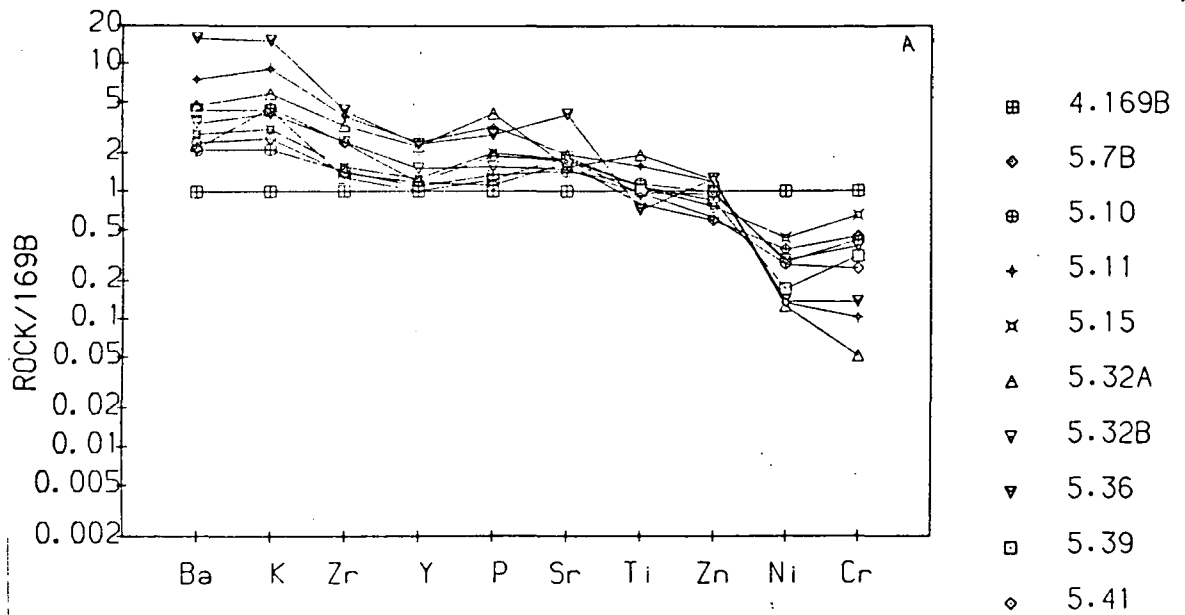


Fig 4.4 a,b Trace element compositions of the Marginal Suite normalised to marginal dyke 169b. 4.4b includes many of the Marginal Suite rocks showing evidence for fractionation.

chamber was walled by Lewisian amphibolite-facies rocks, and had since been emplaced upwards along faults. However, if it has been argued in Chapter 2, the complex is largely in situ, it is difficult to see how liquids residing in the chamber become contaminated with such rocks. However, their data (Fig 1, Palacz and Tait, 1985) do not exclude contamination by rocks of similar isotopic compositions to the Skye acid intrusives. Recent work by R. Greenwood (pers comm) on the Sr and Pb isotopes of Rhum felsites, indicates that they fit these requirements well. Thus evidence in the Marginal Suite for contamination by felsites fits in well with the isotopic evidence for such contamination in the main body of the magma chamber. The new isotopic evidence also supports the idea of a high-level, in situ origin for the ultrabasic complex, walled in part by earlier Tertiary acid rocks, rather than a tectonically emplaced chamber which evolved at depth enclosed by Lewisian rocks.

4.B GABBRO PLUGS AND SHEETS

Most of these bodies are mineralogically and petrographically similar (section 3.C.4), and thus it would seem reasonable to propose that they are also chemically related. Indeed, on Figs 4.2a and 4.2b, they fall roughly on the Marginal Suite fractionation trend.

It is possible to model the major element chemistry of these rocks by subtracting magnesian olivine, plagioclase and diopsidic clinopyroxene from rock 53A, the quenched marginal picrite. However there is not a perfect correlation between the quantities of these phases which have to be removed; thus the evidence is somewhat ambiguous.

Trace element data (Fig 4.6) do not support extensive plagioclase fractionation, as there is no -ve Sr anomaly developed. However, they support the idea of marked olivine fractionation, and perhaps a little clinopyroxene. Sample 53A shows the expected trace element pattern for a high-Mg parent to the gabbros, except for Ba and K which are markedly enriched. This is

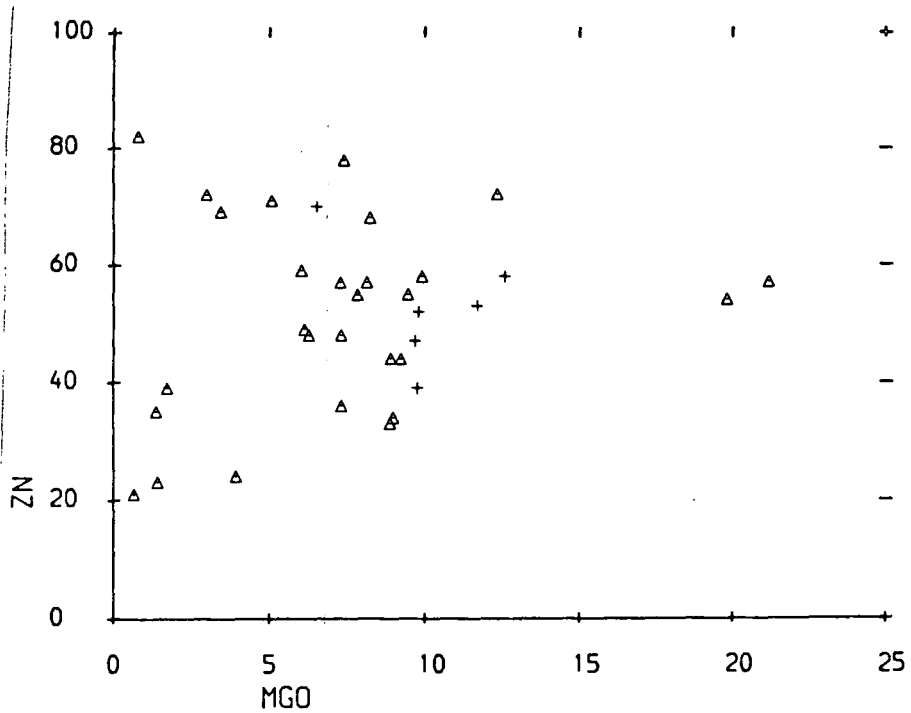


Fig 4.5 MgO vs Zn plot for the Marginal Suite and gabbro plugs and sheets.

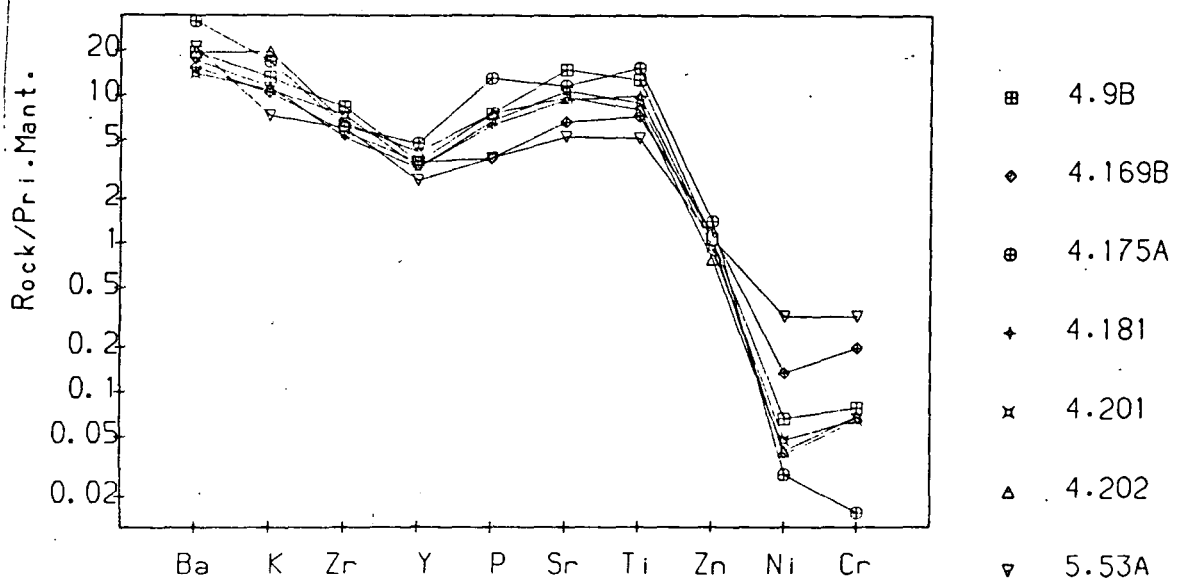


Fig 4.6 Trace element compositions of gabbro plugs and sheets normalised to primordial mantle (Taylor and McClennan, 1985).

almost certainly due to slight contamination by melted country rocks. (see previous section). Ni falls off much faster than Cr in the rocks showing slight Ni and Cr depletion, presumably because the crystallising assemblage was rich in olivine. However the most evolved rocks (lowest Ni and Cr), show relative depletion in Cr, suggesting that Cr-rich phases such as clinopyroxene, or perhaps oxides, had become liquidus phases.

A curious feature shown by these gabbros is the apparent lack of Zr enrichment with fractionation, suggesting that the crystallising assemblages had bulk distribution coefficients of about 1 for Zr.

4.C THE LAYERED ROCKS

As the rocks of the LELS are cumulates, and the compositions are controlled by the relative proportions of three main minerals (Fig 4.7), whole rock analyses are of little use in examining trends in the liquids from which they crystallised. Interpretation is further complicated by evidence for migration of intercumulus liquids, for example the instability of intercumulus orthopyroxene in peridotites, and the replacement of allivalite by peridotite. (see chapters 5 and 6). This implies that intercumulus assemblages need not be fractionates of the same liquids which formed the cumulus crystals in a given rock. Thus concentrations of incompatible elements need not be related to retention of melt in equilibrium with the cumulus phases.

Despite these problems, it is possible to use the whole-rock data to assist in classifying the xenolithic layers in units 4 and 5. Brown (1956) argued that they were intrusive gabbros, whereas the present work has cast doubt on this (chapter 3). In terms of their chemistry they seem to be related to the cumulates, rather than the clearly intrusive gabbro plugs and sheets. This is shown in Fig 4.8. To test this hypothesis more rigorously, the analyses^{of} these three groups of rocks were analysed using cluster analysis.

4.C.1 Cluster Analysis

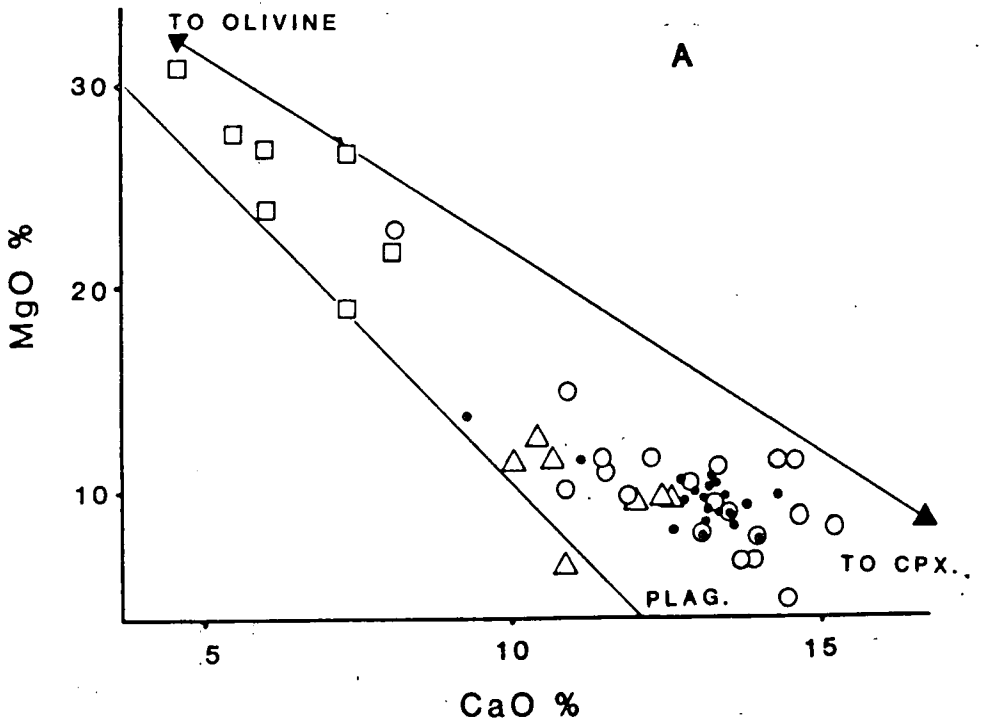


Fig 4.7 MgO vs CaO plot for the LELS rocks. Symbols: squares: peridotites, open circles: allivalites, dots: "sheetrocks", triangles: gabbro plugs and sheets.

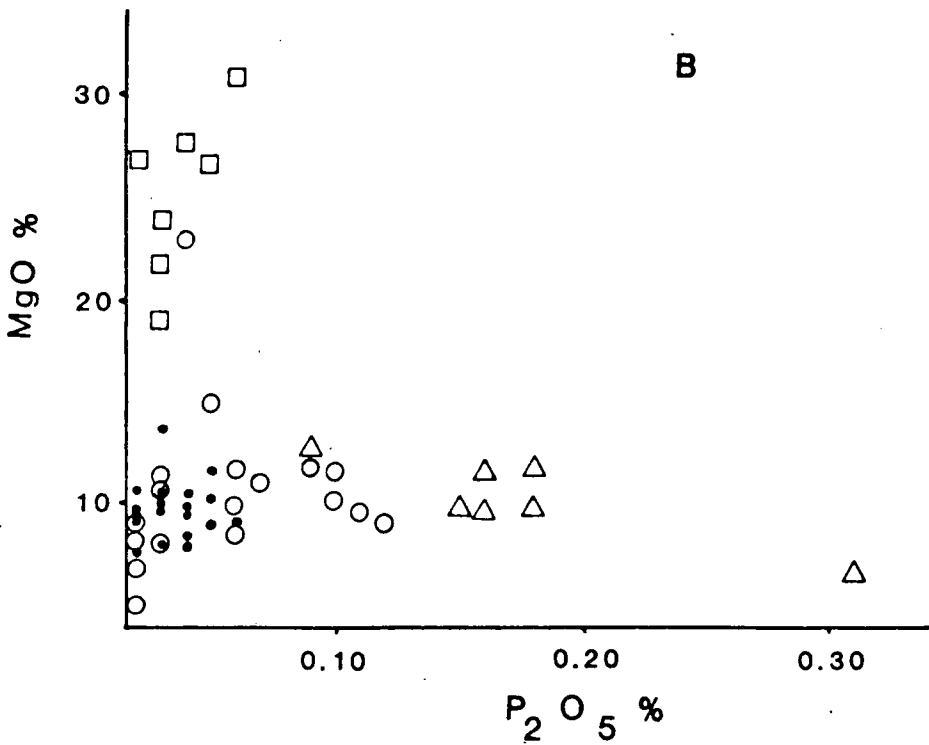


Fig 4.8 MgO vs P₂O₅ plot for the LELS rocks. Symbols as above.

OVERLEAF Fig 4.9 Dendrogram for the LELS allivalites, "sheetrocks", and gabbro plugs and sheets. Sample numbers are shown down the left hand side of the diagram. Prefixes to sample numbers indicate the group to which they belong: 2=allivalites, 3=sheetrocks, 4=gabbro plugs and sheets.

Cluster analysis is a multivariate statistical technique for classifying unknown objects. It makes no assumptions about the data, and seeks to determine any natural groupings or clusters of the data in multidimensional space. A good simple review of the technique can be found in Le Maitre (1982).

The results of cluster analysis obtained on analyses of allivalites, "sheetrocks", and clearly intrusive gabbro plugs and sheets is shown in Fig 4.9. This was performed using the MIDAS statistical package on the Durham University mainframe computer.

Cluster analysis first involves the calculation of a "similarity measure" between every object in the data set. This can be calculated in a number of ways, but the method used here is Euclidean distance, calculated as follows:

$$D_{ij} = \sqrt{\sum_{k=1}^p (X_{ik} - X_{jk})^2}$$

where X_{ik} and X_{jk} are the k^{th} variables of the i^{th} and j^{th} objects respectively, and p is the number of variables. D_{ij} is 0 for identical objects and becomes bigger with increasing dissimilarity. To avoid problems with the combination of % and ppm data used here, the data has been standardised, with equal weight given to all variables.

Having obtained a similarity matrix by the above procedure, the objects can be linked together to form clusters or groups by increasing the distance incrementally such that two objects or clusters combine at each step to form a new cluster. Thus at a distance of 0, all the objects are distinct, but at a distance of 382 all the rocks fall into one cluster. There are various methods for linking objects and clusters; the one used here is complete-linkage. This combines clusters on the basis of minimising the maximum distance between objects in two clusters. It is customary to represent this clustering behaviour on a dendrogram.

Looking at Fig 4.9, it can be seen that the allivalites and sheetrocks all fall inside a common cluster at a distance of 77. The gabbro cluster does not merge with them until a distance of 381. These are the

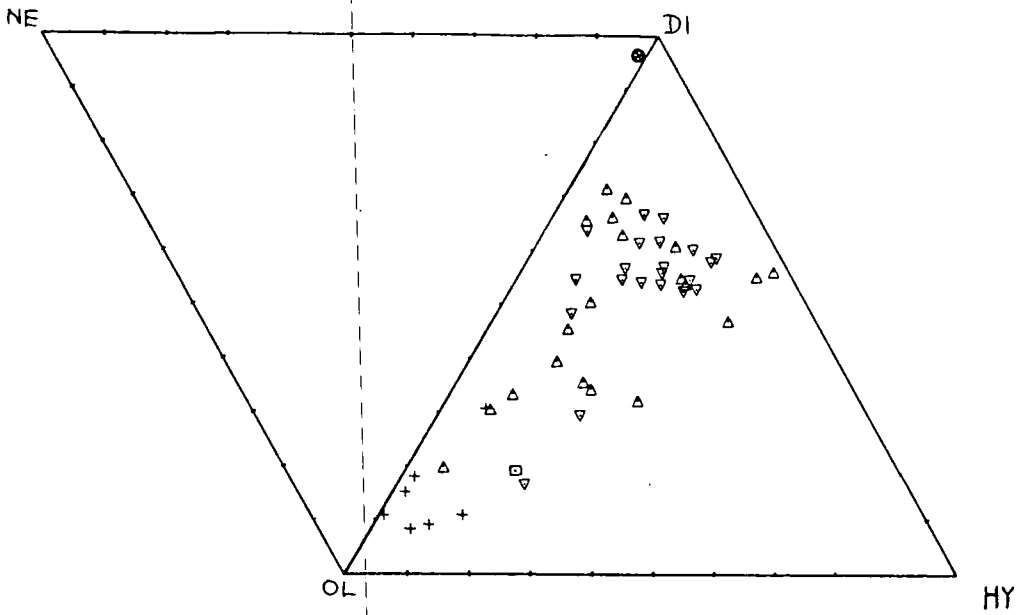


Fig 4.10 Normative compositions of LELS rocks and alkaline vein from unit 3 peridotite. Symbols: crosses = peridotites, up-pointing triangles = allivalites, down-pointing triangles = "sheetrocks", circle with cross = alkaline vein, square = marginal picrite 53A.

two main clusters in the dataset. Within the allivalite/sheetrock cluster, the two groups can also be distinguished although many of the allivalites are more similar to the sheetrocks than they are to other allivalites.

4.C.2 Norms of LELS rocks

CIPW norms were calculated using an assumed Fe³⁺/Fe²⁺ ratio of 0.15 (Brooks, 1976). Most of the LELS rocks are olivine and hypersthene normative with no free quartz and thus are broadly tholeiitic. However the alkaline vein from Unit 3 peridotite (Sample 163) is nepheline normative (Fig 4.10). This rock is also notably rich in P₂O₅ and TiO₂ (Appendix 2).

4.D CONCLUSIONS

(i) The Marginal Suite shows evidence for mixing with both Torridonian sediments, and felsite. However many rocks also show signs of being fractionates. Although picritic rocks occur in the Marginal Suite, and are contaminated, particularly with regard to Ba and K, the intermediate rocks have mostly been produced by mixing of more evolved gabbros with melted country rocks.

(ii) Most of the LELS rocks are olivine-hypersthene normative, although late fractionated veins in peridotites may be nepheline normative.

(iii) The fine-grained, xenolithic layers in the allivalites of units 4 and 5 are chemically similar to the other LELS allivalites. They are distinct from the clearly-intrusive gabbros. While this does not disprove an intrusive origin, taken together with the field and petrographic evidence, it supports their being regarded as part of the layered series.

CHAPTER FIVE

MINERAL CHEMISTRY

A range of minerals from the LELS and associated xenoliths have been analysed by electron microprobe. Data for unit 1 were obtained using WD spectrometry on the Cambridge Instruments Geoscan at Durham University. Additional nickel analyses for sample U1P3 were made by WD analysis at Leicester University. Data for the other units, were obtained using ED spectrometry on the Geoscan at Manchester University Geology Department, except for the sulphide phases which were analysed by EDS on the Cameca microprobe at Manchester.

5.A THE LAYERED ROCKS

5.A.1 Olivine

5.A.1.a Forsterite content

Forsterite content (Fo) ranges from 85.6 to 69.8. The LELS olivines thus show a slightly greater range, and are more iron-rich than those from other parts of the Rhum layered sequence (Table 5.1).

There are marked stratigraphic controls on this variation: the peridotite olivines are more forsteritic than those of the allivalites. These variations are discussed in detail in the following chapter.

	<u>Range</u>	<u>Reference</u>
LELS	86-70	This work
upper ELS	89 ⁽¹⁾ -74 ⁽²⁾	(1) McClurg, 1982 (2) Palacz, 1984
CS	91 ⁽¹⁾ -78 ⁽²⁾	(3) Volker, 1983 (4) McClurg, 1982
WLS	88-78	Dunham and Wadsworth(1978)

Table 5.1 Ranges in olivine composition from different parts of the Rhum complex.

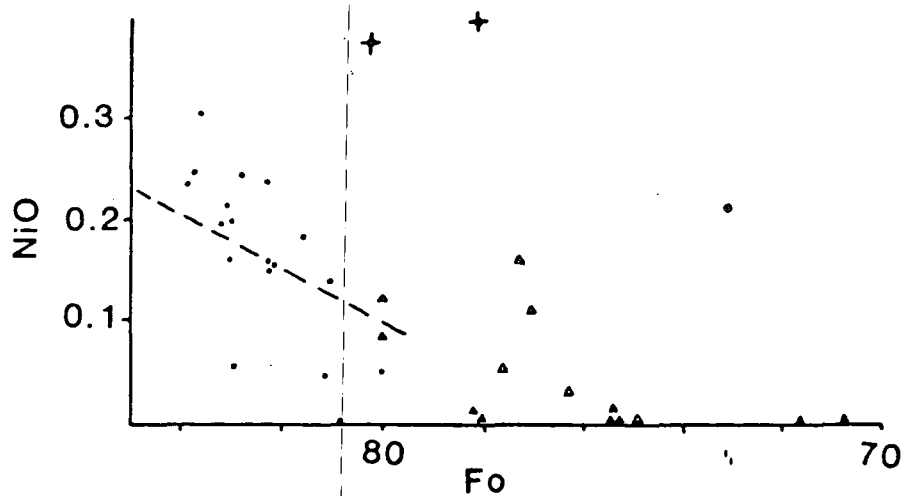


Fig 5.1 Olivine Fo-NiO relationships for unit1. Dashed line indicates Duke and Naldretts (1978) curve separating fields of sulphur-saturated magmas from undersaturated ones. Sample SR209A (crosses) is from the chilled picrite under Beinn nan Stac. Dots: peridotite samples, triangles: allivalite samples.

5.A.1.b Nickel content

Nickel is often used as an indicator of fractionation in magnesian olivines, being highly compatible, as they are less prone to later reequilibration. Only a limited number of reliable nickel analyses are available for LELS olivines, as most of the analyses were performed using ED spectrometry; however some data are available for unit 1, performed using WD analysis at Durham University.

The relationship between olivine Fo content and Ni content has fuelled a number of petrological speculations (egs Duke and Naldrett, 1978; Tait, 1985). Data for unit 1 are shown in Fig 5.1, together with the line separating olivines from sulphide-undersaturated magmas (high Ni) and those from sulphide-saturated assemblages (low Ni) (Duke and Naldrett, 1978). Using this division McClurg (1982) proposed a sulphide-saturated parent for the ELS and sulphide-undersaturated parent magmas for the CS. Tait (1985) has criticized this conclusion, arguing that the olivines with high Ni at a low Fo content in Unit 10 are the result of semi-equilibrium crystallization from highly magnesian magmas, the Fe/Mg ratio equilibrating with that of the magma during cooling, while early high Ni contents are retained. Only tiny quantities of sulphides are seen in unit 10, and Tait does not regard them as having played a significant role in controlling olivine Ni contents. In unit 1 however, Ni-rich sulphides are abundant, and assuming a magmatic origin, must have affected the magma Ni content.

The unit 1 olivines fall on either side of Duke and Naldrett's curve; however all the Unit 1 Ni contents are much lower than those (based on limited data) from a chilled picrite in the Marginal Suite, which shows no evidence for sulphide-saturation. The data show a positive correlation between Fo and Ni contents, but there is much scatter, and within a given sample, Ni may vary considerably. Some of the more evolved olivines in the allivalite are anomalously rich

in Ni.

Additional analyses of Ni in olivines of sample U1P3 revealed a marked heterogeneity in its distribution. Olivine grains not in contact with Ni-rich sulphide blebs have relatively constant NiO contents of 0.10-0.13 wt %. (Mean:0.12). Those in contact with Ni-rich sulphide blebs have variable, and significantly higher NiO contents, between 0.13 and 0.21 wt %. (Mean:0.175). The most Ni rich analyses come from rims of olivine crystals adjoining a pentlandite grain. There are two possibilities: first, that the Ni rich olivines are primary compositions which have somehow been protected from Ni loss during later equilibration, or second, that the low-Ni grains represent initial compositions, which have locally been enriched in Ni by diffusive exchange with the pentlandite. The former is implausible given the lack of a suitable "sink" into which Ni would be likely to migrate from olivine. The pentlandite has an Ni content of 21%; using an olivine NiO content of 0.21%, this gives a partition coefficient, D, of:

$$D^{Ni} = \text{wt \% Ni}_{\text{sulphide}} / \text{wt \% Ni}_{\text{olivine}} = 21 / 0.164 = 128.$$

This is somewhat higher than the experimentally determined values of Boctor (1980,1982), who found an average $D=36$ at 1400°C , for sulphide melt/olivine, but lower than the value obtained by Rajamani and Naldrett (1978) who obtained average $D=274$ at 1255°C for sulphide melt/basalt melt partitioning. Both these results were obtained at lower Ni contents than seen in unit 1, and there is evidence that $f(\text{O}_2)$ may also be an important factor (Boctor,1982), so the agreement is fair. There is also some evidence that D may increase with decreasing temperature (Barnes and Naldrett, 1985). Similar equilibration would explain the anomalously high Ni contents of the evolved olivines in sample U1A1, which is also sulphide-rich.

If the NiO contents of 0.1-0.13% seen in sample U1P3 are primary magmatic, this suggests a Ni-depleted magma, given the Fo content of 83.5, and probably requires that the Ni-rich sulphide melt was

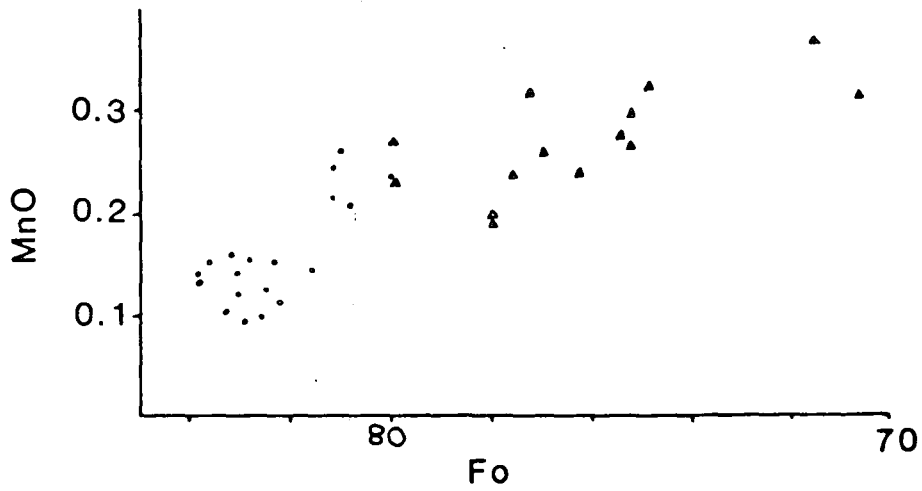


Fig 5.2a Fo content vs MnO for unit 1 olivines.

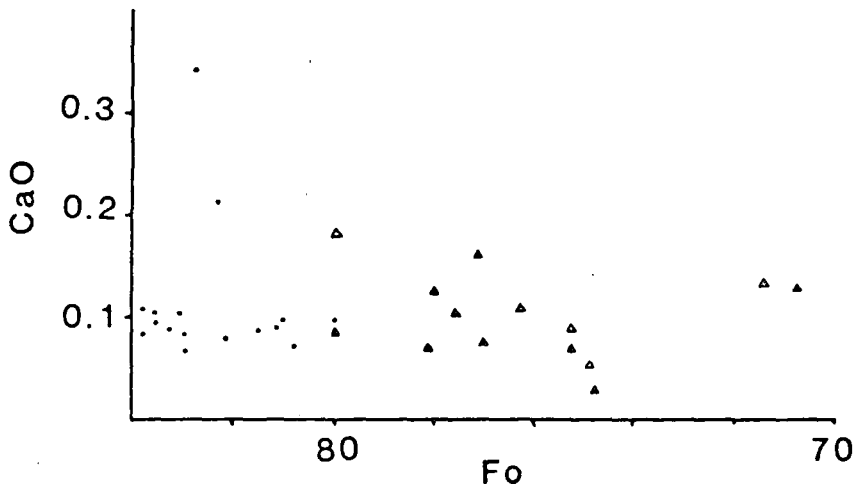


Fig 5.2b Fo content vs CaO for unit 1 olivines.

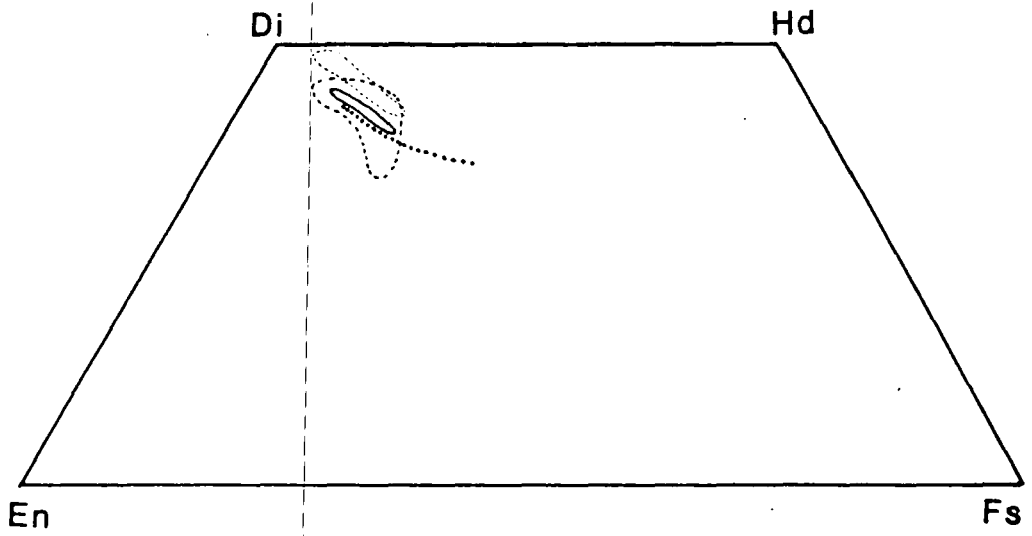


Fig 5.3 Clinopyroxene compositions for LELS rocks. Heavy dashed field: all core compositions, solid line field: mean core compositions. Also marked: dashed line=Skaergaard trend, light dashed field: upper ELS and CS trend (Volker, 1983).

exsolved prior to the crystallisation of olivine, although fractional crystallisation of large amounts of olivine might be able to produce similar effects. As the base of unit 1 is not exposed, it is difficult to choose between these hypotheses.

5.A.1.c Manganese contents

As with Ni, only a few analyses from Unit 1 are available. They show a fairly good linear decrease in MnO with increasing Fo (Fig 5.2a), from about 0.35% MnO at Fo₇₀ to about 0.15% at Fo₈₄. This trend is rather less rich in MnO and has a less steep slope than that found by McClurg (1982) and Volker (1983) for upper ELS and CS olivines.

5.A.1.d Calcium contents

The unit 1 data is shown in Fig 5.2b. There is little correlation with Fo contents, and most olivines contain about 0.1% CaO, similar to the values reported by Simkin and Smith (1970) for basic plutonic rocks, although two analyses from sample U1P2 show anomalously high CaO contents of ca. 0.3% CaO. This is similar to values for quickly cooled basic lavas (Simkin and Smith, 1970). McClurg (1982) and Volker (1983) report CaO contents in the range 0.02% to 0.16% for the upper ELS and CS.

5.A.2 CLINOPYROXENES

Plotted on the traditional pyroxene quadrilateral, the clinopyroxenes of the Lower E.L.S. fall in a banana-shaped field around the Diopside-Salite-Endiopside-Augite boundary (Fig 5.3). The mean core compositions for given rocks define a fairly good linear trend parallel to, but rather more calcic and magnesian than, the Skaergaard trend (Fig 5.3).

Similar relationships were noted by Volker (1983), although his clinopyroxenes (from the Upper E.L.S., C.S. and associated gabbros and dykes), while defining a trend parallel to that of Skaergaard, are more calcic

and magnesian still (Fig 5.3).

It is interesting to note that although there is some overlap between the Upper E.L.S./C.S. field and that of the Lower E.L.S., the Lower E.L.S. pyroxenes cannot be interpreted simply as the products of magmas produced by high level fractionation of the more ultrabasic magmas seen elsewhere on Rhum, because of their lower W_o content at a given Mg/Fe ratio.

Also noteworthy is the fact that the clinopyroxenes from the 'Sheetrocks' fall on a continuous trend from the Lower E.L.S. peridotites, but are markedly less calcic than those from the gabbros and dykes analysed by Volker; perhaps this supports the notion that the sheetrocks are fractionated Lower E.L.S. cumulates, rather than gabbros like those seen elsewhere on the island.

Pyroxene compositions seem to be independent of habit. In samples with both cumulus and intercumulus pyroxene, compositions are almost constant. This has been reported by others (eg Dunham and Wadsworth, 1978).

5.A.2.a Aluminium

Aluminium ranges from 0.17 atoms per 6 oxygens to 0.06 atoms per 6 oxygens. (4.02 - 1.85 wt % Al_2O_3). Al shows a slight +ve correlation with magnesium number (Mgn) of the clinopyroxenes (Fig 5.4a), although there is much scatter. The peridotites show slightly higher Al contents than the allivalites, although the fields overlap. Pyroxenes from the mixed layers tend to have rather low Al contents for a given Mgn. Volker (1983) reported Al_2O_3 contents in the range 4.7 to 3.0 wt % for the CS, and 3.5 - 2.2 wt % for the upper ELS.

Al_{iv} , calculated as (2-Si) on the basis of 6 oxygens, is usually related inversely to the silica activity of the melt from which the clinopyroxenes crystallized (Le Bas, 1962). Al_{iv} shows a slight +ve correlation with Mgn in the allivalites, but in the peridotites there is a suggestion of a -ve correlation (Fig 5.4b). According to Le Bas (1962), increasing Al_{iv} with fractionation is a feature of silica-undersaturated

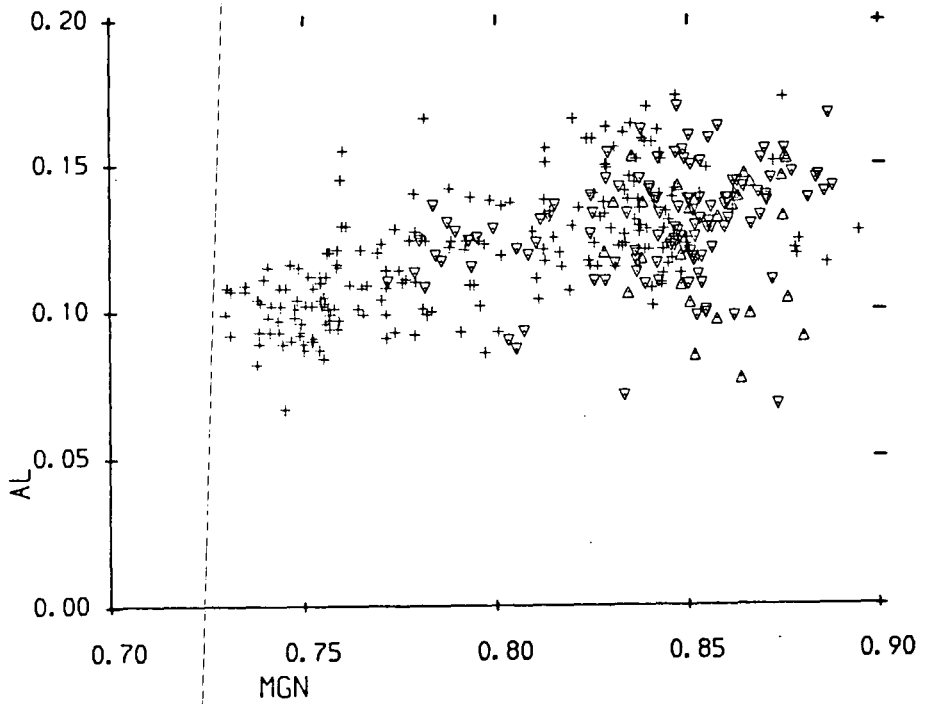


Fig 5.4a Mg/Mg+Fe (atomic)=MGN, vs Al per 6 oxygens for LELS clinopyroxenes. Crosses: allivalites, up-pointing triangles: mixed layers, down-pointing triangles: peridotites.

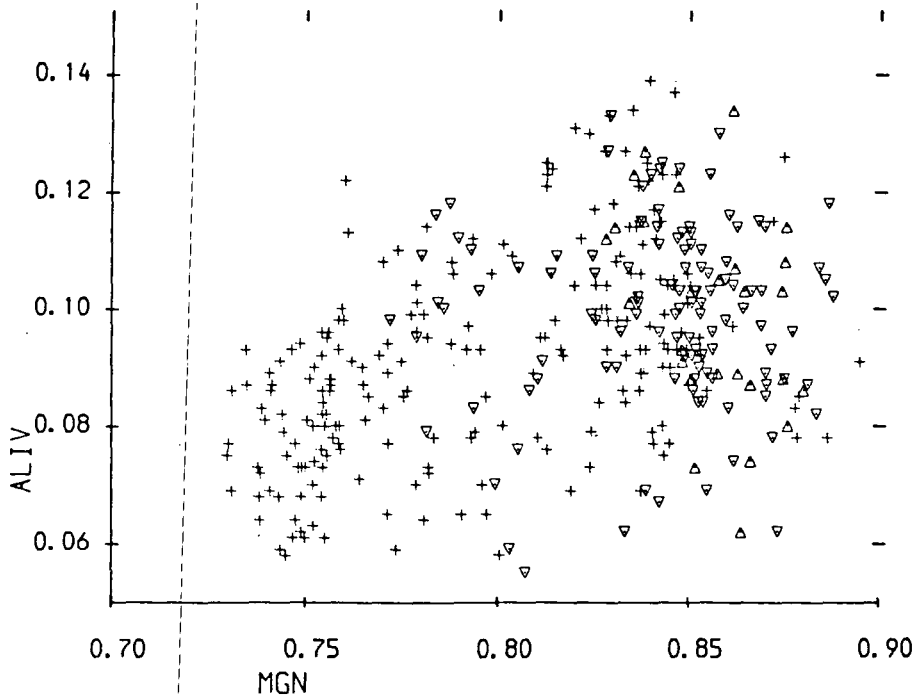


Fig 5.4b Al in tetrahedral sites vs MGN for LELS clinopyroxenes. Symbols as above.



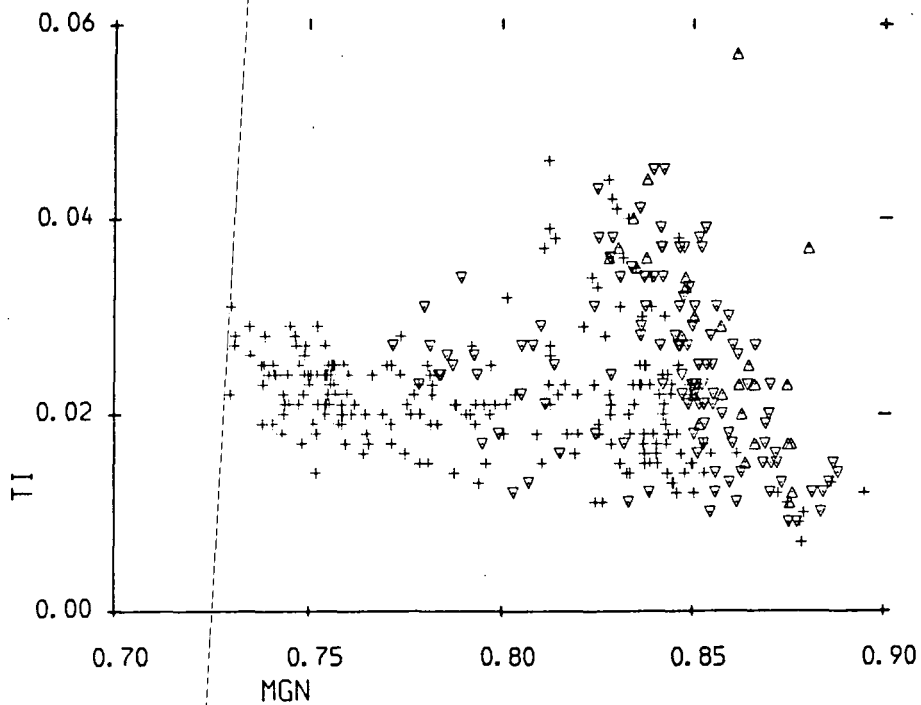


Fig 5.5 MGN vs Ti per 6 oxygens for LELS clinopyroxenes. Crosses: allivalites, up-pointing triangles: mixed layers, down-pointing triangles: peridotites.

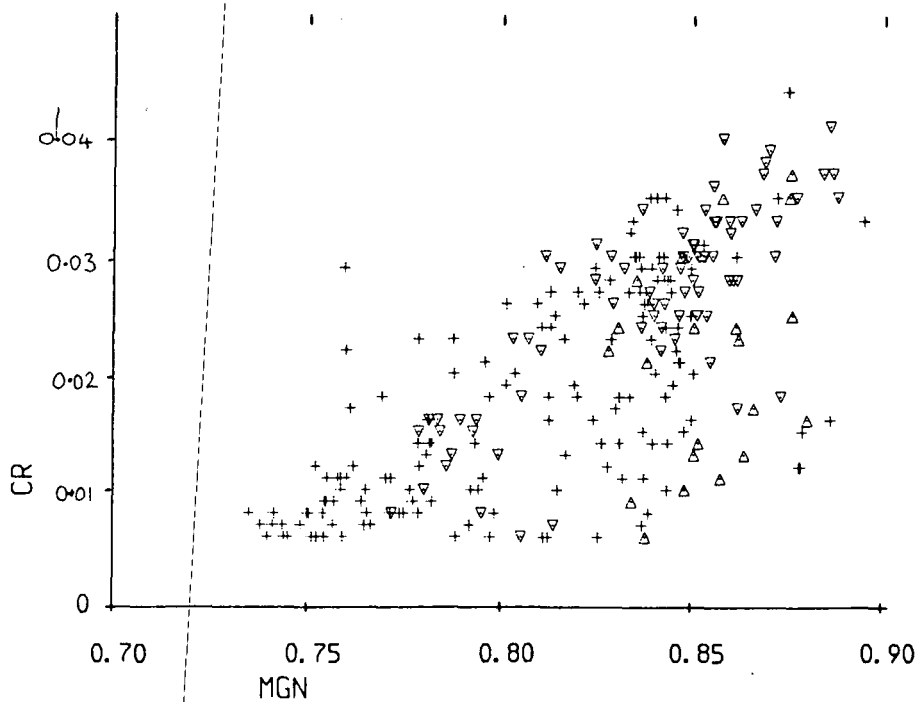


Fig 5.6 MGN vs Cr per 6 oxygens for LELS clinopyroxenes. Symbols as above.

magmas, while decreasing Al_{iv} is a feature of silica-saturated magmas. This suggests two trends in the LELS: an alkaline interstitial peridotite trend, and a tholeiitic allivalite trend. The considerable overlap between these trends can be explained by a certain amount of mobility of the interstitial liquids.

5.A.2.b Titanium

Titanium contents are in the range 0.01 - 0.06 ions per 6 oxygens (0.26 - 2.06wt% TiO_2), although values at the upper end of the scale are not common. Plotted against Mgn, the peridotite pyroxenes are clearly richer in Ti at a given Mgn than those of the allivalites (Fig 5.5). While the latter show little correlation with Mgn, most of the peridotite pyroxenes fall on a trend of increasing in Ti with fractionation. Clinopyroxene Ti contents are often related to the silica activity of the melt (Le Bas, 1962); thus the enhanced Ti contents of peridotite pyroxenes support the notion of an interstitial alkaline trend.

5.A.2.c Chromium

Chromium contents vary from 0.44 ions per 6 Oxygens, to below detection limits (1.53 - 0.0 wt % Cr_2O_3). Cr shows a +ve correlation with Mgn (Fig 5.6), although the scatter is considerable, and the peridotite pyroxenes tend to have higher Cr contents than those of allivalites. Volker reported Cr_2O_3 contents in the range 1.69 - 0.54 for the CS, and 1.32 - 0.46 for the upper ELS.

5.A.2.d Sodium

Sodium contents fall in the range 0.07 - 0.02 ions per 6 oxygens (1.02 - 0.3 wt % Na_2O). Precision for Na using EDS analysis is rather poor; however despite this there is a tendency for the peridotite pyroxenes to have slightly higher Na contents at a given Mgn (Fig 5.7). Volker (1983) reported pyroxene Na contents in the range 0.6 to 0.2 wt %, with a tendency for the CS pyroxenes to have higher contents than those of the

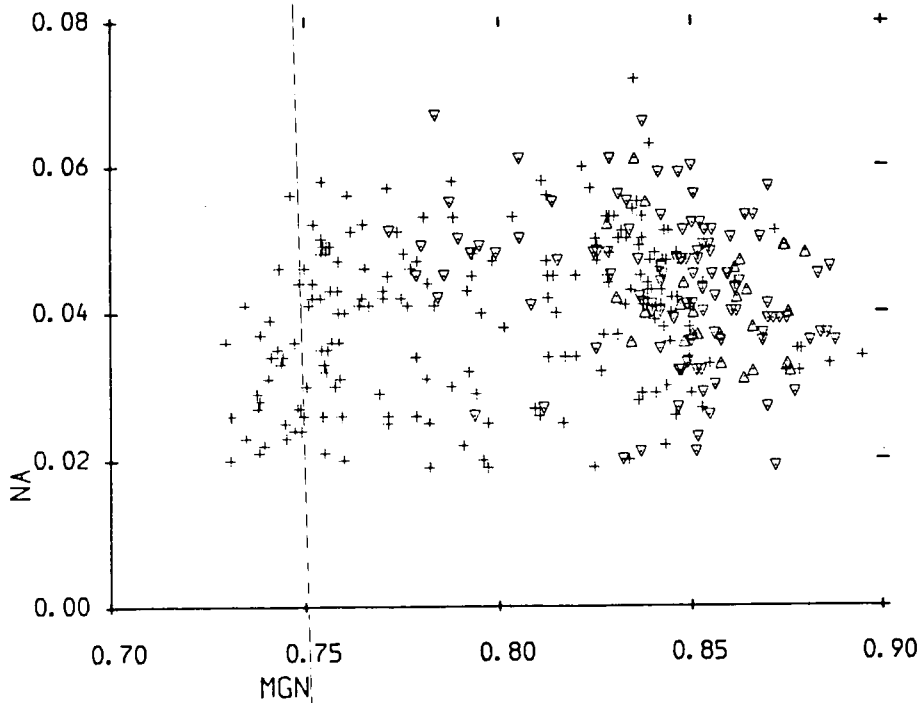


Fig 5.7 MGN vs Na per 6 oxygens for LELS clinopyroxenes. Crosses: allivalites, up-pointing triangles: mixed layers, down-pointing triangles: peridotites.

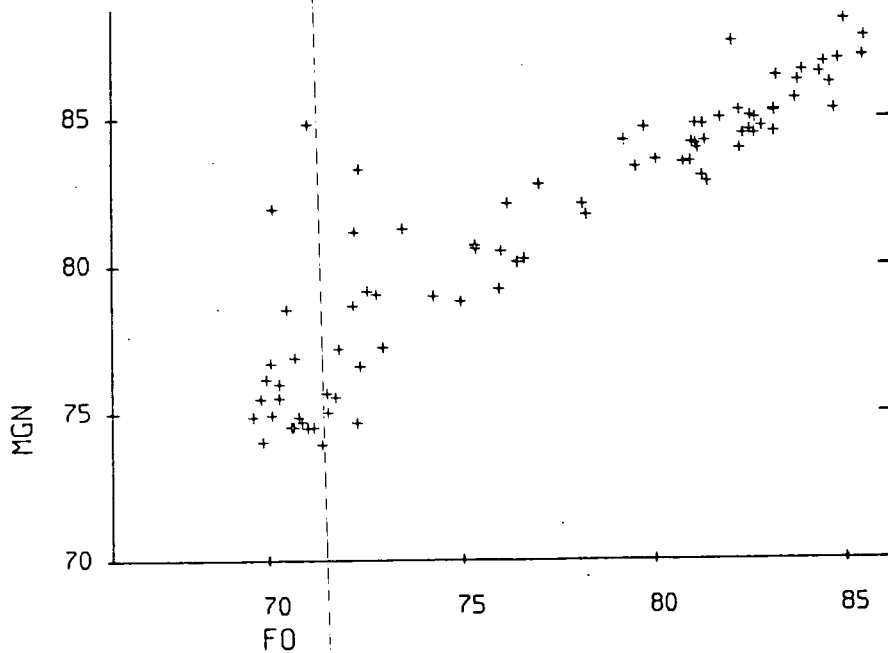


Fig 5.8 Relationship between olivine Fo content and Mgn of clinopyroxenes. Mean values for each sample. Curve shown is from Obata et al (1974) indicating equilibrium at 700°C . The LELS samples lie on the high temperature side of this line.

upper ELS.

5.A.3 Clinopyroxene - olivine relationships

There is a good correlation between Mg# of clinopyroxene and Fo content of olivines in the same rock (Fig 5.8). It has been recognised that slow cooling of an olivine-clinopyroxene pair will result in Fe-Mg exchange between the two phases (eg Speidel and Osborn, 1967) the olivine becoming more Fe-rich, and the pyroxene more magnesian. This has been used as a geothermometer (Obata et al 1974; Powell and Powell, 1974), but poor constraints on the olivine-cpx system (Wood, 1978), and interference by other Fe-Mg phases such as orthopyroxene and spinel, limit its usefulness. Despite these limitations, it is likely that subsolidus Fe-Mg exchange has occurred in the LELS rocks (Fig 5.8).

Another approach is provided by the work of Duke (1976). He determined equations relating Fe/Mg ratios of olivines and clinopyroxenes to those of the liquids from which they crystallised. Applying these to rocks from the LELS (Table 5.2), it can be seen that the clinopyroxenes in a given rock have apparently crystallised from more magnesian liquids than the olivines. This is contrary to what would be expected from the order of crystallisation. Apart from demonstrating that the mineral compositions are not primary, this would also seem to rule out equilibration of both phases with interstitial liquids as being the final control on mineral compositions.

It is likely that elements other than Fe, Mg and perhaps Ca, are less prone to post-cumulus reequilibration due to their high ionic charge, and/or lack of suitable chemical gradients to induce diffusion. However there is no experimental evidence on diffusion rates in clinopyroxenes, and this must be considered a provisional conclusion. There is some indirect evidence that Cr has very slow diffusion rates, in that Duke (1978) found it impossible to attain equilibrium Cr partitioning between clinopyroxene and basic melts.

Sample number	Fo	Mgn	L_{Fo}	L_{Mgn}
U1A2	79.2	84.2	0.875	0.606
U2P1	84.5	86.6	0.613	0.472
U4A3	70.5	78.5	1.395	1.005
U4A15	70.0	76.1	1.429	1.200
U5A1	76.2	82.1	1.041	0.743
U5A17	76.6	80.2	1.017	0.872

Table 5-2 Liquid Fe/Mg ratios calculated from olivines and clinopyroxenes in selected L.E.L.S. rocks, using the equations of Duke (1976). L_{Fo} = molar Fe/Mg ratio of liquid calculated from olivine. L_{Mgn} = molar Fe/Mg ratio of liquid calculated from clinopyroxene.

5.A.4 Plagioclase

Plagioclase has not been analysed extensively as preliminary investigations have revealed extensive within-sample variations. This has also been found by other workers in Rhum rocks (egs Dunham and Wadsworth, 1978; Volker, 1983; Tait, 1985).

The total range recorded (cores and rims) from LELS rocks is from $An_{89.5}$ to $An_{59.1}$, although this is unlikely to be the total range, as it is based on a small number of samples only. The following general points can perhaps be made:

(i) There is little systematic difference between plagioclases in allivalites and poikilitic plagioclases in peridotites. The two groups are indistinguishable on the basis of An content. The most calcic plagioclases are cumulus grains from the lowest part of Unit 1 allivalite, while compositions down to An_{59} have been found at the margins of both cumulus grains in Unit 3 allivalite, and in poikilitic grains from Unit 3 peridotite.

(ii) Zoning, which may be normal, reverse and/or oscillatory, is widespread, and is not always obvious optically.

(iii) The 'sheetrocks' from units 4 and 5 seem to have relatively evolved plagioclases (usually less than An_{70} cores), but do not have rims more sodic than other LELS plagioclases.

(iv) Plagioclase An content is very sensitive to small fluctuations in water pressure, as well as to melt Na/Ca ratios. Given the additional tendency for disequilibrium partitioning of ions during crystal growth (Smith and Lofgren, 1983), the lack of correlation between plagioclase Na/Ca and the Fe/Mg ratio of accompanying phases is perhaps not surprising.

5.A.5 Orthopyroxene

Orthopyroxenes show a range in Mg# from 86 to 71. In all rocks where it has been analysed, orthopyroxene is slightly more magnesian than coexisting

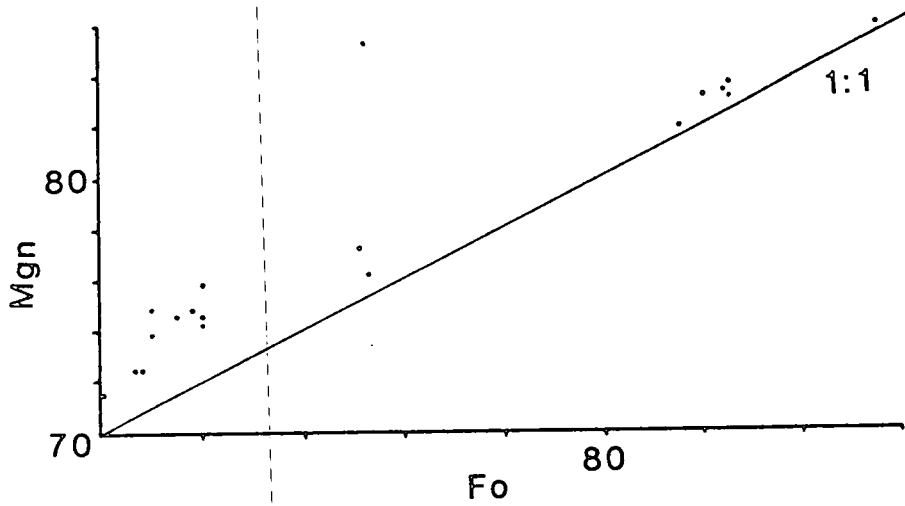


Fig 5.9 Relationship between olivine Fo content and Mgn of orthopyroxenes. Fo content is the mean for a particular sample. En contents may only be based on 1 analysis.

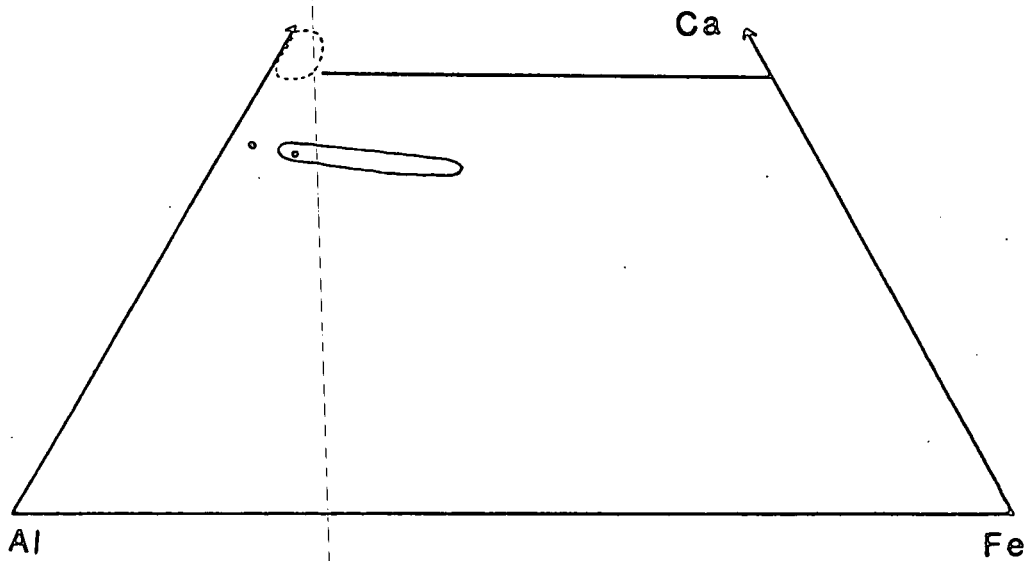


Fig 5.10 Compositions of epidotes from sample U3A2. Dashed field indicates region of clinozoisites formed by replacement of plagioclase (Kitchen, 1985), while the solid field indicates the same author's igneous epidote trend.

olivine, but less magnesian than clinopyroxene in the same rock (Fig 5.9). It is likely that subsolidus equilibration is a major factor in this, as has been found between olivine and clinopyroxene (Section 5.A.3).

5.A.6 Sulphides

Sulphides have been analysed in three specimens from unit 1: U1P2, U1P3, and U1A5. A.R. Butcher and R.A.D. Pattrick kindly carried out these analyses at Manchester University.

There are few differences in chemistry between individual phases in the peridotite and the allivalite, although copper bearing sulphides appear to be modally more abundant in the allivalite (section 3.C). However a few sulphur-rich phases occur only in the allivalite, suggesting a slightly higher sulphur activity in the allivalite. Pyrite and iron-rich violarite, the latter sometimes with a few per cent Co, are the sulphur rich phases (Table 5.3).

A striking feature of the assemblage as a whole, is the rarity of chalcopyrite sensu stricto. Most of the grains analysed as chalcopyrite on the basis of optical properties, are iron-rich, and often metal-deficient, falling between cubanite and chalcopyrite in composition. One analysis corresponds closely to the mineral haycockite ($\text{Cu}_4\text{Fe}_5\text{S}_8$), but others do not correspond to any clearly defined, described phases. They do, however, fall within the intermediate solid solution (iss) field of the system Cu-Fe-S (Craig and Scott, 1982). Within this broad group, two types can be distinguished in the Unit 1 samples: (i) metal deficient (or sulphur enriched - this is not distinguishable on the evidence of probe analysis alone) Cu,Fe,S phases with Cu:Fe 2:1 to 1:1, and (ii), stoichiometric Cu,Fe,S phases with Cu:Fe from 1:1.1 to 1.5:1. The iss field includes the phases cubanite, mooihoekite, talnakhite, haycockite and chalcopyrite, among others, and these are normally the phases formed on cooling iss bulk compositions. However parts of the iss are regarded as being capable of forming metastable superstructures on

Phase:	PYRRH	CU-PYRR	PENT	MD-ISS	ISS	CHPYR	CUB	MACK	HAYCOCK	VIOL
Sample No:	U1A5	U1P2	U1P3	U1P2	U1P3	U1A5	U1P3	U1P2	U1P3	U1A5
Cu wt %	0.00	0.93	0.00	29.39	31.68	34.68	23.50	3.38	30.84	0.01
Ni wt %	0.31	2.55	27.06	0.11	0.00	0.00	0.07	2.69	2.46	23.59
Fe wt %	59.87	59.74	38.37	34.45	34.80	30.98	40.20	56.96	35.03	26.67
Co wt %	0.00	0.00	0.74	0.01	0.00	0.00	0.00	0.00	0.00	7.56
As wt %	0.11	0.50	0.00	0.54	0.13	0.05	0.00	0.19	0.00	0.00
S wt %	39.83	37.27	33.59	35.05	35.60	34.91	34.90	35.19	39.39	41.12
Recalculated on the basis of fixed number of sulphur atoms:										
Cu	0.00	0.10	0.00	3.33	3.53	3.94	2.00	0.38	3.78	0.00
Ni	0.03	0.30	3.50	0.02	0.00	0.00	0.00	0.33	0.33	2.49
Fe	6.87	7.33	5.22	4.50	4.47	4.06	3.95	7.40	4.94	2.96
Co	0.00	0.00	0.10	0.00	0.00	0.00	0.00	0.00	0.00	0.80
As	0.01	0.05	0.00	0.06	0.02	0.01	0.00	0.02	0.00	0.00
S	8	8	8	8	8	8	6	8	8	8
Total Cu+Ni+										
Fe+Co	6.90	7.73	8.82	7.85	8.00	8.00	5.95	8.13	9.05	6.25

Table 5.3 Selected analyses of sulphide minerals from Unit 1.

PYRR: pyrrhotite, CU-PYRR: cuprian pyrrhotite, PENT: pentlandite,
MD-ISS: metal deficient iss, ISS: stoichiometric Cu,Fe,S phases, CHPYR:
chalcopyrite, CUB: cubanite, MACK: mackinawite, HAYCOCK: haycockite?,
VIOL: iron and cobalt rich violarite.

cooling (Craig and Scott, 1982), and this appears to be the case in unit 1.

Phases identified on the basis of microprobe analysis are as follows: pentlandite (25 analyses), pyrrhotite (24 analyses), metal deficient Cu,Fe,S phases (25 analyses), stoichiometric Cu,Fe,S phases (20 analyses; includes chalcopyrite and cubanite), mackinawite (5 analyses), pyrite and haycockite (1 analysis each), and violarite group minerals (2 analyses). Selected analyses of these phases are given in Table 5.3.

The assemblage recorded is fairly typical of magmatic sulphides associated with basic and ultrabasic rocks. Certain phases, eg mackinawite, appear only to form with continued equilibration to low temperatures, while others, principally the poorly defined iron compositions, are thought to be associated with rapid quenching. Given the size of the Rhum intrusion, and the evidence for subsolidus exchange between sulphides and olivines (section 5.A.1.b), rapid cooling seems untenable. Interpretation of this assemblage in terms of published phase diagrams (eg Craig and Killierud, 1969) is thus very difficult; however as Craig and Scott (1982) have said of experimental sulphide phase relations: "...relationships remain enigmatic, obscured by .. extensive solid solutions, unquenchable phases and metastability.". There is no reason to expect natural assemblages to be any better behaved.

5.A.7 Kaersutites

Two kaersutite analyses from sample U2P8 are given in Table 5.4. These are similar in composition to intercumulus kaersutite analyses given by Volker (1983) and Kitchen (1985). The Cr contents are notably high - Cr contents were not given in earlier analyses. Available data (Henderson, 1984), suggests that amphibole would have about the same, or smaller affinity for Cr than clinopyroxene. Cr contents of the latter phase in U2P8 are 0.5% - 0.8%. This may imply that the late-formed kaersutite grew from a Cr-rich liquid, and

Phase:	Kaer	Phlog	Hbl(c)	Hbl(r)	Epi	Unk
SiO ₂	43.45	38.04	48.57	43.26	39.20	42.34
Al ₂ O ₃	10.85	13.61	8.31	11.72	29.17	22.58
FeO*	6.37	9.32	8.72	15.30	5.60	0.09
MgO	16.18	17.53	15.49	10.98	0.38	0.02
CaO	12.12	0.15	12.68	12.46	24.86	25.79
Na ₂ O	2.96	0.74	1.20	2.85	0.29	0.25
K ₂ O	nd	9.52	0.13	0.06	nd	0.16
TiO ₂	4.91	7.37	0.85	0.21	0.00	0.06
Cr ₂ O ₃	1.30	nd	nd	nd	nd	nd
Total	98.14	96.28	95.95	96.84	99.50	91.29

Table 5.4 Selected analyses of minor phases from the LELS. Kaer: kaersutite, Phlog: phlogopite, Hbl(c): green amphibole core, Hbl(r): green amphibole rim, Epi: iron-rich clinozoisite, Unk: unidentified mineral (see also text). FeO*= iron expressed as FeO. nd: not determined.

not a liquid depleted in Cr by extensive crystallisation of chromite and/or clinopyroxene. This thus supports the idea (Section 5.A.2) that peridotites were permeable, and the interstitial liquids were capable of movement and replenishment.

5.A.8 Hydrous minerals in allivalites

Two epidotes from the hydrous assemblage in sample U3A2 have been analysed (Table 5.4). These plot at the Fe-poor end of Kitchen's (1985) igneous trend (Fig 5.10) and away from the field of clinozoisites formed by replacement of plagioclase, supporting a late-magmatic origin for the mineral (Section 3.C.3.b).

Analyses of cores and rims of green euhedral hornblendes from the same assemblage indicates pronounced zoning, the cores being magnesio-hornblende and the rims being edenitic hornblende (nomenclature of Leake, 1978).

Phlogopite from the same sample is highly titanian (Table 5.4).

The unidentified brown mineral (section 3.C.3.b) is a calcium aluminium silicate, presumably with much water, as all analysed grains gave totals around 90-91% (Table 5.4).

5.B SOME ASPECTS OF XENOLITH MINERAL CHEMISTRY

5.B.1 Pigeonite

Inverted pigeonite grains from sample 194c (see section 3.C.3.d) have been analysed. The host-lamellae relationship (Fig 5.11) indicates that these were at the Mg-rich end of the pigeonite stability range in basic rocks. The presence of hypersthene in an adjacent layer in the same rock indicates that this rock was formed at the hypersthene-pigeonite transition, which is commonly at an Mg/Fe ratio of about 70:30 (Brown, 1972). Coexisting plagioclase is An₇₄. Less calcic plagioclases occur in the LELS units, but no such evolved pyroxenes are seen. As plagioclase An content is very dependent on p_{H_2O} ; this may imply that more evolved

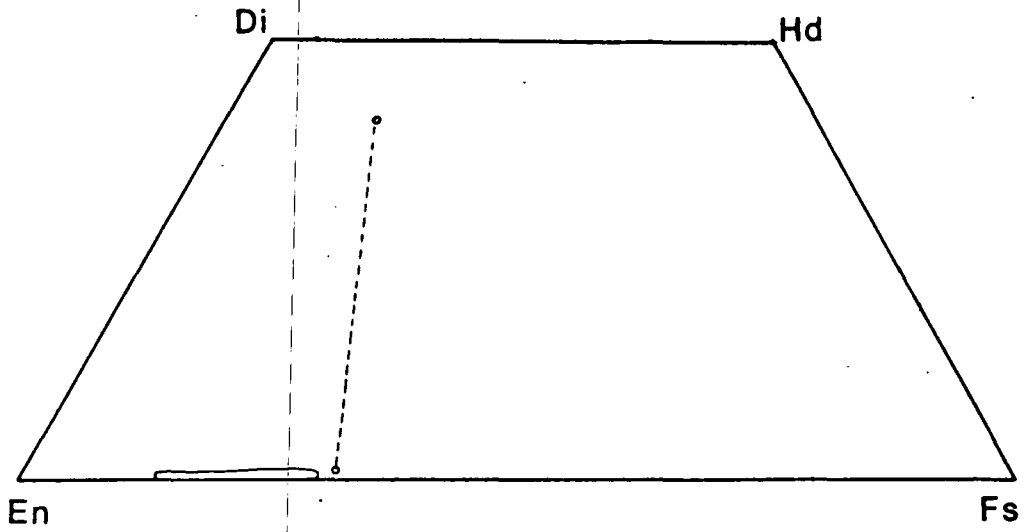


Fig 5.11 Host-lamellae relationship in inverted pigeonite from sample 194C. Solid field is range of LELS orthopyroxenes.

magmas with higher water contents were present in the upper part of the magma chamber, where the rocks now seen as xenoliths were probably formed.

5.B.2 Fassaite-bearing xenoliths

Analyses of phases from sample 20c are given in Table 5.5. This specimen consists of a garnet-rich core surrounded by a rim of fassaite, then a fassaite/magnetite zone passing into plagioclase-augite rock. The analyses of fassaites show several unusual features. They are very low in silica and have low totals with iron calculated as Fe^{2+} . Recalculation of Fe^{3+} by charge balance improves totals considerably, and indicates that these are very highly oxidised pyroxenes. They also contain excessive Ca, requiring a certain amount to be put in the M2 site. This is a common feature of fassaites (Deer et al, 1978). A similar low-silica pyroxene has been described from iron-ore sinters by Dyson and Jukes (1972). This also has Ca in both M1 and M2, and has appreciable Fe^{3+} in tetrahedral sites. Other clinopyroxenes known to contain tetrahedral Fe^{3+} have been described by Virgo (1972). All these pyroxenes share features of the Rhum fassaites: deep yellow colours, strong pleochroism and high dispersion. Thus it seems likely that the Rhum fassaites contain significant tetrahedral Fe^{3+} . However little or nothing is known about Fe^{3+} : Al partitioning between octahedral and tetrahedral sites in such pyroxenes, so this cannot at present be quantified.

The core of the clot consists of intergrown andradite, diopside and vermiculite. The diopside contains almost no iron, and all iron in the garnet is Fe^{3+} (Table 5.5). Thus the Fe^{2+} content of the core is extremely low. Andradite-diopside is a stable assemblage in the system $CaSiO_3-Fe_2O_3-CaMgSi_2O_6$ at $1137^{\circ}C$ (Huckenholz et al, 1968); Andradite is not stable above $1157^{\circ}C$ (op. cit.); above this diopside-haematite-wollastonite_{ss} + liquid would be the stable assemblage. No traces of haematite or wollastonite have been seen in any of the Rhum xenoliths. Unfortunately Huckenholz et

Phase:	Fass1	Fass2	Fass3	Mag	Cpx	Andr	Diop	Verm
SiO2 %	40.66	37.90	44.71	0.72	44.76	34.83	54.06	32.64
Al2O3 %	10.35	12.79	7.09	1.69	6.91	6.08	0.00	13.60
Fe2O3 %	11.29	11.73	4.81	63.63	5.31	23.15	ND	ND
FeO %	1.72	2.16	4.69	31.13	4.50	0.00	0.26	1.60
MgO %	9.08	7.56	10.91	1.37	11.31	0.41	17.46	34.01
CaO %	25.10	24.87	24.47	0.21	24.13	33.78	26.69	0.10
TiO2 %	1.61	2.43	2.25	1.19	2.29	0.56	0.05	0.00
Cr2O3 %	0.06	0.00	0.02	0.37	0.25	0.14	0.00	0.00
Total	99.87	99.45	98.94	100.32	99.46	99.18	98.52	81.95

TABLE 5.5 Selected analyses of minerals from sample 20B.
 Fe2O3 calculated by charge balance in all analyses. Fass1:
 fassaite adjacent to garnet-rich core. Fass2: fassaite from
 near middle of fassaite-rich zone. Fass3: fassaite intergrown
 with magnetite. Mag: magnetite from outer part of
 magnetite-rich zone. Cpx: clinopyroxene just outside
 magnetite-rich zone. Andr: andradite from core of clot. Diop:
 diopside intergrown with andradite. Verm: vermiculite?

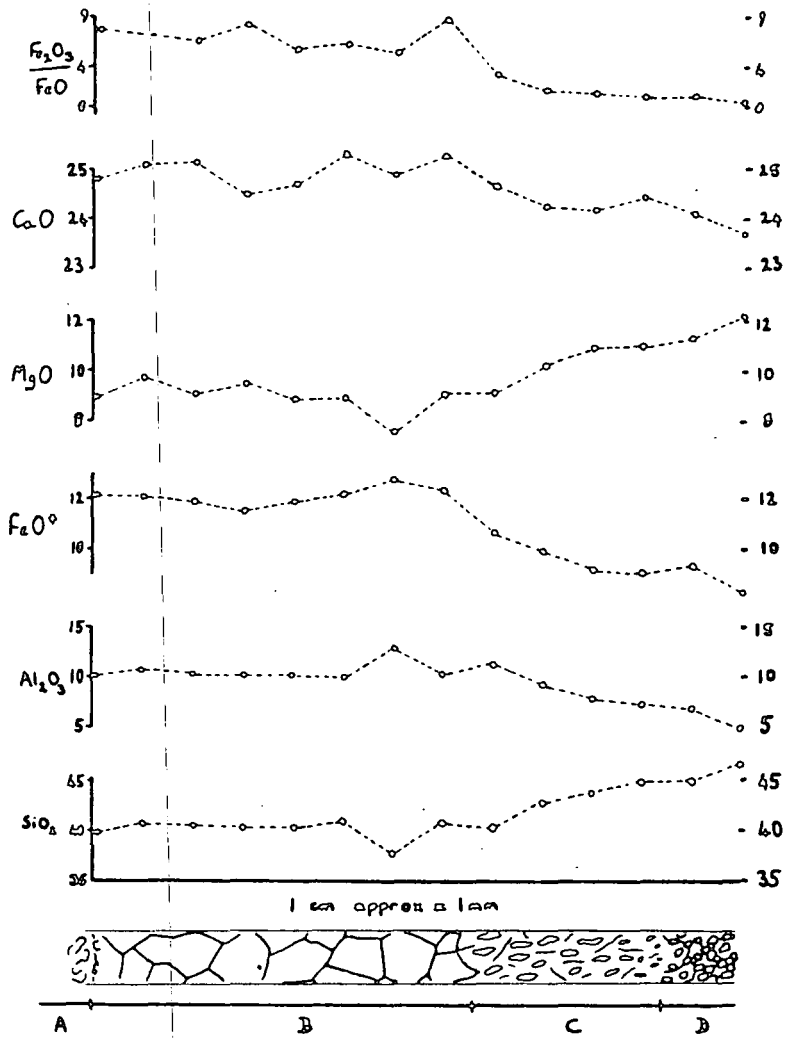


Fig 5.12 Pyroxene compositions in the zone surrounding the garnet/diopside clot (far right) and passing into beerbachite (far left). Fe³⁺ calculated by charge balance. A: garnet/diopside zone, B: fassaite zone, C: fassaite + magnetite zone D: beerbachite

al (1968) do not give $f(O_2)$ conditions for their experimental work, and the dependence of phase relations in this system on f_{O_2} are unknown. The fine intergrowth of andradite and diopside in the Rhum xenoliths suggests inversion from a homogeneous higher temperature phase.

There is a gradation in optical properties of the pyroxene from the core to the margin of the clot (Section 3.C.3.d). The variation in pyroxene composition across this zone is shown in Fig 5.12. Al_2O_3 , Fe^{3+}/Fe^{2+} , total Fe and Ca all tend to decrease from the clot to the enclosing beerbachite, while SiO_2 and MgO show the opposite trend.

The Fe^{3+}/Fe^{2+} ratio indicates a progressive decrease in f_{O_2} from the core of the clot to the beerbachite (Fig 5.12). In the latter the pyroxenes have Fe^{3+}/Fe^{2+} about 0.5 or less, while in the former all iron is Fe_{3+} , held in andradite. The fassaite has intermediate oxidation values. At clinopyroxene Fe^{3+}/Fe^{2+} ratios of 4-0.6, magnetite is intergrown with the fassaite.

As Fe^{3+} must have been diffusing out of the clot, this suggests that at high Fe and f_{O_2} , Fe^{3+} goes into fassaite. At lower Fe levels, and with appreciable Fe^{2+} present, magnetite is the main sink for Fe^{3+} ; and at still lower Fe levels and lower f_{O_2} , 'normal' augitic pyroxene can take up the Fe^{3+} . The coexisting gradient in aluminium concentration will also play an important role in stabilising fassaite.

5.C CONCLUSIONS

(i) The olivines and clinopyroxenes of the LELS show a wider range in composition and are less magnesian than those from other parts of the Rhum ultrabasic complex.

(ii) Subsolidus equilibration has modified the chemistry of the cumulates, particularly with regard to Mg/Fe ratios of ferromagnesian silicates.

(iii) The interstitial clinopyroxenes in peridotites evolve along a different trend to the clinopyroxenes of allivalites. The peridotite trend is

marked by higher Al_{iv} , Ti, Na and Cr.

(iv) Early formed orthopyroxene oikocrysts in allivalites are often replaced by alkaline amphibole-rich assemblages. This suggests that the interstitial liquids in LELS peridotites may have originally been silica-saturated, but were at least partially, displaced by later undersaturated liquids. A possible mechanism for this is discussed in Chapter 7.

(v) Sulphide blebs in Unit 1 may have been exsolved from the magma prior to olivine crystallisation, as olivine Ni contents are low. The chemistry of most sulphide minerals seems to be independent of whether they occur in the peridotite or the allivalite, although pyrite and violarite are restricted to the latter, suggesting higher $f(S_2)$ in the allivalite. The genesis of the sulphides will be further considered in Chapter 7.

(vi) Basaltic xenoliths are associated with very highly oxidised calcium-, aluminium-, and iron-rich amygdale assemblages. Significant diffusion of Fe^{3+} and Al^{3+} outward from these assemblages occurs over distances of 1-2cm.

CHAPTER SIX

CRYPTIC VARIATION

6.A. General

In order to examine the extent of cryptic variation in the L.E.L.S. 90 samples were collected over a 250m vertical section near the Allt nam Ba.

Clinopyroxene and olivine were analysed in all samples where both were present. A few samples lacked one or other phase. Plagioclase was not extensively analysed as preliminary studies indicated that within-sample variation was as great as or greater than that between samples. This has also been found by other workers on Rhum (Dunham and Wadsworth, 1978; Volker, 1983). At least 5 analyses per section were made of clinopyroxene and between 3 and 8 of olivine. In most cases σ was less than 0.3% Fo, or $MgX100/(Mg+Fe)$. In the case of clinopyroxene only core compositions were used, as marginal zoning both of cumulus crystals and poikilitic grains was frequently pronounced.

Even where considerable changes in texture or modal composition are present over the area of a given polished thin section, variations in mineral Mg/Fe ratios are not seen. Thus cryptic variation is not detectable on a small scale in the L.E.L.S. rocks; it seems to be on a larger scale than, and superimposed on the fine scale layering.

Variations in Fo content of olivine and in Mgn of clinopyroxene ($Mgn.=MgX100/(Mg+Fe)$) with height are shown in Fig. 6.1, together with stratigraphic data from the measured section. The range in olivine compositions is from $Fo_{85.6}$ to Fo_{70} ; thus olivine compositions significantly more iron rich than any previously recorded from Rhum - Fo_{74} (Palacz, 1984) - occur in the L.E.L.S.

The most obvious features of the cryptic variation profile are the "peaks" of Fo content associated with peridotites. Nearly every peridotite, even those <20cm thick or present as discontinuous slump horizons within allivalite show this enrichment in Fo

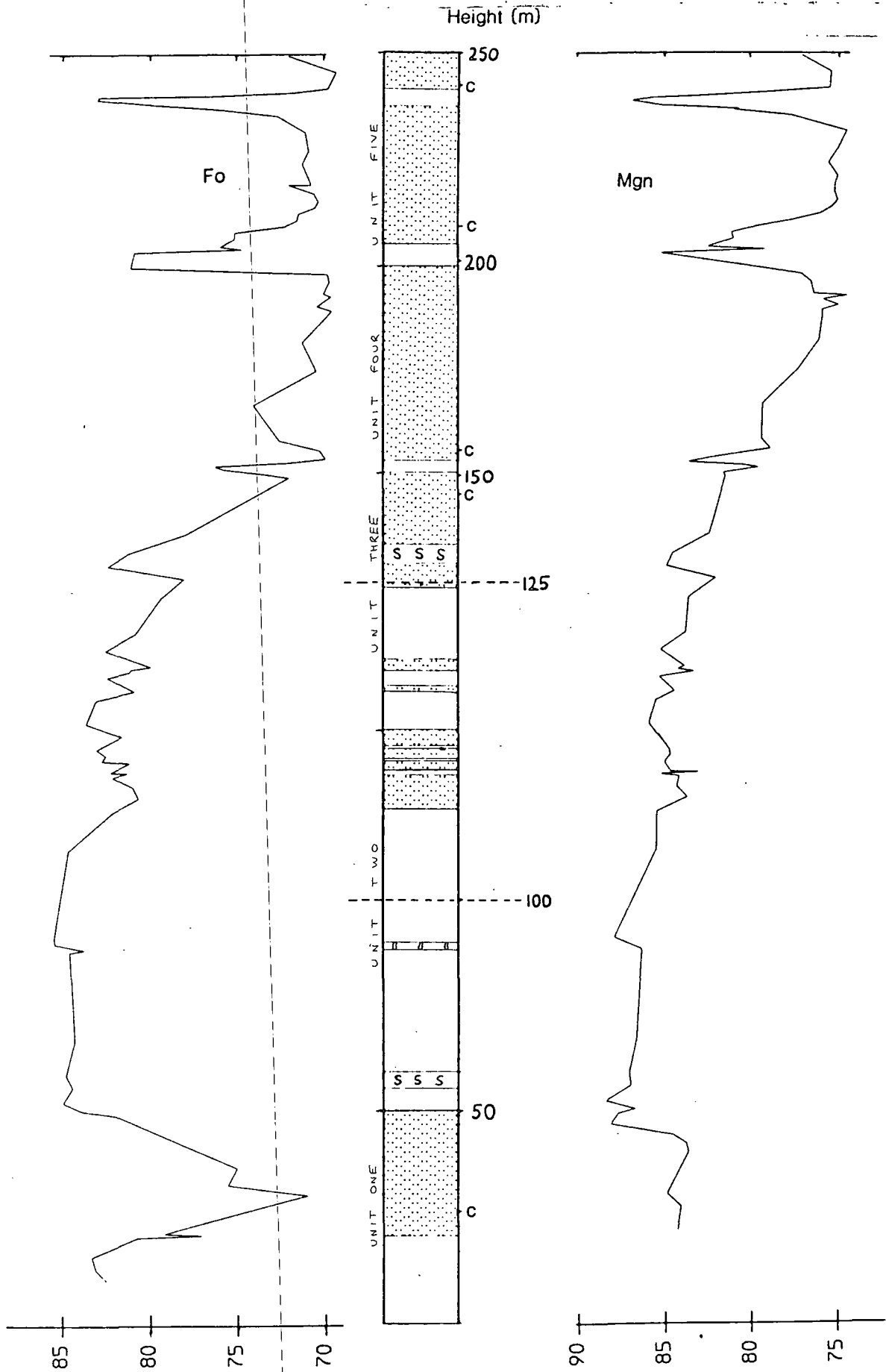


Fig 6.1. Variation of olivine Fo content (left), and clinopyroxene Mgn (right) with height above base of the LELS. C -lowest appearance of cumulus clinopyroxene in each unit. Note expanded vertical scale between 100 and 125 m. Allivalite stippled.

compared with the surrounding feldspar cumulates. Conversely allivalite layers, even where thin or disturbed, are marked by "troughs" of lower Fo content. Progressive depletion of olivine Fo content with height in a unit is not usually seen, although there is a suggestion of general Fo depletion with height particularly in the allivalites of Units 3, 4 and 5. The other obvious feature of the cryptic variation profile is the presence of "reversals" towards the top of allivalite layers - i.e. the most evolved olivines are seen some way below the top of the layer. Conversely the most magnesian olivines in peridotites are seen some way above the base.

The profile shown by the Mgn of clinopyroxene follows that shown by olivine very closely, except in the peridotite of Unit 4 and the central portion of Unit 1 allivalite. The former layer shows a much lower Fo content than other peridotite layers, and indeed the olivines of the overlying allivalite are richer in Fo than the peridotite itself. This may be explained by the presence of gabbroic veins in this area (see section 2c) perhaps indicating that a subsurface gabbro intrusion has modified the chemistry of the cumulates at this level. The situation in Unit 1 is problematic and is discussed later.

6.B Discussion.

There is compelling evidence that the mineral compositions of the L.E.L.S. have been modified by various post-cumulus processes. Work by Henderson and Suddaby (1971), Henderson (1975) and Bevan (1982) has shown, in Rhum and other intrusions that chrome spinels generally show compositions which have been extensively altered by reaction with interstitial liquid and other phases present. If such a process operates in chrome spinel, it seems likely to operate in other phases. Butcher (1985) has shown that late stage veins, representing evolved liquids in the cumulate pile emplaced along fractures, have modified the chemistry of minerals, particularly olivine and chrome spinel in the

surrounding cumulates over distances of 1-2 cm. If re-equilibration can occur over such distances when the rocks are relatively cool and brittle, then with hot interstitial liquids in porous piles the process should also be effective. This may explain the remarkable constancy of olivine compositions in individual samples. Further support for this comes from the fact that olivines are never zoned with respect to Fo, even when co-existing phases show extensive zoning, implying that any zoning has been eradicated by reequilibration. Diffusion profiles around calc-silicate clots in beerbachites from unit 5, also indicate migration of Al and Fe over distances of 1-2cm (chapter 5). It has already been shown (section 5.A.3) that the Fe/Mg ratios of coexisting olivines and clinopyroxenes indicate subsolidus exchange between the two phases, and probably involving the oxide phases and orthopyroxene as well.

The most magnesian clinopyroxene should be seen as the earliest formed cumulus crystals in allivalites, as these represent the first appearance of clinopyroxene on the liquidus. This is not the case. The most magnesian compositions are seen in the poikilitic pyroxene within the Unit 2 peridotite, associated with the most forsteritic olivines. Generally the clinopyroxenes in peridotites are more magnesian than any in the overlying allivalite, and within allivalites intercumulus clinopyroxene low down is more magnesian than the first cumulus grains higher up.

The sympathetic relationship between Mgn of clinopyroxene and Fo content of olivine may provide a clue to this. There is no reason, assuming that mineral compositions are primary, why interstitial i.e. late formed clinopyroxene in a peridotite should mirror the variation in Fo content of the cumulus olivines. The clinopyroxenes crystallized from trapped liquid and would be expected to show no variation, or a random one, with height. The sympathetic variation observed suggests that olivine and clinopyroxene exercise a control on each other's chemistry either by equilibration with late stage migrating liquids in the crystal pile, or by

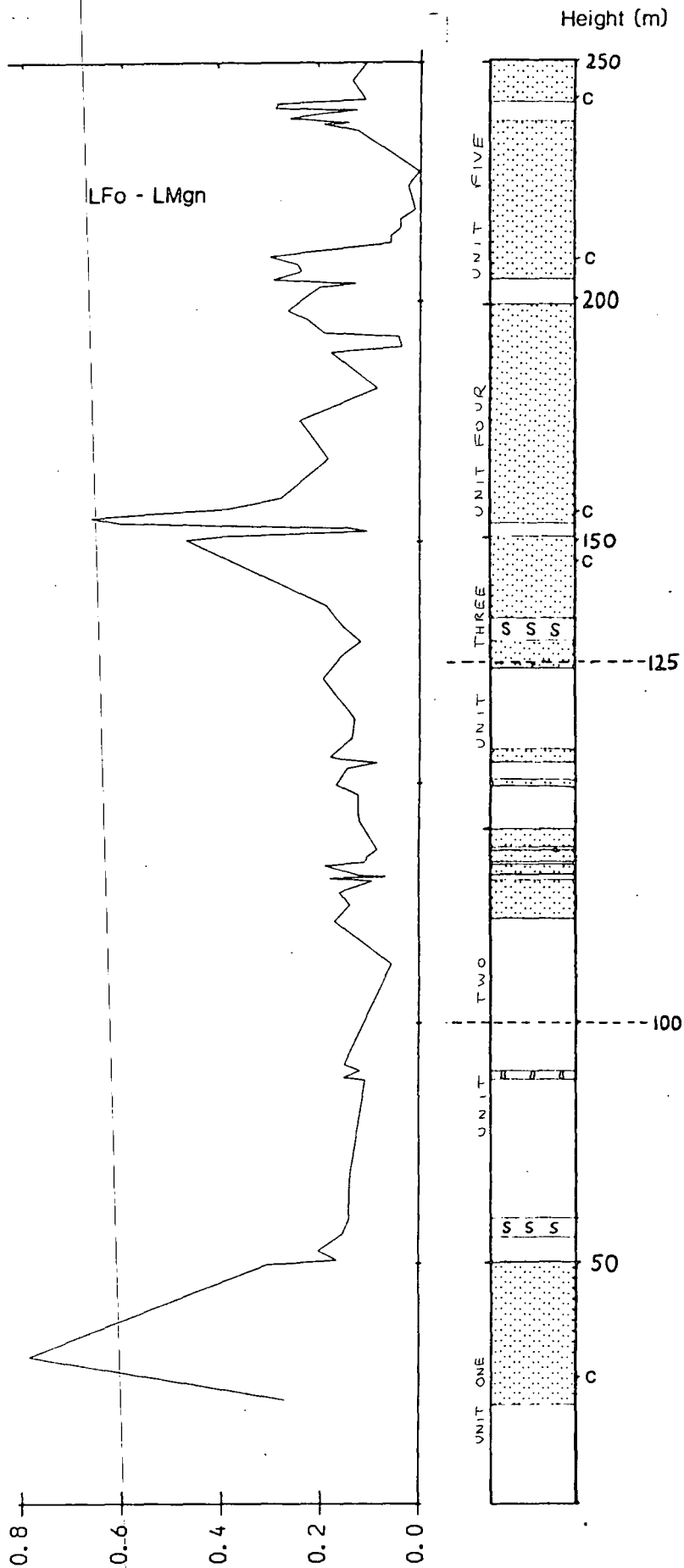


Fig 6.2 Variation in LFo-LMgn with height above base of the LELS. LFo= molar liquid Fe/Mg ratio calculated from olivine, LMgn= molar liquid Fe/Mg ratio calculated from clinopyroxenes, using equations of Duke (1976).

subsolidus Fe/Mg exchange.

The Fe/Mg ratios of liquids in equilibrium with the clinopyroxenes and olivines of the LELS have been calculated using the equations of Duke (1976). Earlier these were used to argue that subsolidus equilibration had indeed occurred. The larger the positive value of $L_{ol} - L_{cpx}$, where L_{cpx} = liquid Fe/Mg ratio calculated from clinopyroxene, and L_{ol} = liquid Fe/Mg ratio calculated from olivine, the greater the degree of equilibration. This parameter will thus be related, among other things, to the rate at which the rocks reach the blocking temperature for olivine-clinopyroxene Fe-Mg exchange. The variation of this parameter with height is shown in Fig 6.2. Values are in the range 0.0 to 0.3, apart from Unit 1 allivalite, and the unit 3/4 contact. At the latter level, there is evidence for late heating of the cumulates by gabbroic vein (section 3.B.4). This may account for the greater degree of equilibration. The situation in unit 1 allivalite is problematical and is discussed later. The allivalites of units 4 and 5 have generally low values similar to, or slightly lower than the other LELS rocks.

The above effects can be divided into two groups: those based on equilibration between solid phases, and those based on liquid/solid reactions. The former seem to have been the final control on mineral compositions, explaining the parallel variation of olivine and clinopyroxene; however it is likely that subsolidus effects are only significant over small distances (a few centimetres at most). To explain the large scale cryptic variation it is necessary to consider the movement of interstitial liquids.

It is clear that the pattern of cryptic variation supports the idea of repeated replenishment of the Rhum magma chamber (Brown, 1956). There are two main models by which the observed peridotite/allivalite layering can be produced in a replenished magma chamber. In the first type, of which the model of Brown (1956), is an example, each new batch of magma crystallises

first olivine, and then olivine + plagioclase as it cools. Brown envisaged a basaltic parent, but this is not essential to the model. In the second type, which was originally proposed by Huppert and Sparks (1980), a dense, high-Mg basalt or picrite is the replenishing magma. This hot, dense liquid ponds at the base of the magma chamber, under the lighter, cooler more evolved liquids which have resulted from the crystallisation of earlier cumulates. As the picritic layer cools, it convects vigorously and crystallises olivine, which decreases the density of the new magma. Eventually the density of the new magma will equal that of the old, and as the temperatures of the layers approach equality, convection slows down, and the interface between the layers breaks down. The allivalites crystallise from "hybrid" magma produced by the mixing of the two layers.

These two models will produce significantly different cryptic variation patterns. In the first case, the onset of olivine + plagioclase (ie allivalite) crystallisation should occur at a constant compositional point in each unit. With the second model this need not be the case, as the onset of crystallisation of olivine + plagioclase is not controlled by the liquidus relationships of the magma, but by the composition of the "hybrid" liquid formed after the breakdown of the picrite layer. If picrite influxes are small, then the composition of this hybrid magma will be dominated by the old residual magma. This could lead to allivalites in successive units showing a more or less continuous evolutionary trend, punctuated by the intervening peridotites.

It is clear from Fig 6.1 that the change from cumulus olivine to cumulus plagioclase + olivine occurs at different compositions in the LELS units. In addition, particularly in units 3, 4 and 5, there is suggestion of continuous iron enrichment with height in the allivalites. This supports the model of Huppert and Sparks (1980).

The pattern of cryptic variation suggests that peridotite layers, with roughly constant Fo contents, at

least where they are thick and undisturbed, are superimposed on an evolving allivalite trend. Thus the peridotites have olivines about Fo_{84-86} , while the allivalites show a range in compositions from about Fo_{83} to Fo_{70} . The composition of the allivalite immediately above a peridotite is thus controlled partly by the composition of the allivalite below. This is particularly well seen in Units 3, 4 and 5, where the allivalite above each peridotite rapidly approaches the composition of that formed prior to the crystallisation of the peridotite layer. This suggests that, after cessation of peridotite crystallisation, the magma overlying the olivine cumulates had only suffered minor replenishment. This can be explained in terms of two factors. Firstly, the peridotites in this part of the sequence are thin, and so the replenishing pulses of picrite may also have been fairly small. Secondly it is likely that the magma from which these evolved allivalites were crystallising was fairly dense (Fig 6.3), thus mixing of the replenishing liquids with the residual magma may well have occurred fairly quickly after their emplacement. The crystallisation of a small amount of olivine would be sufficient to bring the density of the new magma to that of the old. Upon mixing it seems that the new magma was considerably "diluted" by the old. The degree of dilution will depend not only on the volume of the picritic layer, but also the volume of residual magma with which it mixes. It is conceivable that if the residual magma were compositionally stratified, mixing might only involve the lowest and densest layers, producing relatively little dilution of the new magma. In an unstratified, convecting magma chamber the new magma would, upon breakdown of the interface, be mixed with the entire contents of the magma chamber, giving considerable dilution.

The cryptic variation profile (fig 6.1) suggests that mineral compositions in a given peridotite or allivalite layer are affected by the composition of the cumulates above and below. Where the layers are thin, or where a layer has been disturbed or slumped in

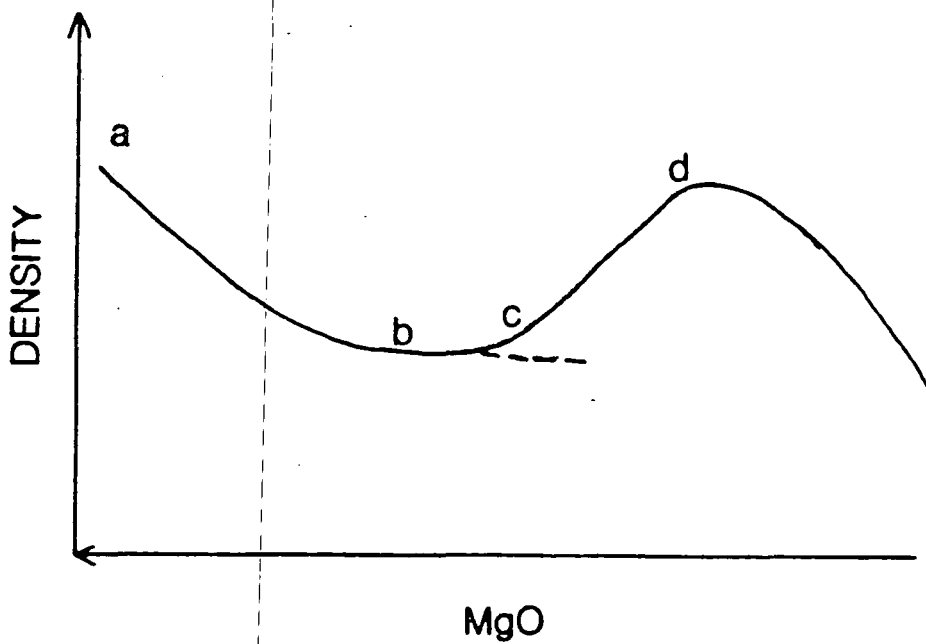


Fig 6.3 Density variation with MgO content of basic liquids shown schematically. Modified from Sparks and Huppert (1984). a - b :decreasing density due to olivine fractionation. c - d: increasing density due to fractionation of abundant plagioclase, and iron enrichment. Dashed line: inhibited density increase in hydrous magmas (Tait, 1984).

with the enclosing cumulates, the compositional contrast is lower than with thick and continuous layers. As the cumulates must have contained appreciable amounts of intercumulus liquid for mixing to occur, it is tempting to view the lowering of the compositional contrast as being due to equilibration with mobile pore liquids. The intercumulus liquid in a peridotite may be considerably more magnesian than that in an allivalite according to the model of Huppert and Sparks (1980). Thus mobilization of pore liquid from a peridotite into an allivalite would cause the allivalite olivines to reequilibrate to more magnesian compositions. Conversely, a thin peridotite mixed with intercumulus liquid from an allivalite would be made over to more iron-rich compositions. The net effect of this process will be to lower the compositional contrast between allivalites and peridotites where pore liquids are mobilized between layers.

While shock-induced mixing can produce these compositional effects in deformed layers, another mechanism is required to explain the reversals in the upper parts of allivalites where contacts are undisturbed. Tait et al (1984) argued that compositionally driven convection can occur in porous crystal piles. Thus if a dense liquid overlies a light liquid occupying pore space, the dense liquid will tend to migrate downwards, displacing the lighter one. This would seem to be a potent mechanism for producing the "reversals". Picritic liquid overlying an allivalite may be denser than the more evolved liquids in the allivalite pore space (Fig 6.3), and would tend to sink into the allivalite, the olivines reequilibrating with the new Mg-rich magma.

It is notable that reversals are small or absent at the tops of the allivalites of units 3, 4 and 5. These are highly evolved allivalites, and this may imply relatively dense, iron-enriched interstitial liquids (Fig 6.3). Picritic magmas would thus have been unable to displace the allivalite pore liquid, and no reversal would be produced. Another factor may have been

the relatively small volume of picritic replenishments in this part of the sequence, as the peridotites are fairly thin.

The problem with this is unit 1 allivalite, which given its highly evolved olivines, would be expected to have pore liquids as dense as those of units 3, 4 and 5. However, unlike the latter units, unit 1 allivalite shows a large reversal, indicating that picritic magma was able to displace pore magma in the upper part of the layer. Unit 1 is also anomalous in that clinopyroxene is very abundant relative to olivine, and the pyroxene is abnormally magnesian.

Water content has a powerful effect on melt density (eg Tait, 1984), and basalts with high water contents may not show a density minimum (Fig 6.3). They would also tend to crystallise very calcic plagioclase, and indeed unit 1 allivalite has the most calcic plagioclase in the LELS (section 5.A.4). This water enrichment might be sufficient to cause interstitial liquids to decrease in density as they fractionated, and allow them to be displaced by picritic liquid associated with the formation of unit 2.

Another anomalous feature of unit 1 is the occurrence of sulphide blebs, and cumulus ilmenites near the base of the allivalite. If these formed before the crystallisation of clinopyroxene, they would deplete the magma in Fe while having a negligible effect on Mg. This might explain the abnormally magnesian nature of the subsequently formed clinopyroxenes. According to this model however, they would have had to form subsequent to the evolved olivines, and this is unlikely, given the occurrence of ilmenite very low down in the allivalite, and the low Ni contents of the olivines, which suggest formation from sulphide-saturated liquids.

Water enrichment may also be able to explain the abundance of clinopyroxene in unit 1 allivalite. In the system Di-An, the stability field of diopside is greatly increased by increasing water pressure (eg Sood, 1981).

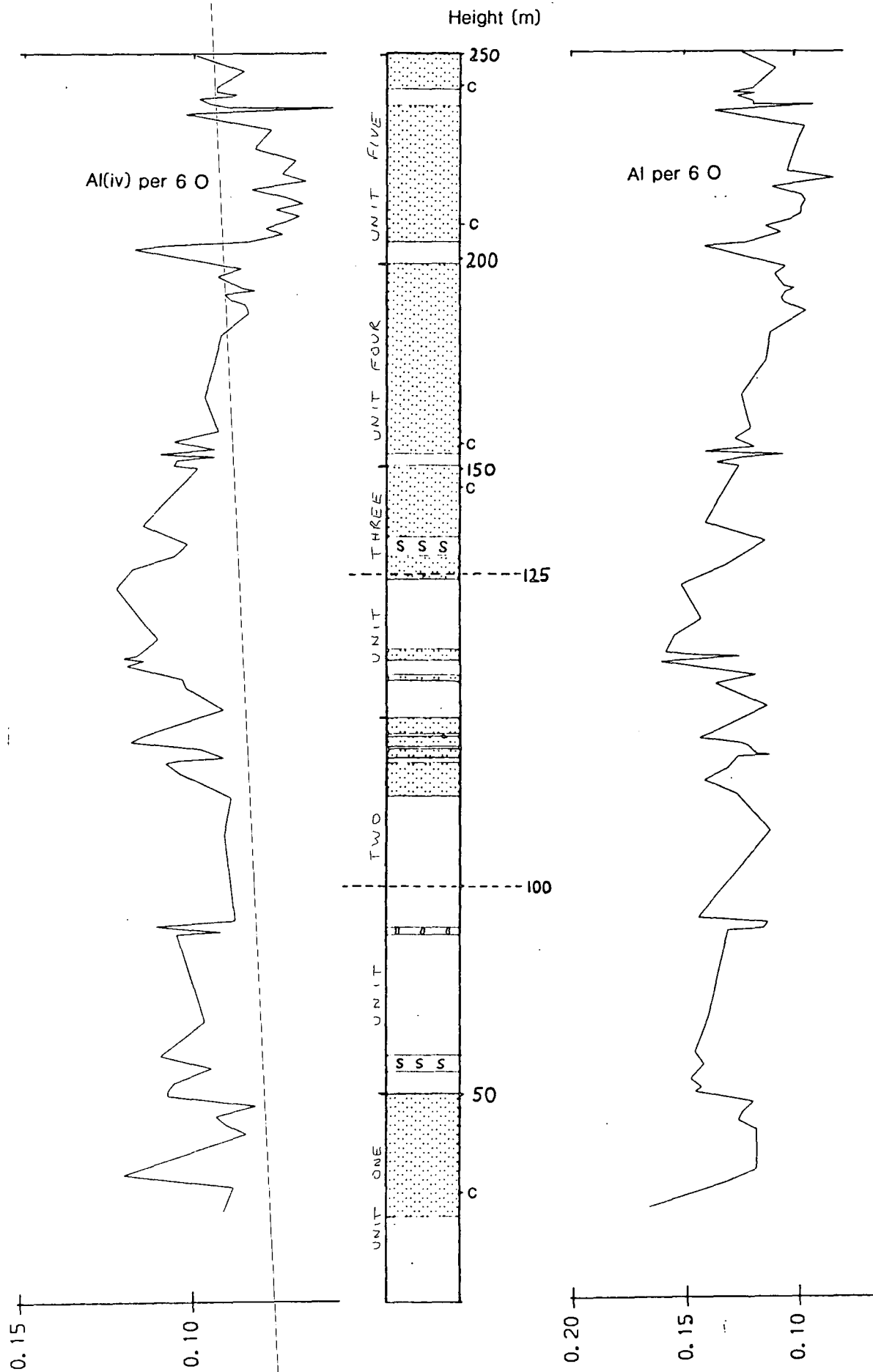


Fig 6.4 Variation of clinopyroxene total Al (right), and tetrahedral Al (left) contents with height above base of the LELS.

6.C Variation in clinopyroxene minor elements

6.c.1 ALUMINIUM

The variation of clinopyroxene aluminium content with height is shown in Fig 6.4. Higher Al contents tend to be associated with peridotites, and the lowest Al contents tend to occur with the most evolved allivalites. The latter may be due to the depletion of Al in the melt by extensive plagioclase crystallisation, or to higher SiO_2 activity during the formation of these rocks. Tetrahedrally coordinated aluminium contents are a more sensitive indicator of silica activity. The variation of Al_{iv} with height is also shown in Fig 6.4. There is a marked decrease in Al_{iv} in the allivalites of units 3, 4 and 5, suggesting increasing silica activity during the formation of these rocks.

6.C.2 TITANIUM

The variation in titanium with height is complex, and generally inter-sample variations are of a similar order of magnitude to the standard deviations for each sample (Fig 6.5). However clinopyroxenes with high Ti contents (>0.03 per 6 O) are restricted to peridotites, and are associated with fingering and replacement in the upper part of unit 2 and the lower part of unit 3. Ti does not show a marked decrease in the allivalites of units 3, 4 and 5, as might be expected from the Al_{iv} behaviour. However Ti enrichment in the liquids from which these fractionated cumulates formed may cancel out the effects of increasing silica activity.

6.C.3 CHROMIUM

Intra-sample Cr variation is considerable; for this reason the values shown on Fig 6.5 are maximum contents for each sample. Cr is highly compatible in clinopyroxene and thus should be a good indicator of fractionation. Like olivine Fo contents, and clinopyroxene Mg, the Cr profile shows marked peaks

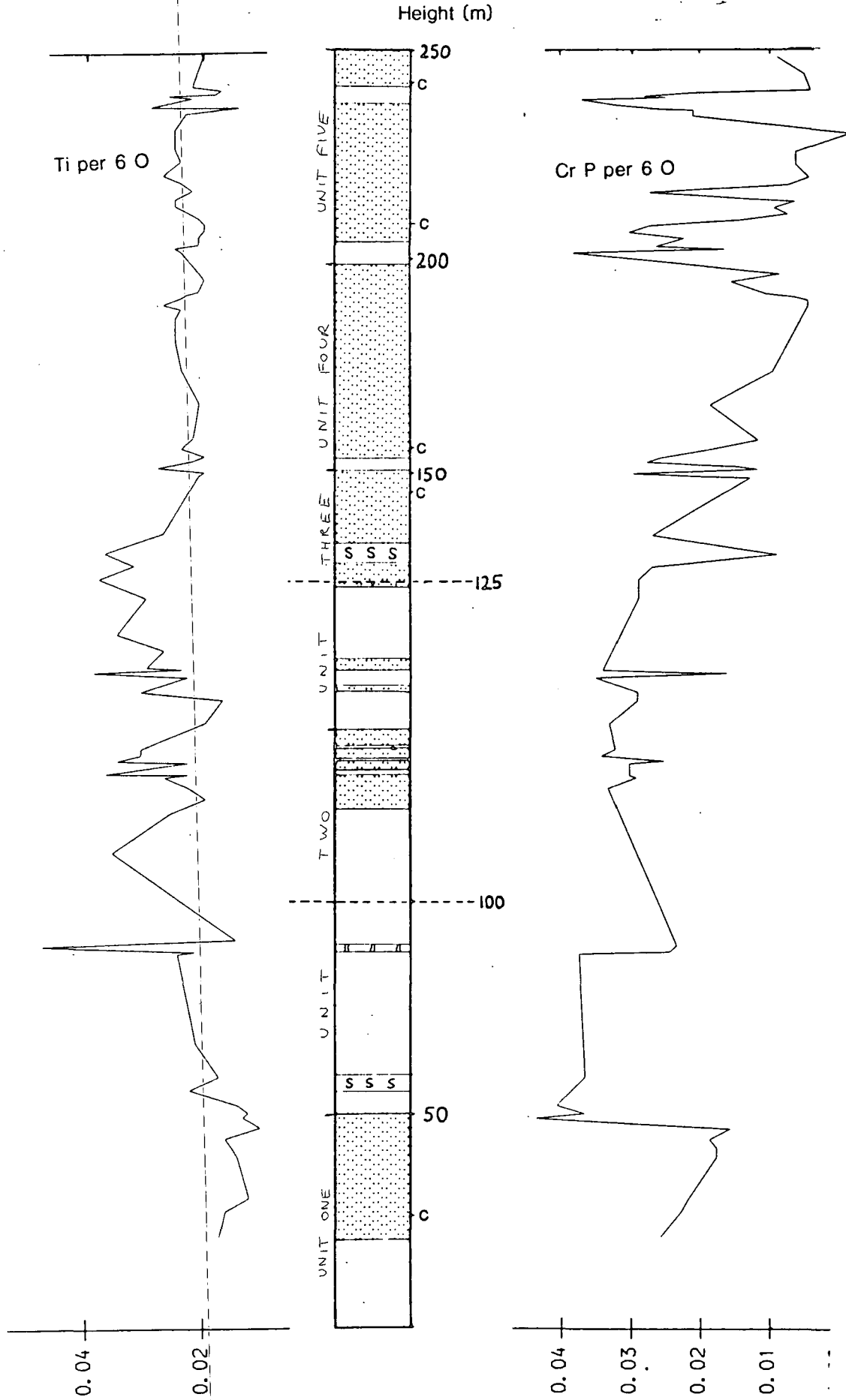


Fig 6.5 Variation of clinopyroxene Ti (left) and Cr (right) contents with height above base on the LELS.

associated with peridotites, and troughs associated with allivalites. Minimum Cr contents are usually seen a little way below the top of allivalites; the topmost part usually shows a reversal with enrichment in Cr, like Mg values.

6.D Conclusions

(i) The LELS shows more extensive cryptic variation than other parts of the Rhum complex.

(ii) Cryptic variation is generally more marked in allivalite layers than in peridotites. Peridotites nearly always have more magnesian olivines and clinopyroxenes than adjacent allivalites, supporting the idea of periodic replenishment of the magma chamber.

(iii) The pattern of cryptic variation supports the model of Huppert and Sparks (1980) for the origin of the large-scale (peridotite/allivalite) layering.

(iv) Post-cumulus processes play an important role in controlling mineral chemistry. Reequilibration of minerals with migrating pore magmas is often significant, and tends to lower the compositional contrast between layers. Subsolidus exchange of Fe and Mg between olivine and clinopyroxene accounts for the parallelism of their cryptic variation patterns.

CHAPTER 7
DISCUSSION AND CONCLUSIONS

7.A. The formation of the LELS

As discussed in chapter 6, the large-scale peridotite/allivalite layering can be explained by a model similar to that of Huppert and Sparks (1980). This involves the peridotites crystallising from hot, dense picritic layers at the base of the magma chamber. The allivalites crystallise from residual liquids

The behaviour of a picritic layer, and the way it breaks down is dependent on the temperature and density contrast between the picritic liquid and that already in the magma chamber (Sparks et al 1984). Generally in Rhum the contacts between peridotites and overlying allivalites are sharp. This may imply that the olivines of the peridotite have settled out prior to the commencement of olivine + plagioclase crystallisation. In the peridotite of unit 5 however, there is a gradational contact between the two layers, marked by centimetre-scale layering between olivine-rich and plagioclase-rich layers, the former becoming thinner and less well defined with height (section 3.B.5). This suggests some overlap in the crystallisation of olivines in the picritic layer and plagioclase + olivine in the magma above. These different contacts can be explained in terms of different temperature and density contrasts between the picrite and the overlying magma.

In the case of sharp contacts the settling out of olivine in the picritic layer seems to have been completed before the reappearance of plagioclase as a cumulus phase. In the case of the gradational contacts the picritic layer seems to have broken down before the olivines had settled out. This could happen if the densities of the two liquids approached equality before the temperatures equalised. The thermal gradient might be sufficient to keep convection going, and keep the olivines suspended, while cumulus plagioclase crystallised from the hybrid liquid. The complex zoning shown by plagioclases in the gradational zone is

consistent with their having formed prior to emplacement of the picrite, and then continuing to grow from more basic, replenished liquid produced by mixing of the liquids.

7.A.1 Types of small-scale layering

In addition to the large-scale layering discussed above, many types of smaller-scale layers occur. The main types are as follows:

(i) Appearance of a cumulus phase. The best example on Rhum is the clinopyroxene rich upper part of unit 9 allivalite (Young and Donaldson, 1985; Palacz, 1984). This merely indicates progressive evolution of the magma from which the cumulates are forming.

(ii) Chromite seams at anorthosite/peridotite contacts. Both the classic chromite seam at the base of unit 12, and the seam seen in unit 3 truncate lamination in the allivalite and seem to have formed by reaction between picritic magma and plagioclase. The allivalite is thermally eroded (ie resorbed) and coated by a reaction crust of chrome-spinel.

(iii) Variation in grain size. Abrupt changes in grain-size generally seem to be associated with lensoid, fine-grained plagioclase-rich layers, which it has been suggested (section 3.C.3.a), are deformed xenoliths. Other abrupt changes in grain size are seen in peridotites, particularly the minor peridotite high up in unit 5, where variations in size and habit of olivines occur. Individual laminae may be only one crystal thick. Despite the evidence for textural equilibration it is likely that these variations reflect fluctuations in the growth conditions of the olivines.

(iv) Variations in the relative proportions of intercumulus phases. This type of layering, termed matrix banding by Dunham (1965), is best developed in peridotites where variations in the proportions of clinopyroxene and plagioclase are spectacularly picked out on weathered surfaces. In the layered series this layering is usually sub-parallel to the general dip, but in peridotite plugs, eg at Sgaorishal, it may be

colloform. The type example, from a plug north of the Long Loch (Dunham, 1965) has been reinterpreted by McClurg (1982) as an early, hydrothermally altered joint-set, but elsewhere this type of layering certainly exists.

(v) Variations in the abundance of intercumulus material. The best examples are the dunite layers developed within peridotites of the upper ELS and CS. These are probably related to the way in which intercumulus material is expelled from a compacting pile of crystals (McKenzie, 1985). This is developed on a very local scale in the peridotites of units 2 and 3 (section 3.C.1.a).

(vi) Slight variations in the relative proportions of cumulus phases. This is almost ubiquitous in the LELS allivalites, and widespread elsewhere on Rhum.

(vii) Sedimentary layering. Layers showing unambiguous evidence of sorting by sedimentary processes are found in Rhum, although rarely. In parts of the CS size and density graded ultrabasic breccias are found, and in unit 9 allivalite on the Askival Plateau, a ripple laminated and cross-bedded sequence occurs. There is some evidence that sinking of chrome-spinels, and by implication, olivines, may have been significant in LELS peridotites (section 3.C.1.a). However, such evidence is lacking in LELS allivalites.

Possible examples of mechanical erosion in the LELS cumulates are seen in the channel-like layers of Unit 3 allivalite (section 3.B.3), and in unit 5 allivalite, where an ilmenite-rich layer truncates underlying layers (Fig 3.9). There is little or no mineralogical or cryptic change across this layer, so an origin by thermal erosion (cf chromite seams) seems unlikely.

7.A.2 The origins of small-scale layering

Evidence for the production of small-scale layering by crystal settling and sedimentary sorting is generally lacking in the LELS, at least in allivalites.

A variety of alternative mechanisms have been proposed, the main varieties of which are reviewed below.

(i) Kinetic effects

Maaloe (1978) argued that rhythmic supersaturation might be important in producing layering in Rhum and Skaergaard. Most phases do not begin to crystallise at their true liquidus temperatures, but require some degree of supercooling and supersaturation before nucleation and crystal growth can operate effectively. He argued that this could cause a crystallising liquid to oscillate about a cotectic with cooling, rather than following the equilibrium path. The products of this oscillatory path would thus alternate in composition, producing a layered sequence. Maaloe argued that this produced the observed small-scale layering within unit 14 allivalite. The process is plausible, although in the case of unit 14 the layering examined by Maaloe consisted of alternations between peridotite and allivalite, and is probably related to minor replenishments of picritic liquid.

Diffusion-controlled oscillating crystallisation is also a possible mechanism (cf Leisegang Rings), but this could only occur in non-convecting liquids where concentration gradients were able to build up above layers of growing crystals.

(ii) Crystallisation from stratified liquids.

The production of layered cumulates by crystallisation from layered liquids has been proposed (eg Irvine, 1980). As discussed earlier there is good evidence that the peridotite layers can be accounted for by crystallisation from short-lived, dense picritic magma layers, however the application of this mechanism to other types of layering is not clear.

If a density gradient exists in a magma chamber cooled from above, or heated from below, stratification of the liquid may occur. A density gradient can be induced in various ways. Entrainment of a light, turbulent boundary layer, produced by sidewall crystallisation, or by melting of low-density country rocks, is one possibility. An upward increase in water

content of the magma might be another. It has been suggested that the Marginal Suite represents, at least in part, a frozen silicic boundary layer to the Rhum magma chamber; thus a density gradient caused by increasing silica-contamination with height seems likely. Heat input from below, by hot dense picritic magma layers, would cause stratification in the magma overlying the picrite. Whether this stratification would persist during crystallisation, and whether it would produce layered cumulates is unknown. However one of the properties of such stratification is that density must decrease upwards from layer to layer. It seems unlikely that the small-scale layers seen within allivalites represent the products of successively less dense liquid layers.

Stratification as described above, will tend to break down from the bottom upwards. One possible effect of this might be that the magma at the base of the chamber would undergo periodic compositional fluctuations as the interfaces between overlying layers broke down and the magmas mixed by convection. Cotectic surfaces in basaltic systems are often curved (eg Irvine, 1977). Thus mixing of liquids at different points on the cotectic can produce "hybrid" liquids deviating from cotectic compositions. This would produce changes in the cumulates observed. This process is not, of course, dependent on the breakdown of stratified liquids. Any periodicity in mixing caused by convection in the magma above the growing crystal pile could in theory produce layering.

(iii) Fluctuating water content.

Phase relations in many silicate systems are sensitive to changes in water content. Increasing water pressure in the system Fo-An-SiO₂ moves the phase boundaries towards more silica-rich compositions (eg Sood, 1981), increasing the size of the olivine stability field in particular. Thus fluctuating water pressure in the magma chamber might be sufficient to produce small changes in the proportions of phases crystallising on a cotectic. The most striking

compositional effect of small changes in water content of basic melts is on the composition of crystallising plagioclase. Thus if this process is significant in producing layering, variations in plagioclase An content should be marked between layers. This has been invoked as a possible explanation for the abundance of clinopyroxene in unit 1 allivalite (section 6.B). More precise application of such explanations on a smaller scale is difficult as plagioclase compositional variation seems to be somewhat haphazard and difficult to interpret (section 5.A.4). However this very lack of correlation between plagioclase An content, and the Fe/Mg ratios of olivine and clinopyroxene, suggests that fluctuating water pressure may have been a feature of the Rhum magma chamber.

In conclusion, it is very difficult to sort out the effects of these different processes. None of the above processes are mutually exclusive, and it is likely that they all play some part. Only rarely can end-member processes be distinguished, most notably layers dominated by settling and sorting processes. Detailed work on plagioclases, which unlike other phases in Rhum, commonly retain growth zoning, and are sensitive to water pressure variations, may provide some means of distinguishing between layers formed by kinetic effects and those formed by larger-scale liquid compositional variations.

7.B. Parental magmas, contamination and evolution.

The general sequence observed in the LELS suggests an olivine-rich tholeiitic parent, as orthopyroxene is a common phase, and inverted pigeonite has been found in a xenolith derived from the upper part of the intrusion. Most of the cumulates are olivine-hypersthene normative with no free quartz. However nepheline-normative rocks are also found, mainly as late veins in peridotites, and the intercumulus phases in LELS peridotites suggest formation from late alkaline magmas.

The earliest attempt to determine the

Name	M9/G	B622	53A	BHY
SiO2	44.80	45.32	45.99	46.80
TiO2	1.07	1.53	0.82	0.80
Al2O3	11.16	12.06	11.63	18.60
Fe2O3	1.70	1.42	1.40	1.20
FeO	11.34	9.47	9.35	7.98
MnO	0.16	0.19	0.17	0.10
MgO	20.50	12.34	19.93	10.90
CaO	9.41	11.47	7.64	10.60
Na2O	1.31	1.92	1.65	2.70
K2O	0.11	0.14	0.16	0.30
P2O5	0.10	0.13	0.09	0.00
CIPW Norms				
Or	0.65	0.83	0.95	1.77
Ab	10.79	16.25	13.96	18.17
An	24.25	23.88	23.86	37.76
Ne	0.16	--	--	2.54
Di	17.47	25.98	10.76	11.98
Hy	--	1.75	10.10	--
Ol	43.61	22.04	35.42	24.52
Mt	2.47	2.06	2.03	1.74
Ilm	2.03	2.91	1.56	1.52
Ap	0.23	0.30	0.21	0.00

Table 7.1 Various proposed parental magmas for the Rhum complex. All norms calculated assuming $Fe^{3+}/Fe^{2+}=0.15$. M9/G: ultrabasic dyke groundmass from McClurg (1982). B622: dyke from McClurg (1982). 53A: variolitic marginal gabbro (this work). BHY: hypothetical parent magma of Brown (1956).

composition of the parental magma was made by Brown (1956). He subtracted the relevant quantities of the cumulus phases from the whole-rock analysis of an allivalite from Unit 3, which he assumed to be a perfect orthocumulate. This gave the composition of a highly aluminous transitional/alkaline basalt. (Table 7.1). This method is likely to be highly inaccurate in view of the difficulty in distinguishing cumulus from intercumulus material in allivalites, and in view of the possibility that the liquid finally trapped in the cumulate was not directly related to that from which the cumulus phases formed. A further difficulty arises from Brown's optical estimates of mineral compositions, which for Unit 3 at least, were probably somewhat in error.

Another approach was used by Tait (1985). He used analyses of Rhum ultrabasic dykes from McClurg (1982) and Forster (1980) as parent liquids and produced a convincing model for the chemical evolution of Unit 10. Analyses of the compositions used are given in Table 7.1. Rocks in this dyke suite are transitional: some eg M9 are nepheline normative while others such as B622 are hypersthene normative.

It had previously been assumed that as the Rhum ultrabasic complex was entirely fault-bounded, it had no chilled margins. However possible chilled margins have been identified under the low-angle contacts at Beinn nan Stac and Sgurr nan Gillean. An analysis of sample 53A from the latter locality is given in Table 7.1. The rock is similar in chemistry to the ultrabasic dykes, but is enriched in Ba and K due to having been emplaced against felsites of low melting point.

These picritic and ultrabasic dykes and marginal rocks would seem to provide good candidates for mildly alkaline or transitional parent magmas. Their close spatial and temporal association with a large ultrabasic magma chamber cannot be fortuitous.

The next problem is to explain the coexistence of tholeiitic and alkaline rocks in the same magma chamber. Campbell (1985), among others, has suggested that continental tholeiites may be produced by

contamination of picrites by silicic continental crust. A similar method may be appropriate to Rhum.

Alkaline rocks are always associated with peridotites in Rhum. According to the model of Huppert and Sparks (1980) and Tait (1985), peridotites evolve from influxes of picritic magma which pond at the base of the magma chamber. Allivalites crystallise from more evolved 'basaltic' liquids with longer residence times in the magma chamber. There is abundant evidence in the Marginal Suite for contamination by melted acid country rocks. If, as has been suggested in Chapter 2, the Marginal Suite represents the original igneous margin of the intrusion, the walls of the intrusion would have been marked by an upward-convecting boundary layer of contaminated magma. If convection in this boundary layer was turbulent, then siliceous contaminated magma would become incorporated into the main body of the magma chamber.

The convective behaviour of boundary layers depends on the Grashof number, G , calculated thus:

$$G = gdrL^3/r_0v^2$$

where g =gravitational acceleration, dr =density difference, L =vertical height of boundary, r_0 =density of magma away from the boundary layer and v =kinematic viscosity of the magma. If G is $> 10^6$ then convection will be turbulent. Using $r_0=2.7 \text{ gcm}^{-3}$, $dr=0.25\text{gcm}^{-3}$, and $v=10^2 \text{ cm}^2\text{s}^{-1}$, as values applicable to Rhum, convection would be turbulent for wall heights greater than about 10^3 cm . It is thus likely that convection was turbulent and contamination would have been carried into the main body of magma. For a rhyolitic magma chamber, Spera et al (1982) calculated the thickness of the convecting boundary layer to be about 100m.

It might be thought that the close proximity to the Marginal Suite of apparently undisturbed layering argues against such a boundary layer. However vertical convecting boundary layers have sharp contacts, particularly in their lower portions where flow may be laminar. Huppert and Turner (1980) illustrate double-

diffusive liquid stratification stably coexisting with a thin turbulent boundary layer in the case of ice-blocks melting into a salinity gradient.

The exact behaviour of the boundary layer in Rhum would be much more difficult to analyse, due to the lithological and thermal complexity of the boundary. Factors which would have to be considered include the viscosity, temperature and density profiles across the country rock - melted country rock - chilled margin - magma zone, the rate of formation and rupturing of the chilled margin, and the style of convection and heat transfer occurring within the main body of magma. The thermal budget of the intrusion would also be important. Replenishment of the chamber would maintain it at a very high temperature; the crystallisation of large quantities of olivine would release enormous quantities of latent heat which would encourage thermal erosion of the wall rocks. This may have been a major mechanism in creating space for the ultrabasic chamber, with the melted country rocks being convected upwards along the intrusion walls and erupted out of the top of the volcano.

The partial entrainment of the contaminated boundary layer into the main body of magma could well be sufficient to cause initially alkaline basalts to evolve along a tholeiitic path. Thus according to this model picritic liquids entering the chamber may have been mildly alkaline, but liquids residing in the chamber for any length of time would be tholeiitic.

This still leaves the problem of early intercumulus orthopyroxene in the LELS peridotites. This could be explained by downward percolation of contaminated tholeiitic liquids into the crystal pile; but orthopyroxene occurrences do not correlate with other evidence for downward movement of evolved liquids (chapter 5).

It is suggested that the orthopyroxene is the result of mixing of the incoming picritic pulse with contaminated liquids in the magma chamber. Depending on the density contrast between the incoming magma and that

in the chamber, and the velocity and direction of intrusion, the incoming magma may form a turbulent plume as it enters the chamber. This would entrain appreciable quantities of the old magma before sinking back to form a layer at the base of the chamber. This could result in the peridotite becoming silica-saturated, and crystallising orthopyroxene. The instability of orthopyroxene in peridotites suggests that later alkaline picritic liquids were able to percolate into the crystal pile, without being contaminated, giving the alkaline trends commonly found in peridotite intercumulus assemblages.

Apart from the LELS, and to a lesser extent, Unit A of the WLS, orthopyroxene is very rare or absent in the the ultrabasic complex. This may partly be related to the proximity of these areas to vertical contacts where turbulent boundary layers would be most likely. Another possibility is that contaminated silicic magmas did not accumulate in the chamber during the formation of most of the complex. More frequent and larger influxes of magma might explain this, as residual magmas were flushed out before significant contamination could build up. Another possibility is the development of a more stable chilled margin during the development of the upper ELS, which may have acted as a barrier to large-scale contamination. A further factor may have been a change in the convective regime in the magma chamber, such that contaminated liquids were not present in the lower part of the chamber, where the cumulates were forming. A stable liquid stratification might confine large-scale entrainment of contaminated liquids to the upper part of the chamber.

7.C. Fingers and replacement

Finger structures provide clear evidence for replacement of allivalite by peridotite in the Rhum complex (Butcher et al, 1985). A brief outline of their main features is given below.

(i) Finger structures post-date the development of lamination, and slump-folds in the

overlying allivalite. However they are earlier than the late-stage veins, which have been observed to cut fingers.

(ii) Finger structures are only seen on the upper surfaces of peridotite layers. Where peridotite overlies allivalite, contacts are either sharp and planar, or show deformational structures such as flames and load-casts.

(iii) Fingers occur on a range of scales from < 1cm, up to 1m or more where they cut right through allivalite layers. In the most extreme examples, only a few relict blocks of allivalite may be left, scattered along strike. It is thus possible that fingering processes have completely removed allivalite horizons, leaving no trace of them.

(iv) Deformation associated with fingers is negligible compared with the scale on which they occur. Allivalite adjacent to fingers generally shows no evidence of deformation, although in specimens from unit 8, single plagioclase crystals are deflected upwards against the finger margin. Elongate olivines within the peridotite of the same finger are aligned parallel to the finger margins, suggesting that the allivalite was behaving more rigidly than the peridotite.

(v) Fingers only seem to be associated with troctolitic or anorthositic allivalites. Allivalites rich in pyroxene have not been observed cut by fingers. This may suggest that the fingering process operates only over a restricted compositional range.

(vi) There is little relationship between the thickness of a peridotite layer and the amplitude of the fingers along its upper surface, although fingers on the upper surfaces on load-casts and other semi-isolated masses of peridotite are always small.

(vii) The Mg/Fe ratios of olivine and clinopyroxene show no significant differences between finger peridotite and adjacent allivalite.

7.C.1 Discussion

While the morphology of finger structures

suggests an origin by loading (cf Anketell et al, 1971), the lack of deformation in the cumulates argues against this. It has been suggested that the interstitial liquid in peridotites may be less dense than that in allivalites (Butcher et al 1985). Thus liquid-liquid loading could occur within the interstices of the crystal pile. According to this model, peridotite pore liquid may not be in equilibrium with plagioclase, and would tend to resorb it, crystallising olivine. However, large fingers occur above thin peridotite layers, and it is doubtful that sufficient pore liquid would be present to resorb significant quantities of plagioclase.

A possible solution to this is provided by the evidence for late-stage alkaline liquids in peridotites. This has been used to argue for replenishment of pore liquid in peridotites by primitive, undersaturated liquids (section 7.B). That evidence for such replenishment is lacking in allivalites is ascribed to their low permeability, perhaps due to more efficient packing of tabular plagioclase compared with the rounded or irregular shapes of olivines in peridotites. In the LELS, those parts of the sequence where fingers are developed have high Ti contents in clinopyroxenes, one of the features of pore liquid replenishment.

It is thus proposed that the peridotites were often able to act as permeable "aquifer" horizons, along which primitive liquids were able to migrate. This is perhaps not a requisite of replacement, but replacement on a large scale requires replenishment of the pore liquid. Where peridotite may be cut off from replenishing liquid as in load casts, the fingers are always small.

The restriction of fingers to the upper surfaces of peridotites may involve a number of factors. First, during compaction of a sequence of several units, pore liquid expelled from the lower parts of peridotites may tend to become ponded below less permeable allivalite layers, producing melt-supported layers which would be highly permeable. Second, the liquids involved in resorbing allivalites may be lighter than the pore

liquids in allivalites affected by replacement. Thus where these liquids overlie allivalite, they would have little tendency to penetrate into it. Another possibility is that while fingers are produced by replacement in situations where allivalite overlies peridotite, in other situations replacement may produce contacts with different morphologies. If planar contacts can be produced by replacement, then the phenomenon may be extremely widespread, but its effects may not be recognisable.

7.D. Evolution of the ultrabasic complex

As discussed in chapter 1, the Rhum complex has been divided into 3 main lithological units: the ELS, WLS and CS. The CS is the latest-formed and has subsided into its present position. This obscures the relationship between the ELS and WLS. Further difficulties are introduced by movements along the Long Loch Fault. Some of this is later than the emplacement of the CS, but it has been suggested that the fault was active before this (Emeleus et al, 1985) and differential movement of the ELS and WLS may have occurred before emplacement of the CS. Thus it is not known whether the ELS and WLS represent different facies in the magma chamber developing simultaneously, or whether one is older than the other. At present it is not possible to resolve this problem directly. However there are certain similarities between the ELS and the WLS. Both are characterised by a general reverse cryptic variation. The Harris Bay member, like the LELS, consists of relatively evolved rocks. Further up the sequence both the WLS and the ELS tend to become more "ultrabasic" with more magnesian olivines and the development of olivine-rich harrisites, although these are fairly rare in the ELS.

If this implies at least a partial temporal overlap between the two series, then conditions must have been extremely variable over quite short distances in the magma chamber. Plagioclase rich rocks are not seen in the WLS, implying that magmas with plagioclase

on the liquidus were never able to crystallise in the western part of the chamber.

Other evidence can be used to argue for the WLS having a lower stratigraphic position than the ELS. The WLS is bounded by the Western Granophyre, while the ELS is in contact with higher level rocks - felsites, explosion breccias and amygdaloidal basalts (seen as xenoliths). Whether this relative disposition of early Tertiary acid rocks occurred before or after the development of the ELS and WLS is uncertain.

7.E. Emplacement of the complex

The interpretation of the low-angle contacts under Beinn nan Stac, Cnapan Breaca and Sgurr nan Gillean, as fragments of the roof to the ultrabasic magma chamber has important implications for the emplacement of the complex (Emeleus et al, 1985). The interpretation of the vertical marginal contacts as also being original igneous contacts means that the Rhum complex is essentially in situ.

This eases some of the problems associated with the model of Emeleus et al (1985). These are principally the lack of evidence for faulting associated with the Marginal Suite and the evidence that the magma chamber was in contact with hydrothermally altered basalts (ie very high level rocks), and largely contaminated by early Tertiary felsite rather than deeper seated country rocks. In addition the model of Emeleus et al (1985) recognises difficulties in envisaging a mechanism by which a semi-solid cylinder of dense ultrabasic rocks could be emplaced upwards to the present level.

It is suggested that final uplift along the Inner Ring Fault (Smith, 1985) preceded the development of the ultrabasic magma chamber. This uplift may have been related to the entry, at lower crustal levels, of large volumes of very hot picritic liquids. Later these magmas were able to reach high crustal levels, forming the Rhum ultrabasic complex we now see.

- Anketell, J.M., Cegla, J. and Dzulynski, S. 1970. On the deformational structures in systems with reversed density gradients. *Annales de la Societe Geologique de Pologne* vol 40, p3-30.
- Bailey, E.B. 1945. Tertiary igneous tectonics of Rhum. *Quarterly Journal of the Geological Society of London* vol. 100, p165 - 191.
- Barnes S.J. and Naldrett A.J. 1985. Geochemistry of the J-M (Howland) Reef of the Stillwater Complex, Minneapolis Adit Area. I. Sulphide Chemistry and Sulphide-Olivine equilibrium. *Economic Geology* vol 80, p627-645.
- Bevan, J.C. 1982. Reaction rims of orthopyroxene and plagioclase around chrome-spinels in olivine from Rhum and Skye. *Contributions to Mineralogy and Petrology* vol. 79, p124 - 129.
- Black, G.P. 1952. The Tertiary Volcanic Succession of the Isle of Rhum, Inverness-shire. *Transactions of the Edinburgh Geological Society* vol 15, p39-51.
- Black, G.P. and Welsh, W. 1961. The Torridonian succession of the Isle of Rhum. *Geological Magazine* vol 98, p265-276.
- Boctor, N.Z. 1980. Partitioning of Ni between olivine and iron monosulphide melt. *Carnegie Institution Washington Yearbook* 80, p352-356.
- Boctor, N.Z. 1982. The effect of $f(O)$, $f(S)$ and temperature on Ni partitioning between olivine and iron sulphide melts. *Carnegie Institution Washington Yearbook* 81, p366-369.
- Brooks, C.K. 1976. The Fe_2O_3/FeO ratio of basalt analyses - an appeal for a standardised procedure. *Bulletin of the Geological Society of Denmark* vol 25, p117-120.
- Brown, G.M. 1956 The layered ultrabasic rocks of Rhum, Inner Hebrides, Scotland. *Philosophical Transactions of the Royal Society of London. B.* vol. 240, p1 - 53.
- Brown, G.M. 1972 Pigeonitic pyroxenes - a review. *Memoirs of the Geological Society of America* vol

- Butcher, A.R. 1984 A study of postcumulus structures in the Rhum layered intrusion, Inner Hebrides, Scotland. Unpublished PhD thesis, University of Manchester.
- Butcher, A.R. 1985 Channelled metasomatism in Rhum layered cumulates - evidence from late-stage veins. Geological Magazine vol. 122 p503-518.
- Butcher, A.R., Young, I.M. and Faithfull, J.W. 1985. Finger structures in the Rhum complex. Geological Magazine vol. 122 p491-502.
- Campbell, I.H. 1985. The difference between oceanic and continental tholeiites: a fluid dynamic explanation. Contributions to Mineralogy and Petrology vol 91, p37-43.
- Campbell, I.H. and Turner, J.S. 1986. The influence of viscosity on fountains in magma chambers. Journal of Petrology vol27, p1-30.
- Craig, J.R. and Killerud, G. 1969 Phase relations in the Cu-Fe-Ni-S system and their application to magmatic ore deposits. In H.D.B. Wilson (Ed), Magmatic Ore Deposits, Economic Geology Monograph 4, p344-358.
- Craig, J.R. and Scott, S.D. 1974. Sulphide Phase Equilibria. In Ribbe, P.H. (Ed), Sulphide Mineralogy, Mineralogical Society of America Reviews in Mineralogy Vol 1, pCS1-CS109.
- Deer, W.A., Howie, R.A., and Zussman, J. 1978. Rock Forming Minerals vol 2A, Single Chain Silicates. Longmans, London, pp668.
- Donaldson, C.H. 1976 An experimental investigation of olivine morphology. Contributions to Mineralogy and Petrology vol.57, p187 - 213.
- Donaldson, C.H. 1982. Origin of some of the Rhum harrisite by segregation of intercumulus liquid. Mineralogical Magazine vol 45, p201-209.
- Donnellan, N.C.B. 1981. Geochemical Studies of the Torridonian Sediments of N.W. Scotland. Unpublished Ph.D. thesis, University of Birmingham.
- Duke, J.M. 1976 Distribution of the period four

- transition elements among olivine, calcic clinopyroxene and mafic silicate liquids: experimental results. *Journal of Petrology* vol.17, p499 - 521.
- Duke, J.M., and Naldrett A.J. 1978. A numerical model of the fractionation of olivine and molten sulphide from komatiite magma. *Earth and Planetary Science Letters* vol 39, p256-266.
- Dunham, A.C. 1962. The petrology and structure of the northern edge of the Tertiary igneous complex of Rhum. Unpublished D.Phil. thesis, Oxford University.
- Dunham, A.C. 1964. A petrographic and geochemical study of back-veining and hybridisation at a gabbro-felsite contact in Coire Dubh, Rhum, Inverness-shire. *Mineralogical Magazine* vol 33, p887-902.
- Dunham, A.C. 1965. A new type of banding in ultrabasic rocks from central Rhum, Invernesshire, Scotland. *American Mineralogist* vol 50, p 1410-1420.
- Dunham, A.C. 1968. The felsites, granophyre, explosion breccias and tuffisites of the north-eastern margin of the Tertiary igneous complex of Rhum, Inverness-shire. *Quarterly Journal of the Geological Society of London* vol 123, p327-352.
- Dunham, A.C. and Emeleus, C.H. 1967. The Tertiary Geology of Rhum, Inner Hebrides. *Proceedings of the Geologists' Association* vol 78, p391-456.
- Dunham, A.C. and Wadsworth, W.J. 1978. Cryptic variation in the Rhum layered intrusion. *Mineralogical Magazine* vol.42, p347 - 356.
- Dunham, A.C. and Wilkinson, F.C.F. 1985. Sulphide Droplets and the Unit 11/12 chromite band, Rhum: a mineralogical study. *Geological Magazine* vol 122, p539-548.
- Dyson, D.J. and Jukes, L.M. 1972. A silica deficient pyroxene from iron-ore sinters. *Mineralogical Magazine* vol 38, p872-877.
- Emeleus, C.H. 1981. A thrust fault at Welshman's Rock, Isle of Rhum. *Scottish Journal of Geology* vol 17,

- Emeleus, C.H. 1985. The Tertiary lavas and sediments of northwest Rhum, Inner Hebrides. *Geological Magazine* vol 122, p 419-437.
- Emeleus, C.H. and Forster, R.M. 1979. *Field Guide to the Tertiary Igneous Rocks of Rhum, Inner Hebrides*. Newbury. Nature Conservancy Council.
- Emeleus, C.H., Wadsworth, W.J., and Smith, N.J. 1985. The early igneous and tectonic history of the Rhum Tertiary Volcanic Centre. *Geological Magazine* vol 122, p451-457.
- Faithfull, J.W. 1985 The Lower Eastern Layered Series of Rhum. *Geological Magazine* vol 122, p459-468.
- Forster M 1980 ^{*A Geochemical and Petrochemical study of the Tertiary minor intrusives of Rhum, N.W. Scotland. PhD Thesis, Univ. of Durham (Unpublished)*}
- Geikie, Sir A. 1897. *The Ancient Volcanoes of Great Britain*, Vol 2. London: Macmillan.
- Gibb, F. 1976. Ultrabasic rocks of Rhum and Skye: the nature of the parent magma. *Journal of the Geological Society of London* vol. 132, p209 - 222.
- Harker, A. 1908. *The geology of the Small Isles of Invernessshire*. Memoir of the Geological Survey of Scotland, 210pp.
- Henderson, P. 1975. Reaction trends of chrome-spinel on Rhum. *Geochimica et Cosmochimica Acta* vol.39, p1039 - 1044.
- Henderson, P. 1982. *Inorganic Geochemistry*. Pergamon. Oxford. 353pp.
- Henderson, P. and Suddaby, P. 1971. Nature and origin of the chrome-spinel of Rhum. *Contributions to Mineralogy and Petrology* vol.33, p21 - 31.
- Huckenholz, H.G., Schairer, J.F., and Yoder, H.S. 1967. Synthesis and Stability of Ferri-diopside. *Carnegie Institution Washington Year Book* 66, p 335-347.
- Hughes, C.J. 1960. An occurrence of tilleyite-bearing limestone in the Isle of Rhum. *Quarterly Journal of the Geological Society of London* vol 97, p384-388.
- Huppert, H.E. and Sparks, R.S.J. 1980. The fluid dynamics of a basaltic magma chamber replenished by influx of hot, dense, ultrabasic liquid. *Contributions to Mineralogy and Petrology* vol.75,

p279 - 289.

- Huppert, H.E. and Turner, J.S. 1980. Ice blocks melting into a salinity gradient. *Journal of Fluid Mechanics* vol 100, p367-384.
- Irvine, T.N. 1977. Chromite crystallisation in the join Mg_2SiO_4 - $CaMgSi_2O_6$ - $CaAl_2Si_2O_8$ - $MgCr_2O_4$ - SiO_2 . *Carnegie Institution Washington Year Book* 76, p465-472.
- Irvine, T.N. 1980. Magmatic infiltration metasomatism, double- diffusive fractional crystallisation and adcumulus growth in the Muskox intrusion and other layered intrusions. In Hargraves, R.B. (ed), *The Physics of Magmatic Processes*. Princeton. 585pp.
- Kitchen, D.E. 1985. The parental magma on Rhum: evidence from alkaline segregations and veins in the peridotites from Salisbury's Dam. *Geological Magazine* vol 122, p 529-537.
- Leake, B.E. 1978. Nomenclature of amphiboles. *Mineralogical Magazine* vol 42, p533-63.
- Le Bas, M.J. 1962. The role of Aluminium in igneous pyroxenes with relation to their parentage. *American Journal of Science* vol 260, p267-288.
- Le Maitre, R.W. 1982. *Numerical Petrology*. Elsevier. Amsterdam. pp281.
- Maaloe, S. 1978. The origin of rhythmic layering. *Mineralogical Magazine*, vol 42, p 337-345.
- Marshall, L.A. and Sparks, R.S.J. 1984. Origins of some mixed- magma and net-veined ring intrusions. *Journal of the Geological Society of London*, vol 141, p171-182.
- McBirney, A.R. and Noyes, R.M. 1978. Crystallisation and layering of the Skaergaard intrusion. *Journal of Petrology* vol.20, p487 - 554.
- McClurg, J.E. 1982. Geology and structure of the northern part of the Rhum ultrabasic complex. Unpublished PhD thesis, University of Edinburgh.
- McKenzie, D.P. 1985. The generation and compaction of partially molten rock. *Journal of Petrology* vol 25, p713-765.
- Obata, M., Banno, S., and Mori, T. 1974. The iron-magnesium partitioning between naturally

- occurring coexisting olivine and Ca-rich clinopyroxene: an application of the simple mixture model to olivine solid solution. Bulletin Societe francaise Mineralogie et Cristallographie vol 97, p101-107.
- Palacz, Z.A. 1984. Isotopic and geochemical evidence for the evolution of a cyclic unit in the Rhum intrusion, north-west Scotland. Nature vol.307, p618 - 620.
- Palacz, Z.A., and Tait, S.R. 1985. Isotopic and geochemical investigation of unit 10 from the Eastern Layered Series of the Rhum Intrusion, Northwest Scotland. Geological Magazine vol 122, p485-490.
- Powell, M., and Powell, R. 1974. An olivine-clinopyroxene geothermometer. Contributions to Mineralogy and Petrology vol 48, p249-263.
- Rajamani, V. and Naldrett, A.J. 1978. Partitioning of Fe,Co,Ni and Cu between sulphide liquid and basaltic melts and the composition of Ni-Cu sulphide deposits. Economic Geology vol 73, p82-93.
- Robins, B. 1982. Finger Structures in the Lille Kufjord Layered Intrusion, Finnmark, Northern Norway. Contributions to Mineralogy and Petrology vol 81, p290-295.
- Simkin, T. and Smith, J.V. 1970. Minor-element distribution in olivine, Journal of Geology vol 78, p304-325.
- Smith, N.J. 1985. The age and structural setting of limestones and basalts on the Main Ring Fault in southeast Rhum. Geological Magazine vol 122, p439-445.
- Smith, R.K. and Lofgren, G.E. 1983. An analytical and experimental study of zoning in plagioclase. Lithos vol 16, p153-168.
- Sood, M., K. 1981 Modern Igneous Petrology. Wiley. New York. 244pp.
- Sparks, R.S.J., and Huppert, H.E. 1984. Density changes during the fractional crystallisation of basaltic magmas: fluid dynamic implications. Contributions

- to Mineralogy and Petrology vol 85, p300-309.
- Sparks, R.S.J., Huppert, H.E., Kerr, R.C., McKenzie, D.P. and Tait, S.R. 1985. Postcumulus processes in layered intrusions. Geological Magazine vol 122, p
- Speidel, D.H. and Osborn, E.F. 1967. Element distribution among coexisting phases in the system $MgO-FeO-Fe_2O_3-SiO_2$ as a function of temperature and oxygen fugacity. American Mineralogist vol 52, p1139-1152.
- Spera, F.J., Yuen, D.A., and Kirschvink, S.J. 1982. Thermal Boundary Layer Convection in Silicic Magma Chambers. Journal of Geophysical Research(B), vol 87, p8755-8767.
- Stolper, E. and Walker, D. 1980. Melt density and the average composition of basalt. Contributions to Mineralogy and Petrology vol.74, p7 - 12.
- Tait, S.R. 1984. Fluid dynamical processes in the formation of layered igneous rocks. Unpublished PhD thesis, University of Cambridge.
- Tait, S.R. 1985. Fluid dynamic and chemical evolution of cyclic unit 10, Rhum, Eastern Layered Series. Geological Magazine vol 122, p469-484.
- Tait, S.R., Huppert, H.E. and Sparks, R.S.J. 1984. The role of compositional convection in the formation of adcumulate rocks. Lithos vol.17, p139 - 146.
- Taylor, S.R. and McClennan, S.M. 1985. The continental crust: its composition and evolution. Blackwell. Oxford. pp312.
- Thy, P. and Esbenson, K.H. 1982. Origin of fine-grained granular rocks in layered intrusions. Geological Magazine vol 119, p405-412.
- Virgo, D. 1972 ⁵⁷Fe Mossbauer Analyses of Fe³⁺ Clinopyroxenes. Carnegie Institution Year Book 71: Washington. p534-538.
- Volker, J.A. 1983. The Geology of the Trallval area, Rhum, Inner Hebrides. Unpublished PhD thesis, University of Edinburgh.
- Wadsworth, W.J. 1961. The ultrabasic rocks of south-west Rhum. Philosophical Transactions of the Royal Society vol B224, p21-64.

- Wager, L.R. and Brown, G.M. 1951. A note on rhythmic layering in the ultrabasic rocks of Rhum. Geological Magazine vol 88, p166-168.
- Wager, L.R., Brown, G.M., and Wadsworth, W.J. 1961. Types of igneous cumulates. Journal of Petrology vol 1, p73-85.
- Williams, C.T. 1978. Uranium-Enriched Minerals in Mesostasis Areas of the Rhum Layered Pluton. Contributions to Mineralogy and Petrology vol 66, p29-39.
- Williams, P.J. 1985. Pyroclastic rocks in the Cnapan Breaca felsite, Rhum. Geological Magazine vol 122, p 447-450.
- Young, I.M. 1984. Mixing of supernatant and interstitial fluids in the Rhum layered intrusion. Mineralogical Magazine vol 48, p345-350.
- Young, I.M. 1984. The evolution of layered plutons - evidence from small scale structures. Unpublished PhD thesis, University of St. Andrews.
- Young, I.M., and Donaldson, C.H. 1985. Formation of granular textured layers and laminae within the Rhum crystal pile. Geological Magazine vol 122, p519-528.
- Wood, B.J. 1976. An olivine-clinopyroxene geothermometer. Contributions to Mineralogy and Petrology vol.56, p297 - 303.

Acknowledgements

This work was carried out under N.E.R.C. grant No.GT4 80 GS25, at Durham University. Thanks are due to Dr. C.H. Emeleus, who supervised the project, and provided much helpful advice and support, and to Dr. A. Peckett. Alan Butcher, Iain Young, Johannes Volker, Steve Tait and Richard Greenwood helped in discussing many aspects of the work. Janet Mclurg kindly allowed the use of some of her data. Dave Plant, Tim Hopkins and Richard Pattrick helped me undertake electron-probe analysis at Manchester University.

Thanks are due to the Nature Conservancy Council for allowing the removal of yet more fragments of the Isle of Rhum. Numerous people helped me during my stay on the island; particular thanks are extended to Peter Duncan, Peter Hancock, Dave Millar, Pam and Angus McIntosh, and Laughton Johnson.

Finally I would like to thank Leicester University Geology Department for allowing me time to complete this work, and Ms Cathryn Burge for moral support, and assistance with typing.

APPENDIX 1

Two sets of standards were used for the determination of major and trace elements in this work. A set of ultrabasic and basaltic compositions, comprising both international standards and Edinburgh University internal standards were used for the major-element determinations. The latter (names prefixed by MO or RE) were kindly supplied by G. Fitton.

Standards used for trace-element analysis were all international standards, covering a wide range of compositions and trace-element concentrations.

Values determined for both sets of standards, together with the recommended values, are given overleaf.

1091

IDENT	SI02	AL203	FE203	MGO	CAO	NA2O	K2O	TI02	MNO	P2O5	TOTAL
1 M01											
MEASURED	43.80	11.80	14.56	11.49	11.33	2.49	1.36	2.95	0.19	0.53	100.52
TRUE	43.21	11.77	14.49	11.39	11.26	2.69	1.47	2.90	0.19	0.60	
DIFF	0.36	-0.03	-0.00	0.04	0.02	-0.21	-0.12	0.03	0.00	-0.07	
2 RE60											
MEASURED	45.75	11.01	12.75	17.67	8.49	1.71	0.48	1.72	0.17	0.22	99.98
TRUE	45.86	10.37	12.56	18.53	8.27	1.80	0.50	1.76	0.18	0.18	
DIFF	-0.10	0.64	0.19	-0.85	0.23	-0.09	-0.02	-0.04	-0.01	0.04	
3 MY54											
MEASURED	41.85	15.47	11.44	6.17	12.84	6.52	2.25	2.53	0.23	0.92	100.24
TRUE	40.97	16.03	11.89	6.46	12.24	6.34	2.32	2.68	0.25	0.82	
DIFF	0.78	-0.59	-0.47	-0.30	0.57	0.16	-0.07	-0.15	-0.02	0.10	
3 NIMP											
MEASURED	50.91	4.72	12.24	27.45	3.00	0.45	0.09	0.22	0.24	0.04	99.34
TRUE	52.75	4.32	13.11	26.15	2.75	0.38	0.09	0.22	0.20	0.02	
DIFF	-1.51	0.43	-0.79	1.48	0.27	0.07	-0.00	0.00	0.04	0.02	
6 M024											
MEASURED	45.81	13.66	14.72	7.59	10.57	3.32	1.06	3.06	0.21	0.65	100.65
TRUE	44.56	13.86	14.52	7.74	10.80	3.45	1.10	3.02	0.21	0.72	
DIFF	0.95	-0.29	0.11	-0.20	-0.30	-0.15	-0.05	0.02	0.00	-0.07	
7 M031											
MEASURED	46.66	12.34	14.44	9.37	11.45	2.07	1.06	2.52	0.19	0.46	100.56
TRUE	46.87	12.19	13.77	9.20	11.84	2.20	0.96	2.38	0.19	0.39	
DIFF	-0.47	0.08	0.59	0.12	-0.46	-0.15	0.10	0.12	0.00	0.07	

	SI02	AL203	FE203	MGO	CAO	NA2O	K2O	TI02	MNO	P2O5	TOTAL
8 RE14											
MEASURED	43.89	8.22	13.94	23.79	6.67	1.32	0.36	1.37	0.18	0.15	99.89
TRUE	43.71	8.96	14.27	23.03	6.30	1.43	0.40	1.40	0.22	0.29	
DIFF	0.23	-0.73	-0.32	0.79	0.38	-0.11	-0.04	-0.03	-0.04	-0.14	
9 M028											
MEASURED	44.78	9.65	14.23	14.84	11.93	1.44	0.93	2.01	0.19	0.35	100.36
TRUE	45.10	8.89	13.86	15.10	12.25	1.43	0.85	2.03	0.20	0.30	
DIFF	-0.48	0.73	0.32	-0.32	-0.36	0.01	0.08	-0.03	-0.01	0.05	
10 BCR1											
MEASURED	55.44	12.93	14.12	2.63	7.44	3.24	1.79	2.34	0.19	0.41	100.54
TRUE	54.58	13.73	13.42	3.48	6.98	3.30	1.70	2.26	0.18	0.36	
DIFF	0.56	-0.87	0.63	-0.86	0.42	-0.07	0.08	0.07	0.01	0.05	
11 PCC1											
MEASURED	43.21	0.37	8.82	45.20	0.31	0.15	0.01	0.02	0.14	0.02	98.25
TRUE	44.18	0.78	8.80	45.53	0.54	0.01	0.01	0.02	0.13	0.0	
DIFF	-0.20	-0.40	0.18	0.47	-0.23	0.14	0.00	-0.00	0.01	0.02	
12 DTS1											
MEASURED	39.55	0.27	8.75	49.32	-0.12	0.17	0.01	0.02	0.14	0.02	98.13
TRUE	40.72	0.24	8.69	50.07	0.15	0.01	0.0	0.01	0.11	0.0	
DIFF	-0.41	0.04	0.23	0.19	-0.28	0.16	0.01	0.01	0.03	0.02	

191

IDENT	SI02	AL203	FE203	MGO	CAO	NA2O	K2O	TI02	MNO	P2O5	TOTAL
13 M09											
MEASURED	42.47	10.06	13.83	16.68	10.09	2.78	0.66	2.74	0.19	0.71	100.22
TRUE	41.86	9.45	13.92	17.32	10.19	2.71	0.71	2.80	0.20	0.83	
DIFF	0.52	0.59	-0.12	-0.67	-0.13	0.06	-0.05	-0.06	-0.01	-0.13	
14 M019											
MEASURED	44.48	11.01	13.65	12.96	11.98	1.99	1.16	2.43	0.19	0.50	100.35
TRUE	44.59	10.17	13.42	13.49	12.34	1.85	1.11	2.38	0.19	0.47	
DIFF	-0.27	0.80	0.19	-0.57	-0.40	0.13	0.04	0.05	0.00	0.02	

TRACE-ELEMENTS

Standard	Ba	Hb	Zr	Y	Sr	Rb	Zn	Cu	Ni	Cr
AGV1	1223/1208	15/15	191/230	22/21.3	606/657	58/67	76/84	58/59.7	27/18.5	9/12.2
BCR1	558/675	9/13.5	115/190	24/37	237/330	31/46.6	89/120	16/18.4	20/15.8	24/17.6
G2	2009/1870	14/13.5	290/300	29/12	533/479	182/168	94/85	28/11.7	21/5.1	4/7
DTS1	55/2.4	1/<3	1/3	0/0	0/0.35	2/0	40/45	10/7	2250/2269	3899/4000
GSP1	1179/1300	26/29	415/500	51/30.4	237/233	244/254	103/98	42/33.5	42/12.5	7/12.5
PCC1	43/1.2	1/1	1/7	0/?	0/0.41	1/0	52/36	13/11.3	2317/2339	2756/2730
GR	1209/1050	38/?	178/180	34/19	599/550	180/175	108/60	358/345	76/55	70/110

Recommended values given following the slash, analysed values before the slash. ? - value not given.

0

APPENDIX 2

The following pages contain XRF analyses obtained during the course of this work. Sample numbers have a prefix in the range 1-6; this indicates the group to which the sample belongs. 1: peridotites. 2: allivalites. 3: "sheetrocks" ie supposedly intrusive gabbros of Brown (1956), now regarded as part of the layered series. 4: intrusive gabbro plugs, sheets and dykes. 5: Marginal Suite. 6: various.

Sample locations are given in the following appendix.

JWF RHUM ROCKS

Name	1.13B	1.152B	1.164A	1.178	1.180	1.195A	2.21	2.37	2.86
SiO2	43.10	41.43	43.02	42.62	41.94	42.70	45.75	47.46	48.23
TiO2	0.22	0.41	0.27	0.20	0.17	0.35	0.16	0.51	0.92
Al2O3	9.37	6.45	9.17	12.22	9.22	8.69	21.79	15.81	14.02
Fe2O3	1.93	1.79	1.42	1.64	1.72	1.63	0.65	1.19	0.99
FeO	12.88	11.94	9.48	10.92	11.45	10.84	4.34	7.92	6.62
MnO	0.22	0.19	0.17	0.18	0.20	0.19	0.09	0.15	0.14
MgO	23.93	30.91	26.62	21.88	26.84	27.60	11.38	11.73	11.58
CaO	6.08	4.61	7.38	8.12	6.08	5.56	13.38	12.29	14.62
Na2O	0.95	0.51	0.79	0.93	0.88	0.85	1.29	1.75	1.58
K2O	0.06	0.16	0.13	0.05	0.05	0.08	0.03	0.14	0.18
P2O5	0.03	0.06	0.05	0.03	0.02	0.04	0.03	0.06	0.10
LOI	0.00	0.00	0.00	0.00	0.00	0.00	0.00	0.00	0.00
Total	98.77	98.46	98.50	98.79	98.57	98.53	98.89	99.01	98.98

CIPW Norms

Or	0.35	0.95	0.77	0.30	0.30	0.47	0.18	0.83	1.06
Ab	8.04	4.32	6.69	7.87	7.45	7.19	10.92	14.81	13.37
An	21.13	14.84	21.10	29.03	21.06	19.66	53.59	34.88	30.64
Di	7.10	6.09	12.09	8.87	7.17	6.11	10.04	20.74	33.08
Hy	8.89	4.75	1.37	1.19	0.49	6.09	2.64	5.95	2.96
Ol	49.98	64.01	53.80	48.72	59.26	55.89	20.22	18.97	14.45
Mt	2.80	2.60	2.06	2.38	2.49	2.36	0.94	1.72	1.44
Ilm	0.42	0.78	0.51	0.38	0.32	0.66	0.30	0.97	1.75
Ap	0.07	0.14	0.12	0.07	0.05	0.09	0.07	0.14	0.23

Trace elements in ppm.

BA	50.0	59.0	54.0	48.0	54.0	70.0	75.0	101.0	84.0
NB	--	1.0	--	--	--	--	--	1.0	1.0
ZR	8.0	17.0	13.0	9.0	6.0	11.0	14.0	34.0	33.0
Y	3.0	4.0	4.0	2.0	2.0	3.0	1.0	6.0	8.0
SR	97.0	63.0	68.0	116.0	72.0	106.0	216.0	190.0	163.0
RB	--	1.0	--	--	--	--	--	1.0	3.0
ZN	80.0	64.0	50.0	61.0	57.0	70.0	21.0	43.0	32.0
CU	103.0	359.0	165.0	268.0	69.0	58.0	95.0	97.0	156.0
NI	572.0	859.0	770.0	711.0	695.0	1030.0	400.0	161.0	151.0
CR	1157.0	2233.0	692.0	839.0	1730.0	2074.0	386.0	226.0	838.0

JWF RHUM ROCKS

Name	2.862	2.87	2.89	2.90	2.91	2.93B	2.164B	2.165C	2.17
SiO2	48.64	48.96	47.69	49.19	45.56	47.37	44.14	49.65	47.88
TiO2	0.91	0.53	0.56	0.92	0.53	1.51	0.28	1.03	0.99
Al2O3	14.13	17.39	18.18	16.22	14.46	14.88	11.10	14.87	17.69
Fe2O3	0.96	0.81	0.99	0.85	1.41	1.46	1.38	1.06	1.15
FeO	6.37	5.42	6.62	5.67	9.43	9.71	9.20	7.05	7.68
MnO	0.13	0.12	0.13	0.12	0.17	0.16	0.17	0.14	0.14
MgO	11.62	8.46	11.04	9.00	14.95	9.91	22.96	9.54	10.13
CaO	14.36	15.26	11.55	14.69	10.92	11.89	8.15	13.31	10.88
Na2O	1.55	1.84	1.85	1.85	1.35	2.05	1.08	1.99	1.92
K2O	0.18	0.18	0.28	0.38	0.15	0.19	0.12	0.30	0.47
P2O5	0.10	0.06	0.07	0.12	0.05	0.06	0.04	0.11	0.10
LOI	0.00	0.00	0.00	0.00	0.00	0.00	0.00	0.00	0.00
Total	98.95	99.03	98.96	99.01	98.98	99.19	98.62	99.04	99.03

CIPW Norms

Or	1.06	1.06	1.65	2.25	0.89	1.12	0.71	1.77	2.78
Ab	13.12	15.57	15.65	15.65	11.42	17.35	9.14	16.84	16.25
An	31.07	38.67	40.48	34.84	32.96	30.85	25.09	30.76	38.27
Di	31.67	29.51	13.16	29.94	16.83	22.57	12.03	27.89	12.16
Hy	6.59	2.60	8.66	4.41	5.17	6.35	3.56	10.52	11.84
Ol	12.10	9.30	16.70	8.66	28.54	15.85	45.46	7.52	13.96
Mt	1.39	1.18	1.44	1.23	2.05	2.11	2.00	1.53	1.67
Ilm	1.73	1.01	1.06	1.75	1.01	2.87	0.53	1.96	1.88
Ap	0.23	0.14	0.16	0.28	0.12	0.14	0.09	0.25	0.23

Trace elements in ppm.

BA	96.0	109.0	116.0	108.0	82.0	89.0	60.0	124.0	140.0
NB	--	--	1.0	1.0	--	1.0	--	--	2.0
ZR	34.0	29.0	40.0	41.0	22.0	26.0	15.0	47.0	52.0
Y	9.0	7.0	7.0	8.0	5.0	6.0	4.0	11.0	9.0
SR	165.0	219.0	241.0	197.0	172.0	208.0	84.0	176.0	195.0
RB	2.0	4.0	1.0	--	--	--	--	3.0	8.0
ZN	35.0	30.0	40.0	30.0	53.0	46.0	51.0	34.0	44.0
CU	152.0	100.0	96.0	123.0	471.0	123.0	75.0	100.0	108.0
NI	156.0	115.0	285.0	124.0	435.0	123.0	807.0	73.0	209.0
CR	851.0	536.0	488.0	628.0	588.0	322.0	1148.0	225.0	157.0

JWF RHUM ROCKS

Name	2.173	2.194B	2.194C	2.194D	2.194D	2.194F	2.195B	2.195C	3.12
SiO2	47.28	50.92	48.48	48.70	48.90	49.36	49.40	47.01	50.06
TiO2	0.84	0.30	0.54	0.32	0.31	0.57	0.22	0.15	0.61
Al2O3	16.43	17.46	21.45	19.84	20.00	17.22	19.34	19.97	15.63
Fe2O3	1.15	0.86	0.96	0.97	0.94	0.97	0.70	0.87	1.01
FeO	7.68	5.71	6.43	6.44	6.26	6.46	4.70	5.78	6.71
MnO	0.15	0.14	0.15	0.14	0.14	0.14	0.12	0.12	0.16
MgO	11.75	8.14	4.91	6.80	6.74	7.97	9.13	10.59	9.07
CaO	11.47	13.13	14.52	13.94	13.73	14.01	13.52	12.91	13.32
Na2O	1.88	2.20	1.73	1.90	2.00	2.26	1.67	1.47	2.23
K2O	0.28	0.11	0.05	0.08	0.08	0.11	0.12	0.10	0.18
P2O5	0.09	0.02	0.02	0.02	0.02	0.03	0.02	0.03	0.06
LOI	0.00	0.00	0.00	0.00	0.00	0.00	0.00	0.00	0.00
Total	99.00	98.98	99.24	99.15	99.12	99.10	98.94	98.99	99.03

CIPW Norms

Or	1.65	0.65	0.30	0.47	0.47	0.65	0.71	0.59	1.06
Ab	15.91	18.62	14.64	16.08	16.92	19.12	14.13	12.44	18.87
An	35.57	37.45	50.63	45.38	45.37	36.53	44.93	47.61	32.11
Di	16.71	22.27	17.51	19.28	18.43	26.58	17.66	13.05	27.15
Hy	6.06	15.77	12.90	9.43	9.67	3.97	14.54	7.54	8.83
Ol	19.63	2.36	0.80	6.46	6.26	9.70	5.49	16.16	8.26
Mt	1.67	1.24	1.40	1.40	1.36	1.41	1.02	1.26	1.46
Ilm	1.60	0.57	1.03	0.61	0.59	1.08	0.42	0.28	1.16
Ap	0.21	0.05	0.05	0.05	0.05	0.07	0.05	0.07	0.14

Trace elements in ppm.

BA	90.0	111.0	100.0	85.0	91.0	96.0	122.0	99.0	105.0
NB	1.0	--	--	--	--	--	1.0	--	--
ZR	41.0	15.0	18.0	18.0	19.0	17.0	17.0	14.0	28.0
Y	8.0	4.0	1.0	2.0	2.0	4.0	3.0	2.0	6.0
SR	174.0	249.0	395.0	383.0	383.0	274.0	265.0	242.0	239.0
RB	2.0	1.0	1.0	--	--	2.0	--	--	3.0
ZN	42.0	32.0	42.0	33.0	34.0	33.0	30.0	29.0	34.0
CU	149.0	115.0	11.0	13.0	13.0	103.0	57.0	126.0	199.0
NI	248.0	83.0	57.0	145.0	154.0	86.0	165.0	236.0	87.0
CR	466.0	250.0	193.0	244.0	246.0	227.0	508.0	593.0	320.0

JWF RHUM ROCKS

Name	3.13A	3.14A	3.14B	3.17A	3.17B	3.18	3.20C	3.20D	3.24
SiO2	50.54	49.98	50.40	47.11	49.91	50.55	49.82	50.04	46.85
TiO2	0.52	0.59	0.50	2.18	0.57	0.37	0.34	0.51	0.70
Al2O3	17.23	16.60	15.96	14.99	16.82	15.78	16.81	16.45	17.74
Fe2O3	0.75	0.78	0.73	1.46	0.97	0.89	0.84	0.94	1.16
FeO	5.00	5.23	4.90	9.71	6.48	5.92	5.62	6.27	7.75
MnO	0.13	0.13	0.14	0.16	0.15	0.15	0.13	0.14	0.14
MgO	8.93	10.23	9.77	8.33	8.32	9.75	9.34	9.58	11.63
CaO	13.52	13.19	14.29	13.11	13.57	13.42	13.77	12.75	11.08
Na2O	2.13	1.98	2.08	2.09	2.09	2.00	2.10	2.07	1.73
K2O	0.14	0.14	0.10	0.14	0.14	0.11	0.15	0.19	0.18
P2O5	0.05	0.05	0.04	0.04	0.04	0.03	0.02	0.04	0.05
LOI	0.00	0.00	0.00	0.00	0.00	0.00	0.00	0.00	0.00
Total	98.94	98.90	98.91	99.31	99.06	98.97	98.94	98.98	99.02

CIPW Norms

Or	0.83	0.83	0.59	0.83	0.83	0.65	0.89	1.12	1.06
Ab	18.02	16.76	17.60	17.69	17.69	16.92	17.77	17.52	14.64
An	37.05	36.00	33.92	31.11	36.11	33.76	36.01	35.04	40.12
Di	23.84	23.31	29.39	27.46	25.06	26.26	25.90	22.53	11.71
Hy	12.57	12.24	8.20	3.06	10.96	13.80	7.08	13.06	9.28
Ol	4.44	7.40	7.10	12.83	5.83	5.52	9.39	7.29	19.08
Mt	1.09	1.14	1.06	2.11	1.41	1.29	1.22	1.36	1.69
Ilm	0.99	1.12	0.95	4.14	1.08	0.70	0.65	0.97	1.33
Ap	0.12	0.12	0.09	0.09	0.09	0.07	0.05	0.09	0.12

Trace elements in ppm.

BA	112.0	123.0	107.0	86.0	120.0	95.0	118.0	120.0	120.0
NB	--	1.0	1.0	1.0	--	--	--	1.0	1.0
ZR	27.0	30.0	26.0	25.0	22.0	17.0	19.0	24.0	29.0
Y	6.0	6.0	6.0	9.0	6.0	5.0	5.0	5.0	5.0
SR	289.0	263.0	260.0	184.0	240.0	238.0	246.0	236.0	221.0
RB	3.0	3.0	3.0	1.0	3.0	--	--	1.0	--
ZN	27.0	33.0	29.0	49.0	35.0	27.0	30.0	37.0	46.0
CU	81.0	110.0	113.0	127.0	109.0	134.0	110.0	143.0	143.0
NI	103.0	125.0	126.0	119.0	122.0	109.0	102.0	151.0	220.0
CR	317.0	368.0	472.0	208.0	354.0	315.0	265.0	298.0	290.0

JWF RHUM ROCKS

Name	3.118	3.123	3.132	3.135	3.139	3.141	3.150	3.179D	3.17
SiO2	49.86	50.01	49.28	49.85	49.33	46.14	49.19	47.83	47.87
TiO2	0.67	0.47	0.29	0.32	0.30	0.40	0.57	0.60	0.33
Al2O3	17.30	17.53	17.00	16.65	17.68	16.71	15.89	15.78	17.00
Fe2O3	1.02	0.87	0.96	0.92	0.92	1.38	0.95	1.16	1.10
FeO	6.82	5.83	6.40	6.13	6.11	9.21	6.32	7.73	7.30
MnO	0.14	0.13	0.14	0.14	0.13	0.17	0.14	0.15	0.14
MgO	8.02	7.73	9.60	9.84	9.09	13.72	10.49	10.65	10.57
CaO	12.59	13.99	13.09	12.96	13.20	9.24	13.26	13.22	12.74
Na2O	2.46	2.33	2.11	2.00	2.08	1.82	1.95	1.80	1.89
K2O	0.16	0.13	0.12	0.12	0.13	0.15	0.19	0.11	0.07
P2O5	0.03	0.02	0.02	0.03	0.02	0.03	0.04	0.03	0.02
LOI	0.00	0.00	0.00	0.00	0.00	0.00	0.00	0.00	0.00
Total	99.07	99.04	99.01	98.97	98.99	98.98	98.99	99.06	99.03

CIPW Norms

Or	0.95	0.77	0.71	0.71	0.77	0.89	1.12	0.65	0.41
Ab	20.82	19.72	17.86	16.92	17.60	15.40	16.50	15.23	15.99
An	35.70	37.00	36.57	36.11	38.53	36.99	34.05	34.66	37.70
Di	21.56	26.12	22.80	22.55	21.66	6.99	25.31	24.84	20.50
Hy	9.01	5.84	7.23	12.32	8.30	8.88	7.48	4.43	5.22
Ol	8.22	7.39	11.86	8.34	10.19	27.01	11.97	16.37	16.94
Mt	1.48	1.27	1.39	1.33	1.33	2.00	1.37	1.68	1.59
Ilm	1.27	0.89	0.55	0.61	0.57	0.76	1.08	1.14	0.63
Ap	0.07	0.05	0.05	0.07	0.05	0.07	0.09	0.07	0.05

Trace elements in ppm.

BA	123.0	113.0	94.0	105.0	110.0	124.0	139.0	86.0	73.0
NB	--	--	--	--	--	1.0	1.0	--	--
ZR	22.0	18.0	15.0	17.0	17.0	23.0	29.0	16.0	14.0
Y	5.0	6.0	5.0	4.0	4.0	2.0	6.0	4.0	3.0
SR	294.0	283.0	245.0	245.0	281.0	427.0	271.0	239.0	251.0
RB	1.0	--	--	--	--	--	--	1.0	1.0
ZN	35.0	32.0	34.0	36.0	35.0	66.0	34.0	37.0	35.0
CU	123.0	51.0	103.0	122.0	104.0	12.0	172.0	111.0	126.0
NI	119.0	86.0	132.0	138.0	144.0	223.0	134.0	154.0	138.0
CR	249.0	220.0	270.0	253.0	382.0	492.0	316.0	189.0	220.0

JWF RHUM ROCKS

Name	3.194A	3.194A	4.9B	4.93A	4.169B	4.175A	4.181	4.201	4.20
SiO2	49.79	49.34	46.66	46.41	46.92	48.54	47.80	47.29	48.74
TiO2	0.48	0.47	2.02	1.41	1.15	2.42	1.58	1.42	1.28
Al2O3	17.81	17.66	14.32	14.32	13.70	14.50	13.57	15.19	14.09
Fe2O3	0.95	0.99	1.42	1.70	1.53	1.66	1.47	1.39	1.27
FeO	6.32	6.60	9.46	11.30	10.17	11.07	9.82	9.29	8.49
MnO	0.14	0.14	0.16	0.18	0.18	0.21	0.18	0.16	0.17
MgO	7.97	8.52	11.70	11.53	12.60	6.53	9.80	9.69	9.75
CaO	13.08	13.02	10.63	10.07	10.41	10.89	12.50	11.96	12.66
Na2O	2.30	2.12	2.26	2.05	2.10	2.87	2.10	2.38	2.05
K2O	0.18	0.16	0.29	0.08	0.23	0.37	0.25	0.24	0.43
P2O5	0.04	0.04	0.18	0.16	0.09	0.31	0.15	0.16	0.18
LOI	0.00	0.00	0.00	0.00	0.00	0.00	0.00	0.00	0.00
Total	99.06	99.06	99.10	99.21	99.08	99.37	99.22	99.17	99.12

CIPW Norms

Or	1.06	0.95	1.71	0.47	1.36	2.19	1.48	1.42	2.54
Ab	19.46	17.94	19.12	17.35	17.77	24.29	17.77	20.14	17.35
An	37.75	38.21	28.08	29.64	27.28	25.60	26.87	30.06	27.98
Di	21.78	21.16	18.96	15.69	19.25	21.80	27.80	22.94	27.28
Hy	8.83	9.53	3.44	9.50	4.86	9.29	4.92	0.08	7.33
Ol	7.79	8.86	21.48	21.05	23.96	8.49	14.91	19.44	11.94
Mt	1.37	1.44	2.06	2.46	2.21	2.41	2.14	2.02	1.85
Ilm	0.91	0.89	3.84	2.68	2.18	4.60	3.00	2.70	2.43
Ap	0.09	0.09	0.42	0.37	0.21	0.72	0.35	0.37	0.42

Trace elements in ppm.

BA	121.0	115.0	99.0	71.0	78.0	160.0	87.0	71.0	98.0
NB	--	--	4.0	--	1.0	2.0	1.0	1.0	1.0
ZR	24.0	21.0	69.0	49.0	47.0	51.0	43.0	61.0	54.0
Y	5.0	5.0	12.0	15.0	12.0	16.0	11.0	11.0	14.0
SR	277.0	273.0	263.0	127.0	117.0	205.0	166.0	190.0	172.0
RB	3.0	--	3.0	--	1.0	--	2.0	3.0	7.0
ZN	34.0	35.0	53.0	52.0	58.0	70.0	52.0	47.0	39.0
CU	87.0	86.0	99.0	53.0	94.0	62.0	79.0	92.0	100.0
NI	135.0	134.0	132.0	201.0	266.0	56.0	76.0	95.0	80.0
CR	289.0	291.0	235.0	480.0	592.0	47.0	195.0	196.0	207.0

JWF RHUM ROCKS

Name	5.53A	5.7B	5.10	5.11	5.15	5.25	5.32A	5.32B	5.36
SiO2	45.99	51.78	50.65	59.17	51.01	47.47	54.41	53.63	63.40
TiO2	0.82	0.91	1.31	1.80	1.23	2.20	2.21	1.11	0.81
Al2O3	11.63	14.62	14.44	13.81	14.84	14.89	13.13	14.28	15.12
Fe2O3	1.40	0.86	1.36	1.09	1.05	1.55	1.50	1.08	0.69
FeO	9.35	5.76	9.10	7.29	7.02	10.34	10.02	7.17	4.60
MnO	0.17	0.13	0.17	0.14	0.14	0.18	0.17	0.14	0.11
MgO	19.83	8.98	8.14	3.45	8.90	8.25	5.08	7.84	2.98
CaO	7.64	12.27	10.88	6.28	11.55	11.79	7.69	9.98	4.02
Na2O	1.65	2.47	2.48	3.57	2.35	2.40	3.26	2.66	3.22
K2O	0.16	1.04	0.49	2.09	0.71	0.14	1.34	0.94	3.49
P2O5	0.09	0.10	0.12	0.29	0.18	0.10	0.37	0.14	0.25
LOI	0.00	0.00	0.00	0.00	0.00	0.00	0.00	0.00	0.00
Total	98.73	98.93	99.14	98.98	98.98	99.31	99.19	98.96	98.69

CIPW Norms

Qtz	--	--	--	11.15	--	--	5.01	2.27	16.28
Or	0.95	6.15	2.90	12.35	4.20	0.83	7.92	5.56	20.63
Ab	13.96	20.90	20.99	30.21	19.89	20.31	27.59	22.51	27.25
An	23.86	25.74	26.83	15.49	27.85	29.45	17.24	24.26	16.50
Di	10.76	27.72	21.54	11.44	22.84	23.22	15.34	19.76	1.49
Hy	10.36	8.92	18.59	12.66	16.15	6.03	18.86	20.63	13.44
Ol	35.05	6.29	3.56	--	3.78	12.83	--	--	--
Mt	2.03	1.25	1.98	1.58	1.53	2.25	2.18	1.56	1.00
Ilm	1.56	1.73	2.49	3.42	2.34	4.18	4.20	2.11	1.54
Ap	0.21	0.23	0.28	0.67	0.42	0.23	0.86	0.32	0.58

Trace elements in ppm.

BA	107.0	169.0	165.0	588.0	221.0	104.0	367.0	268.0	1246.0
NB	--	2.0	2.0	8.0	2.0	--	5.0	2.0	10.0
ZR	50.0	113.0	67.0	183.0	73.0	30.0	154.0	115.0	202.0
Y	9.0	14.0	13.0	29.0	15.0	11.0	27.0	18.0	28.0
SR	93.0	194.0	168.0	228.0	209.0	180.0	181.0	174.0	465.0
RB	2.0	20.0	9.0	47.0	14.0	--	19.0	16.0	81.0
ZN	54.0	34.0	57.0	69.0	44.0	68.0	71.0	55.0	72.0
CU	79.0	42.0	107.0	33.0	98.0	90.0	46.0	90.0	30.0
NI	636.0	92.0	73.0	35.0	113.0	80.0	33.0	76.0	36.0
CR	960.0	259.0	242.0	60.0	380.0	194.0	30.0	216.0	79.0

JWF RHUM ROCKS

Name	5.39	5.41	5.42B	5.42C	5.45	5.46A1	5.46A2	5.46C	5.80
SiO2	52.02	51.73	53.53	53.92	50.46	50.36	50.97	48.96	52.83
TiO2	1.25	1.11	1.37	2.34	1.05	1.07	1.04	2.94	1.63
Al2O3	15.36	14.78	15.18	12.92	14.41	14.42	14.68	13.18	12.41
Fe2O3	1.26	0.85	1.06	1.48	1.11	1.02	0.98	1.66	1.48
FeO	8.41	5.63	7.06	9.84	7.40	6.83	6.52	11.04	9.87
MnO	0.16	0.14	0.13	0.16	0.15	0.15	0.14	0.17	0.20
MgO	6.13	7.31	6.28	6.03	9.22	9.91	9.46	7.39	7.28
CaO	10.87	13.97	10.09	8.04	12.27	12.51	12.37	9.89	10.02
Na2O	2.58	2.71	3.01	2.77	2.31	2.02	2.19	2.93	2.27
K2O	1.00	0.60	1.15	1.49	0.50	0.55	0.49	0.77	1.08
P2O5	0.11	0.17	0.15	0.19	0.15	0.13	0.13	0.38	0.10
LOI	0.00	0.00	0.00	0.00	0.00	0.00	0.00	0.00	0.00
Total	99.15	99.00	99.01	99.18	99.04	98.98	98.97	99.31	99.17

CIPW Norms

Qtz	0.89	--	1.78	4.74	--	--	--	--	2.98
Or	5.91	3.55	6.80	8.81	2.95	3.25	2.90	4.55	6.38
Ab	21.83	22.93	25.47	23.44	19.55	17.09	18.53	24.79	19.21
An	27.38	26.40	24.52	18.43	27.48	28.66	28.79	20.54	20.49
Di	21.23	33.73	20.03	16.66	26.23	26.22	25.56	21.37	23.47
Hy	17.45	5.19	15.94	20.08	12.01	13.90	15.73	10.76	21.18
Ol	--	3.48	--	--	6.87	6.04	3.77	8.43	--
Mt	1.83	1.23	1.54	2.14	1.61	1.49	1.42	2.40	2.15
Ilm	2.37	2.11	2.60	4.44	1.99	2.03	1.98	5.58	3.10
Ap	0.25	0.39	0.35	0.44	0.35	0.30	0.30	0.88	0.23

Trace elements in ppm.

BA	340.0	189.0	315.0	374.0	191.0	217.0	208.0	198.0	238.0
NB	2.0	2.0	2.0	3.0	2.0	2.0	2.0	5.0	2.0
ZR	60.0	65.0	105.0	117.0	45.0	93.0	54.0	66.0	62.0
Y	12.0	14.0	17.0	20.0	13.0	14.0	13.0	25.0	13.0
SR	218.0	205.0	232.0	165.0	197.0	194.0	206.0	169.0	156.0
RB	15.0	11.0	20.0	23.0	5.0	10.0	9.0	9.0	22.0
ZN	49.0	36.0	48.0	59.0	44.0	58.0	55.0	78.0	57.0
CU	59.0	146.0	63.0	53.0	65.0	111.0	115.0	77.0	73.0
NI	45.0	70.0	45.0	47.0	60.0	84.0	82.0	64.0	38.0
CR	181.0	145.0	122.0	56.0	266.0	423.0	456.0	95.0	59.0

JWF RHUM ROCKS

Name	5.80C	5.165B	5.169A	6.48	6.78	6.163P	6.163V	6.179B	6.16
SiO2	51.13	52.15	45.40	69.80	51.87	50.19	54.45	73.27	49.47
TiO2	1.57	0.87	0.76	0.86	0.90	1.54	2.45	0.43	0.34
Al2O3	11.37	19.17	11.14	12.40	14.70	11.28	12.13	11.80	16.68
Fe2O3	2.00	0.65	1.45	0.59	0.86	1.16	0.99	0.21	0.85
FeO	13.31	4.36	9.63	3.90	5.75	7.75	6.58	1.40	5.64
MnO	0.18	0.10	0.17	0.09	0.13	0.15	0.13	0.05	0.13
MgO	7.31	3.91	21.20	0.80	8.88	13.32	4.94	1.40	10.17
CaO	9.32	14.20	7.54	2.44	12.24	9.62	11.51	0.71	13.48
Na2O	2.37	2.92	0.99	3.76	2.43	3.38	5.21	2.75	2.03
K2O	0.78	0.62	0.32	3.72	1.02	0.14	0.19	6.20	0.12
P2O5	0.06	0.11	0.09	0.23	0.11	0.30	0.48	0.08	0.02
LOI	0.00	0.00	0.00	0.00	0.00	0.00	0.00	0.00	0.00
Total	99.40	99.06	98.69	98.59	98.90	98.83	99.06	98.30	98.93

CIPW Norms

Qtz	0.30	1.00	--	26.44	--	--	--	29.67	--
Or	4.61	3.66	1.89	21.98	6.03	0.83	1.12	36.64	0.71
Ab	20.06	24.71	8.38	31.82	20.56	28.60	43.14	23.27	17.18
An	18.09	37.38	25.01	5.98	26.20	15.20	9.16	1.55	36.05
Ne	--	--	--	--	--	--	0.52	--	--
Di	23.06	26.38	9.43	3.95	27.19	24.49	36.48	1.17	24.65
Hy	27.27	3.08	15.71	5.40	10.69	3.89	--	4.69	7.07
Ol	--	--	34.52	--	5.02	20.52	1.45	--	11.35
Mt	2.89	0.95	2.10	0.85	1.25	1.68	1.43	0.30	1.23
Ilm	2.98	1.65	1.44	1.63	1.71	2.92	4.65	0.82	0.65
Ap	0.14	0.25	0.21	0.53	0.25	0.70	1.11	0.19	0.05

Trace elements in ppm.

BA	142.0	171.0	115.0	1184.0	165.0	316.0	194.0	498.0	93.0
NB	1.0	1.0	1.0	14.0	2.0	8.0	4.0	11.0	--
ZR	33.0	59.0	38.0	240.0	113.0	162.0	99.0	161.0	19.0
Y	9.0	10.0	9.0	39.0	14.0	28.0	19.0	49.0	4.0
SR	104.0	262.0	86.0	223.0	197.0	153.0	130.0	69.0	259.0
RB	13.0	12.0	6.0	96.0	25.0	5.0	2.0	212.0	3.0
ZN	48.0	24.0	57.0	82.0	33.0	42.0	40.0	23.0	27.0
CU	33.0	90.0	39.0	27.0	44.0	89.0	102.0	39.0	43.0
NI	37.0	43.0	655.0	27.0	88.0	423.0	93.0	52.0	96.0
CR	74.0	113.0	815.0	2.0	256.0	531.0	76.0	23.0	264.0

JWF RHUM ROCKS

Name 6.20A

SiO2	43.08
TiO2	0.21
Al2O3	15.09
Fe2O3	1.66
FeO	11.06
MnO	0.18
MgO	18.96
CaO	7.37
Na2O	1.23
K2O	0.03
P2O5	0.03
LOI	0.00
Total	98.90

CIPW Norms

Or	0.18
Ab	10.41
An	35.57
Di	0.64
Hy	6.27
Ol	42.97
Mt	2.41
Ilm	0.40
Ap	0.07

Trace elements in ppm.

BA	38.0
NB	--
ZR	7.0
Y	--
SR	144.0
RB	--
ZN	58.0
CU	8.0
NI	564.0
CR	1436.0

APPENDIX 3
SAMPLE LOCALITIES

The localities of most figured samples are given in the text. The positions of samples collected from the measured section are given on the diagram overleaf. The grid references of analysed samples in Appendix 2 are given below:

PERIDOTITES

1.13B	NM39639726	(xenolith)
1.152B	NM40649452	
1.164A	NM40709688	
1.178	NM40179674	(gradational contact)
1.180	NM40189618	
1.195A	NM40269671	

ALLIVALITES

2.21	NM39739701	
2.37	NM40219730	
2.86	NM40479708	
2.87	NM40499729	
2.89	NM40469723	
2.90	NM40389718	
2.91	NM40369716	
2.93B	NM40319707	
2.164B	NM40709688	
2.165C	NM40819676	
2.171	NM40859670	
2.173	NM40879671	
2.194B	NM40299697	(xenolith)
2.194C	''	''
2.194D	''	''
2.194F	''	''
2.195B	NM40269671	
2.195C	''	

" SHEETROCKS "

3.12	NM39679728
3.13A	NM39639726
3.14A	NM39589721
3.14B	''
3.17A	NM39699718
3.18	NM39749716
3.20C	NM39799715
3.20D	''
3.24	NM39829720
3.118	NM40209712
3.123	NM40209711
3.132	NM40189710
3.135	NM40179710
3.139	NM40169710
3.141	NM40159710
3.150	NM40139709
3.179D	NM40449661
3.194A	NM40299697

GABBRO PLUGS, SHEETS, DYKES

4.9B	NM39479753
4.93A	NM40319707 (dyke)
4.169B	NM40989638 (dyke)
4.175A	NM40909672 (sill)
4.181	NM40109613
4.201	NM40489533
4.202	NM40169499

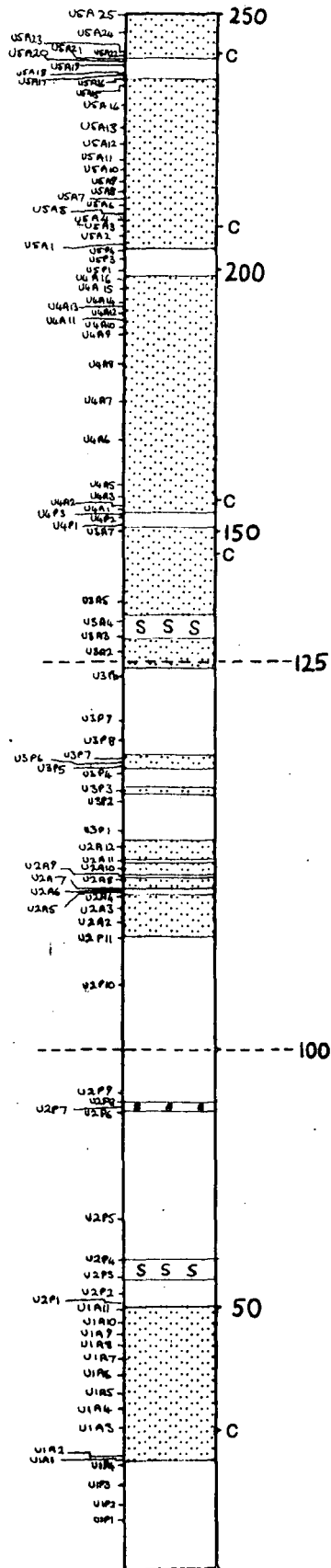
MARGINAL SUITE

5.53A	NM38609549
5.7B	NM39189753
5.10	NM39409747
5.11	NM39379746
5.15	NM39239750
5.25	NM39189753
5.32A	NM40339746
5.32B	' '
5.36	NM40299739
5.39	NM40019742
5.41	NM40429731
5.42B	NM40389735
5.42C	' '
5.45	NM395940
5.46A, C	' '
5.80A	NM40679722
5.80C	' '
5.165B	NM40829676
5.169A	NM40989638 (xenolith)

VARIOUS

6.48	summit of Beinn nan Stac
6.78	NM40649731
6.163P	NM40719696 (mostly peridotite)
6.163V	' ' (vein cutting 163P)
6.179B	NM40449661 (acid sheet)
6.16A	NM39659720 (beerbachite xen.)
6.20A	NM39799715 (' ')

Height (m)



The Lower Eastern Layered Series of Rhum

JOHN W. FAITHFULL*

Department of Geological Sciences, University of Durham, South Road, Durham, DH1 3LE, U.K.

(Received 2 November 1984; accepted 3 April 1985)

Abstract – The Lower Eastern Layered Series (LELS) comprises approximately units 1–5 of previous workers. Remapping has revealed considerable along-strike lithological variation in the units of the LELS. It is suggested, on the basis of field and geochemical evidence, that two layers formerly regarded as ‘conformable intrusive sheets of fine-grained olivine gabbro’, may be evolved allivalite layers rather than later intrusions. Xenolith suites, in these layers and elsewhere, indicate a component derived from the roof or walls of the magma chamber. Cryptic variation is more extensive in the LELS than in other parts of Rhum: olivine forsterite content varies from 85.6 to 70, and clinopyroxene $MgX100/(Mg + Fe)$ varies from 88 to 74. Postcumulus effects and subsolidus re-equilibration have altered the initial compositions of the mineral phases. The data are consistent with a model of repeated replenishment by picritic magma, although the replenishing liquids may have been slightly less magnesian than those subsequently available, during the formation of the upper ELS.

1. Introduction

The Eastern Layered Series (ELS) of Rhum (Brown, 1956) are well known for the spectacular development of large-scale cyclic layering. Brown (1956) divided the sequence into 15 units, each comprising a peridotite layer overlain by an allivalite layer. He interpreted these units as the products of crystallization of pulses of olivine basalt magma. Using the techniques of the time, he could detect no cryptic variation in any of the units, and thus argued that they could only represent a small degree of crystallization at a relatively constant high temperature. He noted that the lower units were orthocumulates, in contrast to the ad- and heterad-cumulates of the upper ELS. Brown mapped two layers of ‘fine-grained olivine gabbro’ conformably intruding the layered rocks, obscuring much of units 4 and 5. Following Bailey (1945) he argued that the layered rocks occurred within a ring fault and that they had been emplaced upwards as a semi-solid cylinder along the fault, lubricated by basaltic magma now seen as a gabbroic ring dyke at the margins of the complex.

The present work is mainly concerned with units 1–5, hereafter referred to as the Lower Eastern Layered Series (LELS).

2. Field relations

Remapping (Fig. 1) has substantially revised Brown’s map of the area, revealing in particular considerable lateral changes in lithology within the LELS. The ‘intrusive conformable sheets of fine-grained olivine gabbro’ have been included in units 4 and 5 of the ELS. The reasons for this are discussed later.

2.a. Marginal relationships

Much of the eastern margin of the ultrabasic complex is a near-vertical ring fault, largely occupied by a heterogeneous gabbroic–dioritic ring dyke known as the marginal gabbro. The contact with the layered rocks is rarely seen, and the few exposures are difficult to interpret due to intense weathering, but over most of the area there is little obvious deformation of the layered rocks near the fault. However, just north of the Allt nam Ba, the allivalites of unit 1 increase sharply in dip towards the marginal gabbro (up to 30–40° to the west) although the contact is not exposed. The Torridonian sediments in this area dip very steeply to the west, in contrast to the regional dip of 10–20° to the northwest. This situation is more consistent with subsidence rather than uplift within the ring fracture.

2.b. The layered rocks

The LELS comprises some 250 m of olivine- and olivine–plagioclase–(clinopyroxene) cumulates. Whereas the upper ELS rocks are mainly adcumulate and heteradcumulate peridotites and troctolites, those in the LELS are orthocumulates, often rich in clinopyroxene. Peridotite forms the bulk of the upper ELS sequence; in the LELS about 60% of the thickness is allivalite. Chrome-spinel seams and harrisite layers are often associated with the upper ELS peridotites, but chromite seams are rare, and harrisites unknown in the LELS.

Lateral lithological variation is a marked feature of the LELS (Fig. 1). This makes the subdivision into five units, as defined in the Allt nam Ba, rather difficult to extend into the northern part of the area.

* Present address: Department of Geology, University of Leicester, LE1 7RH, U.K.

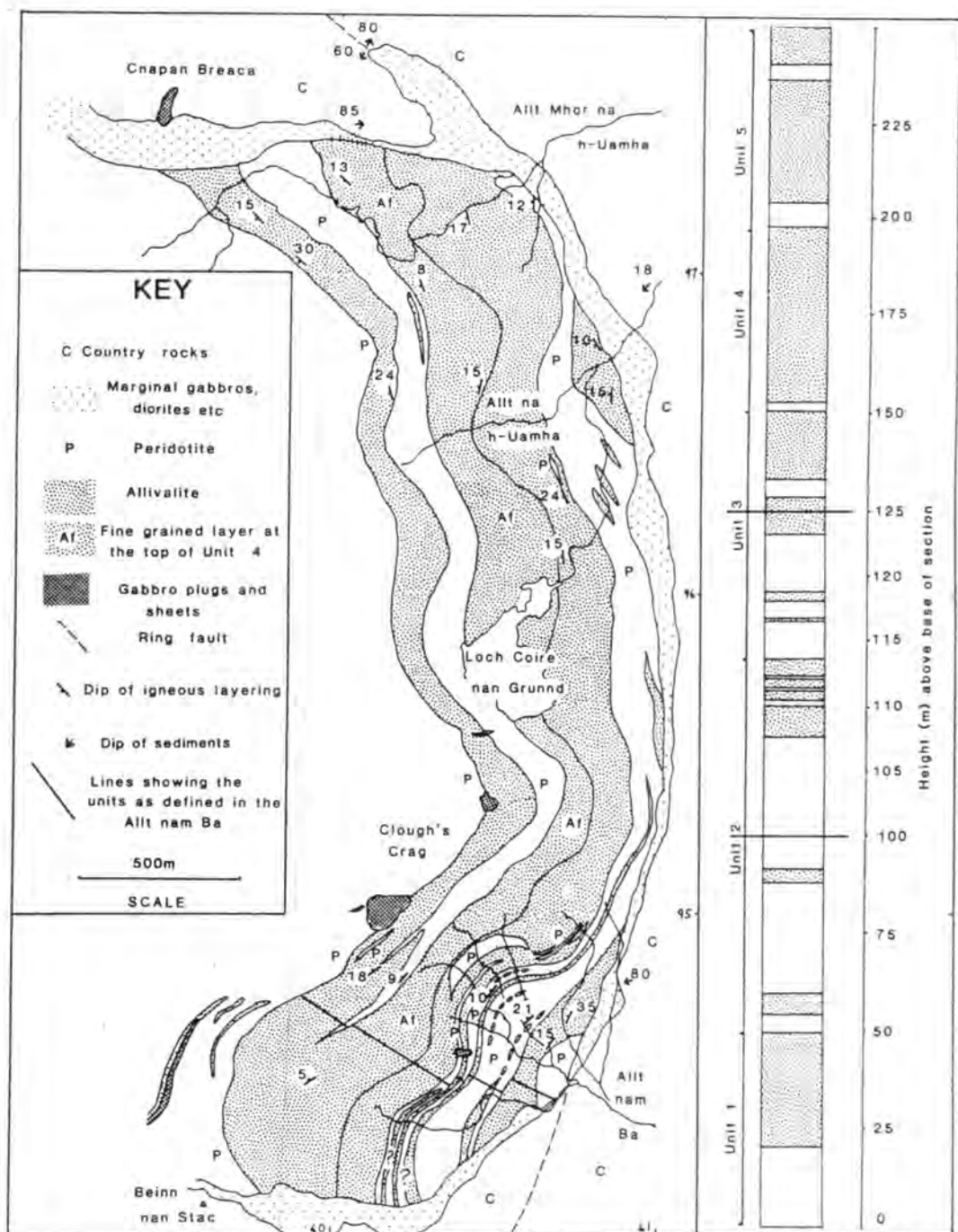


Figure 1. Revised map of the LELS and stratigraphic section. The numbers around the edge of the map are the U.K. National Grid lines at 1 km intervals. The section given above, and the sample traverse were taken from NM 40719452 to NM 40479486, and from NM 40369470 to NM 40109495. Note the expanded vertical scale between 100 m and 125 m on the section.

2.b.1. Unit 1

Unit 1 is only unambiguously exposed in and around the Allt nam Ba. Peridotite exposures in the stream bed are cut by late-stage basic and ultrabasic veins, with irregular orientation. The contact with the allivalite is sharp and planar. The basal parts of the allivalite are troctolitic, and rich (5%) in blebs of sulphide minerals

up to 1 cm across. Olivine is rare or absent through much of the central and upper part of the allivalite. This part of the sequence is marked by discontinuous lensoid layers of clinopyroxene-rich and plagioclase-rich material, the latter rather fine grained. Xenoliths of fine-grained basic rocks (beerbachite) are common in parts of the allivalite. Some of these xenoliths resemble flat slabs, orientated parallel to the layering.

2.b.2. Unit 2

Unit 2 is only well exposed around the Allt nam Ba. The unit is a complex one containing many subsidiary peridotites and allivalites. The unit is about 65 m thick, most of this being peridotite. The contact with unit 1 is planar, sharp, with no chrome-spinel seam. A few metres above the base the peridotite contains a slumped and contorted layer of allivalite, which thins and disappears to the north. Such deformed layers are common in units 2 and 3. They are marked by low-angle folding and the development of load structures of peridotite into allivalite. Despite the intensity of the small-scale deformation these disturbed layers are concordant with the enclosing rocks. Another such layer occurs about 15 m below the main allivalite.

The main allivalite is a clinopyroxene-poor troctolite resembling the classic allivalites of the upper ELS. This allivalite contains three small peridotite layers. Each of these has an undulating upper surface with 'fingers' of peridotite extending up into the overlying rock. These 'fingers' cut sharply across recumbent slump folds in the overlying allivalite with no visible deformation. These are considered in detail elsewhere (Butcher, Young & Faithfull, this issue).

2.b.3. Unit 3

Unit 3 is the most extensive in the LELS, exhibiting considerable lateral changes in lithology. The boundary with unit 4 is only clear-cut in the south; to the north the allivalite of unit 3 merges with that of unit 4, due to the northward thinning of unit 4 peridotite. In the Allt nam Ba section, unit 3 contains several subsidiary allivalites and peridotites, and the main allivalite is troctolitic in the basal parts. Elsewhere, the main allivalite is largely an unlaminated clinopyroxene-rich type, with troctolite confined to thin discontinuous layers. These clinopyroxene-rich rocks closely resemble gabbros, and parts of the sequence have in the past been mapped as such, despite the lack of visible contacts and the presence of layering. Xenoliths are fairly common in the clinopyroxene-rich facies. Beerbachite, troctolite, peridotite and gabbro are all represented.

Below the main unit 3 allivalite, east of Loch Coire nan Grund, peridotite overlies a thin troctolite layer, not traceable away from this locality. This contact is notable for the development of three chrome-spinel seams, the only ones seen in the LELS.

2.b.4. Unit 4

The peridotite taken as the base of unit 4 in the Allt nam Ba is only 2–3 m thick and has a rather weathered and altered appearance. It cannot be traced far to the north. In the Allt nam Ba the basal part of unit 4 allivalite is a well-layered, rather weathered troctolite;

this passes up into unlayered clinopyroxene and Fe–Ti oxide-rich material with abundant xenoliths of beerbachite and ultrabasic rocks. To the north of the Allt nam Ba the troctolitic facies is not well developed, and the orthocumulates of unit 3 pass up into those of unit 4 with no clear boundary. This thick allivalite is referred to as unit 3/4 allivalite. The xenoliths becomes increasingly abundant with height in unit 4 until suddenly there is a decrease in grain size, over about 2 m. This finer grained layer was mapped by Brown (1956) as an 'intrusive sheet of fine-grained olivine gabbro'. However, the lack of obviously intrusive contacts, and the presence of layering structures and xenoliths in both the fine-grained layer and the underlying allivalite suggest that it may be part of the layered series.

A wide variety of xenoliths occurs in these rocks. Beerbachite blocks, up to 10 m long, with clots and veins of calc-silicate minerals, finely laminated anorthosites and troctolites, peridotite and gabbro are all represented. These display a number of mineralogical curiosities. Ferri-fassaite, green in the field, bright yellow in thin section, is common in the calc-silicate rocks, together with grossular, plagioclase, and other minerals. This intimate association of calc-silicates with beerbachite strongly suggests that these xenoliths may represent thermally metamorphosed amygdaloidal basalts. One of the fine-grained anorthosite xenoliths (rather similar to the fine-grained plagioclase layers in unit 1) contains a layer rich in poikilitic crystals of inverted pigeonite—indicating that feldspar cumulates more fractionated than any we now see were forming in the Rhum magma chamber.

2.b.5. Unit 5

Unit 5 peridotite is not well exposed but, where exposed, the contact with the overlying allivalite is gradational, over a distance of about 1 m. Such gradational peridotite–allivalite contacts are unusual in the LELS; normally such contacts are sharp and abrupt. In this instance the contact is marked by a zone of fine scale (1–5 cm) olivine-rich and plagioclase-rich layers, the olivine-rich layers becoming thinner and less clearly marked upwards.

The allivalite of unit 5 corresponds to the upper 'intrusive sheet of fine-grained olivine gabbro' of Brown (1956). As with the lower sheet, it is difficult to disprove an intrusive origin, although the gradational lower contact, lack of net veining, and the presence of good internal layering suggest similarities with the LELS allivalites rather than the clearly intrusive gabbros.

Unit 5 allivalite is not so rich in xenoliths as the fine-grained facies of unit 4, although beerbachite and gabbro xenoliths are locally common. The allivalite is well layered, and in places concentrations of Fe–Ti oxides occur (Fig. 2). The upper part of this allivalite



Figure 2. Layering in unit 5 allivalite. A prominent Fe-Ti oxide-rich layer occurs at the level marked X-X.

develops, in places, a rather pale, well-layered facies, which Brown (1956) interpreted as relics of the allivalite which had been intruded by the sheet; explicit evidence for this is, however, lacking.

2.c. Gabbro plugs and sheets

Previous maps of the LELS have shown differing numbers of small gabbro intrusions in a variety of places. Much of this confusion has stemmed from the rather 'gabbroic' appearance of the LELS rocks, together with the extent of lateral lithological variation, which was not previously recognized. Most of these have been reinterpreted as clinopyroxene-rich allivalite. However, several small plugs and inclined sheets of gabbro have been mapped on the basis of transgressive or chilled margins and lack of layering. Two of these are intruded across the upper contact of unit 5 allivalite, cutting both it and the overlying peridotite.

Around the unit 3-unit 4 boundary in the area below Clough's Crag, thin gabbroic veins are common. This, together with the rather altered appearance of cumulates in the area, may indicate the proximity of a gabbro intrusion, perhaps below the present erosion level. This disruption occurs near the base of the xenolithic layer in unit 4 allivalite and may have been used by Brown (1956) as evidence for the intrusive origin of this layer. Away from this area no such effects are seen, however, and it is suggested that there is no connection between the two.

3. Petrography

Accounts of the petrography of the LELS are given in Harker (1908) and in Brown (1956). An outline of new observations is given below.

3.a. Peridotite petrography

Olivines are usually granular-rounded in shape; however, in places, particularly the peridotites in units

4 and 5, elongate crystals occur. These invariably display lamination. In the small peridotite layer within unit 5 allivalite, the elongate olivines appear to show two intersecting laminations (Fig. 3a). While this may be a depositional feature related to cross-lamination, it may also be caused by rotational shear during compaction of the crystal mush, or during growth *in situ*. In several specimens there is a suggestion that chrome-spinel crystals are concentrated along the upper surfaces of olivine crystals (Fig. 3b). Such structures have been described by J. A. Volker (unpubl. Ph.D. thesis, Univ. Edinburgh, 1983) from Trallval on Rhum, where he considered them evidence for sinking of chrome-spinel crystals in the interstitial liquid.

Sulphide minerals are common in trace quantities (< 0.1%), but in unit 1 peridotite they are locally abundant (1-5% of the rock), forming poikilitic blebs up to 7 mm across. Primary phases are pentlandite, pyrrhotite, chalcopyrite and cubanite. A little native copper occurs associated with alteration.

3.b. Allivalite petrography

Allivalites are characterized by the presence of cumulus plagioclase, which may or may not show lamination. Where the crystals are poikilitically enclosed in clinopyroxene, they are never laminated, even if those outside are (Fig. 3c); and the crystals inside are usually smaller than the crystals outside, unlike in olivines in peridotite (Fig. 3d). This implies that lamination, at least in allivalites, is not a depositional feature, but is developed at a late stage, probably due to compaction or shear of the crystal mush.

Very fine-grained plagioclase-rich rocks occur as layers and laminae in places. In these, the plagioclase crystals form interlocking grains, and sometimes develop triple-junction grain boundaries. They are well layered and laminated on a small scale, with variations in the size of the plagioclase and in the abundance of mafic minerals defining the layering. These rocks are common in units 1 (Fig. 3e) and 3, and as xenoliths in unit 4 allivalite, where they occasionally contain poikilitic crystals of inverted pigeonite (Fig. 3f).

Olivine crystals are usually inclusion-free, and lack the rounded-granular habit typical of olivine in peridotite. Habit does not seem to be rigorously controlled by position within a unit, although poikilitic olivine is rare in the basal parts of allivalites. Elongate or skeletal olivines are lacking in allivalites. In the slumped layers peridotite and allivalite are partly mixed; two populations of cumulus grains can be seen in thin section: the cumulus plagioclases and rather irregular cumulus olivines of the allivalite, and the rounded olivines and chrome-spinels of the peridotite.



Figure 3a. Intersecting laminations in peridotite from unit 5. Olivines parallel to the bottom of the photograph are in extinction. Scale bar = 0.5 mm.



Figure 3d. Laminated olivine crystals in peridotite from unit 5. Note that lamination is not affected by enclosure in clinopyroxene. Scale bar = 0.5 mm.



Figure 3b. Chrome-spinel concentrations on the upper surfaces of olivine crystals from unit 2 peridotite. Scale bar = 0.5 mm.



Figure 3e. Boundary between a fine-grained and a coarse-grained layer in unit 1 allivalite. Note the development of triple junctions in the fine-grained layer. Scale bar = 0.5 mm.



Figure 3c. Laminated plagioclase crystals in allivalite from unit 5. Note that crystals enclosed in the clinopyroxene do not show lamination. Scale bar = 0.5 mm.

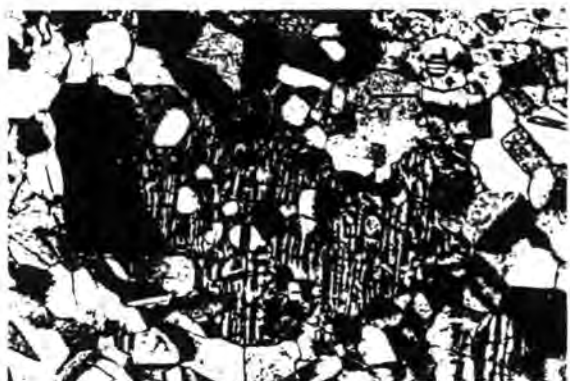


Figure 3f. Inverted pigeonite in fine-grained plagioclase-rich cumulate, Xenolith in unit 4 allivalite. Scale bar = 0.1 mm.

Pale green clinopyroxene is found in most rocks, sometimes showing marginal zoning. Exsolution is not common but, particularly in units 3, 4 and 5, lamellae of opaque phases or orthopyroxene are occasionally seen. Orthopyroxene, although fairly common as an interstitial mineral, has only been seen as cumulus crystals in a xenolith from the upper part of unit 4.

Fe-Ti oxides are the dominant opaque phase in the LELS allivalites, even in the troctolitic types of units 2 and 3. They occur mostly as interstitial blebs, although in unit 1 allivalite large cumulus ilmenites occur near the base.

Sulphides are normally absent from allivalites, with two exceptions. The basal part of unit 1 allivalite

contains about 5% of large sulphide blebs. These consist of intergrown pyrrhotite, pentlandite, chalcopyrite, cubanite and mackinawite. Smaller blebs of high-Ni pentlandite, pyrrhotite and chalcopyrite are also common. Further up in unit 1, the only sulphides seen are small, sometimes composite grains of pyrrhotite and chalcopyrite. Another sulphide-rich layer occurs in unit 3/4 in the Allt Mhor na h-Uamha, where a plagioclase- and clinopyroxene-rich layer contains about 4% of tiny pyrrhotite and chalcopyrite blebs.

3.c. Petrography of the gabbro plugs and sheets

The main minerals are clinopyroxene and plagioclase. The former is usually pale brown, with marked normal zoning. Sector zoning is well developed in some rocks. Habit varies, from euhedral prisms to ophitic intergrowths with plagioclase. The latter forms narrow laths, generally showing strong continuous normal zoning. Other minerals present are: Fe-Ti oxides, as large irregular grains; olivine, usually as large altered grains; and green amphibole. A fine-grained mesostasis is often present, usually altered to chlorite; this is one of the best features for distinguishing the gabbros from the clinopyroxene-rich allivalites.

4. Bulk-rock chemistry

As the LELS rocks are cumulates, bulk rock analyses are of little use in establishing the evolution of liquids in the magma chamber. The rock compositions are controlled mainly by the proportions of olivine, clinopyroxene, and plagioclase (Fig. 4a).

The status of the 'fine-grained sheets of olivine gabbro' (Brown, 1956) has already been questioned on the basis of field relations (sections 2.b.4 and 5). Comparison of these rocks with the clearly intrusive gabbro sheets and plugs, and the 'normal' allivalites, reveals a close affinity with the allivalites (Fig. 4b). This does not disprove an intrusive origin, but perhaps supports the notion that these rocks are related to the layered series rather than the gabbros.

5. Cryptic variation

In order to examine the extent of cryptic variation in the LELS 90 samples were collected over a 250 m vertical section near the Allt nam Ba.

Clinopyroxene and olivine were analysed in all samples. Plagioclase was not extensively analysed as preliminary studies indicated that within-sample variation was as great as or greater than that between samples. This has also been found by other workers on Rhum (Dunham & Wadsworth, 1978; Volker, unpubl. Ph.D. thesis, Univ. Edinburgh, 1983). At least five analyses per section were made of clinopyroxene and between three and eight of olivine. In nearly all

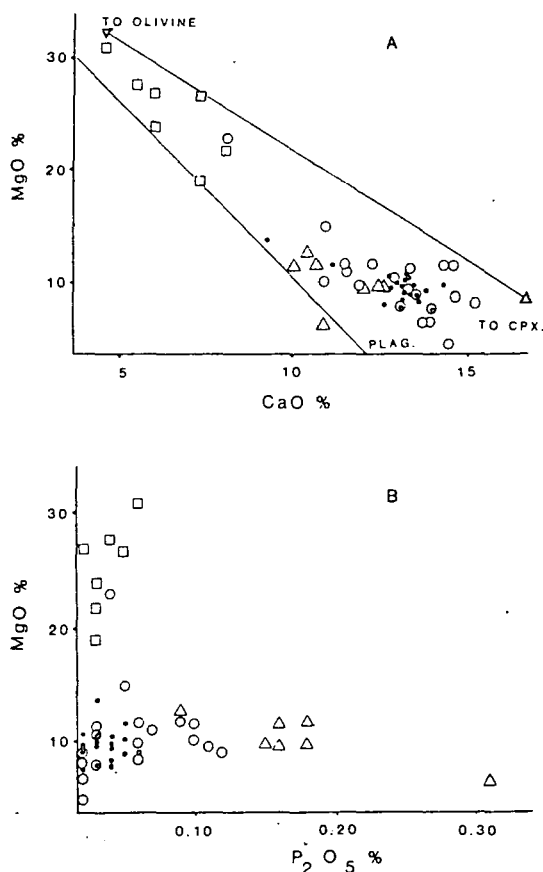


Figure 4a, b. Bulk-rock variation diagrams for the rocks of the LELS. Symbols: \square , peridotite; \circ , allivalites; \circ , 'intrusive sheets' of Brown (1956); \triangle , gabbro plugs and sheets.

cases σ was less than 0.3% Fo, or $Mg \times 100 / (Mg + Fe)$. In the case of clinopyroxene only core compositions were used, as marginal zoning both of cumulus crystals and poikilitic grains was frequently pronounced.

Even where considerable changes in texture or modal composition are present over the area of a given polished thin section, variations in mineral chemistry are not seen. Thus cryptic variation is not detectable on a small scale in the LELS rocks; it seems to be on a larger scale than, and superimposed on, the fine-scale layering.

Variations in Fo content of olivine and in Mg of clinopyroxene ($Mgn = Mg \times 100 / (Mg + Fe)$) with height are shown in Figure 5, together with stratigraphic data from the measured section. The range in olivine compositions is from $Fo_{85.6}$ to Fo_{70} ; thus olivine compositions significantly more iron-rich than any previously recorded from Rhum- Fo_{74} (Palacz, 1984) - occur in the LELS.

The most obvious features of the cryptic variation profile are the 'peaks' of Fo content associated with peridotites. Nearly every peridotite, even those < 20 cm thick or present as discontinuous slump horizons within allivalite, shows this enrichment in Fo

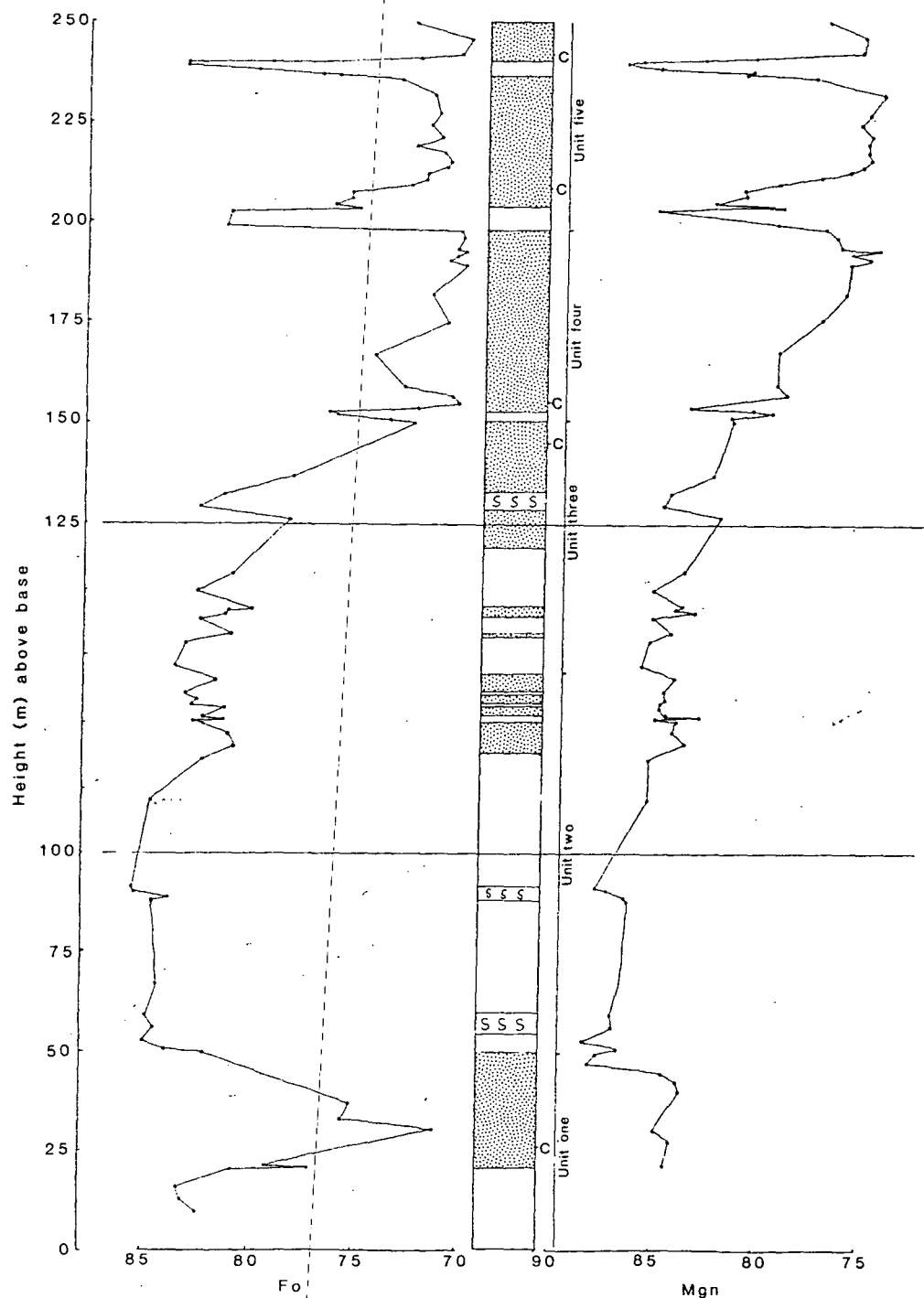


Figure 5. Cryptic variation in the LELS, as shown by olivine Fo content and Mg# of clinopyroxene (see text). Key: stipple = allivalite; S = slumped, mixed layers; blank = peridotite. C = lowest occurrence of cumulus clinopyroxene in each unit. Note the expanded vertical scale between 100 m and 125 m.

compared with the surrounding feldspar cumulates. Conversely allivalite layers, even where thin or disturbed, are marked by 'troughs' of lower Fo content. Progressive depletion of olivine Fo content with height in a unit is not usually seen, although there is a suggestion of general Fo depletion with height, particularly in the allivalites of units 3, 4 and 5. The

other obvious feature of the cryptic variation profile is the presence of 'reversals' towards the top of allivalite layers - i.e. the most evolved olivines are seen some way below the top of the layer. Conversely the most magnesian olivines in peridotites are seen some way above the base.

The profile shown by the Mg# of clinopyroxene

follows that shown by olivine very closely, except in the peridotite of unit 4 and the central portion of unit 1 allivalite. The former layer shows a much lower Fo content than other peridotite layers, and indeed the olivines of the overlying allivalite are richer in Fo than the peridotite itself. This may be explained by the presence of gabbroic veins in this area (see section 2.c), perhaps indicating that a subsurface gabbro intrusion has modified the chemistry of the cumulates at this level. The situation in unit 1 is problematic and is discussed in section 6.c.

6. Discussion

6.a. Mineral chemistry

There is compelling evidence that the mineral compositions of the LELS have been modified by various postcumulus processes. Work by Henderson & Suddaby (1971), Henderson (1975) and Bevan (1982) has shown, in Rhum and other intrusions, that chrome-spinels generally show compositions which have been extensively altered by reaction with interstitial liquid and other phases present. If such a process operates in chrome-spinel, it seems likely to operate in other phases. Butcher (this volume) has shown that late-stage veins, representing evolved liquids in the cumulate pile emplaced along fractures, have modified the chemistry of minerals, particularly olivine and chrome-spinel in the surrounding cumulates over distances of 1–2 cm. If re-equilibration can occur over such distances when the rocks are relatively cool and brittle, then with hot interstitial liquids in porous piles the process should also be effective. This may explain the remarkable constancy of olivine compositions in individual samples. Further support for this comes from the fact that olivines are never zoned with respect to Fo, even when co-existing phases show extensive zoning, implying that any zoning has been eradicated by re-equilibration.

The cryptic variation profile (Fig. 5) suggests that mineral compositions in a given peridotite or allivalite layer are affected by the composition of the cumulates above and below. Where the layers are thin, or where a layer has been disturbed or slumped in with the enclosing cumulates, the compositional contrast is lower than with thick and continuous layers.

The most magnesian clinopyroxene should be seen as the earliest formed cumulus crystals in allivalites, as these represent the first appearance of clinopyroxene on the liquidus. This is not the case. The most magnesian compositions are seen in the poikilitic pyroxene within the unit 2 peridotite, associated with the most forsteritic olivines. Generally the clinopyroxenes in peridotites are more magnesian than any in the overlying allivalite, and within allivalites intercumulus clinopyroxene low down is more magnesian than the first cumulus grains higher up.

The sympathetic relationship between Mgn of

Table 1. Liquid Fe–Mg ratios calculated from olivines and clinopyroxenes in selected LELS rocks, using the equations of Duke (1976)

Sample number	Fo	Mgn	L_{Po}	L_{Mgn}
U1A2	79.2	84.2	0.875	0.606
U2P1	84.5	86.6	0.613	0.472
U4A3	70.5	78.5	1.395	1.005
U4A15	70.0	76.1	1.429	1.200
U5A1	76.2	82.1	1.041	0.743
U5A17	76.6	80.2	1.017	0.872

L_{Po} = molar Fe–Mg ratio of liquid calculated from olivine.
 L_{Mgn} = molar Fe–Mg ratio of liquid calculated from clinopyroxene.

clinopyroxene and Fo content of olivine may provide a clue to this. There is no reason, assuming that mineral compositions are primary, why interstitial (i.e. late-formed) clinopyroxene in a peridotite should mirror the variation in Fo content of the cumulus olivines. The clinopyroxenes crystallized from trapped liquid and would be expected to show no variation, or a random one, with height. The sympathetic variation observed suggests that olivine and clinopyroxene exercise a control on each other's chemistry either by equilibration with late-stage migrating liquids in the crystal pile, or by subsolidus Fe–Mg exchange. Duke (1976) gives equations for calculating the Fe–Mg ratios of mafic melts in equilibration with olivines and clinopyroxenes. Applying these to rocks from the LELS (Table 1) it can be seen that clinopyroxenes in a given rock have apparently crystallized from more magnesian liquids than the olivines, contrary to what would be expected from the order of crystallization. Apart from demonstrating that the mineral compositions are not primary, this would seem to rule out equilibration of both phases with interstitial liquids as being the final control on mineral compositions. The extent of equilibration is difficult to gauge due to poor constraints on the olivine–clinopyroxene system (Wood, 1976) and interference by other phases, particularly oxide minerals.

The above effects can be divided into two groups: those based on equilibration between solid phases, and those based on liquid–solid reactions. The former seem to have been the final control on mineral compositions, explaining the parallel variation of olivine and clinopyroxene; however, it is likely that subsolidus effects are only significant over small distances (a few centimetres at most). To explain the large-scale cryptic variation it is necessary to consider the movement of interstitial liquids (section 6.c).

6.b. Parental magmas

Various liquids have been proposed as parental magmas for the Rhum layered rocks (Brown, 1956; Gibb, 1976; Dunham & Wadsworth, 1978; Huppert & Sparks, 1980). Recent unpublished work (Forster,

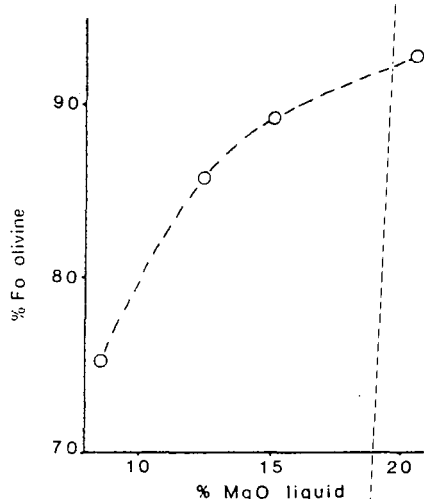


Figure 6. Variation of Fo content of olivine primocrysts, with % MgO of liquid for selected dykes analysed by McClurg (unpubl. Ph.D. thesis, Univ. Edinburgh, 1982).

unpubl. Ph.D. thesis, Univ. Durham, 1980; and McClurg, unpubl. Ph.D. thesis, Univ. Edinburgh, 1982) has proved the existence of ultrabasic liquids with up to 21% MgO in the Rhum dyke suite. Such magmas would seem ideal parent magmas for the ultrabasic complex, being capable of crystallizing large amounts of forsteritic olivine without the enormous volumes of magma required for a basaltic parent liquid.

The relationship between primocryst Fo content and liquid MgO content of dykes analysed by McClurg (unpubl. Ph.D. thesis, Univ. Edinburgh, 1982) is shown in Figure 6. Applying this diagram to the LELS rocks, a liquid of about 13% MgO would account for the most magnesian olivines observed ($Fo_{85.6}$). However, this can only be regarded as a minimum value, as the observed Fo contents in the LELS are likely to be somewhat lower than when they first crystallized. An analysis by J. E. McClurg of a dyke near to this composition is given in Table 2.

6.c. The formation of the LELS

The alternations between peridotite and allivalite have, since the work of Brown (1956), been ascribed to the repeated replenishment of the magma chamber. This is supported by the pattern of cryptic variation, in which peridotites have more magnesian olivines than the overlying and underlying allivalites.

Recent work on the behaviour of open-system magma chambers (Huppert & Sparks, 1980) suggests that replenishment of a basic magma chamber by picritic liquids would result in ponding of the hot, dense new magma under the lighter, cooler residual magma. Olivine crystallizes from the picrite, which converts strongly as it loses heat to the overlying liquid. As olivine crystallizes, the density of the magma

Table 2. Analysis of dyke B622

Major element oxides (%)		Trace elements (ppm)	
SiO ₂	45.32	Ni	350
Al ₂ O ₃	12.92	Cr	751
Fe ₂ O ₃	12.17	V	333
MgO	12.34	Cu	160
CaO	11.47	Sc	36
Na ₂ O	1.92	Pb	4
K ₂ O	0.14	Rb	1
TiO ₂	1.53	Sr	239
MnO	0.19	Ba	24
P ₂ O ₅	0.13	Th	0
		Y	19
		Zr	94
		Nb	1
		La	7
		Ce	12
		Nd	8

Analysis of dyke from unpublished Ph.D. thesis of J. E. McClurg (Univ. Edinburgh, 1982), with permission. A similar liquid may have been parental to the LELS.

in the lower layer decreases. Eventually the temperatures and densities of the layers approach equality, and the boundary between them breaks down. This marks the end of peridotite formation. The fractionation of picritic-tholeiitic melts is often marked by a density minimum at around the point where plagioclase begins to crystallize in quantity (Stolper & Walker, 1980; Huppert & Sparks, 1980). Thus the magmas from which the more fractionated allivalites (units 1, 3, 4, 5) crystallized may have been denser than those which formed the more primitive troctolitic types (unit 2, most of the upper ELS units). A picritic melt emplaced into cooler, more evolved magma will thus mix more quickly than one emplaced into hotter magma with a composition around the density minimum, due to the lower density contrast. It will also lose heat faster; this may explain the abundance of elongate olivine crystals in the peridotites of units 4 and 5, as such habits are encouraged by fast cooling (Donaldson, 1976).

If the picritic liquid is denser than the interstitial liquid in the underlying crystal pile, it may sink into it, displacing the evolved liquids (Tait, Huppert & Sparks, 1984; Sparks *et al.*, this issue). This would seem to be a potent mechanism for producing the reversals in cryptic variation seen at the top of allivalites, the olivines re-equilibrating with the new Mg-rich magma. Reversals are small or absent at the tops of unit 3 and unit 4 allivalites; perhaps the density of the interstitial liquid in these evolved cumulates was such that convective exchange with the overlying picritic liquid was not possible. A problem here is the large reversal shown by unit 1 allivalite which, given the evolved nature of the olivines, might be expected to have had interstitial liquid as dense as that in units 3 and 4. However, unit 1 allivalite shows evidence for early (cumulus) Fe-Ti oxides (section 3.b). Early crystallization of such phases may have caused a

continuous decrease in density with fractionation, allowing the picritic liquid to sink in. Conditions of higher f_{O_2} could account for such behaviour. Such early removal of Fe from the magma might also explain the magnesian character of the clinopyroxenes in unit 1 allivalite.

The model of Tait, Huppert & Sparks (1984) predicts that while evolved orthocumulates are forming at the magma chamber floor, evolved adcumulates will be forming at the roof. It is interesting to note that evolved adcumulates (including the pigeonite-bearing xenolith) are associated with roof- or wall derived xenolithic material. This assemblage also includes thermally metamorphosed amygdaloidal basalt, suggesting that the Rhum magma chamber may have been in contact with Tertiary basalts.

The LELS rocks are in general less ultrabasic than those elsewhere in Rhum, both in terms of the abundance of peridotite and in terms of the rather more evolved mineral compositions. This may be due to replenishment by smaller pulses of picritic liquid, which would crystallize less peridotite and allow the accumulation of lower-temperature, more evolved cumulates. The frequent emplacement of large picritic pulses would, in addition to producing large volumes of peridotite, tend to maintain the chamber at a high temperature, thus giving the primitive compositions typical of the upper ELS cumulates.

Acknowledgements. This work was carried out under N.E.R.C. grant No. GT4 80 GS25, at Durham University. Thanks are due to Dr C. H. Emeleus, who supervised the project, and provided much helpful advice. Alan Butcher, Iain Young, Johannes Volker and Steve Tait helped in discussing many aspects of the work. Janet McClurg kindly allowed the use of some of her data. Special thanks are due to Ms. Cathryn Burge for assistance, not least in typing and in the preparation of diagrams.

References

- BAILEY, E. B. 1945. Tertiary igneous tectonics of Rhum. *Quarterly Journal of the Geological Society of London* **100**, 165–91.
- BEVAN, J. C. 1982. Reaction rims of orthopyroxene and plagioclase around chrome-spinels in olivine from Rhum and Skye. *Contributions to Mineralogy and Petrology* **79**, 124–9.
- BROWN, G. M. 1956. The layered ultrabasic rocks of Rhum, Inner Hebrides, Scotland. *Philosophical Transactions of the Royal Society of London B* **240**, 1–53.
- BUTCHER, A. R. 1985. Channelled metasomatism in Rhum layered cumulates – evidence from late-stage veins. *Geological Magazine* **122**, 503–18.
- BUTCHER, A. R., YOUNG, I. M. & FAITHFULL, J. W. 1985. Finger structures in the Rhum complex. *Geological Magazine* **122**, 491–502.
- DONALDSON, C. H. 1976. An experimental investigation of olivine morphology. *Contributions to Mineralogy and Petrology* **57**, 187–213.
- DUNHAM, A. C. & WADSWORTH, W. J. 1978. Cryptic variation in the Rhum layered intrusion. *Mineralogical Magazine* **42**, 347–56.
- DUKE, J. M. 1976. Distribution of the period four transition elements among olivine, calcic clinopyroxene and mafic silicate liquids: experimental results. *Journal of Petrology* **17**, 499–521.
- GIBB, F. G. F. 1976. Ultrabasic rocks of Rhum and Skye: the nature of the parent magma. *Journal of the Geological Society of London* **132**, 209–22.
- HARKER, A. 1908. *The Geology of the Small Isles of Inverness-shire*. Memoir of the Geological Survey of Scotland, 210 pp.
- HENDERSON, P. 1975. Reaction trends of chrome-spinel on Rhum. *Geochimica et Cosmochimica Acta* **39**, 1039–44.
- HENDERSON, P. & SUDDABY, P. 1971. Nature and origin of the chrome-spinel of Rhum. *Contributions to Mineralogy and Petrology* **33**, 21–31.
- HUPPERT, H. E. & SPARKS, R. S. J. 1980. The fluid dynamics of a basaltic magma chamber replenished by influx of hot, dense, ultrabasic liquid. *Contributions to Mineralogy and Petrology* **75**, 279–89.
- PALACZ, Z. A. 1984. Isotopic and geochemical evidence for the evolution of a cyclic unit in the Rhum intrusion, north-west Scotland. *Nature* **307**, 618–20.
- SPARKS, R. S. J., HUPPERT, H. E., KERR, R. C., MCKENZIE, D. P. & TAIT, S. R. 1985. Postcumulus processes in layered intrusions. *Geological Magazine* **122**, 555–68.
- STOLPER, E. & WALKER, D. 1980. Melt density and the average composition of basalt. *Contributions to Mineralogy and Petrology* **74**, 7–12.
- TAIT, S. R., HUPPERT, H. E. & SPARKS, R. S. J. 1984. The role of compositional convection in the formation of adcumulate rocks. *Lithos* **17**, 139–46.
- WOOD, B. J. 1976. An olivine-clinopyroxene geothermometer. *Contributions to Mineralogy and Petrology* **56**, 297–303.

Finger structures in the Rhum Complex

ALAN R. BUTCHER,* IAIN M. YOUNG† & JOHN W. FAITHFULL‡

* Department of Geology, University of Manchester, M13 9PL, U.K.

† Department of Geology, University of St Andrews, St Andrews, Fife, Scotland, U.K.

‡ Department of Geological Sciences, University of Durham, Science Laboratories, Durham, DH1 3LE, U.K.

(Received 2 November 1984; accepted 13 March 1985)

Abstract – Finger-like protrusions of peridotite are developed on Rhum where peridotite is overlain by allivalite. These structures, which were described by Brown as 'upward-growing pyroxene structures', are found in the following environments: at the main intra-unit junctions; along the upper surface of subsidiary peridotites in certain allivalites; and along the lower surface of allivalite blocks in some peridotites.

The structures generally take the form of parallel-sided or tapering protrusions with circular cross-sections. The tops of fingers are conical or hemispherical in shape. Typical dimensions are: finger amplitude, 2–5 cm; finger diameter, up to 3 cm; and finger wavelength, 5–10 cm. Peridotite in the finger is modally and texturally similar to the underlying layer, varieties range from feldspathic peridotite to dunitic peridotite. In the field the fingers apparently cut through layering, laminae and lamination without any associated disruption of the planar structures.

Two contrasting mechanisms of formation are discussed: vertical deformation of crystal mushes, and metasomatic replacement. On balance, we prefer to interpret the fingers as evidence for the replacement of pre-existing allivalite by secondary peridotite. Replacement was achieved by pore magma from the underlying peridotite migrating upwards into the overlying allivalite, in response to compaction. This pore magma was able to resorb plagioclase but crystallize olivine and pyroxene in its place.

1. Introduction

Recent detailed mapping on Rhum has established that the layered intrusion can be envisaged as an early well layered series of rocks, now comprising the Eastern Layered Series (ELS) and Western Layered Series (WLS), intruded by a later, transgressive body of largely unlayered ultrabasic rocks comprising the Central Series (CS) (unpub. Ph.D. theses by J. E. McClurg, 1982, and J. A. Volker, 1983, Univ. Edinburgh). The layered series may be further subdivided into major cyclic units (Brown, 1956): such a unit is defined as an olivine-rich lower layer (peridotite) overlain by an upper plagioclase-rich layer (allivalite).

Conventionally, the cyclicity of the Rhum stratigraphy has been interpreted as the result of periodic replenishment of the magma chamber (Brown, 1956; Wadsworth, 1961), although Young (unpub. Ph.D. thesis, Univ. St Andrews, 1984) has tentatively proposed contemporaneous crystallization of different types of cumulates in a vertically zoned magma chamber. The basic assumption in the interpretation of the layers has been that the present lithostratigraphy is essentially a primary feature. However, compositional modification by pervasive or channelled

metasomatism may have occurred (J. A. Volker, unpub. Ph.D. thesis, Univ. Edinburgh, 1983; Butcher, this issue).

In this paper we describe structures, termed 'finger structures', which indicate that modal replacement of allivalite by peridotite has occurred on Rhum, on both a local and massive scale, producing rocks texturally and compositionally indistinguishable from presumed cumulates in the intrusion. The importance of this conclusion for interpretations of Rhum lithostratigraphy is assessed and a tentative, qualitative model for the formation of these secondary rocks is proposed.

2. The finger structures

The contacts between peridotite and overlying allivalite on Rhum are commonly characterized by finger-shaped protrusions of peridotite into allivalite. These structures were first described by Brown (1956), who compared them to the 'fingers of an outstretched hand' and named them upward-growing pyroxene structures. Since they do not necessarily contain pyroxene, and have not formed by pyroxene growing upwards, we propose that they be called 'finger structures' on account of their geometry. This is in keeping with the terminology used by Robins (1982) for describing similar structures in the Lille Kufjord intrusion.

Finger structures are commonly developed through-

Present addresses: * Institute for Geological Research on the Bushveld Complex, University of Pretoria, Hillcrest, Pretoria, 0002, Republic of South Africa. † Department of Geology, University of Leicester, University Road, Leicester LE1 7RH, U.K.

out the ELS and CS, but only three areas have been studied in detail: the Hallival-Askival area (ELS); the Minishal area (CS); and the Long Loch area (CS). Fingers have not been found in the WLS.

2.a. The Hallival-Askival area

Figure 1 summarizes the principle localities where finger structures are developed. The three main environments are: (i) along the main intra-unit contacts (e.g. Units 6-11); (ii) along the upper surface of subsidiary peridotite layers in certain allivalites (e.g. Units 2, 8, 12, 13, 14); and (iii) along the lower surface of allivalite blocks in peridotite (e.g. Units 9, 10, 11). Because fingers at intra-unit contacts are the same as those in (ii) above, only fingers from environments (ii) and (iii) are described.

2.a.1. Fingers associated with subsidiary peridotites

Unit 2, Allt nam Bà. Unit 2 of the ELS contains a number of subsidiary peridotites within the allivalite, best exposed in the Allt nam Bà (Fig. 1).

Figure 2a shows that the allivalite (6.5 m thick) contains three thin peridotite layers. Each of these has a sharp planar base and a fingered top, although the fingers are rather small (1-3 cm in amplitude). The allivalite above the lowest peridotite has well developed recumbent slump folds - these are sharply cut across by the fingers (Fig. 3).

To the north the peridotites thicken somewhat, and deformation becomes more marked with the peridotite layers becoming locally discontinuous due to loading, with flame structures of allivalite injecting the peridotites. Fingering is more prominent on the upper surfaces of the peridotite layers than it is to the south.

A few tens of metres to the north the allivalite presents a different spectacle. The upper part has been extensively disrupted by finger development, with merging of subsidiary peridotites leaving only a few relic fragments of plagioclase-cumulate (Fig. 2b). The peridotites often show 'inverted mushroom' style load structures, the upper surfaces of which show the development of fingers.

Unit 8, northeast Askival Plateau. The fingers at this locality (Fig. 1) are the same as Brown's (1956) 'upward-growing pyroxene structure'. A schematic strike section of the exposure is given in Figure 4.

At the southeastern end, up to six minor peridotite horizons can be distinguished. Finger structures are developed along the upper contacts of layers A, B (Fig. 5a,b), E and F. The lower contacts are either planar or slumped (load structures?). Towards the northwest, exposure is incomplete and only the bottom two layers (A and B) are found. Both layers thin away towards this direction and merge with the allivalite.

Close inspection of weathered surfaces shows that the fingers cross-cut the feldspar lamination in the allivalite (Fig. 5b). Peridotite in the finger is texturally similar to the underlying layer (a general increase in clinopyroxene content is apparent in both at the northwestern end of the section). Layer B (figured by Brown, 1956, plate 2, fig. 20) contains fingers of variable orientation: some are vertical; others preferentially lean in one direction.

Thin sections of samples from layers A and B (Fig. 6) show that the finger structures are formed of tabular olivines enclosed by large poikilitic clinopyroxene crystals (Brown, 1956). Plagioclase only occurs as rare interstitial patches.

Brown (1956) made several important microfabric observations on fingers from this locality. He noted that the tabular olivines near the edge of the finger are orientated parallel to the periphery of the structure, while in the core they are random, as is seen in Figure 6. He also established that tabular crystals of olivine and plagioclase in the overlying allivalite are orientated roughly horizontal, except at the contact with the structure where they are rotated out of alignment and now lie sub-parallel to it. This can also be seen in Figure 6 (the deflection of the lamination is not sufficiently dramatic to be picked out on a weathered surface; see Fig. 5b). Peridotite 1 cm below the base of the finger in Figure 6 is a typical, well-laminated olivine cumulate. At distances greater than 3 cm below the finger, the cumulus olivines change in shape from tabular to anhedral.

Unit 14, west Hallival. The allivalite section of Unit 14 directly below the summit of Hallival contains several layers of olivine cumulate, but all are classed as belonging to one unit for practical reasons (after Brown, 1956). A measured section through the allivalite on the western side of Hallival (Fig. 1) is given in Figure 7a.

The main intra-unit junction is gradational but in the overlying allivalite the subsidiary peridotites all have sharp contacts (except where indicated in Fig. 7a). Finger structures were recorded by Brown (1956) in this part of Unit 14; Figure 7a shows they are ubiquitous, and only three peridotite horizons do not contain them along their upper contacts. Some of the structures are remarkably regular and finger-like (e.g. Fig. 7b,c); others are highly irregular (Fig. 7d).

Three different peridotite horizons have been sampled (Fig. 7a; samples HF9, HF4, HF3) and all show that the Unit 14 fingers are texturally unlike those already described from Unit 8. Firstly, the finger peridotite consists of anhedral rather than tabular olivines. Secondly, the clinopyroxene grains (and occasional plagioclase) which enclose the anhedral olivines do not form well-developed oikocrysts. Thirdly, the allivalite is unlaminated in all samples.

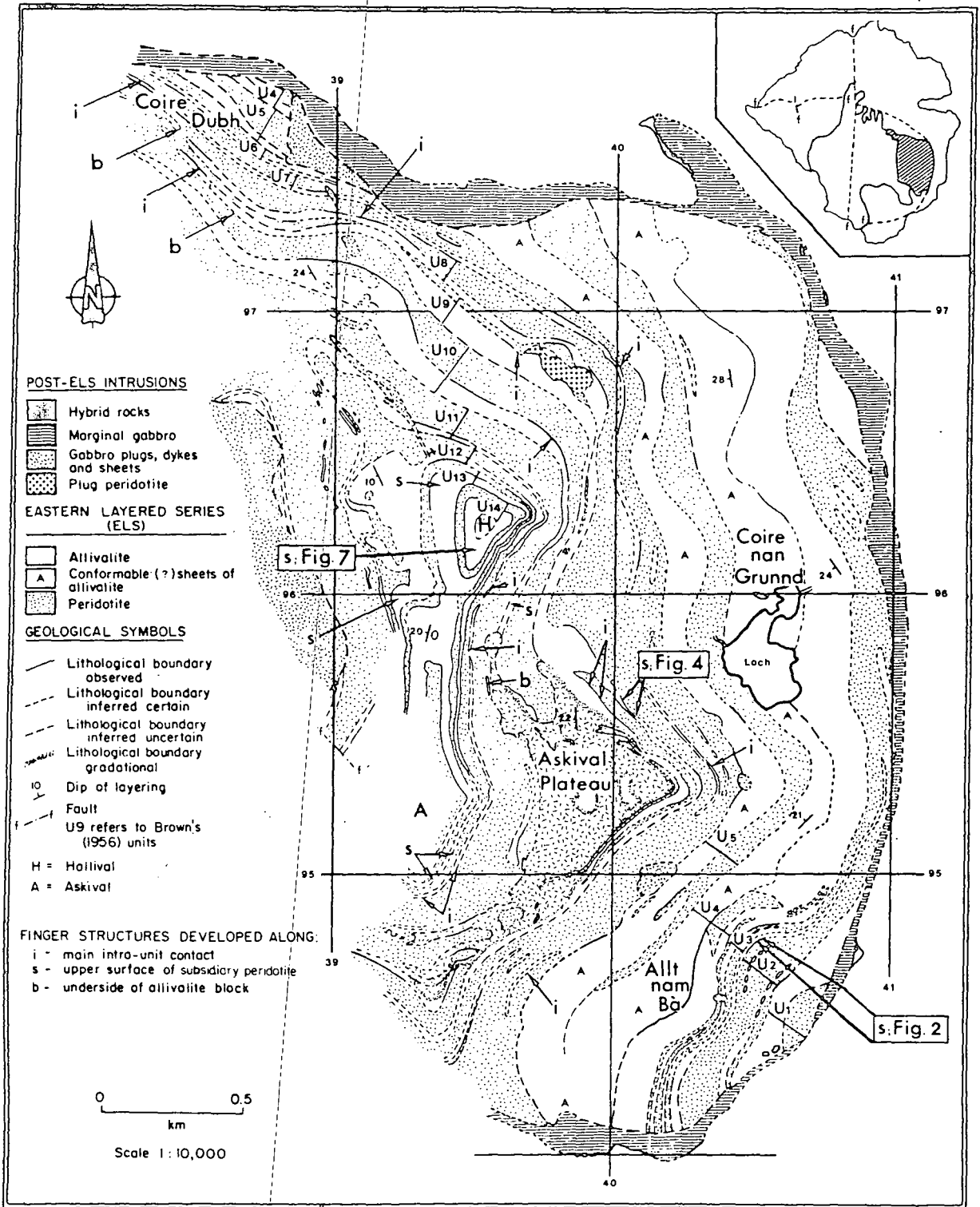


Figure 1. Geological map of the Hallival and Askival area showing the principal localities where finger structures are developed.

2.a.2. Fingers associated with allivalite blocks

The peridotite sections of Units 9, 10 and 11 contain imperistent horizons of allivalite blocks in northwest Coire Dubh, southeast Coire Dubh and the Askival

Plateau area, respectively (Fig. 1). The orientation of layering in the blocks is similar to that found in the surrounding peridotite suggesting they are not xenoliths but instead relic fragments of an originally continuous allivalite layer (or layers). The blocks all

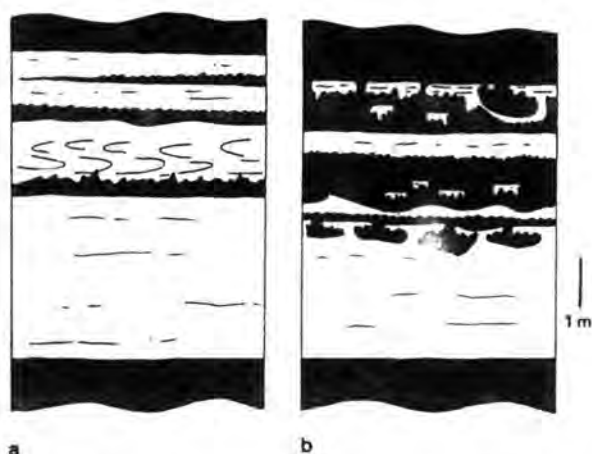


Figure 2. Stratigraphy of Unit 2 allivalite at two localities (a, b) in the Allt nam Bà. Black, peridotite; blank, allivalite. See text for details.



Figure 3. Finger structures cutting slump folds in Unit 2, Allt nam Bà.

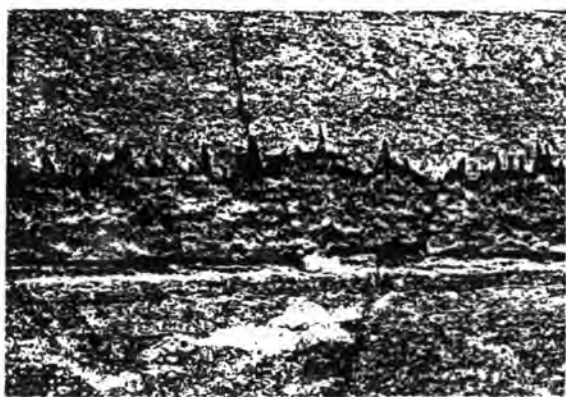


Figure 5. Finger structures associated with subsidiary peridotite layer B in Unit 8 allivalite, northeast Askival Plateau. (a) Fingers are developed along the upper contact, while the lower contact is planar. Scale: hand lens, 3 cm long. (b) Close-up of the fingers in (a). The weathered surface of the overlying allivalite shows igneous lamination of cumulus olivine and plagioclase grains.

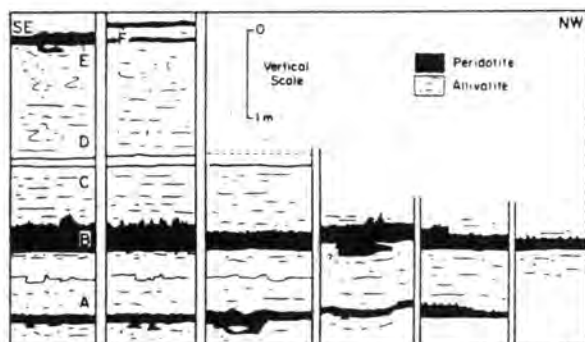


Figure 4. Schematic strike section of Unit 8 allivalite, northeast Askival Plateau, showing structures developed at the upper contacts of subsidiary peridotite horizons. Lateral distance represented by the section is approximately 100 m (see Fig. 1).

have highly irregular lower surfaces which are invariably finger-shaped (Fig. 8). Some have planar upper surfaces containing a chrome-spinel layer which continues undeformed in the surrounding peridotite up to 1.5 m away from the block (Fig. 8).

2.b. The Minishal area

The northern margin of the CS forms a broad tongue-shaped area east of Minishal (Fig. 9) consisting largely of undifferentiated peridotite, cut by intrusive ultrabasic breccia zones and a late gabbro (J. E. McClurg, unpub. Ph.D. thesis, Univ. Edinburgh, 1982).

At a locality southeast of Minishal (Fig. 9), a cliff exposure reveals a breccia zone containing a layer of allivalite (maximum thickness 3.5 m), which tapers out to the east and is unexposed at the western end. The layer is surrounded by a matrix of feldspathic peridotite. Along the lower contact, the matrix

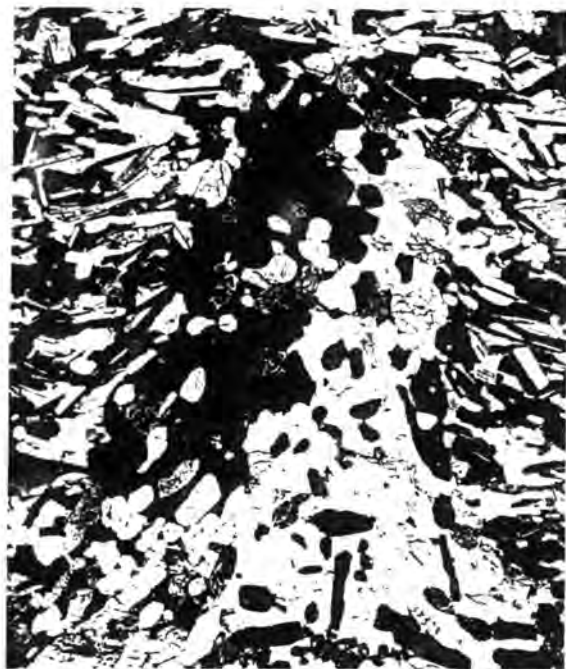


Figure 6. Photomicrograph of sample GMBFC; a finger structure developed at the top of peridotite layer A, Unit 8 allivalite, northeast Askival Plateau. Crossed polars; field of view 2 cm wide.

peridotite protrudes upwards into the allivalite in the form of impressive finger structures (some up to 50 cm in amplitude). The upper contact does not show these structures but it is highly irregular. Diffuse sub-horizontal layering is present throughout the allivalite; most of the fingers are normal to the layering, although some have been found to lean preferentially in one direction.

Prominent subvertical channels cut through the allivalite layer but these are interpreted as largely a weathering phenomenon related to the presence of joints or other planes of weakness. It is possible however, that some channels may have originally been filled by pipe-shaped peridotite protrusions from the layer below, and that the peridotite has since been removed by preferential weathering.

A further interesting feature of this exposure is that at the eastern end there are two fragments of allivalite in the peridotite about 0.5 m below the layer. Both fragments have planar upper contacts, finger-shaped lower contacts, and are completely surrounded (in 2-D) by peridotite.

A specimen of a peridotite finger taken from the middle of the exposure consists of anhedral olivine; hydrous intercumulus phases (brown amphibole, brown mica; 1–5 vol. %); intercumulus clinopyroxene; and secondary alteration minerals (chlorite, serpentine). Plagioclase was detected in some thin sections. The allivalite surrounding the finger is weakly laminated; a few plagioclase tablets at the contact are deflected upwards.

2.c. The Long Loch area

On the western shores of Long Loch (Fig. 9) there are spectacular sections through a well-layered sequence of the Central Series, mapped by J. E. McClurg (unpub. Ph.D. thesis, Univ. Edinburgh, 1982) as belonging to the Long Loch Member (or Long Loch Group of J. A. Volker, unpub. Ph.D. thesis, Univ. Edinburgh, 1983).

A schematic strike section of the sequence west of the loch is given in Figure 10. Three compositionally distinct units are shown. Unit A at the base is an unlayered olivine-rich cumulate. This is overlain by an allivalite (Unit B) containing several modally graded layers (olivine-rich base, plagioclase-rich top). Unit C is a layer consisting of normally size-graded fragments of peridotite set in a feldspathic matrix. A slumped horizon of feldspathic peridotite (Unit B, a) occurs near to the top of Unit B.

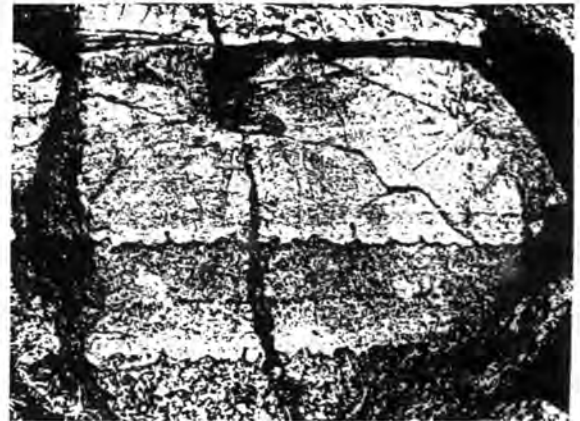
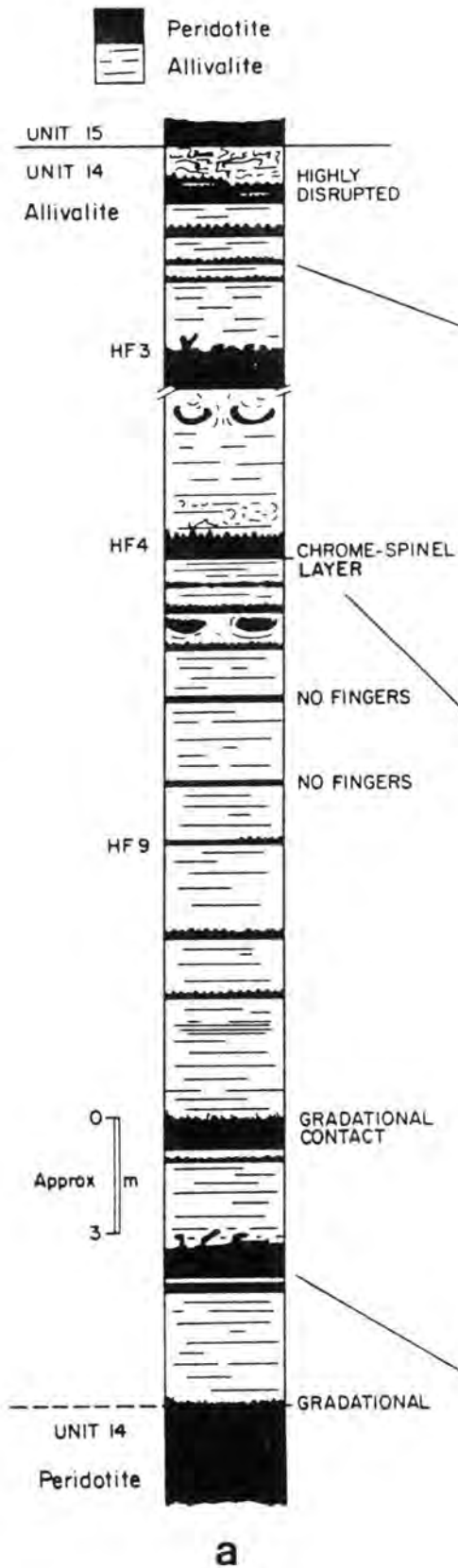
Exposure is sufficiently good to be able to examine in detail the junctions between each unit. Figure 10 indicates the various types of structure observed. They include:

Flame structures: these are flame-shaped protrusions of allivalite into overlying peridotite. They are developed at the contact between Units B and C, and also at the interfaces between individual graded layers in Unit B (flames are omitted from Unit B in Fig. 10 for clarity).

Finger structures: these occur at the Unit A–B junction (Fig. 11); along the upper surface of Unit B, a; and within individual graded layers in Unit B.

Finger structures in Unit B can be seen to develop across the section from north to south. At the northern end, there are up to 7 modally graded layers. Laterally, however, the olivine-rich bases of some layers start to develop finger-shaped interfaces with the overlying plagioclase-rich portion of the layer (Fig. 10), but only where the gradation from one into the other takes place abruptly (across a zone less than 1 cm in thickness). In the middle and southern end of the section some peridotite fingers extend right through the plagioclase-rich section and coalesce with the olivine cumulates at the base of the overlying graded layer. Layering in the allivalite near to the transgressive finger structures is always undeformed.

Samples suitable for detailed analysis of the Long Loch structures have not been obtained because of extraction difficulties, but a thin section of the Unit A–B contact shows the peridotite is petrographically similar to the Minishal structures. Intercumulus amphibole, mica and clinopyroxene enclose anhedral olivines. The allivalite in this section is unlayered.



b



c



d



Figure 8. Block of layered allivalite in feldspathic peridotite, Unit 11, Askival Plateau. A chrome-spinel layer (c) is present along the upper surface of the block which extends into the surrounding peridotite.

3. Mineral compositions

A preliminary microprobe study has been carried out on samples of six different finger structures, and the results are summarized in Figure 12.

3.a. Olivine and clinopyroxene

All samples analysed show there are no significant differences in the compositions of olivine and clinopyroxene between finger peridotite and the overlying allivalite. There are also no systematical changes in the composition of these minerals either with position within a finger (e.g. Minishal; A, B) or with position in peridotite below a finger (e.g. Unit 8; 1-3). All olivine is unzoned; clinopyroxene is normally zoned at the extreme margins of some grains (only core compositions are given in Fig. 12).

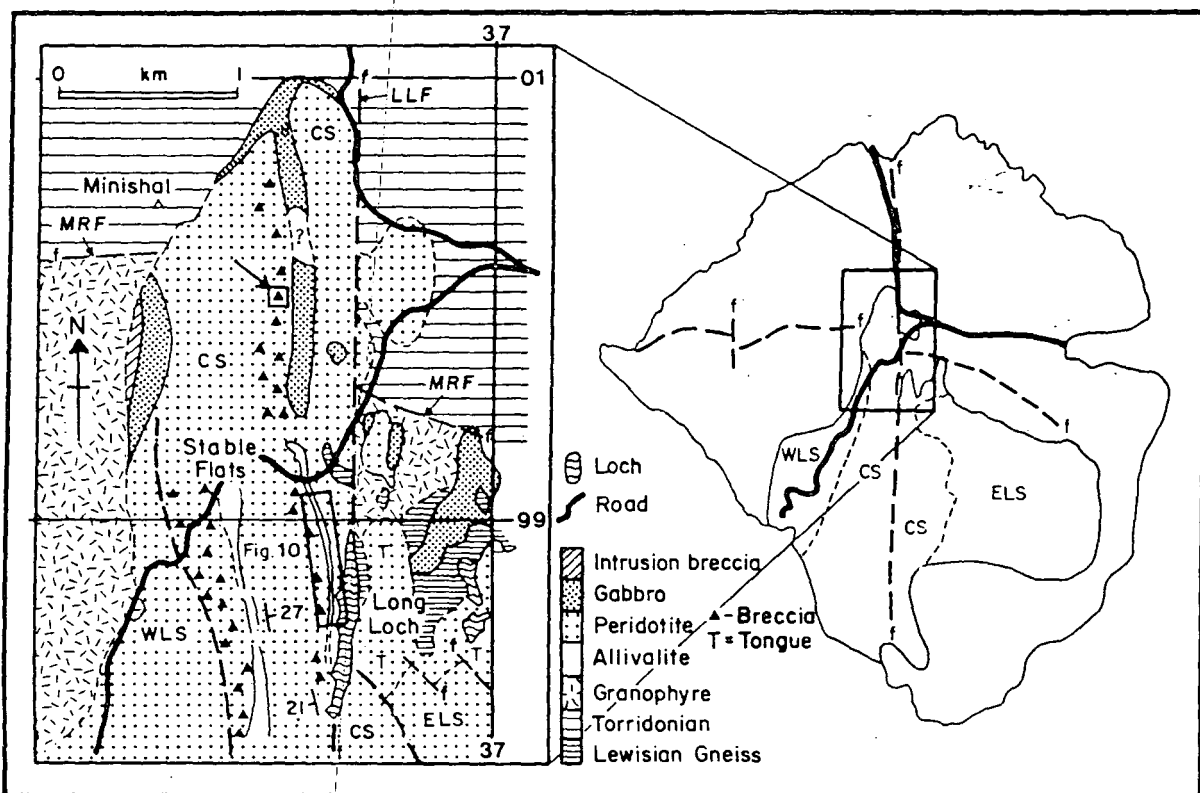


Figure 9. Sketch map of the geology of the Minishal and Long Loch areas, modified after J. E. McClurg (unpub. Ph.D thesis, Univ. Edinburgh, 1982). Symbols: LLF, Long Loch Fault; MRF, Main Ring Fault. Arrowed box indicates the position of the Minishal locality referred to in the text; rectangular box shows the area covered by Figure 10.

Figure 7. Finger structures in Unit 14 allivalite, west Hallival. (a) Sketch stratigraphic section through Unit 14 allivalite, showing the contacts along which finger structures are developed (schematically represented by bulges along upper surfaces of subsidiary peridotite layers). (b) Two peridotite layers with weakly developed finger structures along their upper contacts. (c) Regular shaped finger structures. The lower contact of the peridotite is characteristically planar. Note the complex slump structures in the allivalite above the fingers, and the feldspathic veins cutting both peridotite and allivalite. Scale: 50 pence coin, middle of exposure. (d) Irregular shaped protrusions of peridotite (generally plate-like), developed above a well-layered subsidiary olivine cumulate.

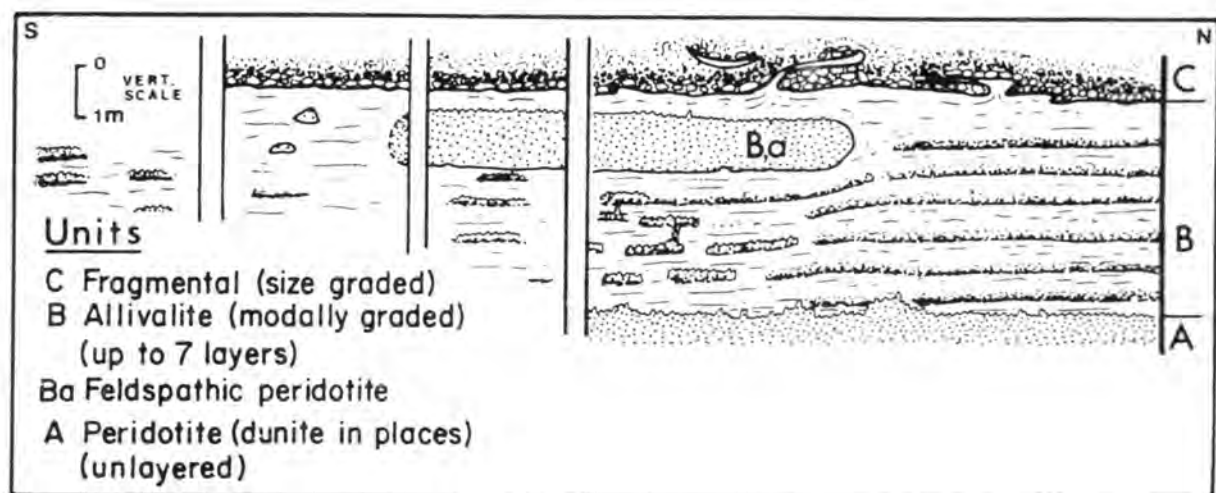


Figure 10. Schematic strike section of the well-layered CS sequence west of Long Loch. Lateral distance represented by the section is approximately 0.75 km.



Figure 11. Peridotite fingers cutting layered allivalite. Unit A-B contact, Long Loch area (see also Robins, 1982, fig. 6).

3.b. Plagioclase

Relative to plagioclase in the allivalite, finger plagioclase shows a greater compositional range, and is generally more Na-rich.

4. Summary

The following general observations have been made on Rhum finger structures:

(a) Fingers only develop where peridotite is overlain by allivalite. From their present lithologies this indicates a positive or gravitationally stable density stratification, i.e. the relatively denser peridotite is at the bottom.

(b) The contact between the peridotite and the allivalite is always exceptionally abrupt. Fingers do not form along gradational contacts.

(c) Only the upper surface of the peridotite layer

develops fingers. The lower surface is characteristically planar.

(d) Fingers are found in a variety of environments: (i) at the main intra-unit contacts; (ii) along the upper surface of subsidiary peridotites in certain allivalites; (iii) along the lower surface of allivalite blocks in some peridotites.

(e) The geometry of the structures at any given locality is often remarkably consistent. They generally take the form of parallel-sided or tapering protrusions with circular cross-sections. The tops of fingers are conical or hemispherical in shape. Typical amplitudes for most fingers are 2–5 cm; diameters up to 3 cm. Distances between individual fingers are also regular; typical wavelengths measure 5–10 cm. The long axis of the finger is usually orientated normal to the layering, although some have been found that are vertically orientated or preferentially lean in one direction.

However, not all of the structures are finger-shaped: pipe-like structures (2 m long; diameters up to 10 cm) and plate-like structures also occur. On encountering more mafic layers in the allivalite, fingers sometimes widen, but have never been noted to narrow. No consistent correlations between finger geometry and the thickness, lithology or texture of the underlying peridotite layer have been found.

(f) Inspection of weathered surfaces suggests that peridotite in the finger is modally and texturally similar to the underlying layer. Varieties range from feldspathic peridotite to dunitic peridotite.

(g) Finger structures cross-cut slumped allivalite and therefore post-date slumping events in the feldspathic cumulates. A finger in Unit 2 (ELS) is cut by a late-stage ultrabasic vein.

(h) In terms of mineral chemistry, finger peridotite and overlying allivalite are essentially the same in composition, except for plagioclase which is more Na-rich in the finger.

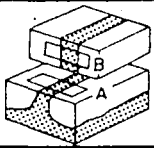
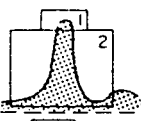


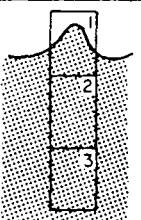

Location	Parts of finger covered by thin section	OLIVINE		CPX		PLAGIOCLASE	
		Fo ALLIV.	Fo FING.	Mgr A	Mgr F	An A	An F
Minishal (CS)	 MINBB	84.3	84.2	84.9	86.2	86.4-82.8	76.1-61.7
	MINBA	84.8	84.9	—	86.0	85.9-83.3	80.5-61.6
Unit 14 Allivalite	 HF3, ₁	83.6	82.7	85.5	—	86.5-84.5	84.5-69.2
	HF3, ₂	82.9	82.8	85.0	85.0	88.4-85.2	87.3-78.8
	 HF4	84.7	84.2	85.8	85.9	89.5-85.9	88.2-64.2
Unit 11 Allivalite	 APG4, ₂	84.5	85.2	88.5	87.8	84.4-82.2	77.2-57.8
Unit 8 Allivalite	 GMBFA, ₁	82.0	81.7	86.1	85.1	85.2-83.3	—
	GMBFA, ₂	—	82.0	—	85.0	—	82.0-75.3
	GMBFA, ₃	—	81.6	—	84.1	—	75.7-72.8
	 GMBFC	81.0	80.9	83.8	85.4	85.2-80.1	85.4-71.5

Figure 12. Summary of electron microprobe data of finger structures from the Minishal area (CS) and the Hallival-Askival area (Units 8, 11 and 14). Fo and Mgr, 100 Mg/(Mg+Fe) ratios. An, 100 Ca/(Ca+Na) ratio; values given are ranges of plagioclase 'core' compositions. Analyses were made on a modified Cambridge Instrument Company Geoscan fitted with a Link Systems model 290-2KX energy-dispersive spectrometer. Average compositions for all phases were determined from at least 5 analysed spots of 5 different crystals.

5. Discussion

In a recent paper, Robins (1982) has suggested an origin for the finger structures in the Lille Kufjord and Rhum intrusions. His conclusion is that they are not deformational structures but formed by metasomatic replacement of allivalite by peridotite.

In the discussion below, three different mechanisms of formation are considered in the light of the new field, textural and mineralogical observations on the Rhum fingers:

- deposition of allivalite on an irregular peridotite floor;
- deformation of crystal mushes;
- metasomatic replacement.

5.a. Deposition on an irregular floor

One possible explanation of the Rhum fingers is that they represent the morphology of the peridotite floor prior to deposition of the allivalite. This might explain fingers with small amplitudes (e.g. Fig. 7b, c) but not pipe-like structures or other more complex shaped

protrusions (e.g. Fig. 7d). Also, transgressive relationships suggest the fingers formed after deposition of the allivalite and not before it (Figs 3 and 11).

5.b. Vertical deformation of a crystal mush

A more plausible mechanism is that the finger structures formed by vertical deformation of an unconsolidated olivine cumulate into overlying, relatively more consolidated, allivalite. However, this is extremely difficult to reconcile with: (i) the overwhelming field evidence that layered allivalite near to cross-cutting fingers is apparently undeformed; (ii) the structures having formed at contacts where there is a normal density gradient (as suggested by the present rock densities). Analogous deformation structures in layered clastic sediments always develop in reverse density gradients (Anketell, Cegla & Dzulynski, 1970). The morphology of the fingers is also different from the mushroom-like load structures described by Thy & Wilson (1980) from the Fongen-Hyllingen intrusion.

5.b.1. Lack of deformation

Deformation is not obvious at outcrop scale (Fig. 11), but there is some evidence from thin sections that disruption of laminated crystals has taken place. For example, in Unit 8 tabular olivines in the finger lie parallel with the margins of the structure, whereas in the peridotite below the finger they lie parallel with the general orientation of the layering. Also, lamination in the allivalite is deflected upwards at the finger contacts. However, we consider the deformation to be on too small a scale if the fingers had formed by a process involving only diapiric intrusion of peridotite into allivalite.

5.b.2. Relative density

Lee (1981) has described similar structures from the Bushveld Intrusion which formed in normal density gradients. The structures, termed 'flames' rather than 'fingers' by Lee (1981), occur where anorthosite overlies chromitite or pyroxenite; and norite over harzburgite or chromitite. Because these structures are similar in many respects to those in reverse density gradients in clastic sediments, Lee has inferred that interstitial liquid played an important part in controlling the relative density and viscosity of the adjacent cumulate layers.

A similar mechanism for the Rhum structures is suggested by the recognition of a density minimum in the MORB liquid line of descent (Stolper & Walker, 1980; Sparks, Meyer & Sigurdsson, 1980). Huppert & Sparks (1980) consider that liquids parental to the Rhum peridotites were picritic and those parental to the allivalite were basaltic. Assuming this to be the case, liquid trapped within the olivine cumulates must initially have become less dense on fractionation of olivine, whereas that trapped in the allivalites must initially have become more dense on fractionation. Thus, it is possible that liquid present in the olivine cumulates was initially, or became, less dense than that in the feldspar-rich cumulates. Field evidence (section 2.a.1) indicates that the allivalite contained a low porosity at the time of finger formation (i.e. fingers post-date slumping and lamination). Calculations by one of us (IMY) suggest that an allivalite mush containing, for example, 30% interstitial liquid will only be more dense than a peridotite mush if the latter contains 80% liquid or more (the densities of the liquids in the allivalite and peridotite are assumed to be 2.75 and 2.70 g/cm³, respectively). Unreasonably large amounts of interstitial liquid are needed in the peridotite (up to 80%) before gravitational instability can be induced.

Although loading of two crystal mushes with the properties outlined above overcomes the relative density problem, this mechanism cannot account for the field evidence that peridotite has apparently been

generated at the expense of allivalite, and that fingers transgress allivalite layers causing negligible distortion in comparison with their size. We therefore believe that finger formation requires some mechanism in addition to simple loading of crystal mushes.

5.c. Metasomatic replacement

This involves the selective replacement of pre-existing allivalite by secondary peridotite within the crystal pile. Perhaps the most attractive feature of metasomatic replacement as a model for finger formation is that it may take place on a volume-for-volume basis (Irvine, 1980).

5.c.1. Mechanism

In this model we envisage a situation just prior to the finger formation event where a peridotite layer of high porosity was overlain by an allivalite layer of relatively low porosity. We assume the interstitial liquid in the peridotite at that time was lighter than that in the overlying allivalite (section 5.b.2).

We now suggest the two layers underwent compaction. Compaction was most effective in the peridotite because of the loosely packed crystal framework and the lower density of the interstitial melt (McKenzie, 1984); thus liquid in the peridotite was driven upwards into the allivalite in the form of fingers. Because this liquid was not in equilibrium with the allivalite, this would result in resorption of both feldspar and olivine in the allivalite until all of the feldspar was consumed, assuming strictly isothermal conditions. However, if the peridotite liquid was relatively hotter than that in the allivalite mush, cooling of this liquid as it was expelled upwards would allow feldspar alone to be resorbed and olivine to crystallize (Bowen, 1928; McBirney, 1979). In either case resorption of feldspar would be accompanied, or succeeded by, crystallization of olivine.

The compaction-metasomatism process outlined above involves the flow of liquid in only one direction and is therefore similar to Robins' (1982) model. Following Irvine (1980), Robins explained finger structures in the Lille Kufjord and Rhum intrusions as the result of metasomatic replacement by upward migrating intercumulus liquid.

A possible alternative model, which relies on fluid dynamic instability rather than compaction as the mechanism for expelling liquid from the peridotite, is well illustrated by the experiments of Sparks *et al.* (this issue). They describe finger-like protrusions developing where heavier fluid sinks into a porous media of light fluid. In the present study this could correspond to dense melt in the allivalite sinking and light melt in the peridotite rising; flow of liquids in this model is therefore in two directions. If liquid-liquid loading was the mechanism of finger formation, then

the possible subsequent metasomatic effects of dense allivalite pore magma sinking into the peridotite should be found; i.e. downward protruding allivalite fingers. This is not the case, and we therefore prefer to interpret the peridotite fingering as the manifestation of a compaction-metasomatism process. Indeed, effective exchange of melts was probably not possible if, at the time of finger formation, the allivalite was well compacted and of a low porosity, as suggested by field observations.

5.c.2. Textures and mineral chemistry

Metasomatic replacement is now generally accepted as a likely process in layered intrusions (e.g. Skaergaard and Duke Island: Irvine, 1980; Bushveld: Cameron & Desborough, 1964 and Schiffries, 1982). The recognition therefore that replacement may have also taken place on Rhum is particularly interesting because most finger peridotite shows typical cumulate textures – apart from its transgressive behaviour it cannot be distinguished from normal olivine cumulates (thought to have formed by primary igneous processes). Indeed, there is no textural evidence at thin section scale to suggest that any reaction has taken place between crystals and upward infiltrating liquid (e.g. rounded or embayed plagioclase tablets near to finger contacts, reaction rims, etc.).

The microfabrics exhibited by tabular olivines in some fingers (e.g. Unit 8) are not difficult to reconcile with a replacement model. An alternative to the deformational interpretation (section 5.b.1) is that the tabular olivines (Fig. 6) are not primary cumulus crystals, but instead were precipitated from the metasomatizing pore magma. If this assumption is correct, then their present orientation parallel to the periphery of the structure can be explained by the upward moving magma having forcefully shouldered them aside and effectively 'plastering' them to the sides of the growing finger (see Irvine (1980, p. 362), where upward flow of intercumulus liquid in the Muskox Intrusion was thought to be sufficient to align cumulus olivine crystals). Alternatively, the olivine crystals may have grown in their present position in response to physico-chemical gradients during assimilation of the allivalite.

The upward deflection of cumulus plagioclase laths adjacent to the fingers is also not problematic. This can be tentatively ascribed to slight movement at the contact during crystallization of the secondary peridotite. Also, rotation of the laths indicates interstitial liquid was present in the allivalite at that time.

Our observation that fingers are developed along the lower surfaces of allivalite blocks in certain peridotites (section 2.a.2) is taken by us to provide more definite evidence for metasomatic replacement on Rhum; they therefore lend support to the theory that finger

structures in other environments (e.g. at intra-unit contacts, in subsidiary peridotites, etc.) also formed by replacement. We explain the blocks as having formed by the incomplete replacement of subsidiary allivalite layers by secondary peridotite. A mechanism involving plastic deformation can largely be discounted because the chrome-spinel layers which continue in the peridotite from blocks are undeformed (section 2.a.2). Thus the blocks are held to record replacement on a massive scale.

Perhaps one of the most puzzling features of the Rhum structures is the remarkably constant compositions shown by minerals in peridotite directly below a finger, within a finger, and in allivalite overlying a finger (Fig. 12). Intuitively, one might expect a difference if the peridotite had formed by replacement and the allivalite by primary igneous processes. However, it could be argued that further infiltration metasomatism has modified any chemical effects resulting from finger formation.

6. Conclusions

Finger-like protrusions of peridotite are not geological curiosities on Rhum – they occur throughout the ELS and CS in several different environments where peridotite is overlain by allivalite.

We have argued that finger formation is best explained by metasomatic replacement (Robins, 1982). There is overwhelming evidence at outcrop scale that fingers transgress layers without causing perceptible distortion, and this is consistent with the allivalite having been replaced by secondary peridotite on a volume-for-volume basis. When deformation fabrics are found, they are on a scale which is considered too small if the fingers had formed only by injection of peridotite into allivalite.

The model we propose requires a peridotite of high porosity to be overlain by an allivalite of low porosity. Intercumulus liquid in the peridotite should be lighter than that in the allivalite. The process of finger formation starts when the two layers undergo compaction, allowing relatively light pore liquid in equilibrium with the peridotite to move upwards into the overlying allivalite in the form of fingers. This liquid resorbs plagioclase in the allivalite but crystallizes olivine and clinopyroxene in its place, producing secondary olivine-cumulates indistinguishable from other peridotites in the intrusion. The upward deflection of plagioclase laths in the allivalite near to the structures suggests slight movement occurred at the contact during crystallization of the secondary peridotite.

Thus, finger structures found where allivalite overlies peridotite are taken to provide evidence for postcumulus replacement on a local scale (i.e. within the finger-shaped area now occupied by the structure), whereas fingers associated with allivalite blocks indicate replacement on a massive scale (i.e. large

portions of the Rhum stratigraphy have been obliterated and only relic blocks now remain).

This conclusion obviously has far-reaching implications for the interpretations of layered intrusions. The present structures have all been recognized because of their form and obvious discordant relationships with the layered rocks. However, there is a possibility that replacement may take place even where discordant relationships are not obvious, i.e. where the evidence for fingering may be on a very different scale (smaller amplitude to wavelength ratio), or even absent. Complete replacement of allivalite layers without relic blocks must also be considered.

Also, the present study suggests that tabular or anhedral crystals (e.g. olivine) cannot always be assumed to be cumulus in status. Many apparent variations in cryptic layering may therefore only represent postcumulus crystallization of secondary bodies. It is clear then that extreme care must be taken in interpreting magma evolution from cryptic variation profiles through cyclic units on Rhum.

As most of the conclusions reached in this paper have come from field observations, future work on Rhum should include detailed chemical studies on the layers identified here as having been formed by replacement. This will allow an even better assessment of the extent to which postcumulus processes have determined the present textural and chemical features on Rhum.

Acknowledgements. This study would not have been possible without the permission of the Nature Conservancy Council to work on Rhum, and the award of Research Studentships by the Natural Environment Research Council, for which we are all grateful. Dr R. S. J. Sparks is thanked for suggesting ways of improving our ideas on finger formation. Mrs Marina Potgieter drafted the figures, and Mrs Ina Bornman typed the manuscript.

References

- ANKETELL, J. M., CEGLA, J. & DZULYNSKI, S. 1970. On the deformational structures in systems with reversed density gradients. *Annales de la Société Géologique de Pologne* **40**, 3–30.
- BOWEN, N. L. 1928. *The Evolution of the Igneous Rocks*. Princeton University Press. 334 pp.
- BROWN, G. M. 1956. The layered ultrabasic rocks of Rhum, Inner Hebrides. *Philosophical Transactions of the Royal Society of London* **B240**, 1–53.
- BUTCHER, A. R. 1985. Channelled metasomatism in Rhum layered cumulates – evidence from late-stage veins. *Geological Magazine* **122**, 503–18.
- CAMERON, E. N. & DESBOROUGH, G. A. 1964. Origin of certain magnetite-bearing pegmatites in the eastern Bushveld Complex, South Africa. *American Mineralogist* **62**, 1082–96.
- HÜPPERT, H. E. & SPARKS, R. S. J. 1980. The fluid dynamics of a basaltic magma chamber replenished by influx of hot, dense ultrabasic magma. *Contributions to Mineralogy and Petrology* **75**, 279–89.
- IRVINE, T. N. 1980. Magnetic infiltration metasomatism, double-diffusive fractional crystallization, and adcumulus growth in the Muskox intrusion and other layered intrusions. In *Physics of Magmatic Processes* (ed. R. B. Hargraves), pp. 325–83. Princeton, N.J.: Princeton University Press.
- LEE, C. A. 1981. Post-deposition structures in the Bushveld Complex mafic sequence. *Journal of the Geological Society of London* **138**, 327–41.
- MCBIRNEY, A. R. 1979. Effects of assimilation. In *The Evolution of the Igneous Rocks* (ed. H. S. Yoder, Jr.), pp. 307–38. Princeton, N.J.: Princeton University Press.
- MCKENZIE, D. P. 1984. The generation and compaction of partially molten rock. *Journal of Petrology* **25**, 713–65.
- ROBINS, B. 1982. Finger structures in the Lille Kufjord layered intrusion, Finnmark, Northern Norway. *Contributions to Mineralogy and Petrology* **81**, 290–5.
- SCHIFFRIES, C. M. 1982. The petrogenesis of a platiniferous dunite pipe in the Bushveld Complex: infiltration metasomatism by a chloride solution. *Economic Geology* **77**, 1439–53.
- SPARKS, R. S. J., HÜPPERT, H. E., KERR, R. C., MCKENZIE, D. P. & TAIT, S. R. 1985. Postcumulus processes in layered intrusions. *Geological Magazine* **122**, 555–68.
- SPARKS, R. S. J., MEYER, P. & SIGURDSSON, H. 1980. Density variation amongst mid-ocean ridge basalts: implications for magma mixing and the scarcity of primitive lavas. *Earth and Planetary Science Letters* **46**, 419–30.
- STOLPER, E. & WALKER, D. 1980. Melt density and the average composition of basalt. *Contributions to Mineralogy and Petrology* **74**, 7–12.
- THY, P. & WILSON, J. R. 1980. Primary igneous load-cast deformation structures in the Fongen-Hyllingen layered basic intrusion, Trondheim Region, Norway. *Geological Magazine* **117**, 363–74.
- WADSWORTH, W. J. 1961. The layered ultrabasic rocks of south-west Rhum, Inner Hebrides. *Philosophical Transactions of the Royal Society of London* **B244**, 21–64.

